

TECHNISCHE UNIVERSITÄT KAISERSLAUTERN

Analysis of Systems of Hyperbolic Partial Differential Equations Coupled to Switched Differential Algebraic Equations

Vom Fachbereich Mathematik der
Technischen Universität Kaiserslautern
zur Verleihung des akademischen Grades
Doktor der Naturwissenschaften
(Doctor rerum naturalium)
genehmigte

Dissertation

von
Damla KOÇOĞLU

Gutachter:
Prof. Dr. Stephan TRENN
Prof. Dr. Falk HANTE

AG Technomathematik
Fachbereich Mathematik

12. Dezember 2020

D386

Abstract

Simplified ODE models describing blood flow rate are governed by the pressure gradient. However, assuming the orientation of the blood flow in a human body correlates to a positive direction, a negative pressure gradient forces the valve to shut, which stops the flow through the valve, hence, the flow rate is zero, whereas the pressure rate is formulated by an ODE. Presence of ODEs together with algebraic constraints and sudden changes of system characterizations yield systems of switched differential-algebraic equations (swDAEs). Alternating dynamics of the heart can be well modelled by means of swDAEs. Moreover, to study pulse wave propagation in arteries and veins, PDE models have been developed. Connection between the heart and vessels leads to coupling PDEs and swDAEs. This model motivates to study PDEs coupled with swDAEs, for which the information exchange happens at PDE boundaries, where swDAE provides boundary conditions to the PDE and PDE outputs serve as inputs to swDAE. Such coupled systems occur, e.g. while modelling power grids using telegrapher's equations with switches [63], water flow networks with valves [76, 80] and district heating networks with rapid consumption changes [21]. Solutions of swDAEs might include jumps, Dirac impulses and their derivatives of arbitrary high orders. As outputs of swDAE read as boundary conditions of PDE, a rigorous solution framework for PDE must be developed so that jumps, Dirac impulses and their derivatives are allowed at PDE boundaries and in PDE solutions. This is a wider solution class than solutions of small bounded variation (BV), for instance, used in [19] where nonlinear hyperbolic PDEs are coupled with ODEs. Similarly, in [5, 71, 73], the solutions to switched linear PDEs with source terms are restricted to the class of BV. However, in the presence of Dirac impulses and their derivatives, BV functions cannot handle the coupled systems including DAEs with index greater than one. Therefore, hyperbolic PDEs coupled with swDAEs with index one will be studied in the BV setting and with swDAEs whose index is greater than one will be investigated in the distributional sense. To this end, the 1D space of piecewise-smooth distributions is extended to a 2D piecewise-smooth distributional solution framework. 2D space of piecewise-smooth distributions allows trace evaluations at boundaries of the PDE. Moreover, a relationship between solutions to coupled system and switched *delay* DAEs is established. The coupling structure in this thesis forms a rather general framework. In fact, any arbitrary network, where PDEs are represented by edges and (switched) DAEs by nodes, is covered via this structure. Given a network, by rescaling spatial domains which modifies the coefficient matrices by a constant, each PDE can be defined on the same interval which leads to a formulation of a single PDE whose unknown is made up of the unknowns of each PDE that are stacked over each other with a block diagonal coefficient matrix. Likewise, every swDAE is reformulated such that the unknowns are collected above each other and coefficient matrices compose a block diagonal coefficient matrix so that each node in the network is expressed as a single swDAE. The results are illustrated by numerical simulations of the power grid and simplified circulatory system examples. Numerical results for the power grid display the evolution of jumps and Dirac impulses caused by initial and boundary conditions as a result of instant switches. On the other hand, the analysis and numerical results for the simplified circulatory system do not entail a Dirac impulse, for otherwise such an entity would destroy the entire system. Yet jumps in the flow rate in the numerical results can come about due to opening and closure of valves, which suits clinical and physiological findings. Regarding physiological parameters, numerical results obtained in this thesis for the simplified circulatory system agree well with medical data and findings from literature when compared for the validation.

Zusammenfassung

Modelle, die auf gewöhnlichen Differentialgleichungen (GDGL) führen, die die Blutflussrate beschreiben, werden durch den Druckgradienten bestimmt. Wird die Orientierung des Blutflusses im menschlichen Körper als positive Richtung angenommen, so führt ein negativer Druckgradient zur Umkehrung der Flussrichtung und zum Schließen der Herzklappen. Der Blutfluss wird gestoppt und die Flussrate fällt auf Null. Der Verlauf der Druckänderung, die Druckrate, wird dabei mithilfe einer DGL beschrieben. Unterliegen die DGL algebraischen Beschränkungen und plötzlichen Änderungen der Systemcharakterisierungen, führt dies zu Systemen geschalteter differential – algebraischer Gleichungen (DAGL). Die alternierende Dynamik des Herzens kann mithilfe von geschalteten DAGL gut modelliert werden. Darüber hinaus wurden zur Untersuchung der Pulswellenausbreitung in Arterien und Venen Modelle, die auf partiellen Differentialgleichungen (PDGL) führen, entwickelt. Die Verbindung zwischen dem Herzen und den Gefäßen führt zur Kopplung von PDGL und geschalteten DAGL. Dieses Modell motiviert zur Untersuchung von mit geschalteten DAGL gekoppelten PDGL, bei denen der Informationsaustausch an den PDGL-Grenzen stattfindet. Dabei liefern die geschalteten DAGL die von den PDGL benötigten Randbedingungen, während die Ausgabewerte der PDGL als Eingabewerte der geschalteten DAGL dienen. Solche gekoppelten Systeme treten z.B. bei der Modellierung von Stromnetzen mithilfe von Telegraphengleichungen mit Schaltern [63], Wasserflussnetzen mit Ventilen [76, 80] und Fernwärmenetzen mit schnellen Verbrauchsänderungen [21] auf. Lösungen geschalteter DAGL können Sprünge, Dirac-Impulse und ihre Ableitungen beliebig hoher Ordnungen umfassen. Da sich die Ergebnisse von geschalteten DAGL als Randbedingungen von PDGL lesen, muss ein strenger Lösungsrahmen für PDGL entwickelt werden, sodass Sprünge, Dirac-Impulse und ihre Ableitungen an den PDGL-Grenzen und in PDGL-Lösungen erlaubt sind. Dies ist eine breitere Lösungsklasse als die Funktionen der beschränkten Variation (BV), die z.B. in [19] verwendet werden, wo nichtlineare hyperbolische PDGL mit DGL gekoppelt sind. In ähnlicher Weise sind in [5, 71, 73] die Lösungen für geschaltete lineare PDGL mit Quelltermen auf die Klasse der BV beschränkt. Bei Vorhandensein von Dirac-Impulsen und ihren Ableitungen können BV-Funktionen jedoch nicht mit den gekoppelten Systemen einschließlich DAGL mit Index größer als eins umgehen. Daher werden hyperbolische PDGL, die mit DAGL mit Index eins gekoppelt sind, in der BV-Einstellung und mit DAGL, deren Index größer als eins ist, auf die Klasse der Distributionen untersucht. Zu diesem Zweck wird der eindimensionale Raum stückweise glatter Distributionen auf ein zweidimensionales stückweise glattes Lösungsframework erweitert. Der zweidimensionale Raum stückweise glatter Verteilungen erlaubt Randwerte an den Grenzen der PDGL. Darüber hinaus wird eine Beziehung zwischen Lösungen des gekoppelten Systems und den geschalteten retardierten DAGL hergestellt. Die Kopplungsstruktur, die hier untersucht wird, bildet einen eher allgemeinen Rahmen. Tatsächlich wird jedes beliebige Netzwerk, in dem PDGL durch Kanten und (geschaltete) DAGL durch Knoten repräsentiert werden, über diese Struktur abgedeckt. Die Ergebnisse anhand numerische Simulationen des Stromnetzes und vereinfachter Beispiele des Herz-Kreislaufsystems veranschaulicht werden. Die numerischen Ergebnisse für das Stromnetz zeigen die Entwicklung von Sprüngen und Dirac-Impulsen, die durch die, von Sofortschaltern beeinflussten, Anfangs- und Randbedingungen verursacht werden. Dementgegen beinhalten die Analyse und die numerischen Ergebnisse für das vereinfachte Zirkulationssystem keinen Dirac-Impuls, denn sonst würde eine solche Entität das gesamte System zerstören. Dennoch können Sprünge in der Flussrate in den numerischen Ergebnissen durch Öffnen und Schließen der Klappen entstehen, was den klinischen und physiologischen Befunden entspricht. Was die physiologischen Parameter betrifft, so stimmen die numerischen Ergebnisse für das vereinfachte Kreislaufsystem gut mit medizinischen Daten und Befunden aus der Literatur überein.

Acknowledgements

I want to thank my supervisors Prof. Dr. Stephan Trenn and Dr. Raul Borsche for offering and sharing their knowledge, helping me improve myself scientifically and always being supportive, helpful and understanding. Their excellence guidance and fruitful feedback shaped my academic qualifications. My doctoral studies are funded by Deutsche Forschungsgemeinschaft (DFG). Therefore, I would like to thank DFG for their financial support.

Contents

Abstract	iii
Acknowledgements	vii
1 Introduction	1
2 Hyperbolic partial differential equations	5
2.1 Semilinear balance laws	5
2.2 Linear conservation laws	22
3 Theory of distributions	31
3.1 Preliminary Notions	31
3.2 Distributions in time domains	32
3.3 Operations on distributions	34
3.4 The space $\mathbb{D}_{\text{pw}C^\infty}(T)$ of piecewise smooth distributions	36
4 Switched differential algebraic equations	41
4.1 Mathematical structure	41
4.2 Distributional swDAEs	44
5 Coupling hyperbolic balance laws with switched DAEs of index one	47
5.1 Coupled system	47
6 Theory of distributions in time and space	55
6.1 Distributions in time and space domains	55
6.2 The space $\mathbb{D}_{\text{pw}C^\infty}(T \times X)$ of piecewise smooth distributions	59
7 Distributional solutions for linear hyperbolic PDEs	69
7.1 Scalar advection equation	69
7.2 Linear systems of partial differential equations	72
8 Coupling linear PDE systems with switched DAE systems	77
8.1 System class	77
8.2 The coupled system	91
8.3 Numerical results	95
9 Appendix	125
9.1 Zeno behavior	125
9.2 Algorithm for the power grid example	127
9.3 Algorithm for the circulatory system example	129

Chapter 1

Introduction

In this thesis, a rigorous solution theory is developed for systems where a system of linear hyperbolic partial differential equations (PDEs) is coupled with a system of switched differential algebraic equations (DAEs) via boundary conditions (BC), see Figure 1.1 as an overview. Furthermore, the well-posedness of a switched system which is composed of semi-

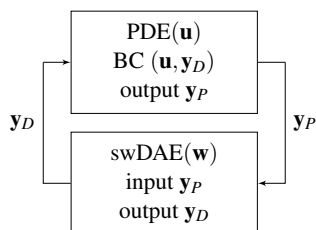


FIGURE 1.1: Coupling of a PDE with a switched DAE via boundary condition.

linear hyperbolic balance laws and DAEs is studied, where the system is given as follows

$$\partial_t \mathbf{u}(t, x) + \mathbf{A}_\sigma(t, x) \partial_x \mathbf{u}(t, x) = \mathbf{s}_\sigma(t, x, \mathbf{u}(t, x)), \quad (1.1a)$$

$$\mathbf{P}_\sigma(t) \begin{pmatrix} \mathbf{u}(t, 0^+) \\ \mathbf{u}(t, 1^-) \end{pmatrix} = \mathbf{P}_{\mathbf{w}, \sigma}(t) \mathbf{w}(t) + \mathbf{p}_\sigma(t), \quad (1.1b)$$

$$\mathbf{E}_\sigma \dot{\mathbf{w}} = \mathbf{H}_\sigma \mathbf{w} + \mathbf{K}_{0, \sigma}(t) \mathbf{u}(t, 0^+) + \mathbf{K}_{1, \sigma}(t) \mathbf{u}(t, 1^-) + \mathbf{f}(t), \quad (1.1c)$$

where the unknown \mathbf{u} satisfies the system of semi-linear hyperbolic partial differential equations (1.1a), and \mathbf{w} is the solution to the linear DAE (1.1c) whose index is one. The functions \mathbf{u} and \mathbf{w} are linked together through the boundary conditions (1.1b) of the PDE and the vector field of the DAE (1.1c). The complete system (1.1) is subject to some external switching, governed by the parameter σ . Such systems occur in many real applications, for example, when modeling power grids using the telegrapher's equations [63] including switches (e.g. induced by disconnecting lines), water flow networks with valves [76, 80], gas transport [11, 41, 42], supply chain models including processor breakdown [3, 53], district heating systems with rapid consumption changes [21] and blood flow with simplified valve models in the heart [94]. Similar systems, but with nonlinear PDEs, are also used for modelling the human circulatory system [102, 103, 104] or for controlling traffic flow [38, 56] with autonomous vehicles. Similar to [72], the closed loop setting illustrated in Figure 1.1 can include general network structures where edges represent PDEs and nodes stand for switched DAEs (swDAEs). After rescaling the spatial domain of each PDE, the coefficient matrices for PDEs are modified by a constant factor. As every PDE is defined on the same space interval due to rescaling, all PDEs in the network can be then viewed as a single PDE whose unknown consists of the unknowns of PDEs that are stacked over each other. Moreover, the coefficient matrix of the resulting PDE is a block diagonal matrix composed of coefficient matrices of each PDE. In a similar fashion, all swDAEs can be grouped together such that

there is only one swDAE system whose unknown comprises the unknowns of given swDAEs; and whose coefficient matrices are block diagonal, which are made up of coefficient matrices of the corresponding swDAEs.

In the literature, the coupling between hyperbolic PDEs and ODEs at the boundary has been studied in different settings; see [19, 20, 29, 34, 35, 57, 58] and references therein. In the case of nonlinear systems of hyperbolic balance laws, the obtained results hold only locally in time and with small total variation, [18, 19]. Instead, the setting in this thesis allows to prove the existence of a global in time solution without any restrictions on the total variation of the initial data. This is in accordance with the results obtained in the Ph.D. thesis [71] by Falk Hante about the well-posedness of switched linear balance laws on bounded domains. It should be remarked that the results obtained in [71] do not cover the case in this thesis. This is due to the fact that (1.1) is a so-called *loop system*; i.e., the boundary condition (1.1b) at one side can depend on the trace of the solution at the other side. The present setting can also include the case of networks. In the BV setting, only the special case of DAEs of index one is treated. This is due to the fact that solutions to DAEs with index greater than one are in general distributions; hence, they do not have the minimum regularity that source terms of hyperbolic PDEs require. The results are global in time as long as the inputs have a finite (not necessarily small) total variation. In this thesis, the well-posedness of (1.1) is proven by using an iterative converging procedure, based on the solutions to both PDEs and DAEs. Concerning the hyperbolic balance laws (1.1a)-(1.1b), the well-known definition of broad solutions is employed, see for example [24], based on the concept of characteristic curves. Using the Banach fixed point theorem, the results on bounded intervals, which are studied in [71], are extended to the case of looped systems. Moreover, suitable bounds on the total variation are obtained, which allow one to consider the traces of the solution at the boundaries. Regarding DAEs, well-known results and estimates are employed, see [81].

In this coupled system, the values of the switched DAE provide the boundary conditions for the PDE and the values of the PDE at its boundaries serve as an input to the DAE. As an initial example, consider the linear advection equation with the initial and boundary conditions with the output

$$\begin{aligned}
 & \partial_t v(t, x) + \partial_x v(t, x) = 0, \quad t \in [0, \infty), \quad x \in [0, \infty), \\
 \text{IC} \quad & v(0, x) = v_0(x), \\
 \text{BC} \quad & v(t, 0^+) =: b(t), \\
 \text{output} \quad & y_P(t) := v(t, 0).
 \end{aligned} \tag{1.2}$$

There exists a unique solution to (1.2) as it is well-known from the classical hyperbolic PDE theory.

Consider now the following DAE of the form $\mathbf{E}\dot{\mathbf{w}} = \mathbf{H}\mathbf{w} + \mathbf{B}q$ with the output

$$\begin{aligned}
 \begin{bmatrix} 1 & 0 \\ 0 & 0 \end{bmatrix} \begin{bmatrix} \dot{w} \\ \dot{z} \end{bmatrix} &= \begin{bmatrix} 1 & 0 \\ 0 & 1 \end{bmatrix} \begin{bmatrix} w \\ z \end{bmatrix} - \begin{bmatrix} 0 \\ 1 \end{bmatrix} q, \\
 y_D(t) &:= \begin{bmatrix} 0 & 1 \end{bmatrix} \begin{bmatrix} w \\ z \end{bmatrix},
 \end{aligned} \tag{1.3}$$

where $q : [0, \infty) \rightarrow \mathbb{R}$ is some input of the system. There exists a unique solution to the DAE if and only if the matrix pair (\mathbf{E}, \mathbf{H}) is regular; i.e., $\det(s\mathbf{E} - \mathbf{H})$ is not the zero polynomial for $s \in \mathbb{R}$, [130]. Consider now the coupling between these two systems, (1.2) with (1.3), via their inputs and outputs; i.e., $b(t) = y_D(t)$ and $q(t) = y_P(t)$. According to these coupling rules, however, it is not possible to describe a well-defined coupled system as the output of the PDE is equals to its boundary condition, which yields an algebraic loop for the DAE as

follows

$$y_D(t) = b(t) = y_P(t) = q(t),$$

which makes the coupling ill-posed. Here, the delicate issue takes place while designating the coupling rules so that the information PDE provides as an input to the swDAE needs to be specified in terms of only outgoing waves of the PDE.

Solutions of switched DAEs in general contain jumps and derivatives thereof, i.e. Dirac impulses [130, 132], hence the solution concept of the PDE has to be extended to allow for jumps and Dirac impulses at the boundary. In particular, this is a wider class compared to the solutions of small bounded variation, e.g. used in [19] where a nonlinear hyperbolic PDE is coupled to an ODE. Similarly, in [5, 73], the investigations of switched linear PDEs with source terms are restricted to solutions with bounded variation. In [123], Dirac impulses are introduced at the position of an interface of nonlinear PDEs. A more general appearance of Dirac impulses is allowed in [36, 141] for a partially linear system. Since arbitrary high derivatives of Dirac impulses can occur as solutions of switched DAEs, the aforementioned approaches are not suitable to handle the coupled systems studied here. Indeed, the first main contribution is a suitable extension of the 1D piecewise-smooth distributional solution framework, which was developed to handle switched DAEs in [130, 131], to a 2D piecewise-smooth distributional solution framework. This solution space allows trace evaluation on the boundaries of the domain. Towards the main existence and uniqueness result for solutions of the coupled system, a relationship between the solutions of the coupled systems and the solution of switched *delay* DAEs is established as well. For the latter, a recent existence and uniqueness result for delay DAEs in [133] is generalized. After defining a 2D solution space, a condition is stated on systems to be coupled such that the coupling is well-defined.

This thesis is structured as follows. First, several results about the well-posedness of linear hyperbolic balance laws are summarized and the classical solution theory of linear hyperbolic PDEs in Chapter 2, theory of distributions in Chapter 3 and the solution theory of switched DAEs in Chapter 4 are reviewed. In Chapter 5, the coupled problem of hyperbolic balance laws and switched DAEs is investigated. Then, distributions in a 2D space are defined in Chapter 6. Later, a novel distributional solution framework for linear hyperbolic PDEs is introduced in Chapter 7, which is then used in the distributional setting to study coupled systems with linear transport equations and linear swDAEs of arbitrary index in Chapter 8 and to establish a link between the coupled system and the solutions of switched delay DAEs. Finally, the results are illustrated by numerical simulations of a simple power grid and blood flow examples.

Chapter 2

Hyperbolic partial differential equations

Exploiting hyperbolic partial differential equations is an effective tool to model physical systems and engineering problems. Furthermore, they enjoy wide range of applications, such as describing traffic flow, [22, 32, 33, 75, 137], open channel hydraulics [31], irrigation systems [88], chemical processes [137], transmission line networks [91, 122], gas flow networks [10, 137], blood flow networks [96, 98, 105], air traffic management [12], supply-chain models [7, 62, 70], cell movement in biology [47, 100] and heat exchangers [144]. Many of the aforementioned PDE systems can be modeled as balance or conservation laws. This chapter begins with some existing results of semilinear balance laws and method of characteristics. The existing theoretical results are reviewed and extended such that looped systems are included. By using the Banach fixed point theorem, the results on bounded intervals are extended to the case of looped systems. Moreover, suitable bounds on the total variation are obtained, which allow to consider the traces of the solution at the boundaries. For linear conservation laws, an explicit solution formula to these systems in terms of their initial and boundary data is provided. Finally, the formulation of the solution to linear conservation laws at boundaries is expressed in terms of boundary data and solutions at previous time shifts which depend on the domain and wave speeds.

2.1 Semilinear balance laws

Consider the following semilinear initial boundary value problem (IBVP)

$$\partial_t \mathbf{u}(t, x) + \mathbf{A}(t, x) \partial_x \mathbf{u}(t, x) = \mathbf{s}(t, x, \mathbf{u}(t, x)), \quad (2.1a)$$

$$\begin{pmatrix} \mathbf{P}_a^0(t) & \mathbf{P}_a^1(t) \\ \mathbf{P}_b^0(t) & \mathbf{P}_b^1(t) \end{pmatrix} \begin{pmatrix} \mathbf{u}(t, a) \\ \mathbf{u}(t, b) \end{pmatrix} = \mathbf{b}(t), \quad (2.1b)$$

$$\mathbf{u}(t_0, x) = \mathbf{u}^{t_0}(x), \quad (2.1c)$$

where $x \in [a, b]$, $t \geq t_0$ with the following assumptions:

(H-1): The map $\mathbf{A} : [t_0, \infty) \times [a, b] \rightarrow \mathbb{R}^{n \times n}$ is a \mathbf{C}^2 function.

(H-2): The source term $\mathbf{s} : [t_0, \infty) \times [a, b] \times \mathbb{R}^n \rightarrow \mathbb{R}^n$ is bounded, measurable with respect to t , and Lipschitz continuous with respect to x and \mathbf{u} . In particular, there exists $L_s > 0$ such that

$$|\mathbf{s}(t, x, \mathbf{u})| \leq L_s, \quad |\mathbf{s}(t, x_1, \mathbf{u}_1) - \mathbf{s}(t, x_2, \mathbf{u}_2)| \leq L_s |x_1 - x_2| + L_s |\mathbf{u}_1 - \mathbf{u}_2|$$

for every $t \geq t_0$, $x, x_1, x_2 \in [a, b]$, and $\mathbf{u}, \mathbf{u}_1, \mathbf{u}_2 \in \mathbb{R}^n$.

(H-3): The system is strictly hyperbolic; i.e., $\mathbf{A}(t, x)$ has n real and distinct eigenvalues, namely $\lambda_1(t, x) < \dots < \lambda_n(t, x)$, and corresponding left $\mathbf{l}_i(t, x)$ and right $\mathbf{r}_i(t, x)$ eigenvectors for each $i = 1, \dots, n$. It is further assumed that

$$\|\mathbf{r}_i\|_2 = 1, \quad \mathbf{l}_j \cdot \mathbf{r}_i = \begin{cases} 1, & \text{if } i = j, \\ 0, & \text{if } i \neq j, \end{cases}$$

where $\|\cdot\|_2$ is the Euclidean norm.

(H-4): There exist $c > 0$ and $\ell \in \{1, 2, \dots, n-1\}$ such that $\lambda_\ell(t, x) < -c$ and $\lambda_{\ell+1}(t, x) > c$ for every $(t, x) \in [t_0, \infty) \times [a, b]$.

(H-5): $\mathbf{P}_a^0, \mathbf{P}_a^1 \in \mathbf{C}^0(\mathbb{R}; \mathbb{R}^{(n-\ell) \times n})$ and $\mathbf{P}_b^0, \mathbf{P}_b^1 \in \mathbf{C}^0(\mathbb{R}; \mathbb{R}^{\ell \times n})$ are locally Lipschitz continuous and satisfy

$$\det \begin{pmatrix} \mathbf{P}_a^0(t) [\mathbf{r}_{\ell+1}(t, a) \cdots \mathbf{r}_n(t, a)] & \mathbf{P}_a^1(t) [\mathbf{r}_1(t, b) \cdots \mathbf{r}_\ell(t, b)] \\ \mathbf{P}_b^0(t) [\mathbf{r}_{\ell+1}(t, a) \cdots \mathbf{r}_n(t, a)] & \mathbf{P}_b^1(t) [\mathbf{r}_1(t, b) \cdots \mathbf{r}_\ell(t, b)] \end{pmatrix} \neq 0$$

for every $t \in [t_0, \infty)$.

Remark 2.1

Left- and right eigenvectors \mathbf{l}_i and \mathbf{r}_i of $\mathbf{A}(t, x)$ are Lipschitz continuous with respect to t and x , by the implicit function theorem. Hence, by Rademacher's theorem, [106], partial derivatives of \mathbf{l}_i and \mathbf{r}_i exist everywhere up to a set of measure zero.

2.1.1 The method of characteristics

Under the previous assumptions, the system (2.1) can be rewritten in a diagonal form by defining the $n \times n$ matrices \mathbf{L} and \mathbf{R} as

$$\mathbf{L}(t, x) = [\mathbf{l}_1(t, x) \cdots \mathbf{l}_n(t, x)]^\top \quad \text{and} \quad \mathbf{R}(t, x) = [\mathbf{r}_1(t, x) \cdots \mathbf{r}_n(t, x)],$$

whose components are respectively the left- and right eigenvectors of the matrix $\mathbf{A}(t, x)$, and the $n \times n$ diagonal matrix $\Lambda(t, x)$, which is composed of the eigenvalues of $\mathbf{A}(t, x)$. Note that, the Assumptions (H-3) and (H-4) imply that the matrices \mathbf{L} , \mathbf{R} , and Λ are non-singular. Multiplying Equation (2.1a) with the matrix \mathbf{L} on the left decouples the left hand side into a system of scalar equations

$$\mathbf{v}_t(t, x) + \Lambda(t, x)\mathbf{v}_x(t, x) = \mathbf{h}(t, x, \mathbf{v}(t, x)), \quad (2.2)$$

where

$$\mathbf{h}(t, x, \mathbf{u}) := \mathbf{L}(t, x)\mathbf{s}(t, x, \mathbf{u}(t, x)) + [\mathbf{L}_t(t, x) + \Lambda(t, x)\mathbf{L}_x(t, x)]\mathbf{v}(t, x), \quad (2.3)$$

with $\mathbf{h} = [h_1 \cdots h_n]^\top$ and the characteristic variable $\mathbf{v} = [v_1 \cdots v_n]^\top$ such that

$$v_i(t, x) = \mathbf{l}_i(t, x) \cdot \mathbf{u}(t, x), \quad \forall i = 1, 2, \dots, n. \quad (2.4)$$

Note that multiplying Equation (2.1a) with the matrix \mathbf{R}^{-1} on the left would decouple the equation into scalar equations as in (2.2), as well.

Remark 2.2

As a result of Remark (2.1), the maps h_i , for $i = 1, 2, \dots, n$, are measurable with respect to t and x ; and locally Lipschitz continuous with respect to \mathbf{v} .

Solutions to (2.1) are considered in the sense of broad solutions, which are based on the concept of characteristic curves.

Definition 2.3

An absolutely continuous function $t \mapsto x_i(t; \tau, \sigma)$ is called *i-th characteristic curve* if it satisfies

$$\frac{d}{dt}x_i(t; \tau, \sigma) = \lambda_i(t, x_i(t; \tau, \sigma)) \quad \text{with} \quad x_i(\tau; \tau, \sigma) = \sigma,$$

almost everywhere on $[t_0, \infty) \times [a, b]$, where $x_i(t; \tau, \sigma)$ is defined.

The system (2.2) consists of n scalar advection equations of the form

$$\partial_t v_i(t, x) + \lambda_i(t, x) \partial_x v_i(t, x) = h_i(t, x, \mathbf{v}(t, x)), \quad (2.5)$$

where $\lambda_i(t, x)$ is the wave speed for $i = 1, \dots, n$.

Each equation in (2.5) can be reduced to an ODE along the integral curve $x_i(t; \tau, \sigma)$ in the vector field $(1, \lambda_i)$ passing through (τ, σ) . Let

$$\frac{dt}{d\tau} = 1, \quad \frac{dx}{d\tau} x_i(t; \tau, \sigma) = \lambda_i(t, x_i(t; \tau, \sigma)),$$

with $x_i(\tau; \tau, \sigma) = \sigma$, then it holds

$$\begin{aligned} \frac{d}{d\tau} v_i(t, x_i(t; \tau, \sigma)) &= \partial_t v_i(t, x_i(t; \tau, \sigma)) \frac{dt}{d\tau} + \partial_x v_i(t, x_i(t; \tau, \sigma)) \frac{dx}{d\tau} \\ &= \partial_t v_i(t, x_i(t; \tau, \sigma)) + \lambda_i(t, x_i(t; \tau, \sigma)) \partial_x v_i(t, x_i(t; \tau, \sigma)) \\ &= h_i(t, x_i(t; \tau, \sigma), \mathbf{v}(t, x_i(t; \tau, \sigma))). \end{aligned}$$

As a result, each equation in (2.5) for $i = 1, \dots, n$ can be considered as an ordinary differential equation of the form

$$\frac{d}{d\tau} v_i(t; \tau, \sigma) = h_i(t, x_i(t; \tau, \sigma), \mathbf{v}(t, x_i(t; \tau, \sigma))),$$

along the characteristic curves $x_i(t; \tau, \sigma)$.

Let $\mathbf{v}_-(t, x)$ and $\mathbf{v}_+(t, x)$ be vectors composed of left- and right- going characteristic variables such that

$$\mathbf{v}_-(t, x) := [v_1 \dots v_\ell]^\top \quad \text{and} \quad \mathbf{v}_+(t, x) := [v_{\ell+1} \dots v_n]^\top,$$

where $\mathbf{v}_- : [t_0, \infty) \times [a, b] \rightarrow \mathbb{R}^\ell$ and $\mathbf{v}_+ : [t_0, \infty) \times [a, b] \rightarrow \mathbb{R}^{n-\ell}$.

Remark 2.4

By defining

$$\mathbf{R}^-(t, x) := [\mathbf{r}_1(t, x) \dots \mathbf{r}_\ell(t, x)] \quad \text{and} \quad \mathbf{R}^+(t, x) := [\mathbf{r}_{\ell+1}(t, x) \dots \mathbf{r}_n(t, x)],$$

the boundary condition (2.1b) can be rewritten in the form

$$\begin{pmatrix} \mathbf{N}_a(t) & \mathbf{M}_a(t) \\ \mathbf{M}_b(t) & \mathbf{N}_b(t) \end{pmatrix} \begin{pmatrix} \mathbf{v}_+(t, a) \\ \mathbf{v}_-(t, b) \end{pmatrix} = \mathbf{b}(t) - \hat{\mathbf{N}}(t) \begin{pmatrix} \mathbf{v}_-(t, a) \\ \mathbf{v}_+(t, b) \end{pmatrix}, \quad (2.6)$$

with

$$\begin{aligned} \mathbf{N}_a(t) &= \mathbf{P}_a^0(t) \mathbf{R}^+(t, a), & \mathbf{M}_a(t) &= \mathbf{P}_a^1(t) \mathbf{R}^-(t, b), & \mathbf{M}_b(t) &= \mathbf{P}_b^0(t) \mathbf{R}^+(t, a), \\ \mathbf{N}_b(t) &= \mathbf{P}_b^1(t) \mathbf{R}^-(t, b), & \text{and} & & \hat{\mathbf{N}}(t) &= \begin{pmatrix} \mathbf{P}_a^0 \mathbf{R}^-(t, a) & \mathbf{P}_a^1 \mathbf{R}^+(t, b) \\ \mathbf{P}_b^0 \mathbf{R}^-(t, a) & \mathbf{P}_b^1 \mathbf{R}^+(t, b) \end{pmatrix}. \end{aligned}$$

Due to Assumption (H-5), the $n \times n$ matrix

$$\hat{\mathbf{M}}(t) := \begin{pmatrix} \mathbf{N}_a(t) & \mathbf{M}_a(t) \\ \mathbf{M}_b(t) & \mathbf{N}_b(t) \end{pmatrix}$$

is invertible; and hence Equation (2.6) can be rewritten as

$$\begin{pmatrix} \mathbf{v}_+(t, a) \\ \mathbf{v}_-(t, b) \end{pmatrix} = (\hat{\mathbf{M}}(t))^{-1} \mathbf{b}(t) - (\hat{\mathbf{M}}(t))^{-1} \hat{\mathbf{N}}(t) \begin{pmatrix} \mathbf{v}_-(t, a) \\ \mathbf{v}_+(t, b) \end{pmatrix}, \quad (2.7)$$

that is,

$$\begin{cases} \mathbf{v}_+(t, a) = \mathbf{b}^+(t) + \mathbf{N}^+(t) \begin{pmatrix} \mathbf{v}_-(t, a) \\ \mathbf{v}_+(t, b) \end{pmatrix}, \\ \mathbf{v}_-(t, b) = \mathbf{b}^-(t) + \mathbf{N}^-(t) \begin{pmatrix} \mathbf{v}_-(t, a) \\ \mathbf{v}_+(t, b) \end{pmatrix}, \end{cases} \quad (2.8)$$

with appropriate choices $\mathbf{b}^-(t) \in \mathbb{R}^\ell$, $\mathbf{b}^+(t) \in \mathbb{R}^{n-\ell}$, $\mathbf{N}^-(t) \in \mathbb{R}^{\ell \times n}$ and $\mathbf{N}^+(t) \in \mathbb{R}^{(n-\ell) \times n}$.

Remark 2.5

Since the map \mathbf{A} is of class \mathbf{C}^2 , it holds that the eigenvalues and the eigenvectors have the same regularity. In particular the source term \mathbf{h} , defined in (2.3), for the diagonal equation (2.2) satisfies the following estimates: For every $T > t_0$, there exists a constant $L_{\mathbf{h}} > 0$ such that

$$|\mathbf{h}(t, x, \mathbf{v})| \leq L_{\mathbf{h}}, \quad |\mathbf{h}(t, x_1, \mathbf{v}_1) - \mathbf{h}(t, x_2, \mathbf{v}_2)| \leq L_{\mathbf{h}} |x_1 - x_2| + L_{\mathbf{h}} |\mathbf{v}_1 - \mathbf{v}_2|,$$

for a.e. $t \in [t_0, T]$ and for every $x, x_1, x_2 \in [a, b]$ and $\mathbf{v}, \mathbf{v}_1, \mathbf{v}_2 \in \mathbb{R}^n$.

Remark 2.6

By Assumption (H-4), the function $t \mapsto x_i(t; \tau, \sigma)$ is invertible as the eigenvalues are bounded away from zero. In the sequel, the inverse function is denoted by $x \mapsto t_i(x; \tau, \sigma)$.

In the following, regarding hyperbolic balance laws, broad solutions, see for example [24], based on the concept of characteristic curves, are defined.

Definition 2.7

Fix $T > t_0$. A function $\mathbf{u} : \mathbf{C}^0([t_0, T]; \mathbf{L}^1((a, b); \mathbb{R}^n))$ is a *broad solution* to (2.1) if, defining for every $i \in \{1, \dots, n\}$ the i -th component v_i of \mathbf{u} as in Equation (2.4), and consequently writing \mathbf{u} as

$$\mathbf{u}(t, x) = \sum_{i=1}^n v_i(t, x) \mathbf{r}_i(t, x) = \mathbf{R}(t, x) \mathbf{v}(t, x) \quad \text{on } [t_0, T] \times [a, b], \quad (2.9)$$

the following conditions hold:

- (1):** For every $i \in \{1, \dots, n\}$, $\tau \in [t_0, T]$, and for a.e. $\sigma \in [a, b]$, the equation

$$\frac{d}{d\tau} v_i(t; x_i(t; \tau, \sigma)) = h_i(t, x_i(t; \tau, \sigma), \mathbf{v}(t, x_i(t; \tau, \sigma))),$$

holds for a.e. t , where the characteristic curve $x_i(t; \tau, \sigma)$ exists.

- (2):** The boundary condition (2.1b), or the alternative formulation (2.7), holds for a.e. $t \in [t_0, T]$.

- (3):** For every $i \in \{1, \dots, n\}$, the initial condition

$$v_i(t_0, x) = \mathbf{I}_i(t_0, x) \cdot \mathbf{u}^{t_0}(x)$$

holds for a.e. $x \in [a, b]$.

In the following lemma, a priori estimate on the total variation of broad solutions to (2.2) is established. As it will be seen in the sequel, the bound on the total variation will yield the well-posedness of solutions to (2.1).

Lemma 2.8

Assume that hypotheses **(H-1)**-**(H-5)** hold and that $x \in [0, 1]$ and $t_0 = 0$ for brevity. Let \mathbf{v} be a broad solution to (2.2) with boundary conditions (2.8). Then, for every $0 < t \leq \frac{1}{\lambda_{\max}}$, where $\lambda_{\max} := \max_{i=1, \dots, n} |\lambda_i|$, there exists a constant $C > 0$, depending on λ_{\max} , \mathbf{h} , \mathbf{N}^+ , and on \mathbf{N}^- , such that

$$\begin{aligned} \mathbf{TV}(\mathbf{v}(t, \cdot)) &\leq C(1 + \mathbf{TV}(\bar{\mathbf{v}}) + \mathbf{TV}(\mathbf{b}^+) + \mathbf{TV}(\mathbf{b}^-)) \exp(Ct) \\ &\quad + C(\|\mathbf{v}\|_{\mathbf{L}^\infty} + \|\mathbf{b}^+\|_{\mathbf{L}^\infty} + \|\mathbf{b}^-\|_{\mathbf{L}^\infty}) \exp(Ct). \end{aligned} \quad (2.10)$$

Proof. First, note that the choice $t \leq \frac{1}{\lambda_{\max}}$ implies that the characteristic curves starting from one boundary do not reach the other boundary within time $\frac{1}{\lambda_{\max}}$. Denote by L a uniform bound and a Lipschitz constant for \mathbf{h} in $\left[0, \frac{1}{\lambda_{\max}}\right] \times [0, 1] \times \mathbb{R}^n$; see Remark 2.5. Since \mathbf{v} is a broad solution to (2.2), for every $i \in \{1, \dots, \ell\}$ and $0 \leq t \leq \frac{1}{\lambda_{\max}}$,

$$v_i(t, x) = \begin{cases} \bar{v}_i(x_i(0; t, x)) + \int_0^t h_i(\tau, x_i(\tau; t, x), \mathbf{v}(\tau, x_i(\tau; t, x))) d\tau, & \text{if } x < x_i(t; 0, 1), \\ m_i^1(t_i(1; t, x)) + \int_{t_i(1; t, x)}^t h_i(\tau, x_i(\tau; t, x), \mathbf{v}(\tau, x_i(\tau; t, x))) d\tau, & \text{if } x > x_i(t; 0, 1), \end{cases} \quad (2.11)$$

while, for every $i \in \{\ell + 1, \dots, n\}$ and $0 \leq t \leq \frac{1}{\lambda_{\max}}$,

$$v_i(t, x) = \begin{cases} m_i^0(t_i(0; t, x)) + \int_{t_i(0; t, x)}^t h_i(\tau, x_i(\tau; t, x), \mathbf{v}(\tau, x_i(\tau; t, x))) d\tau, & \text{if } x < x_i(t; 0, 0), \\ \bar{v}_i(x_i(0; t, x)) + \int_0^t h_i(\tau, x_i(\tau; t, x), \mathbf{v}(\tau, x_i(\tau; t, x))) d\tau, & \text{if } x > x_i(t; 0, 0), \end{cases} \quad (2.12)$$

where t_i denotes the inverse of the i -th characteristic curve, see Remark 2.6, m_i^0 and m_i^1 are i -th elements of $\mathbf{v}_+(t, a)$ and $\mathbf{v}_-(t, b)$, respectively, see (2.8), such that

$$\begin{pmatrix} m_1^0(t) \\ m_2^0(t) \\ \vdots \\ m_n^0(t) \end{pmatrix} = \mathbf{b}^+(t) + \mathbf{N}^+(t) \begin{pmatrix} \mathbf{v}_-(t, 0) \\ \mathbf{v}_+(t, 1) \end{pmatrix}, \quad (2.13)$$

$$\begin{pmatrix} m_1^1(t) \\ m_2^1(t) \\ \vdots \\ m_n^1(t) \end{pmatrix} = \mathbf{b}^-(t) + \mathbf{N}^-(t) \begin{pmatrix} \mathbf{v}_-(t, 0) \\ \mathbf{v}_+(t, 1) \end{pmatrix}.$$

For $i \in \{1, \dots, \ell\}$ and $0 < t \leq \frac{1}{\lambda_{\max}}$, one has

$$\begin{aligned} \mathbf{TV}(v_i(t, \cdot)) &= \mathbf{TV}(v_i(t, \cdot); [0, x_i(t; 0, 1)]) + \mathbf{TV}(v_i(t, \cdot); (x_i(t; 0, 1), 1]) \\ &\quad + |v_i(t, x_i(t; 0, 1)^+) - v_i(t, x_i(t; 0, 1)^-)|. \end{aligned} \quad (2.14)$$

while, for $i \in \{\ell + 1, \dots, n\}$ and $0 < t \leq \frac{1}{\lambda_{\max}}$,

$$\begin{aligned} \mathbf{TV}(v_i(t, \cdot)) &= \mathbf{TV}(v_i(t, \cdot); [0, x_i(t; 0, 0)]) + \mathbf{TV}(v_i(t, \cdot); (x_i(t; 0, 0), 1]) \\ &\quad + |v_i(t, x_i(t; 0, 0)^+) - v_i(t, x_i(t; 0, 0)^-)|. \end{aligned} \quad (2.15)$$

Consider the first term on the right hand side of (2.14) and points $0 \leq x_0 \leq \dots \leq x_N < x_i(t; 0, 1)$. By using (2.11), the following is obtained

$$\begin{aligned} \sum_{j=1}^N |v_i(t, x_j) - v_i(t, x_{j-1})| &\leq \mathbf{TV}(\bar{v}_i) + \sum_{j=1}^N \int_0^t |h_i(\tau, x_i(0; t, x_j), \mathbf{v}(\tau, x_i(0; t, x_j))) \\ &\quad - h_i(\tau, x_i(0; t, x_{j-1}), \mathbf{v}(\tau, x_i(0; t, x_{j-1})))| d\tau \\ &\leq \mathbf{TV}(\bar{v}_i) + Lt + L \int_0^t \mathbf{TV}(\mathbf{v}(\tau, \cdot)) d\tau, \end{aligned}$$

and hence

$$\mathbf{TV}(v_i(t, \cdot); [0, x_i(t; 0, 1)]) \leq \mathbf{TV}(\bar{v}_i) + Lt + L \int_0^t \mathbf{TV}(\mathbf{v}(\tau, \cdot)) d\tau. \quad (2.16)$$

Similarly, the first term on the right hand side of (2.15) can be estimated by

$$\mathbf{TV}(v_i(t, \cdot); (x_i(t; 0, 0), 1]) \leq \mathbf{TV}(\bar{v}_i) + Lt + L \int_0^t \mathbf{TV}(\mathbf{v}(\tau, \cdot)) d\tau. \quad (2.17)$$

Consider now the second term on the right hand side of (2.14) and points $x_i(t; 0, 1) < x_0 \leq \dots \leq x_N \leq 1$. By using (2.11), one obtains

$$\begin{aligned} \sum_{j=1}^N |v_i(t, x_j) - v_i(t, x_{j-1})| &\leq \sum_{j=1}^N |m_i^1(t_i(1; t, x_j)) - m_i^1(t_i(1; t, x_{j-1}))| \\ &\quad + \sum_{j=1}^N \left| \int_{t_i(1; t, x_j)}^t h_i(\tau, x_i(\tau; t, x_j), \mathbf{v}(\tau, x_i(\tau; t, x_j))) d\tau \right. \\ &\quad \left. - \int_{t_i(1; t, x_{j-1})}^t h_i(\tau, x_i(\tau; t, x_{j-1}), \mathbf{v}(\tau, x_i(\tau; t, x_{j-1}))) d\tau \right|. \end{aligned}$$

Defining $K := \sup_{t \in [0, \frac{1}{\lambda_{\max}}]} \left\{ \sup_{\xi \in \mathbb{R}^n \setminus \{0\}} \frac{|\mathbf{N}^-(t)(\xi)|}{|\xi|}, \sup_{\xi \in \mathbb{R}^n \setminus \{0\}} \frac{|\mathbf{N}^+(t)(\xi)|}{|\xi|} \right\}$ and using the relations (2.11), (2.12), and (2.13) yield

$$\begin{aligned} \sum_{j=1}^N |m_i^1(t_i(1; t, x_j)) - m_i^1(t_i(1; t, x_{j-1}))| &\leq \mathbf{TV}(\mathbf{b}^-) + Kn\mathbf{TV}(\bar{\mathbf{v}}) + 2KnLt \\ &\quad + KnL \int_0^t \mathbf{TV}(\mathbf{v}(\tau; \cdot)) d\tau, \end{aligned}$$

while using the assumptions on \mathbf{h} and triangular inequalities

$$\begin{aligned} &\sum_{j=1}^N \left| \int_{t_i(1; t, x_j)}^t h_i(\tau, x_i(\tau; t, x_j), \mathbf{v}(\tau, x_i(\tau; t, x_j))) d\tau \right. \\ &\quad \left. - \int_{t_i(1; t, x_{j-1})}^t h_i(\tau, x_i(\tau; t, x_{j-1}), \mathbf{v}(\tau, x_i(\tau; t, x_{j-1}))) d\tau \right| \\ &\leq 2Lt + L \int_0^t \mathbf{TV}(\mathbf{v}(\tau; \cdot)) d\tau. \end{aligned}$$

Therefore, the second term on the right hand side of (2.14) can be estimated by

$$\begin{aligned} \mathbf{TV}(v_i(t, \cdot); (x_i(t; 0, 1), 1]) &\leq \mathbf{TV}(\mathbf{b}^-) + Kn\mathbf{TV}(\bar{\mathbf{v}}) + 2(Kn+1)Lt \\ &\quad + (Kn+1)L \int_0^t \mathbf{TV}(\mathbf{v}(\tau; \cdot)) d\tau. \end{aligned} \tag{2.18}$$

Similarly, the second term on the right hand side of (2.15) can be estimated by

$$\begin{aligned} \mathbf{TV}(v_i(t, \cdot); [0, x_i(t; 0, 0)]) &\leq \mathbf{TV}(\mathbf{b}^+) + Kn\mathbf{TV}(\bar{\mathbf{v}}) + 2(Kn+1)Lt \\ &\quad + (Kn+1)L \int_0^t \mathbf{TV}(\mathbf{v}(\tau; \cdot)) d\tau. \end{aligned} \tag{2.19}$$

Consider now the third term on the right hand side of (2.14). By using the relations (2.11), (2.12), (2.13), and the assumptions on \mathbf{h} , one obtains

$$\begin{aligned}
& \left| v_i(t, x_i(t; 0, 1)^+) - v_i(t, x_i(t; 0, 1)^-) \right| \leq \left| \lim_{\tau \rightarrow 0^+} m_i^1(\tau) \right| + |\bar{v}_i(1^-)| \\
& \quad + \left| \int_0^t h_i(\tau, x_i(\tau; t, x_i(t; 0, 1)), \mathbf{v}(\tau, x_i(\tau; t, x_i(t; 0, 1))^+)) d\tau \right. \\
& \quad \left. - \int_0^t h_i(\tau, x_i(\tau; t, x_i(t; 0, 1)), \mathbf{v}(\tau, x_i(\tau; t, x_i(t; 0, 1))^-)) d\tau \right| \\
& \leq |\mathbf{b}^-(0^+)| + (2K + 1) \|\bar{\mathbf{v}}\|_{\mathbf{L}^\infty} + L \int_0^t \mathbf{TV}(v(\tau, \cdot)) d\tau.
\end{aligned} \tag{2.20}$$

Similarly, the third term on the right hand side of (2.15) can be estimated by

$$\begin{aligned}
& \left| v_i(t, x_i(t; 0, 0)^+) - v_i(t, x_i(t; 0, 0)^-) \right| \\
& \leq |\mathbf{b}^+(1^-)| + (2K + 1) \|\bar{\mathbf{v}}\|_{\mathbf{L}^\infty} + L \int_0^t \mathbf{TV}(v(\tau, \cdot)) d\tau.
\end{aligned} \tag{2.21}$$

Inserting (2.16), (2.18) and (2.20) into (2.14) yields

$$\begin{aligned}
\mathbf{TV}(v_i(t, \cdot)) & \leq \mathbf{TV}(\bar{v}_i) + \mathbf{TV}(\mathbf{b}^-) + Kn\mathbf{TV}(\bar{\mathbf{v}}) + (2Kn + 3)Lt \\
& \quad + (Kn + 3)L \int_0^t \mathbf{TV}(\mathbf{v}(\tau, \cdot)) d\tau \\
& \quad + |\mathbf{b}^-(0^+)| + (2K + 1) \|\bar{\mathbf{v}}\|_{\mathbf{L}^\infty}.
\end{aligned} \tag{2.22}$$

A similar estimate for (2.15) holds. Consequently,

$$\begin{aligned}
\mathbf{TV}(\mathbf{v}(t, \cdot)) & \leq (1 + Kn^2) \mathbf{TV}(\bar{\mathbf{v}}) + \ell \mathbf{TV}(\mathbf{b}^-) + (n - \ell) \mathbf{TV}(\mathbf{b}^+) \\
& \quad + (2Kn + 3)nLt + n(2K + 1) \|\bar{\mathbf{v}}\|_{\mathbf{L}^\infty} + \ell |\mathbf{b}^-(0^+)| \\
& \quad + (n - \ell) |\mathbf{b}^+(1^-)| + (2 + Kn)nL \int_0^t \mathbf{TV}(\mathbf{v}(\tau, \cdot)) d\tau.
\end{aligned}$$

An application of Gronwall Lemma implies that (2.10) holds. \square

The following is an existence and uniqueness theorem to systems of the form (2.1) and the basic idea is the same as [24, Theorem 3.2], where the result is proved in the case of no boundaries. The proof in the case of two *separate* boundaries, which is considered in the work [71], does not cover the situation in this thesis. This is due to the fact that the boundary data depend on the trace of the solution at the other boundary.

Theorem 2.9

Let $x \in [0, 1]$, $T > 0$, $\mathbf{u}(0, x) =: \bar{\mathbf{u}}$ and let hypotheses **(H-1)**-**(H-5)** hold. There exists a process

$$\mathcal{P} : [0, T] \times \mathcal{D} \rightarrow \mathbf{L}^1((0, 1); \mathbb{R}^n)$$

where

$$\mathcal{D} = \{(\bar{\mathbf{u}}, \mathbf{b}) \in \mathbf{L}^1((0, 1); \mathbb{R}^n) \times \mathbf{L}^1((0, T); \mathbb{R}^n) : \mathbf{TV}(\bar{\mathbf{u}}) + \mathbf{TV}(\mathbf{b}) < +\infty\}$$

satisfying:

(1): $\mathbf{u}(t, \cdot) = \mathcal{P}(t, \bar{\mathbf{u}}, \mathbf{b})$ is the solution to (2.1) in the sense of Definition 2.7.

(2): $\mathcal{P}(0, \bar{\mathbf{u}}, \mathbf{b}) = \bar{\mathbf{u}}$ for every $(\bar{\mathbf{u}}, \mathbf{b}) \in \mathcal{D}$.

(3): For every $0 \leq t_1 \leq t_2 \leq T$ and $(\bar{\mathbf{u}}, \mathbf{b}) \in \mathcal{D}$, it holds:

$$\mathcal{P}(t_2, \bar{\mathbf{u}}, \mathbf{b}) = \mathcal{P}(t_2 - t_1, \mathcal{P}(t_1, \bar{\mathbf{u}}, \mathbf{b}), \mathbf{b}(\cdot + t_1)).$$

(4): There exists $L > 0$ such that

$$\|\mathcal{P}(t, \bar{\mathbf{u}}, \mathbf{b}) - \mathcal{P}(t, \bar{\mathbf{u}}_0, \tilde{\mathbf{b}})\|_{\mathbf{L}^1(0,1)} \leq L \left[\|\bar{\mathbf{u}} - \bar{\mathbf{u}}_0\|_{\mathbf{L}^1(0,1)} + \|\mathbf{b} - \tilde{\mathbf{b}}\|_{\mathbf{L}^1(0,T)} \right] \quad (2.23)$$

for a.e. $t \in [0, T]$ and for all $\bar{\mathbf{u}}, \bar{\mathbf{u}}_0 \in \mathbf{L}^1(0, 1)$, and $\mathbf{b}, \tilde{\mathbf{b}} \in \mathbf{L}^1(0, T)$.

(5): There exists $L > 0$ such that, for a.e. $t \in [0, T]$,

$$\begin{aligned} \mathbf{TV}_{[0,1]}(\mathcal{P}(t, \bar{\mathbf{u}}, \mathbf{b})) &\leq Le^{Lt} \left[1 + \mathbf{TV}_{[0,1]}(\bar{\mathbf{u}}) + \mathbf{TV}_{[0,t]}(\mathbf{b}) \right] \\ &\quad + Le^{Lt} \left[\|\bar{\mathbf{u}}\|_{\mathbf{L}^\infty(0,1)} + \|\mathbf{b}\|_{\mathbf{L}^\infty(0,t)} \right]. \end{aligned} \quad (2.24)$$

(6): There exists $L > 0$ such that, for a.e. $t \in [0, T]$,

$$\begin{aligned} \|\mathcal{P}(\cdot, \bar{\mathbf{u}}, \mathbf{b})(0^+) - \mathcal{P}(\cdot, \bar{\mathbf{u}}_0, \tilde{\mathbf{b}})(0^+)\|_{\mathbf{L}^1(0,t)} &\leq L \|\bar{\mathbf{u}} - \bar{\mathbf{u}}_0\|_{\mathbf{L}^1(0,1)} \\ &\quad + L \|\mathbf{b} - \tilde{\mathbf{b}}\|_{\mathbf{L}^1(0,T)} \end{aligned} \quad (2.25)$$

(7): There exists $L > 0$ such that, for a.e. $t \in [0, T]$,

$$\begin{aligned} \|\mathcal{P}(\cdot, \bar{\mathbf{u}}, \mathbf{b})(1^-) - \mathcal{P}(\cdot, \bar{\mathbf{u}}_0, \tilde{\mathbf{b}})(1^-)\|_{\mathbf{L}^1(0,t)} &\leq L \|\bar{\mathbf{u}} - \bar{\mathbf{u}}_0\|_{\mathbf{L}^1(0,1)} \\ &\quad + L \|\mathbf{b} - \tilde{\mathbf{b}}\|_{\mathbf{L}^1(0,T)}. \end{aligned} \quad (2.26)$$

Proof. The local existence and uniqueness of solutions will be proven by employing the contraction mapping theorem. Global existence is then shown by using the a priori estimates and local existence and uniqueness of solutions. By Remark 2.4, the proof is focused on the diagonal version of system (2.1) and is divided in various steps as follows.

Local existence and uniqueness. Fix an initial condition $\bar{\mathbf{u}} \in \mathbf{L}^1((0, 1); \mathbb{R}^n)$ with finite total variation and a boundary condition $\mathbf{b} \in \mathbf{L}^1((0, T); \mathbb{R}^n)$ with finite total variation. Denote with $\bar{\mathbf{v}}(x) = \mathbf{L}(0, x) \bar{\mathbf{u}}(x)$ the corresponding initial condition for the diagonal system (2.2) and with $\mathbf{b}^-, \mathbf{b}^+$ the corresponding boundary conditions; see (2.8). Define

$$K = \sup_{t \in [0, T]} \left\{ \sup_{\xi \in \mathbb{R}^n \setminus \{0\}} \frac{|\mathbf{N}^-(t)(\xi)|}{|\xi|}, \sup_{\xi \in \mathbb{R}^n \setminus \{0\}} \frac{|\mathbf{N}^+(t)(\xi)|}{|\xi|} \right\} \quad (2.27)$$

$$M = n(2K + 1) \mathbf{TV}(\bar{\mathbf{v}}) + n \mathbf{TV}(\mathbf{b}) + 2n \|\bar{\mathbf{v}}\|_{\mathbf{L}^\infty} + 1 \quad (2.28)$$

$$\lambda_{\max} = \max \{ |\lambda_i(s, x)| : i \in \{1, \dots, n\}, s \in [0, T], x \in [0, 1] \} \quad (2.29)$$

$$\Lambda = \max \left\{ \|\lambda_i\|_{\mathbf{C}^1([0, T] \times [0, 1])} : i \in \{1, \dots, n\} \right\}. \quad (2.30)$$

Note that both λ_{\max} and Λ are finite due to **(H-1)** and **(H-3)**. Choose $\bar{t} \in (0, T]$ such that

$$\bar{t} < \min \left\{ \frac{1}{\lambda_{\max}}, \frac{1}{nL(4K + 2KM + 3M + 3)} \right\} \quad (2.31)$$

and

$$n(2 + nK)e^{\Lambda \bar{t}} L \bar{t} \leq \frac{1}{2}, \quad (2.32)$$

where L is a uniform bound and a Lipschitz constant for \mathbf{h} in $[0, T] \times [0, 1] \times \mathbb{R}^n$; see Remark 2.5.

Note that the choice of \bar{t} implies that every characteristic curve starting from a boundary does not arrive to the other boundary within time \bar{t} . Now, the aim is to construct a map whose fixed points are solutions to the diagonal IBVP and hence to (2.1). First, introduce the space

$$X = \left\{ \mathbf{v} \in \mathbf{C}^0([0, \bar{t}]; \mathbf{L}^1([0, 1]; \mathbb{R}^n)) : \begin{array}{l} \sup_{i \in \{1, \dots, n\}} \sup_{t \in [0, \bar{t}]} \mathbf{TV}(v_i(t)) \leq M \\ \mathbf{v}(0) = \bar{\mathbf{v}} \end{array} \right\}, \quad (2.33)$$

equipped with the norm

$$\|\mathbf{v}\|_X := \sum_{i=1}^n \|v_i\|_{\mathbf{C}^0([0, \bar{t}]; \mathbf{L}^1([0, 1]; \mathbb{R}))} = \sum_{i=1}^n \sup_{t \in [0, \bar{t}]} \int_0^1 |v_i(t, x)| dx, \quad (2.34)$$

so that X is a Banach space. Now define the operator

$$\begin{aligned} \mathbf{M}: X &\longrightarrow X \\ \mathbf{v} &\longmapsto \mathbf{M}(\mathbf{v}) = (M_1(\mathbf{v}), \dots, M_n(\mathbf{v})), \end{aligned}$$

according to the following four cases.

(1): For every $i \in \{1, \dots, \ell\}$, $0 < t \leq \bar{t}$, and $x \in [0, x_i(t; 0, 1)]$, define

$$M_i(\mathbf{v})(t, x) = \bar{v}_i(x_i(0; t, x)) + \int_0^t h_i(\tau, x_i(\tau; t, x), \mathbf{v}(\tau, x_i(\tau; t, x))) d\tau. \quad (2.35)$$

It is claimed that for every $0 \leq t \leq \bar{t}$,

$$\mathbf{TV}(M_i(\mathbf{v})(t, \cdot); [0, x_i(t; 0, 1)]) \leq \mathbf{TV}(\bar{v}_i) + L(1 + M)\bar{t}, \quad (2.36)$$

and that

$$\mathbf{TV}(M_i(\mathbf{v})(\cdot, 0); [0, \bar{t}]) \leq \mathbf{TV}(\bar{v}_i) + L(2 + M)\bar{t}. \quad (2.37)$$

For later use, for $0 \leq t \leq \bar{t}$ denote

$$\mathbf{M}_{b,0}(\mathbf{v})(t) = \begin{pmatrix} M_1(\mathbf{v})(t, 0^+) \\ \vdots \\ M_\ell(\mathbf{v})(t, 0^+) \end{pmatrix}, \quad (2.38)$$

which is well defined by (2.35) and has a finite total variation by (2.37).

To prove (2.36), fix $N \in \mathbb{N} \setminus \{0\}$, a time $0 \leq t \leq \bar{t}$, and points $0 \leq x_0 < \dots < x_N \leq x_i(t; 0, 1)$; using the notation $\tilde{x}_j(\tau) = x_i(\tau; t, x_j)$, one has

$$\begin{aligned} \sum_{j=1}^N |M_i(\mathbf{v})(t, x_j) - M_i(\mathbf{v})(t, x_{j-1})| &\leq \underbrace{\sum_{j=1}^N |\bar{v}_i(\tilde{x}_{j-1}(\tau)) - \bar{v}_i(\tilde{x}_{j-1}(\tau))|}_{I_1} \\ &+ \underbrace{\sum_{j=1}^N \left| \int_0^t h_i(\tau, \tilde{x}_j(\tau), \mathbf{v}(\tau, \tilde{x}_j(\tau))) - h_i(\tau, \tilde{x}_{j-1}(\tau), \mathbf{v}(\tau, \tilde{x}_{j-1}(\tau))) d\tau \right|}_{I_2}. \end{aligned}$$

Clearly, the term I_1 is estimated by $\mathbf{TV}(\bar{v}_i)$. For the term I_2 , one has

$$\begin{aligned} I_2 &\leq \sum_{j=1}^N \int_0^t |h_i(\tau, \tilde{x}_j(\tau), \mathbf{v}(\tau, \tilde{x}_j(\tau))) - h_i(\tau, \tilde{x}_{j-1}(\tau), \mathbf{v}(\tau, \tilde{x}_{j-1}(\tau)))| d\tau \\ &+ \sum_{j=1}^N \int_0^t |h_i(\tau, \tilde{x}_{j-1}(\tau), \mathbf{v}(\tau, \tilde{x}_j(\tau))) - h_i(\tau, \tilde{x}_{j-1}(\tau), \mathbf{v}(\tau, \tilde{x}_{j-1}(\tau)))| d\tau \\ &\leq L \sum_{j=1}^N \int_0^t (|\tilde{x}_j(\tau) - \tilde{x}_{j-1}(\tau)| + |\mathbf{v}(\tau, \tilde{x}_j(\tau)) - \mathbf{v}(\tau, \tilde{x}_{j-1}(\tau))|) d\tau \\ &\leq Lt + LMt, \end{aligned}$$

and thus, (2.36) is obtained.

To prove (2.37), fix $N \in \mathbb{N} \setminus \{0\}$ and times $0 \leq t_0 < \dots < t_N \leq \bar{t}$; by using the notation $\hat{x}_j(\tau) = x_i(\tau; t_j, 0)$, one has

$$\begin{aligned} \sum_{j=1}^N |M_i(\mathbf{v})(t_j, 0) - M_i(\mathbf{v})(t_{j-1}, 0)| &\leq \underbrace{\sum_{j=1}^N |\bar{v}_i(\hat{x}_j(0)) - \bar{v}_i(\hat{x}_{j-1}(0))|}_{I_3} \\ &+ \underbrace{\sum_{j=1}^N \left| \int_0^{t_{j-1}} (h_i(\tau, \hat{x}_j(\tau), \mathbf{v}(\tau, \hat{x}_j(\tau))) - h_i(\tau, \hat{x}_{j-1}(\tau), \mathbf{v}(\tau, \hat{x}_j(\tau)))) d\tau \right|}_{I_4} \\ &+ \underbrace{\sum_{j=1}^N \left| \int_0^{t_{j-1}} (h_i(\tau, \hat{x}_{j-1}(\tau), \mathbf{v}(\tau, \hat{x}_j(\tau))) - h_i(\tau, \hat{x}_{j-1}(\tau), \mathbf{v}(\tau, \hat{x}_{j-1}(\tau)))) d\tau \right|}_{I_5} \\ &+ \underbrace{\sum_{j=1}^N \left| \int_{t_{j-1}}^{t_j} h_i(\tau, \hat{x}_j(\tau), \mathbf{v}(\tau, \hat{x}_j(\tau))) d\tau \right|}_{I_6}. \end{aligned}$$

Clearly, the term I_3 is estimated by $\mathbf{TV}(\bar{v}_i)$. For the remaining terms I_4 , I_5 , and I_6 , one has

$$\begin{aligned} I_4 &\leq L \sum_{j=1}^N \int_0^{t_{j-1}} |\hat{x}_j(\tau) - \hat{x}_{j-1}(\tau)| d\tau \leq L\bar{t} \\ I_5 &\leq L \sum_{j=1}^N \int_0^{t_{j-1}} |\mathbf{v}(\tau, x_i(\tau; t_j, 0)) - \mathbf{v}(\tau, x_i(\tau; t_{j-1}, 0))| d\tau \leq LM\bar{t} \\ I_6 &\leq L\bar{t}, \end{aligned}$$

therefore, (2.37) is proved.

(2): For every $i \in \{\ell + 1, \dots, n\}$, $0 < t \leq \bar{t}$, and $x \in [x_i(t; 0, 0), 1]$, the following is defined

$$M_i(\mathbf{v})(t, x) = \bar{v}_i(x_i(0; t, x)) + \int_0^t h_i(\tau, x_i(\tau; t, x), \mathbf{v}(\tau, x_i(\tau; t, x))) d\tau. \quad (2.39)$$

Similarly, one obtains, for every $0 \leq t \leq \bar{t}$,

$$\mathbf{TV}(M_i(\mathbf{v})(t, \cdot); (x_i(t; 0, 0), 1]) \leq \mathbf{TV}(\bar{v}_i) + L(1 + M)\bar{t} \quad (2.40)$$

and that

$$\mathbf{TV}(M_i(\mathbf{v})(\cdot, 1); [0, \bar{t}]) \leq \mathbf{TV}(\bar{v}_i) + L(2 + M)\bar{t}. \quad (2.41)$$

For $0 \leq t \leq \bar{t}$, denote

$$\mathbf{M}_{b,1}(\mathbf{v})(t) = \begin{pmatrix} M_{\ell+1}(\mathbf{v})(t, 1^-) \\ \vdots \\ M_n(\mathbf{v})(t, 1^-) \end{pmatrix}, \quad (2.42)$$

which is well defined by (2.39) and has a finite total variation by (2.41).

(3): For every $i \in \{1, \dots, \ell\}$, $0 < t \leq \bar{t}$, and $x \in (x_i(t; 0, 1), 1]$, define

$$M_i(\mathbf{v})(t, x) = m_i^1(t_i(1; t, x)) + \int_{t_i(1; t, x)}^t h_i(\tau, x_i(\tau; t, x), \mathbf{v}(\tau, x_i(\tau; t, x))) d\tau, \quad (2.43)$$

where t_i denotes the inverse of the i -th characteristic curve, and m_i^1 is the i -th element of the following vector

$$\begin{pmatrix} m_1^1(t) \\ m_2^1(t) \\ \vdots \\ m_n^1(t) \end{pmatrix} = \mathbf{b}^-(t) + \mathbf{N}^-(t) \begin{pmatrix} \mathbf{M}_{b,0}(\mathbf{v})(t) \\ \mathbf{M}_{b,1}(\mathbf{v})(t) \end{pmatrix}, \quad (2.44)$$

see (2.8), (2.38), and (2.42).

It is claimed that for every $0 \leq t \leq \bar{t}$

$$\begin{aligned} \mathbf{TV}(M_i(\mathbf{v})(t, \cdot); (x_i(t; 0, 1), 1]) &\leq \mathbf{TV}(\mathbf{b}^-) + 2K\mathbf{TV}(\bar{v}_i) \\ &\quad + L(4K + 2KM + M + 2)\bar{t}. \end{aligned} \quad (2.45)$$

To prove (2.45), fix $N \in \mathbb{N} \setminus \{0\}$, a time $0 \leq t \leq \bar{t}$, and points $x_i(t; 0, 1) \leq x_0 < \dots < x_N \leq 1$; by using the notations $\tilde{x}_j(\tau) = x_i(\tau; t, x_j)$ and $\tilde{t}_j = t_i(1; t, x_j)$, one has

$$\begin{aligned} & \sum_{j=1}^N |M_i(\mathbf{v})(t, x_j) - M_i(\mathbf{v})(t, x_{j-1})| \leq \underbrace{\sum_{j=1}^N |m_i^1(\tilde{t}_j) - m_i^1(\tilde{t}_{j-1})|}_{I_7} \\ & + \underbrace{\sum_{j=1}^N \left| \int_{\tilde{t}_j}^t (h_i(\tau, \tilde{x}_j(\tau), \mathbf{v}(\tau, \tilde{x}_j(\tau))) - h_i(\tau, \tilde{x}_j(\tau), \mathbf{v}(\tau, \tilde{x}_{j-1}(\tau)))) d\tau \right|}_{I_8} \\ & + \underbrace{\sum_{j=1}^N \left| \int_{\tilde{t}_j}^t (h_i(\tau, \tilde{x}_j(\tau), \mathbf{v}(\tau, \tilde{x}_{j-1}(\tau))) - h_i(\tau, \tilde{x}_{j-1}(\tau), \mathbf{v}(\tau, \tilde{x}_{j-1}(\tau)))) d\tau \right|}_{I_9} \\ & + \underbrace{\sum_{j=1}^N \left| \int_{\tilde{t}_j}^{\tilde{t}_{j-1}} h_i(\tau, \tilde{x}_{j-1}(\tau), \mathbf{v}(\tau, \tilde{x}_{j-1}(\tau))) d\tau \right|}_{I_{10}}. \end{aligned}$$

By using (2.27), (2.37), (2.41), and (2.44), one obtains

$$\begin{aligned} I_7 & \leq \mathbf{TV}(\mathbf{b}^-) + K \mathbf{TV}(\mathbf{M}_{b,0}(\mathbf{v})(\cdot)) + K \mathbf{TV}(\mathbf{M}_{b,1}(\mathbf{v})(\cdot)) \\ & \leq \mathbf{TV}(\mathbf{b}^-) + 2K [\mathbf{TV}(\tilde{v}_i) + L(2+M)\bar{t}]. \end{aligned}$$

For the remaining terms I_8 , I_9 , and I_{10} , one has

$$\begin{aligned} I_8 & \leq L \sum_{j=1}^N \int_{\tilde{t}_j}^t |\mathbf{v}(\tau, \tilde{x}_j(\tau)) - \mathbf{v}(\tau, \tilde{x}_{j-1}(\tau))| d\tau \leq LM\bar{t}, \\ I_9 & \leq L \sum_{j=1}^N \int_{\tilde{t}_j}^t |\tilde{x}_j(\tau) - \tilde{x}_{j-1}(\tau)| d\tau \leq L\bar{t}, \\ I_{10} & \leq \sum_{j=1}^N \int_{\tilde{t}_j}^{\tilde{t}_{j-1}} |h_i(\tau, \tilde{x}_{j-1}(\tau), \mathbf{v}(\tau, \tilde{x}_{j-1}(\tau)))| d\tau \leq L\bar{t}, \end{aligned}$$

which prove (2.45).

(4): For every $i \in \{\ell + 1, \dots, n\}$, $0 < t \leq \bar{t}$, and $x \in [0, x_i(t; 0, 0))$, define

$$M_i(\mathbf{v})(t, x) = m_i^0(t_i(0; t, x)) + \int_{t_i(0; t, x)}^t h_i(\tau, x_i(\tau; t, x), \mathbf{v}(\tau, x_i(\tau; t, x))) d\tau, \quad (2.46)$$

where t_i denotes the inverse of the i -th characteristic curve, and m_i^0 is the i -th element of the following

$$\begin{pmatrix} m_1^0(t) \\ m_2^0(t) \\ \vdots \\ m_n^0(t) \end{pmatrix} = \mathbf{b}^+(t) + \mathbf{N}^+(t) \begin{pmatrix} \mathbf{M}_{b,0}(\mathbf{v})(t) \\ \mathbf{M}_{b,1}(\mathbf{v})(t) \end{pmatrix}, \quad (2.47)$$

see (2.8).

Similarly, it is deduced that, for every $0 \leq t \leq \bar{t}$,

$$\begin{aligned} \mathbf{TV}(M_i(\mathbf{v})(t, \cdot); [0, x_i(t; 0, 0)]) &\leq \mathbf{TV}(\mathbf{b}^+) + 2K\mathbf{TV}(\bar{v}_i) \\ &\quad + L(4K + 2KM + M + 2)\bar{t}. \end{aligned} \quad (2.48)$$

By using (2.35) and (2.43), note also that it holds, for every $i \in \{1, \dots, \ell\}$ and $0 < t \leq \bar{t}$,

$$\left| \lim_{x \rightarrow x_i(t; 0, 1)^-} M_i(\mathbf{v})(t, x) - \lim_{x \rightarrow x_i(t; 0, 1)^+} M_i(\mathbf{v})(t, x) \right| \leq 2 \|\bar{v}_i\|_{\mathbf{L}^\infty} + LM\bar{t}. \quad (2.49)$$

The same inequality holds in the case $i \in \{\ell + 1, \dots, n\}$.

By using (2.36), (2.40), (2.45), (2.48) and (2.49), one observes, for every $0 \leq t \leq \bar{t}$ and $i \in \{1, \dots, n\}$,

$$\begin{aligned} \mathbf{TV}(M_i(\mathbf{v})(t, \cdot)) &\leq \mathbf{TV}(\mathbf{b}) + (2K + 1)\mathbf{TV}(\bar{v}_i) + 2\|\bar{v}_i\|_{\mathbf{L}^\infty} \\ &\quad + L(4K + 2KM + 3M + 3)\bar{t} \end{aligned} \quad (2.50)$$

and hence, by the choice of \bar{t} (2.31),

$$\mathbf{TV}(\mathbf{M}(\mathbf{v})(t, \cdot)) \leq M, \quad (2.51)$$

which implies that the operator $\mathbf{M}(\mathbf{v})$ is well defined. Note that the proof that $t \mapsto \mathbf{M}(\mathbf{v})(t)$ is continuous from $[0, \bar{t}]$ to $\mathbf{L}^1((0, 1); \mathbb{R}^n)$ is straightforward and hence omitted.

Fix $\mathbf{v}, \mathbf{v}^* \in X$. For every $t \in [0, \bar{t}]$ and $i \in \{1, \dots, \ell\}$, one has

$$\begin{aligned} \|M_i(\mathbf{v})(t, \cdot) - M_i(\mathbf{v}^*)(t, \cdot)\|_{\mathbf{L}^1} &= \int_0^1 |M_i(\mathbf{v})(t, x) - M_i(\mathbf{v}^*)(t, x)| dx \\ &\leq \int_0^{x_i(t; 0, 1)} |M_i(\mathbf{v})(t, x) - M_i(\mathbf{v}^*)(t, x)| dx + \int_{x_i(t; 0, 1)}^1 |M_i(\mathbf{v})(t, x) - M_i(\mathbf{v}^*)(t, x)| dx. \end{aligned}$$

By using (2.35) and the change of variable $\xi = x_i(\tau; t, x)$, one obtains

$$\begin{aligned} \int_0^{x_i(t; 0, 1)} |M_i(\mathbf{v})(t, x) - M_i(\mathbf{v}^*)(t, x)| dx &\leq \int_0^{x_i(t; 0, 1)} \int_0^t |h_i(\tau, x_i(\tau; t, x), \mathbf{v}(\tau, x_i(\tau; t, x))) \\ &\quad - h_i(\tau, x_i(\tau; t, x), \mathbf{v}^*(\tau, x_i(\tau; t, x)))| d\tau dx \\ &\leq L \int_0^{x_i(t; 0, 1)} \int_0^t |\mathbf{v}(\tau, x_i(\tau; t, x)) - \mathbf{v}^*(\tau, x_i(\tau; t, x))| d\tau dx \end{aligned}$$

$$\leq e^{\Lambda \bar{t}} L \int_0^t \int_0^1 |\mathbf{v}(\tau, \xi) - \mathbf{v}^*(\tau, \xi)| d\xi d\tau \leq e^{\Lambda \bar{t}} L \bar{t} \|\mathbf{v} - \mathbf{v}^*\|_X.$$

By using (2.43), the following is obtained

$$\begin{aligned} \int_{x_i(t;0,1)}^1 |M_i(\mathbf{v})(t,x) - M_i(\mathbf{v}^*)(t,x)| dx &\leq K \underbrace{\int_{x_i(t;0,1)}^1 |\mathbf{M}_{b,0}(\mathbf{v})(t_i(1;t,x)) - \mathbf{M}_{b,0}(\mathbf{v}^*)(t_i(1;t,x))| dx}_{I_{11}} \\ &+ K \underbrace{\int_{x_i(t;0,1)}^1 |\mathbf{M}_{b,1}(\mathbf{v})(t_i(1;t,x)) - \mathbf{M}_{b,1}(\mathbf{v}^*)(t_i(1;t,x))| dx}_{I_{12}} + I_{13}, \end{aligned}$$

where

$$\begin{aligned} I_{13} = \int_{x_i(t;0,1)}^1 \int_{t_i(1;t,x)}^t & |h_i(\tau, x_i(\tau; t, x), \mathbf{v}(\tau, x_i(\tau; t, x))) \\ & - h_i(\tau, x_i(\tau; t, x), \mathbf{v}^*(\tau, x_i(\tau; t, x)))| d\tau dx. \end{aligned}$$

For the term I_{11} , using (2.35) and (2.38), it holds that

$$\begin{aligned} I_{11} &\leq \sum_{j=1}^{\ell} \int_{x_i(t;0,1)}^1 |M_j(\mathbf{v})(t_i(1;t,x), 0) - M_j(\mathbf{v}^*)(t_i(1;t,x), 0)| dx \\ &\leq \sum_{j=1}^{\ell} \int_{x_i(t;0,1)}^1 \left| \int_0^{t_i(1;t,x)} h_j(\tau, x_j(\tau; t_i(1;t,x), 0), \mathbf{v}(\tau, x_j(\tau; t_i(1;t,x), 0))) \right. \\ &\quad \left. - h_j(\tau, x_j(\tau; t_i(1;t,x), 0), \mathbf{v}^*(\tau, x_j(\tau; t_i(1;t,x), 0))) \right| d\tau dx \\ &\leq L \sum_{j=1}^{\ell} \int_{x_i(t;0,1)}^1 \int_0^{t_i(1;t,x)} |\mathbf{v}^*(\tau, x_j(\tau; t_i(1;t,x), 0)) \\ &\quad - \mathbf{v}^*(\tau, x_j(\tau; t_i(1;t,x), 0))| d\tau dx \\ &\leq L \ell e^{\Lambda \bar{t}} \bar{t} \|\mathbf{v} - \mathbf{v}^*\|_X. \end{aligned}$$

Similarly, the following can be obtained

$$I_{12} \leq L (n - \ell) e^{\Lambda \bar{t}} \bar{t} \|\mathbf{v} - \mathbf{v}^*\|_X.$$

For the remaining term I_{13} , by using the change of variable $\xi = x_i(\tau; t, x)$, the following is obtained

$$I_{13} \leq L \int_{x_i(t;0,1)}^1 \int_{t_i(1;t,x)}^t |\mathbf{v}(\tau, x_i(\tau; t, x)) - \mathbf{v}^*(\tau, x_i(\tau; t, x))| d\tau dx$$

$$\leq e^{\Lambda \bar{L}} \int_0^t \int_0^1 |\mathbf{v}(\tau, \xi) - \mathbf{v}^*(\tau, \xi)| d\tau d\xi \leq e^{\Lambda \bar{L}} \bar{L} \|\mathbf{v} - \mathbf{v}^*\|_X.$$

Therefore, for every $t \in [0, \bar{t}]$ and $i \in \{1, \dots, \ell\}$, it holds

$$\|M_i(\mathbf{v})(t, \cdot) - M_i(\mathbf{v}^*)(t, \cdot)\|_{\mathbf{L}^1} \leq (2 + Kn) e^{\Lambda \bar{L}} \bar{L} \|\mathbf{v} - \mathbf{v}^*\|_X. \quad (2.52)$$

Analogous calculations allow to prove that, for every $i \in \{\ell + 1, \dots, n\}$ and $t \in [0, \bar{t}]$,

$$\|M_i(\mathbf{v})(t, \cdot) - M_i(\mathbf{v}^*)(t, \cdot)\|_{\mathbf{L}^1} \leq (2 + Kn) e^{\Lambda \bar{L}} \bar{L} \|\mathbf{v} - \mathbf{v}^*\|_X. \quad (2.53)$$

Hence, using (2.32), (2.34), (2.52), and (2.53), for every $t \in [0, \bar{t}]$, it holds

$$\begin{aligned} \|\mathbf{M}(\mathbf{v}) - \mathbf{M}(\mathbf{v}^*)\|_X &\leq \sum_{i=1}^n \sup_{t \in [0, \bar{t}]} \|M_i(\mathbf{v})(t, \cdot) - M_i(\mathbf{v}^*)(t, \cdot)\|_{\mathbf{L}^1([0, 1]; \mathbb{R})} \\ &\leq n (2 + Kn) e^{\Lambda \bar{L}} \bar{L} \|\mathbf{v} - \mathbf{v}^*\|_X \leq \frac{1}{2} \|\mathbf{v} - \mathbf{v}^*\|_X, \end{aligned}$$

which proves that \mathbf{M} is a contraction; hence, a unique solution exists in the time interval $[0, \bar{t}]$.

Global existence in $[0, T]$. Assume by contradiction that the solution \mathbf{v} does not exist on the whole time interval $[0, T]$ and define

$$\widehat{T} = \sup \{t \in [0, T] : \mathbf{v} \text{ is defined in } [0, t]\}. \quad (2.54)$$

By contradiction $\widehat{T} < T$. Moreover

$$\lim_{t \rightarrow \widehat{T}^-} \mathbf{TV}(\mathbf{v}(t, \cdot)) = +\infty, \quad (2.55)$$

otherwise the construction in the first part of the proof can be applied, violating the maximality of \widehat{T} .

If $\widehat{T} \leq \lambda_{\max}$, then Lemma 2.8 implies that $\mathbf{TV}(\mathbf{v}(t, \cdot))$ is bounded in the time interval $[0, \widehat{T}]$, contradicting (2.55).

If $\widehat{T} \leq \lambda_{\max}$, then one can apply the previous considerations on time intervals of length λ_{\max} , obtaining a contradiction with the definition of \widehat{T} .

Stability estimates in $[0, T]$. Here, the proofs are briefly sketched for the \mathbf{L}^1 -estimates (2.23), (2.25), and (2.26). Only the case $t \leq \bar{t}$ is considered, the final estimates follow by an iterative procedure. One starts with the four cases in the construction of \mathbf{M} . Let \mathbf{v} and \mathbf{v}^* be the solutions to the diagonal system (2.2) with the initial and boundary conditions $\bar{\mathbf{v}}$, \mathbf{b} and respectively $\bar{\mathbf{v}}^*$ and \mathbf{b}^* .

(1): For $i \in \{1, \dots, \ell\}$, $t \leq \bar{t}$, and $x \in [0, \bar{x}_i]$, where $\bar{x}_i = x_i(t; 0, 1)$, one obtains

$$\begin{aligned} &\int_0^{\bar{x}_i} |M_i(\mathbf{v})(t, x) - M_i(\mathbf{v}^*)(t, x)| dx \\ &\leq \|\bar{\mathbf{v}} - \bar{\mathbf{v}}^*\|_{\mathbf{L}^1(0, 1)} + \int_0^{\bar{x}_i} \int_0^t |h_i(\tau, x_i(\tau; t, x), \mathbf{v}(\tau, x_i(\tau; t, x))) \\ &\quad - h_i(\tau, x_i(\tau; t, x), \mathbf{v}^*(\tau, x_i(\tau; t, x)))| d\tau dx \end{aligned}$$

$$\leq \|\bar{\mathbf{v}} - \bar{\mathbf{v}}^*\|_{\mathbf{L}^1(0,1)} + L \int_0^t \|\mathbf{v}(\tau, \cdot) - \mathbf{v}^*(\tau, \cdot)\|_{\mathbf{L}^1(0,1)} d\tau.$$

Similarly, for $\tilde{t} \in (0, t)$, it can be deduced the estimate for the trace

$$\begin{aligned} \int_{\tilde{t}}^t |M_i(\mathbf{v})(\tau, 0^+) - M_i(\mathbf{v}^*)(\tau, 0^+)| d\tau &\leq \int_{\tilde{t}}^t |\bar{v}_i(x_i(\tilde{t}; \tau, 0)) - \bar{v}_i^*(x_i(\tilde{t}; \tau, 0))| d\tau \\ &\quad + \int_{\tilde{t}}^t \int_0^t |h_i(\tau, x_i(\theta; \tau, 0), \mathbf{v}(\tau, x_i(\theta; \tau, 0))) \\ &\quad - h_i(\tau, x_i(\theta; \tau, 0), \mathbf{v}^*(\tau, x_i(\theta; \tau, 0)))| d\theta d\tau \\ &\leq \|\bar{\mathbf{v}} - \bar{\mathbf{v}}^*\|_{\mathbf{L}^1(0,1)} + L \int_0^t \|\mathbf{v}(\tau, \cdot) - \mathbf{v}^*(\tau, \cdot)\|_{\mathbf{L}^1(0,1)} d\tau. \end{aligned} \quad (2.56)$$

(2): In the same way, for $i \in \{\ell + 1, \dots, n\}$, $t \leq \bar{t}$, and $x \in [\bar{x}_i, 1]$, where $\bar{x}_i = x_i(t; 0, 0)$,

$$\int_{\bar{x}_i}^1 |M_i(\mathbf{v})(t, x) - M_i(\mathbf{v}^*)(t, x)| dx \leq \|\bar{\mathbf{v}} - \bar{\mathbf{v}}^*\|_{\mathbf{L}^1(0,1)} + L \int_0^t \|\mathbf{v}(\tau, \cdot) - \mathbf{v}^*(\tau, \cdot)\|_{\mathbf{L}^1(0,1)} d\tau,$$

and for $\tilde{t} \in (0, t)$

$$\begin{aligned} \int_{\tilde{t}}^t |M_i(\mathbf{v})(\tau, 1^-) - M_i(\mathbf{v}^*)(\tau, 1^-)| d\tau \\ \leq \|\bar{\mathbf{v}} - \bar{\mathbf{v}}^*\|_{\mathbf{L}^1(0,1)} + L \int_0^t \|\mathbf{v}(\tau, \cdot) - \mathbf{v}^*(\tau, \cdot)\|_{\mathbf{L}^1(0,1)} d\tau. \end{aligned} \quad (2.57)$$

(3): For $i \in \{1, \dots, \ell\}$, $t \leq \bar{t}$, and $x \in [\bar{x}_i, 1]$, where $\bar{x}_i = x_i(t; 0, 1)$, by using (2.56) and (2.57), the following is obtained

$$\begin{aligned} \int_{\bar{x}_i}^1 |M_i(\mathbf{v})(t, x) - M_i(\mathbf{v}^*)(t, x)| dx &\leq \int_{\bar{x}_i}^1 |m_i(t_i(1; t, x)) - m_i^*(t_i(1; t, x))| dx \\ &\quad + \int_{\bar{x}_i}^1 \int_{t_i(1; t, x)}^t |h_i(\tau, x_i(\tau; t, x), \mathbf{v}(\tau, x_i(\tau; t, x))) \\ &\quad - h_i(\tau, x_i(\tau; t, x), \mathbf{v}^*(\tau, x_i(\tau; t, x)))| d\tau dx \\ &\leq \|\mathbf{b} - \mathbf{b}^*\|_{\mathbf{L}^1(0,T)} \\ &\quad + K \sum_{j=1}^{\ell} \int_{t_j(1; t, \bar{x}_i)}^t |M_j(\mathbf{v})(\tau, 0^+) - M_j(\mathbf{v}^*)(\tau, 0^+)| d\tau \\ &\quad + K \sum_{j=\ell+1}^n \int_{t_j(1; t, \bar{x}_i)}^t |M_j(\mathbf{v})(\tau, 1^-) - M_j(\mathbf{v}^*)(\tau, 1^-)| d\tau \end{aligned}$$

$$\begin{aligned}
& + L \int_0^t \|\mathbf{v}(\tau, \cdot) - \mathbf{v}(\tau, \cdot)\|_{\mathbf{L}^1(0,1)} d\tau \\
& \leq \|\mathbf{b} - \mathbf{b}^*\|_{\mathbf{L}^1(0,T)} + nK \|\bar{\mathbf{v}} - \bar{\mathbf{v}}^*\|_{\mathbf{L}^1(0,1)} \\
& \quad + nKL \int_0^t \|\mathbf{v}(\tau, \cdot) - \mathbf{v}(\tau, \cdot)\|_{\mathbf{L}^1(0,1)} d\tau.
\end{aligned}$$

(4): Analogous calculations imply that for $i \in \{\ell + 1, \dots, n\}$, $t \leq \bar{t}$, and $x \in [0, \bar{x}_i]$, with $\bar{x}_i = x_i(t; 0, 0)$

$$\begin{aligned}
\int_0^{\bar{x}_i} |M_i(\mathbf{v})(t, x) - M_i(\mathbf{v}^*)(t, x)| dx & \leq \|\mathbf{b} - \mathbf{b}^*\|_{\mathbf{L}^1(0,T)} + nK \|\bar{\mathbf{v}} - \bar{\mathbf{v}}^*\|_{\mathbf{L}^1(0,1)} \\
& \quad + nKL \int_0^t \|\mathbf{v}(\tau, \cdot) - \mathbf{v}(\tau, \cdot)\|_{\mathbf{L}^1(0,1)} d\tau.
\end{aligned}$$

By combining the estimates that are obtained in the previous four cases, one has

$$\begin{aligned}
\|\mathbf{v}(t, \cdot) - \mathbf{v}^*(t, \cdot)\|_{\mathbf{L}^1} & \leq 2\|\mathbf{b} - \mathbf{b}^*\|_{\mathbf{L}^1(0,T)} + (2nK + 2) \|\bar{\mathbf{v}} - \bar{\mathbf{v}}^*\|_{\mathbf{L}^1(0,1)} \\
& \quad + (2nKL + 2) \int_0^t \|\mathbf{v}(\tau, \cdot) - \mathbf{v}(\tau, \cdot)\|_{\mathbf{L}^1(0,1)} d\tau,
\end{aligned}$$

for every $t \leq \bar{t}$. By using Gronwall Lemma, one obtains (2.23). Moreover, estimates (2.25) and (2.26) follow from (2.56), (2.57), and (2.23).

Total variation estimate. The total variation estimate (2.24) follows from Lemma 2.8. \square

2.2 Linear conservation laws

In this section, the following conservation law is studied

$$\partial_t \mathbf{u}(t, x) + \mathbf{A} \partial_x \mathbf{u}(t, x) = \mathbf{0}, \quad (2.58)$$

where $x \in \mathbb{R}$, $t \geq t_0 \in \mathbb{R}$, $\mathbf{A} \in \mathbb{R}^{n \times n}$ with Assumptions (H-3)-(H-4) and initial condition (2.1c).

By applying the coordinate transformation $\mathbf{v} = \mathbf{R}^{-1} \mathbf{u}$, it can be seen that the system (2.58) is equivalent to a decoupled system of scalar PDEs, $i = 1, 2, \dots, n$,

$$\partial_t v_i(t, x) + \lambda_i \partial_x v_i(t, x) = 0, \quad (2.59)$$

with the initial condition

$$v_i(t_0, x) =: v_i^{t_0}(x), \quad (2.60)$$

where $v_i^{t_0} = \mathbf{l}_i \mathbf{u}^{t_0}$, where \mathbf{l}_i is the i -th left eigenvector. In order to give a solution formula in a compact form, two shift operators are defined as follows.

Definition 2.10: 2D shift operator for functions

Denote with $\mathcal{F}(A \rightarrow B)$ the set of all functions from some set A to some set B . Let $T \subseteq \mathbb{R}$

and $X \subseteq \mathbb{R}$, then the *time shift operator* $\mathcal{S}_{\text{time}}^{\lambda, x_0}$ with speed $\lambda \in \mathbb{R}$ and initial position $x_0 \in X$ is

$$\mathcal{S}_{\text{time}}^{\lambda, x_0} : \mathcal{F}(T \rightarrow \mathbb{R}) \mapsto \mathcal{F}(T \times X \rightarrow \mathbb{R}), \quad f \mapsto [(t, x) \mapsto f(t - \frac{x - x_0}{\lambda})],$$

with the convention that $f(s) = 0$ if $s \notin T$. The *space shift operator* $\mathcal{S}_{\text{space}}^{\lambda, t_0}$ with speed $\lambda \in \mathbb{R}$ and initial time $t_0 \in T$ is

$$\mathcal{S}_{\text{space}}^{\lambda, t_0} : \mathcal{F}(X \rightarrow \mathbb{R}) \mapsto \mathcal{F}(T \times X \rightarrow \mathbb{R}), \quad g \mapsto [(t, x) \mapsto g(x - \lambda(t - t_0))],$$

with the convention that $f(y) = 0$ if $y \notin X$.

By the *method of characteristics*, [44], it is easily seen that the unique solution of each scalar PDE (2.59) with differentiable initial data $v_i^{t_0}$ is given by $v_i(t, x) = v_i^0(x - \lambda_i(t - t_0))$ or, equivalently, in terms of the space shift operator by

$$v_i = \mathcal{S}_{\text{space}}^{\lambda_i, t_0} v_i^{t_0}.$$

Corollary 2.11

2D time shift operator for functions $\mathcal{S}_{\text{time}}^{\lambda, x_0}$ commutes with (partial) derivative operator ∂_t and 2D space shift operator for functions $\mathcal{S}_{\text{space}}^{\lambda, t_0}$ commutes with (partial) derivative operator ∂_x , where $\lambda, x_0, t_0 \in \mathbb{R}$

$$\mathcal{S}_{\text{time}}^{\lambda, x_0} \partial_t^{(n)} f(t) = \partial_t^{(n)} \mathcal{S}_{\text{time}}^{\lambda, x_0} f(t), \quad \text{and} \quad \mathcal{S}_{\text{space}}^{\lambda, t_0} \partial_x^{(n)} f(x) = \partial_x^{(n)} \mathcal{S}_{\text{space}}^{\lambda, t_0} f(x),$$

for $f : \mathbb{R} \rightarrow \mathbb{R}$ and $n \in \mathbb{N}$.

Proof. Let $f : \mathbb{R} \rightarrow \mathbb{R}$ and $\mathcal{S}_{\text{time}}^{\lambda, x_0}$ be the time shift operator. It holds, for $n = 1$,

$$\begin{aligned} \partial_t \mathcal{S}_{\text{time}}^{\lambda, x_0} f(t) &= \partial_t f\left(t - \frac{x - x_0}{\lambda}\right) \\ &= f'\left(t - \frac{x - x_0}{\lambda}\right) \\ &= \mathcal{S}_{\text{time}}^{\lambda, x_0} f'(t) \\ &= \mathcal{S}_{\text{time}}^{\lambda, x_0} \partial_t f(t). \end{aligned}$$

Assume the claim holds for $n \geq 1$. Then, for $n + 1$, one obtains

$$\begin{aligned} \mathcal{S}_{\text{time}}^{\lambda, x_0} \partial_t^{(n+1)} f(t) &= \mathcal{S}_{\text{time}}^{\lambda, x_0} \partial_t^{(n)} \partial_t f(t) \\ &= \partial_t^{(n)} \mathcal{S}_{\text{time}}^{\lambda, x_0} \partial_t f(t) \\ &= \partial_t^{(n+1)} \mathcal{S}_{\text{time}}^{\lambda, x_0} f(t), \end{aligned}$$

hence, by induction, the claim follows. Analogous steps can be conducted to prove the commutativity of $\mathcal{S}_{\text{space}}^{\lambda, t_0}$ and ∂_x . \square

In the original coordinates, the solution \mathbf{u} to (2.58) is given as in the following lemma.

Lemma 2.12

Consider the system (2.58) satisfying Assumption **(H-3)** with differentiable initial data \mathbf{u}^{t_0} . Then the unique solution is given by

$$\mathbf{u} = \sum_{i=1}^n \Pi_i \mathcal{S}_{\text{space}}^{\lambda_i, t_0} \mathbf{u}^{t_0} =: \mathcal{S}_{\text{space}}^{\Lambda, \mathbf{R}, t_0} \mathbf{u}^{t_0}, \quad (2.61)$$

where $\Pi_i := \mathbf{R} \operatorname{diag}(\mathbf{e}_i) \mathbf{R}^{-1}$, $\mathbf{e}_i \in \mathbb{R}^n$ is the i -th directional unit vector, and the space shift operator $\mathcal{S}_{\text{space}}^{\lambda, t_0}$ is canonically extended to $\mathcal{S}_{\text{space}}^{\lambda, t_0} : \mathcal{F}(X \rightarrow \mathbb{R}^n) \mapsto \mathcal{F}(T \times X \rightarrow \mathbb{R}^n)$ by applying the space shift to each component of the vector-valued functions.

Remark 2.13

The operator $\mathcal{S}_{\text{space}}^{\Lambda, \mathbf{R}, t_0} : \mathcal{F}(X \rightarrow \mathbb{R}^n) \mapsto \mathcal{F}(T \times X \rightarrow \mathbb{R}^n)$ is also an extension of $\mathcal{S}_{\text{space}}^{\lambda, t_0}$; however, it is not a canonical extension due to the structure of the eigenvector matrix \mathbf{R} unless $\mathbf{R} = \mathbf{I}$.

The following simple example illustrates the reasoning behind Remark 2.13.

Example 2.14

Consider the coefficient matrix $\mathbf{A} = \begin{bmatrix} 0 & 1 \\ 1 & 0 \end{bmatrix}$ whose eigenvalues are $\lambda_1 = -1$, $\lambda_2 = 1$ and the matrix of right eigenvectors $\mathbf{R} = \begin{bmatrix} 1 & 1 \\ -1 & 1 \end{bmatrix}$ and the vector $\mathbf{u}^{t_0} = (u_1^{t_0} \ u_2^{t_0})^\top$. Then from the formula (2.61), it follows

$$\mathcal{S}_{\text{space}}^{\Lambda, \mathbf{R}, t_0} \mathbf{u}^{t_0} = \frac{1}{2} \begin{pmatrix} \mathcal{S}_{\text{space}}^{\lambda_1, t_0} u_1^{t_0} - \mathcal{S}_{\text{space}}^{\lambda_1, t_0} u_2^{t_0} + \mathcal{S}_{\text{space}}^{\lambda_2, t_0} u_1^{t_0} + \mathcal{S}_{\text{space}}^{\lambda_2, t_0} u_2^{t_0} \\ -\mathcal{S}_{\text{space}}^{\lambda_1, t_0} u_1^{t_0} + \mathcal{S}_{\text{space}}^{\lambda_1, t_0} u_2^{t_0} + \mathcal{S}_{\text{space}}^{\lambda_2, t_0} u_1^{t_0} + \mathcal{S}_{\text{space}}^{\lambda_2, t_0} u_2^{t_0} \end{pmatrix},$$

while the canonical extension $\mathcal{S}_{\text{space}}^{\Lambda, \mathbf{I}, t_0}$ yields the following

$$\mathcal{S}_{\text{space}}^{\Lambda, \mathbf{I}, t_0} \mathbf{u}^{t_0} = \begin{pmatrix} \mathcal{S}_{\text{space}}^{\lambda_1, t_0} u_1^{t_0} \\ \mathcal{S}_{\text{space}}^{\lambda_2, t_0} u_2^{t_0} \end{pmatrix}.$$

2.2.1 Bounded spatial domain

When the spatial domain is assumed to be bounded, say $x \in [a, b]$, for the system (2.58), it is necessary to prescribe some boundary conditions at the boundaries $x = a$ and/or $x = b$. Hence, in addition to Assumptions **(H-3)** and **(H-4)**, assumptions on boundary characteristics must be considered, as well.

In Figure 2.1, characteristics emerging from initial and boundary conditions of a linear PDE, which has two unknowns for which $\lambda_1 < 0$ and $\lambda_2 > 0$ hold, are depicted.

The boundary conditions, say $\mathbf{b}^a(t)$ and $\mathbf{b}^b(t)$ at $x = a$ and $x = b$, respectively, for the PDE system (2.58) with the initial condition (2.1c) are defined as

$$\begin{aligned} \mathbf{P}_a \mathbf{u}(t, a) &= \mathbf{b}^a(t), \\ \mathbf{P}_b \mathbf{u}(t, b) &= \mathbf{b}^b(t), \end{aligned} \quad t > t_0, \quad (2.62)$$

where $\mathbf{P}_a \in \mathbb{R}^{(n-\ell) \times n}$, $\mathbf{P}_b \in \mathbb{R}^{\ell \times n}$, $\mathbf{b}^a : \mathbb{R} \rightarrow \mathbb{R}^{n-\ell}$ and $\mathbf{b}^b : \mathbb{R} \rightarrow \mathbb{R}^\ell$.

In this section, the following modified assumptions on the system and on boundary conditions which are originated from **(H-5)** are considered.

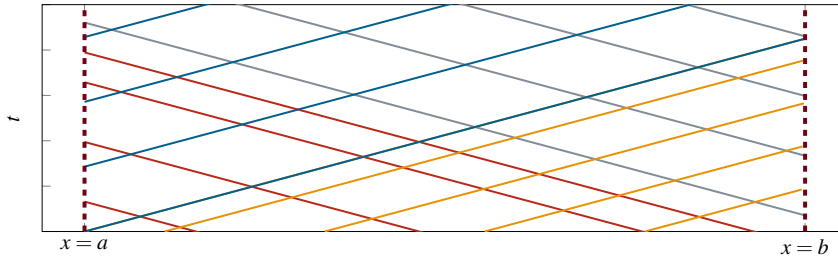


FIGURE 2.1: Left- and right going characteristics for a linear PDE with two unknowns over the domain $[t_0, \infty) \times [a, b]$, $a < b$. Lines with negative slope are for $\lambda_1 < 0$ and with positive slope for $\lambda_2 > 0$. Each different color represents inputs from initial or boundary conditions for λ_1 and λ_2 . Information travels along characteristics.

(H'-3): The system (2.58) is hyperbolic; i.e., \mathbf{A} has n real and distinct eigenvalues, namely $\lambda_1 \leq \lambda_2 \leq \dots \leq \lambda_n$ where $\lambda_i \neq 0$ for each $i = 1, \dots, n$, and corresponding left \mathbf{l}_i and right \mathbf{r}_i eigenvectors for each $i = 1, \dots, n$.

(H'-5): $\mathbf{P}_a \in \mathbb{R}^{(n-\ell) \times n}$ is such that

$$\det(\mathbf{P}_a \mathbf{R}^+(t, a)) \neq 0$$

for $t \in [t_0, \infty)$. Thus, there exists an $(n-\ell) \times (n-\ell)$ invertible matrix $\mathbf{M}_2(t)$ with entries $m_{i,j}(t)$ such that

$$\mathbf{M}_2(t) = \mathbf{P}_a \mathbf{R}^+(t, a),$$

where $\mathbf{R}^+(t, a)$ is the submatrix of $\mathbf{R}(t, a)$ whose columns are the eigenvectors corresponding to the eigenvalues $\lambda_{\ell+1} > 0$ for $\ell \in \{1, 2, \dots, n-1\}$. Further, the $(n-\ell) \times n$ matrix can be defined as

$$\mathbf{M}(t) := [\mathbf{M}_1(t) \ \mathbf{M}_2(t)] = \mathbf{P}_a \mathbf{R}(t, a),$$

where $\mathbf{M}_1 \in \mathbb{R}^{(n-\ell) \times \ell}$ is some matrix.

(H'-6): $\mathbf{P}_b \in \mathbb{R}; \mathbb{R}^{\ell \times n}$ is such that

$$\det(\mathbf{P}_b \mathbf{R}^-(t, b)) \neq 0$$

for $t \in [t_0, \infty)$. Thus, there exists an $\ell \times \ell$ invertible matrix \mathbf{N}_1 with entries $n_{i,j}(t)$ such that

$$\mathbf{N}_1(t) = \mathbf{P}_b \mathbf{R}^-(t, b),$$

where $\mathbf{R}^-(t, b)$ is the submatrix of $\mathbf{R}(t, b)$ whose columns are the eigenvectors corresponding to the eigenvalues $\lambda_\ell < 0$ for $\ell \in \{1, 2, \dots, n-1\}$. Similarly, the $\ell \times n$ matrix can be defined as

$$\mathbf{N}(t) := [\mathbf{N}_1(t) \ \mathbf{N}_2(t)] = \mathbf{P}_b \mathbf{R}(t, b),$$

where $\mathbf{N}_2 \in \mathbb{R}^{\ell \times (n-\ell)}$ is some matrix.

The boundary conditions in terms of characteristic variables can then be written

$$\begin{aligned} [\mathbf{M}_1(t) \ \mathbf{M}_2(t)] \begin{pmatrix} \mathbf{v}_-(t, a) \\ \mathbf{v}_+(t, a) \end{pmatrix} &= \mathbf{b}^a(t), \\ [\mathbf{N}_1(t) \ \mathbf{N}_2(t)] \begin{pmatrix} \mathbf{v}_-(t, b) \\ \mathbf{v}_+(t, b) \end{pmatrix} &= \mathbf{b}^b(t), \end{aligned}$$

which yields

$$\begin{aligned}\mathbf{v}_+(t, a) &= -(\mathbf{M}_2(t))^{-1} \mathbf{M}_1(t) \mathbf{v}_-(t, a) + \mathbf{M}_2^{-1} \mathbf{b}^a(t), \\ \mathbf{v}_-(t, b) &= -(\mathbf{N}_1(t))^{-1} \mathbf{N}_2(t) \mathbf{v}_+(t, b) + \mathbf{N}_1^{-1} \mathbf{b}^b(t).\end{aligned}\quad (2.63)$$

The decoupled system (2.5) on the bounded domain $[a, b]$, on the other hand, has $\mathbf{v}_+ : [t_0, \infty) \times [a, b] \rightarrow \mathbb{R}^{n-\ell}$ incoming waves (the waves that enter the domain at the boundary) and $\mathbf{v}_- : [t_0, \infty) \times [a, b] \rightarrow \mathbb{R}^\ell$ outgoing waves at $x = a$ regarding characteristics. Similarly, at $x = b$, the same system has \mathbf{v}_- incoming waves and \mathbf{v}_+ outgoing waves.

The boundary conditions (2.62) for the characteristic variables are of the form

$$\begin{aligned}\mathbf{M}\mathbf{v}(t, a) &= \mathbf{b}^a(t), \\ \mathbf{N}\mathbf{v}(t, b) &= \mathbf{b}^b(t),\end{aligned}\quad t > t_0, \quad (2.64)$$

where $\mathbf{M} = [\mathbf{M}_1 \quad \mathbf{M}_2] \in \mathbb{R}^{(n-\ell) \times n}$ and $\mathbf{N} = [\mathbf{N}_1 \quad \mathbf{N}_2] \in \mathbb{R}^{\ell \times n}$ are given by

$$\begin{bmatrix} \mathbf{P}_a \mathbf{R}^- & \mathbf{P}_a \mathbf{R}^+ \\ \mathbf{P}_b \mathbf{R}^- & \mathbf{P}_b \mathbf{R}^+ \end{bmatrix} = \begin{bmatrix} \mathbf{M}_1 & \mathbf{M}_2 \\ \mathbf{N}_1 & \mathbf{N}_2 \end{bmatrix},$$

where \mathbf{R}^- , \mathbf{R}^+ are submatrices of \mathbf{R} such that $\mathbf{R}^- := [\mathbf{r}_1 \dots \mathbf{r}_\ell]$ and $\mathbf{R}^+ := [\mathbf{r}_{\ell+1} \dots \mathbf{r}_n]$; and \mathbf{M}_2 , \mathbf{N}_1 are invertible matrices, and, therefore, (2.64) can be resolved further as (2.63).

Remark 2.15

In the case that the wave speed $\lambda_i = 0$, the equation (2.59) is simply $\partial_t v_i = 0$, meaning that the change in the solution with respect to time is zero, with the initial condition given as in (2.60). Hence, the solution is given by the initial condition $v_i(t, x) = v_i^{t_0}(x)$.

2.2.2 Explicit solution formula in terms of characteristic variables

Consider the system (2.5) with the initial condition (2.60) and the boundary conditions (2.64). To ease the notation, let $K^- := \{1, \dots, \ell\}$ and $K^+ := \{\ell + 1, \dots, n\}$. The solution to each scalar PDE in (2.5) can be found individually in terms of the initial condition $v_i^{t_0}(x)$ and boundary conditions $v_i(t, a) =: v_i^L(t)$, $v_i(t, b) =: v_i^R(t)$. The solution $\mathbf{v}(t, x)$ is expressed in terms of $\mathbf{v}_-(t, x)$ and $\mathbf{v}_+(t, x)$ separately below.

For the left-going waves, the solution is of the form

$$v_i(t, x) = \begin{cases} \left(\mathcal{S}_{\text{space}}^{\lambda_i, t_0} v_i^{t_0} \right)(t, x), & \text{if } x - b \leq \lambda_i(t - t_0), \\ \left(\mathcal{S}_{\text{time}}^{\lambda_i, b} v_i^R \right)(t, x), & \text{if } x - b > \lambda_i(t - t_0), \end{cases}$$

where $i \in K^-$, $t \geq t_0$ and $x \in [a, b]$.

Then the vector of all the left-going waves, $\mathbf{v}_-(t, x)$, is formulated as

$$\mathbf{v}_-(t, x) = \sum_{i \in K^-} \text{diag}(\mathbf{e}_i) \left[\mathbb{1}_{\{x-b \leq \lambda_i(t-t_0)\}} \mathcal{S}_{\text{space}}^{\lambda_i, t_0} \mathbf{v}_-^{t_0} + \mathbb{1}_{\{x-b > \lambda_i(t-t_0)\}} \mathcal{S}_{\text{time}}^{\lambda_i, b} \mathbf{v}_-^R \right](t, x),$$

where $\mathbf{e}_i \in \mathbb{R}^\ell$ is the i -th directional unit vector for $i \in K^-$, $\mathbf{v}_-^{t_0} : [a, b] \rightarrow \mathbb{R}^\ell$ the initial condition, and $\mathbf{v}_-^R : [t_0, \infty) \rightarrow \mathbb{R}^\ell$ the boundary condition at $x = b$. At the left boundary $x = a$, the values of the vector $\mathbf{v}_-(t, a)$ can be written as follows

$$\mathbf{v}_-(t, a) = \sum_{i \in K^-} \text{diag}(\mathbf{e}_i) \left(\mathcal{S}_{\text{time}}^{\lambda_i, b} \mathbf{v}_-^R \right)(t, a),$$

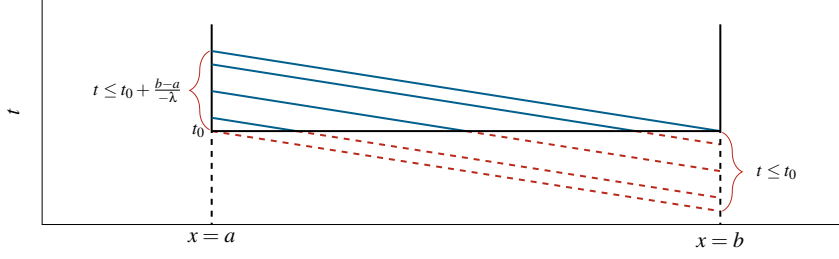


FIGURE 2.2: The Cauchy-Kovalevskaya procedure, an illustration of the extension of initial condition for $t < t_0$ for a single wave with negative velocity and initial time t_0 . The red lines show the extension on the boundary for $x \in [a, b]$ while blue lines represent the information from initial condition.

where

$$\left(\mathcal{S}_{\text{time}}^{\Lambda^-, \mathbf{I}, b} \mathbf{v}_-^R \right) (t, a) := \sum_{i \in K^-} \text{diag}(\mathbf{e}_i) \left(\mathcal{S}_{\text{space}}^{\lambda_i, t_0} \mathbf{v}_-^{t_0} \right) (t, a), \quad \text{on } \left[t_0, t_0 + \frac{b-a}{-\lambda_i} \right],$$

which can be interpreted as the extension of the boundary condition for negative times in terms of the initial values, see Figure 2.2 (cf. the Cauchy-Kovalevskaya procedure, [44]).

In a similar fashion, the solution to right-going waves is of the form

$$v_j(t, x) = \begin{cases} \left(\mathcal{S}_{\text{space}}^{\lambda_j, t_0} v_j^{t_0} \right) (t, x), & \text{if } x - a \geq \lambda_j(t - t_0), \\ \left(\mathcal{S}_{\text{time}}^{\lambda_j, a} v_j^L \right) (t, x), & \text{if } x - a < \lambda_j(t - t_0), \end{cases}$$

where $j \in K^+$ and $x \in [a, b]$.

Similarly, the solution for the right-going waves $\mathbf{v}_+(t, x)$ is

$$\mathbf{v}_+(t, x) = \sum_{j \in K^+} \text{diag}(\mathbf{e}_j) \left[\mathbb{1}_{\{x-a \geq \lambda_j(t-t_0)\}} \mathcal{S}_{\text{space}}^{\lambda_j, t_0} \mathbf{v}_+^{t_0} + \mathbb{1}_{\{x-a < \lambda_j(t-t_0)\}} \mathcal{S}_{\text{time}}^{\lambda_j, a} \mathbf{v}_+^L \right] (t, x),$$

where $\mathbf{e}_j \in \mathbb{R}^{n-\ell}$ is the j -th directional unit vector for $j \in K^+$, and $\mathbf{v}_+^{t_0} : [a, b] \rightarrow \mathbb{R}^{n-\ell}$ the initial condition, and $\mathbf{v}_+^L : [t_0, \infty) \rightarrow \mathbb{R}^{n-\ell}$ the boundary condition at $x = a$.

At the right boundary $x = b$, the solution for the right-going waves $\mathbf{v}_+(t, b)$ can be written as

$$\mathbf{v}_+(t, b) = \sum_{j \in K^+} \text{diag}(\mathbf{e}_j) \left(\mathcal{S}_{\text{time}}^{\lambda_j, a} \mathbf{v}_+^L \right) (t, b),$$

where

$$\left(\mathcal{S}_{\text{time}}^{\Lambda^+, \mathbf{I}, a} \mathbf{v}_+^L \right) (t, b) := \sum_{i \in K^+} \text{diag}(\mathbf{e}_i) \left(\mathcal{S}_{\text{space}}^{\lambda_i, t_0} \mathbf{v}_+^{t_0} \right) (t, b), \quad \text{on } \left[t_0, t_0 + \frac{b-a}{\lambda_i} \right].$$

The solutions $\mathbf{v}_-(t, x)$ and $\mathbf{v}_+(t, x)$ together form the solution $\mathbf{v}(t, x)$ to the system (2.5) with the initial condition (2.60) and the boundary conditions (2.64). Hence, $\mathbf{v}(t, x)$ is given by

$$\begin{aligned} \mathbf{v}(t, x) = & \sum_{i \in K^-} \begin{bmatrix} \text{diag}(\mathbf{e}_i) \\ \mathbf{0}_{n-\ell, \ell} \end{bmatrix} \left[\mathbb{1}_{\{x-b \leq \lambda_i(t-t_0)\}} \mathcal{S}_{\text{space}}^{\lambda_i, t_0} \mathbf{v}_-^{t_0} + \mathbb{1}_{\{x-b > \lambda_i(t-t_0)\}} \mathcal{S}_{\text{time}}^{\lambda_i, b} \mathbf{v}_-^R \right] (t, x) \\ & + \sum_{j \in K^+} \begin{bmatrix} \mathbf{0}_{\ell, n-\ell} \\ \text{diag}(\mathbf{e}_j) \end{bmatrix} \left[\mathbb{1}_{\{x-a \geq \lambda_j(t-t_0)\}} \mathcal{S}_{\text{space}}^{\lambda_j, t_0} \mathbf{v}_+^{t_0} + \mathbb{1}_{\{x-a < \lambda_j(t-t_0)\}} \mathcal{S}_{\text{time}}^{\lambda_j, a} \mathbf{v}_+^L \right] (t, x), \end{aligned}$$

where $\mathbf{e}_i \in \mathbb{R}^\ell$ and $\mathbf{e}_j \in \mathbb{R}^{n-\ell}$. Using the formulae (2.63), the vector values of the solution at $x = a$ and $x = b$ then are of the form

$$\begin{aligned}\mathbf{v}(t, a) &= \begin{bmatrix} \mathbf{0}_{\ell, n-\ell} \\ \mathbf{M}_2^{-1} \end{bmatrix} \mathbf{b}^a(t) + \begin{bmatrix} \mathbf{I}_{\ell, \ell} & \mathbf{0}_{\ell, n-\ell} \\ -\mathbf{M}_2^{-1} \mathbf{M}_1 & \mathbf{0}_{n-\ell, n-\ell} \end{bmatrix} \sum_{i \in K^-} \begin{bmatrix} \text{diag}(\mathbf{e}_i) \\ \mathbf{0}_{n-\ell, \ell} \end{bmatrix} \left(\mathcal{S}_{\text{time}}^{\lambda_i, b} \mathbf{v}_-^R \right) (t, a), \\ \mathbf{v}(t, b) &= \begin{bmatrix} \mathbf{N}_1^{-1} \\ \mathbf{0}_{n-\ell, \ell} \end{bmatrix} \mathbf{b}^R(t) + \begin{bmatrix} \mathbf{0}_{\ell, \ell} & -\mathbf{N}_1^{-1} \mathbf{N}_2 \\ \mathbf{0}_{n-\ell, \ell} & \mathbf{I}_{n-\ell, n-\ell} \end{bmatrix} \sum_{j \in K^+} \begin{bmatrix} \mathbf{0}_{\ell, n-\ell} \\ \text{diag}(\mathbf{e}_j) \end{bmatrix} \left(\mathcal{S}_{\text{time}}^{\lambda_j, a} \mathbf{v}_+^L \right) (t, b),\end{aligned}$$

where $\mathbf{I}_{\ell, \ell} \in \mathbb{R}^{\ell \times \ell}$ and $\mathbf{I}_{n-\ell, n-\ell} \in \mathbb{R}^{(n-\ell) \times (n-\ell)}$ are identity matrices.

2.2.3 Solution framework for the linear hyperbolic system

In this section, the solution $\mathbf{u}(t, x)$ to the system (2.58) with the initial and boundary conditions (2.1c) and (2.62) will be formulated by using the results from Section 2.2.2. As the change of coordinates explained in Section 2.2.1 allows to pass from the linear hyperbolic PDE system to the decoupled system (2.59), the inversion of the coordinate change; i.e., $\mathbf{u} = \mathbf{R}\mathbf{v}$, is of use to formulate the solution $\mathbf{u}(t, x)$ similarly.

Let $\mathbf{u}^L := \mathbf{u}(t, a)$, $\mathbf{u}^R := \mathbf{u}(t, b)$ be the boundary values of the solution \mathbf{u} and $\Pi_i := \mathbf{R} \text{diag}(\mathbf{e}_i) \mathbf{R}^{-1}$, where $\mathbf{e}_i \in \mathbb{R}^n$ is the i -th directional unit vector. Then

$$\begin{aligned}\mathbf{u}(t, x) &= \sum_{i \in K^-} \Pi_i \left(\mathbb{1}_{\{x-b \leq \lambda_i(t-t_0)\}} \mathcal{S}_{\text{space}}^{\lambda_i, t_0} \mathbf{u}^{t_0} + \mathbb{1}_{\{x-b > \lambda_i(t-t_0)\}} \mathcal{S}_{\text{time}}^{\lambda_i, b} \mathbf{u}^R \right) (t, x) \\ &\quad + \sum_{j \in K^+} \Pi_j \left(\mathbb{1}_{\{x-a \geq \lambda_j(t-t_0)\}} \mathcal{S}_{\text{space}}^{\lambda_j, t_0} \mathbf{u}^{t_0} + \mathbb{1}_{\{x-a < \lambda_j(t-t_0)\}} \mathcal{S}_{\text{time}}^{\lambda_j, a} \mathbf{u}^L \right) (t, x),\end{aligned}\tag{2.65}$$

is the solution to the IBVP.

Lemma 2.16

Consider the PDE (2.58) on $[t_0, \infty) \times [a, b]$ satisfying Assumptions (H-3), (H'-5) and (H'-6) with some given initial trajectory \mathbf{u}^{t_0} as in (2.1c) and boundary conditions $\mathbf{b}^a, \mathbf{b}^b$ as in (2.62). Let \mathbf{u}^L and \mathbf{u}^R satisfy the following

$$\begin{aligned}\mathbf{u}^L(t) &= \begin{cases} \sum_{i \in K^-} \Pi_i \left(\mathcal{S}_{\text{space}}^{\lambda_i, t_0} \mathbf{u}^{t_0} \right) (t, a), & t \leq t_0 + \frac{b-a}{\lambda_i}, \\ \mathbf{F}_a \mathbf{b}^a(t) + \sum_{k=1}^n \mathbf{D}_k^{ab} \left(\mathcal{S}_{\text{time}}^{\lambda_k, b} \mathbf{u}^R \right) (t, a), & t > t_0 + \frac{b-a}{\lambda_k}, \end{cases} \\ \mathbf{u}^R(t) &= \begin{cases} \sum_{j \in K^+} \Pi_j \left(\mathcal{S}_{\text{space}}^{\lambda_j, t_0} \mathbf{u}^{t_0} \right) (t, b), & t \leq t_0 + \frac{b-a}{\lambda_j}, \\ \mathbf{F}_b \mathbf{b}^b(t) + \sum_{k=1}^n \mathbf{D}_k^{ba} \left(\mathcal{S}_{\text{time}}^{\lambda_k, a} \mathbf{u}^L \right) (t, b), & t > t_0 + \frac{b-a}{\lambda_k}, \end{cases}\end{aligned}\tag{2.66}$$

where $\Pi_p := [\mathbf{R}^- \ \mathbf{R}^+] \text{diag}(\mathbf{e}_p) [\mathbf{R}^- \ \mathbf{R}^+]^{-1}$, with $\mathbf{e}_p \in \mathbb{R}^n$, $K^- = \{1, \dots, \ell\}$, $K^+ = \{\ell+1, \dots, n\}$,

$$\mathbf{F}_a = \mathbf{R} \begin{bmatrix} \mathbf{0}_{\ell, n-\ell} \\ \mathbf{M}_2^{-1} \end{bmatrix}, \quad \mathbf{F}_b = \mathbf{R} \begin{bmatrix} \mathbf{N}_1^{-1} \\ \mathbf{0}_{n-\ell, \ell} \end{bmatrix},\tag{2.67}$$

$$\mathbf{D}_p^{ab} = \mathbf{R} \begin{bmatrix} \mathbf{I}_{\ell, \ell} & \mathbf{0}_{\ell, n-\ell} \\ -\mathbf{M}_2^{-1} \mathbf{M}_1 & \mathbf{0}_{n-\ell, n-\ell} \end{bmatrix} \mathbf{R}^{-1} \Pi_p,\tag{2.68a}$$

$$\mathbf{D}_p^{ba} = \mathbf{R} \begin{bmatrix} \mathbf{0}_{\ell,\ell} & -\mathbf{N}_1^{-1} \mathbf{N}_2 \\ \mathbf{0}_{n-\ell,\ell} & \mathbf{I}_{n-\ell,n-\ell} \end{bmatrix} \mathbf{R}^{-1} \Pi_p, \quad (2.68b)$$

and where it is assumed that $\mathbf{u}^{t_0}(x) = 0$ for $x \notin [a, b]$. Then every classical solution is given by

$$\mathbf{u}(t, x) = \sum_{i \in K^-} \Pi_i \left(\mathcal{S}_{\text{time}}^{\lambda_i, b} \mathbf{u}^R \right) (t, x) + \sum_{j \in K^+} \Pi_j \left(\mathcal{S}_{\text{time}}^{\lambda_j, a} \mathbf{u}^L \right) (t, x).$$

For any initial condition $\mathbf{u}^{t_0}(x)$, and boundary conditions $\mathbf{b}^a(t)$, $\mathbf{b}^b(t)$, there exist unique solutions $\mathbf{u}^L(t)$ and $\mathbf{u}^R(t)$ given in (2.66).

Proof. As from the previous discussion above, by the method of characteristics, a solution $\mathbf{u}(t, x)$ to the initial boundary value problem (2.58) with the initial condition \mathbf{u}^{t_0} and boundary conditions \mathbf{b}^a , \mathbf{b}^b is of the form

$$\begin{aligned} \mathbf{u}(t, x) &= \sum_{i \in K^-} \Pi_i \left(\mathbb{1}_{\{x-b \leq \lambda_i(t-t_0)\}} \mathcal{S}_{\text{space}}^{\lambda_i, t_0} \mathbf{u}^{t_0} + \mathbb{1}_{\{x-b > \lambda_i(t-t_0)\}} \mathcal{S}_{\text{time}}^{\lambda_i, b} \mathbf{u}^R \right) (t, x) \\ &+ \sum_{j \in K^+} \Pi_j \left(\mathbb{1}_{\{x-a \geq \lambda_j(t-t_0)\}} \mathcal{S}_{\text{space}}^{\lambda_j, t_0} \mathbf{u}^{t_0} + \mathbb{1}_{\{x-a < \lambda_j(t-t_0)\}} \mathcal{S}_{\text{time}}^{\lambda_j, a} \mathbf{u}^L \right) (t, x), \end{aligned}$$

which satisfies the initial condition $\mathbf{u}(t_0, x) = \mathbf{u}^{t_0}$. The partial derivatives are

$$\begin{aligned} \partial_t \mathbf{u} &= \sum_{i \in K^-} \Pi_i \left((-\lambda_i) \mathbb{1}_{\{x-b \leq \lambda_i(t-t_0)\}} \mathcal{S}_{\text{space}}^{\lambda_i, t_0} (\mathbf{u}^{t_0})' + \mathbb{1}_{\{x-b > \lambda_i(t-t_0)\}} \mathcal{S}_{\text{time}}^{\lambda_i, b} (\mathbf{u}^R)' \right) (t, x) \\ &+ \sum_{j \in K^+} \Pi_j \left((-\lambda_j) \mathbb{1}_{\{x-a \geq \lambda_j(t-t_0)\}} \mathcal{S}_{\text{space}}^{\lambda_j, t_0} (\mathbf{u}^{t_0})' + \mathbb{1}_{\{x-a < \lambda_j(t-t_0)\}} \mathcal{S}_{\text{time}}^{\lambda_j, a} (\mathbf{u}^L)' \right) (t, x), \\ \partial_x \mathbf{u} &= \sum_{i \in K^-} \Pi_i \left(\mathbb{1}_{\{x-b \leq \lambda_i(t-t_0)\}} \mathcal{S}_{\text{space}}^{\lambda_i, t_0} (\mathbf{u}^{t_0})' + \left(-\frac{1}{\lambda_i}\right) \mathbb{1}_{\{x-b > \lambda_i(t-t_0)\}} \mathcal{S}_{\text{time}}^{\lambda_i, b} (\mathbf{u}^R)' \right) (t, x) \\ &+ \sum_{j \in K^+} \Pi_j \left(\mathbb{1}_{\{x-a \geq \lambda_j(t-t_0)\}} \mathcal{S}_{\text{space}}^{\lambda_j, t_0} (\mathbf{u}^{t_0})' + \left(-\frac{1}{\lambda_j}\right) \mathbb{1}_{\{x-a < \lambda_j(t-t_0)\}} \mathcal{S}_{\text{time}}^{\lambda_j, a} (\mathbf{u}^L)' \right) (t, x), \end{aligned}$$

which proves $\partial_t \mathbf{u} + \Lambda \partial_x \mathbf{u} = \mathbf{0}$ and concludes the proof of existence.

Let $\tilde{t}_i := t - \frac{b-x}{-\lambda_i}$, for $i \in K^-$ and $\hat{t}_j := t - \frac{x-a}{\lambda_j}$, for $j \in K^+$. With the manipulations

$$\begin{aligned} \mathbf{u}^R(\tilde{t}_i) &= \mathbf{u}^{t_0}(b - \lambda_i \tilde{t}_i), \quad \text{for } \tilde{t}_i < t_0, \\ \mathbf{u}^L(\hat{t}_j) &= \mathbf{u}^{t_0}(a - \lambda_j \hat{t}_j), \quad \text{for } \hat{t}_j < t_0, \end{aligned}$$

with the convention that $\mathbf{u}^{t_0}(x) = 0$ for $x \notin [a, b]$. The solution $\mathbf{u}(t, x)$ can now be written as

$$\mathbf{u}(t, x) = \sum_{i \in K^-} \Pi_i \left(\mathcal{S}_{\text{time}}^{\lambda_i, b} \mathbf{u}^R \right) (t, x) + \sum_{j \in K^+} \Pi_j \left(\mathcal{S}_{\text{time}}^{\lambda_j, a} \mathbf{u}^L \right) (t, x), \quad (2.69)$$

where $x \in [a, b]$ and the boundary values $\mathbf{u}^L(t)$ and $\mathbf{u}^R(t)$ are defined as in (2.66) and $\mathbf{u}^{t_0}(x) = 0$ for $x \notin [a, b]$. If $\tilde{\mathbf{u}}(t, x)$ is another solution, by linearity $\hat{\mathbf{u}}(t, x) := \mathbf{u}(t, x) - \tilde{\mathbf{u}}(t, x)$ solves

$$\partial_t \hat{\mathbf{u}}(t, x) + \mathbf{A} \partial_x \hat{\mathbf{u}}(t, x) = \mathbf{0}, \quad (2.70)$$

with the initial condition $\hat{\mathbf{u}}(t_0, x) = \mathbf{0}$ and boundary conditions $\hat{\mathbf{b}}^a(t) = \mathbf{0}$, $\hat{\mathbf{b}}^b(t) = \mathbf{0}$. A solution $\hat{\mathbf{u}}(t, x)$ to (2.70) is given by the formula (2.69) which yields $\hat{\mathbf{u}}(t, x) = \mathbf{0}$. Hence, $\mathbf{u}(t, x) = \tilde{\mathbf{u}}(t, x)$. As a result, there exist unique solutions $\mathbf{u}^L(t)$, $\mathbf{u}^R(t)$ given in (2.66). \square

Definition 2.17: 1D time shift operator for functions

In addition to the 2D shift operator defined as in Definition 2.10, the 1D time shift operator $\mathcal{S}_{\text{time}}^\tau$ with $\tau \in \mathbb{R}$ for functions $f : T \subseteq \mathbb{R} \rightarrow \mathbb{R}$ is analogously defined as follows

$$\begin{aligned} \mathcal{S}_{\text{time}}^\tau : \mathcal{F}(T \rightarrow \mathbb{R}) &\mapsto \mathcal{F}(T \rightarrow \mathbb{R}), \\ f &\mapsto [t \mapsto f(t - \tau)], \end{aligned} \quad (2.71)$$

where \mathcal{F} is the set of all functions from some set T to \mathbb{R} and with the convention that $f(s) = 0$ if $s \notin T$ for $f \in \mathcal{F}$.

Remark 2.18

Similar to Corollary 2.11, 1D time shift operator for functions $\mathcal{S}_{\text{time}}^\tau$ with $\tau \in \mathbb{R}$ commutes with the derivative operator.

Remark 2.19

Let $\mathbf{u}_{ab}(t) := \left(\mathbf{u}^L(t)^\top, \mathbf{u}^R(t)^\top \right)^\top \in \mathbb{R}^{2n}$, where $\mathbf{u}^L(t)$ and $\mathbf{u}^R(t)$ satisfy (2.66). Below, \mathbf{u}_{ab} is expressed in a compressed form in terms of the 1D time shift operator $\mathcal{S}_{\text{time}}^\tau$

$$\mathbf{u}_{ab}(t) = \begin{bmatrix} \mathbf{F}_a & \mathbf{0}_{n,n-r} \\ \mathbf{0}_{n,r} & \mathbf{F}_b \end{bmatrix} \begin{bmatrix} \mathbf{b}^a(t) \\ \mathbf{b}^b(t) \end{bmatrix} + \sum_{k=1}^n \begin{bmatrix} \mathbf{0}_{n,n} & \mathbf{D}_k^{ab} \\ \mathbf{D}_k^{ba} & \mathbf{0}_{n,n} \end{bmatrix} (\mathcal{S}_{\text{time}}^{\tau_k} \mathbf{u}_{ab}(t)), \quad (2.72)$$

where $\tau_k = \frac{b-a}{\text{sgn}(\lambda_k)\lambda_k}$, the matrices $\mathbf{F}_a, \mathbf{F}_b, \mathbf{D}_k^{ab}, \mathbf{D}_k^{ba}$, for $k = 1, 2, \dots, n$, are given in (2.67)-(2.68) and extensions of initial conditions as boundary conditions for $t \leq t_0 + \frac{b-a}{\text{sgn}(\lambda_k)\lambda_k}$, are adapted as in the proof of Lemma 2.16. Then the equality (2.72) follows from the equations in (2.66).

Chapter 3

Theory of distributions

A function f from a set A to a set B uniquely relates each element of A with an element of B . Therefore, evaluation of functions $\tau \mapsto f(\tau)$ is an operation defined for elements of the domain of the function f . On the other hand, measuring physical quantities at a point is not possible in real world. What can be measured is, however, their mean values over some neighborhood of a certain point. These mathematical objects are called *distributions*, which generalize the notion of functions. These generalized functions act on a set of so-called *test functions*. In this chapter, following the works [30, 40, 78, 90, 130], the theory of distributions is briefly explained.

3.1 Preliminary Notions

In this section, some preliminary notions which are employed throughout this thesis are reviewed.

Definition 3.1: Support of a function

The *support* of a function $f : \Omega \subseteq \mathbb{R}^d \rightarrow \mathbb{R}$, $d \in \mathbb{N} \setminus \{0\}$, is

$$\text{supp } f(\tau) = \text{cl}\{\tau \in \Omega \mid f(\tau) \neq 0\}.$$

Definition 3.2: Test functions

The space of test functions is denoted by C_0^∞ and is defined as

$$C_0^\infty(\mathbb{R}^d; \mathbb{R}) := \left\{ f \in C^\infty(\mathbb{R}^d; \mathbb{R}) \mid \text{supp } f(\tau) \text{ is compact} \right\},$$

where $d \in \mathbb{N} \setminus \{0\}$ and $C^\infty(\mathbb{R}^d; \mathbb{R})$ is the space of real-valued functions that are infinitely differentiable.

The space of test functions $C_0^\infty(\mathbb{R}^d; \mathbb{R})$ is a topological vector space, [16]. In the sequel, the space $C^\infty(\mathbb{R}^d; \mathbb{R})$ is assumed to be equipped with the topology given in [16].

Definition 3.3: Convergence in $C_0^\infty(\mathbb{R}; \mathbb{R})$

The sequence $\varphi_n \in C_0^\infty(\mathbb{R}^d; \mathbb{R})$ converges to $\varphi \in C_0^\infty(\mathbb{R}^d; \mathbb{R})$ if there exists a compact set $K \subseteq \mathbb{R}^d$ such that $\text{supp } \varphi_n \subseteq K$ for all $n \in \mathbb{N}$ and the sequence $\{\varphi_n^{(k)}\}$ converges uniformly to $\varphi^{(k)}$ in K for every $k = (k_1, k_2, \dots, k_d)$ with $k_i \in \mathbb{N}$ for $i = 1, 2, \dots, d$ as $n \rightarrow \infty$; i.e.,

$$\lim_{n \rightarrow \infty} \sup_{\tau \in \mathbb{R}^d} \left| \varphi_n^{(k)}(\tau) - \varphi^{(k)}(\tau) \right| \rightarrow 0, \quad \forall k \in \mathbb{N}^d,$$

where

$$\varphi^{(k)} := \partial_{\tau_1}^{(k_1)} \partial_{\tau_2}^{(k_2)} \dots \partial_{\tau_d}^{(k_d)} \varphi.$$

Definition 3.4: Locally integrable functions

A Lebesgue measurable function $f : \Omega \subseteq \mathbb{R}^d \rightarrow \mathbb{R}$ is called *locally integrable* if

$$\int_K |f(\tau)| \, d\tau < \infty,$$

on all compact subsets $K \subset \Omega$. The space of locally integrable functions is denoted by $L^1_{\text{loc}}(\mathbb{R}^d; \mathbb{R})$.

3.2 Distributions in time domains

In this section, taking the definitions from Section 3.1 into account with $d = 1$, distributions in \mathbb{R} are studied.

Definition 3.5: Distributions

A functional $D : C_0^\infty(\mathbb{R}; \mathbb{R}) \rightarrow \mathbb{R}$ is called a *distribution* if it is linear and continuous. Linearity in this context means

$$D(\alpha\varphi_1 + \beta\varphi_2) = \alpha D(\varphi_1) + \beta D(\varphi_2),$$

for all $\alpha, \beta \in \mathbb{R}$ and $\varphi_1, \varphi_2 \in C_0^\infty$. As the space of test functions is equipped with the suitable topology, continuity is characterized by the limit property. In other words, if φ_n converges to φ in C_0^∞ , then

$$\lim_{n \rightarrow \infty} D(\varphi_n) = D(\varphi).$$

The space of distributions is denoted by $\mathbb{D}(C_0^\infty(\mathbb{R}; \mathbb{R}); \mathbb{R})$ (or in short \mathbb{D}), which is, by definition, the dual space of $C_0^\infty(\mathbb{R}; \mathbb{R})$.

Lemma 3.6: Regular distributions

Let $f \in L^1_{\text{loc}}(\mathbb{R}; \mathbb{R})$. A *regular distribution* $f_{\mathbb{D}}$ that is induced by f is defined by

$$\begin{aligned} f_{\mathbb{D}} : C_0^\infty &\rightarrow \mathbb{R} \\ \varphi &\mapsto \int_{\mathbb{R}} \varphi f. \end{aligned} \tag{3.1}$$

The space of regular distributions is given by

$$\mathbb{D}_{\text{reg}} = \{f_{\mathbb{D}} \mid f \in L^1_{\text{loc}}(\mathbb{R}; \mathbb{R})\}.$$

Regular distributions are distributions.

Proof. Assume that $\varphi \in C_0^\infty(\mathbb{R}; \mathbb{R})$ and $\text{supp } \varphi = K$. Then, K is a compact set and the integral (3.1) is well-defined

$$f_{\mathbb{D}} = \int_K f \varphi < \infty,$$

where $f \in L^1_{\text{loc}}(\mathbb{R}; \mathbb{R})$. Hence, $f_{\mathbb{D}}$ is well-defined. The linearity follows from

$$f_{\mathbb{D}}(\alpha\varphi_1 + \beta\varphi_2) = \int_{K_1} f(\alpha\varphi_1 + \beta\varphi_2) = \alpha f_{\mathbb{D}}(\varphi_1) + \beta f_{\mathbb{D}}(\varphi_2),$$

where $\varphi_1, \varphi_2 \in C_0^\infty(\mathbb{R}; \mathbb{R})$, $\alpha, \beta \in \mathbb{R}$ and $\text{supp } \varphi_1, \text{supp } \varphi_2 \subseteq K_1$. To show continuity of $f_{\mathbb{D}}$, suppose the sequence φ_n converges to φ in $C_0^\infty(\mathbb{R}; \mathbb{R})$ as in Definition 3.3. Therefore, $\text{supp } \varphi, \text{supp } \varphi_n \subseteq K_1$ and thus

$$\lim_{n \rightarrow \infty} |f_{\mathbb{D}}(\varphi) - f_{\mathbb{D}}(\varphi_n)| \leq \lim_{n \rightarrow \infty} \int_{K_1} |f| |\varphi_n - \varphi| \leq \lim_{n \rightarrow \infty} \sup_{\tau \in \mathbb{R}} |\varphi_n - \varphi| \int_{K_1} |f| \rightarrow 0,$$

since φ_n converges uniformly to φ . □

Remark 3.7

Functions that belong to the space $L^1_{\text{loc}}(\mathbb{R}; \mathbb{R})$ are not required to exhibit any nice behavior. For example, the function $f(\tau) = e^{|\tau|}$ belongs to the space $L^1_{\text{loc}}(\mathbb{R}; \mathbb{R})$ but $f \notin L^1(\mathbb{R}; \mathbb{R})$.

Example 3.8

The Heaviside function $H_0 \in L^1_{\text{loc}}(\mathbb{R}; \mathbb{R})$ defined as

$$H_0(\tau) = \begin{cases} 1, & \text{if } \tau \geq 0, \\ 0, & \text{if } \tau < 0, \end{cases}$$

induces a regular distribution; i.e., for all $\varphi \in C_0^\infty(\mathbb{R}; \mathbb{R})$

$$(H_0)_{\mathbb{D}}(\varphi) := \int_{\mathbb{R}} H_0 \varphi = \int_0^\infty \varphi < \infty,$$

as the support of φ is bounded.

Example 3.9: Dirac impulse

The Dirac impulse δ_τ at $\tau \in \mathbb{R}$ given by

$$\begin{aligned} \delta_\tau : C_0^\infty(\mathbb{R}; \mathbb{R}) &\rightarrow \mathbb{R} \\ \varphi &\mapsto \delta_\tau(\varphi) := \varphi(\tau), \end{aligned}$$

is a distribution which is not induced by any locally integrable function.

Definition 3.10: Singular distributions

Distributions that are not induced by any locally integrable function are called *singular*.

Dirac impulse δ_τ , $\tau \in \mathbb{R}$, given in Example 3.9 is a well-known singular distribution.

Proposition 3.11

The space of regular distributions \mathbb{D}_{reg} is a proper subspace of distribution space \mathbb{D} , [78].

3.3 Operations on distributions

Derivatives of distributions Let $f \in L^1_{\text{loc}}(\mathbb{R}; \mathbb{R})$ such that its derivative f' exists and is in $L^1_{\text{loc}}(\mathbb{R}; \mathbb{R})$. The derivative of distribution induced by f is

$$\begin{aligned} (f_{\mathbb{D}})' &= \int_{\mathbb{R}} f' \varphi \\ &= - \int_{\mathbb{R}} f \varphi' \\ &= -f_{\mathbb{D}}(\varphi'), \quad \forall \varphi \in C_0^\infty(\mathbb{R}; \mathbb{R}), \end{aligned}$$

where φ vanishes at $\mp\infty$ as it has a bounded support. Hence, the derivative of an arbitrary distribution can also be defined similarly.

Definition 3.12

The *distributional derivative* of $D \in \mathbb{D}$ is

$$\begin{aligned} D' := \dot{D} &:= \frac{d_{\mathbb{D}}}{d\tau} D : \mathbb{D} \rightarrow \mathbb{D} \\ D &\mapsto -D(\varphi'), \end{aligned}$$

where $\varphi \in C_0^\infty(\mathbb{R}; \mathbb{R})$.

Proposition 3.13

For $D \in \mathbb{D}$, the distributional derivative D' is linear and continuous, hence in \mathbb{D} . Any distribution $D \in \mathbb{D}$ is infinitely differentiable as test functions are elements of $C^\infty(\mathbb{R}; \mathbb{R})$. Hence, higher order derivatives of a distribution $D \in \mathbb{D}$ are

$$\begin{aligned} \left(\frac{d_{\mathbb{D}}}{d\tau}\right)^{(k)} : \mathbb{D} &\rightarrow \mathbb{D} \\ D &\mapsto (-1)^{(k)} D \left(\left(\frac{d}{d\tau}\right)^{(k)} \varphi \right), \end{aligned}$$

for $k \in \mathbb{N}$. Furthermore,

$$\left(f^{(k)}\right)_{\mathbb{D}} = (f_{\mathbb{D}})^{(k)},$$

where $f \in C^k(\mathbb{R}; \mathbb{R})$, [30].

Example 3.14

The distributional derivative of the Heaviside function H_τ is the Dirac impulse δ_τ

$$\begin{aligned} \frac{d_{\mathbb{D}}}{d\tau} (H_\tau)_{\mathbb{D}}(\varphi) &= -(H_\tau)_{\mathbb{D}} \left(\frac{d_{\mathbb{D}}}{d\tau} \varphi \right) \\ &= - \int_{\mathbb{R}} H_\tau \varphi' \end{aligned}$$

$$\begin{aligned}
&= - \int_{\tau}^{\infty} \varphi' \\
&= \varphi(\tau) = \delta_{\tau}(\varphi), \quad \forall \tau \in \mathbb{R}.
\end{aligned}$$

Definition 3.15

The addition of any distributions $D_1, D_2 \in \mathbb{D}$ is defined as, [30],

$$\begin{aligned}
D_1 + D_2 : \mathcal{C}_0^{\infty}(\mathbb{R}; \mathbb{R}) &\rightarrow \mathbb{R} \\
\varphi &\mapsto D_1(\varphi) + D_2(\varphi), \quad \forall \varphi \in \mathcal{C}_0^{\infty}(\mathbb{R}; \mathbb{R}).
\end{aligned}$$

Definition 3.16

The multiplication of any distribution $D \in \mathbb{D}$ with any smooth function $g \in \mathcal{C}^{\infty}(\mathbb{R}; \mathbb{R})$ is defined as, [30],

$$\begin{aligned}
gD : \mathcal{C}_0^{\infty}(\mathbb{R}; \mathbb{R}) &\rightarrow \mathbb{R} \\
\varphi &\mapsto D(g\varphi), \quad \forall \varphi \in \mathcal{C}_0^{\infty}(\mathbb{R}; \mathbb{R}), \quad g\varphi \in \mathcal{C}_0^{\infty}(\mathbb{R}; \mathbb{R}).
\end{aligned}$$

Corollary 3.17

For $D \in \mathbb{D}$ and $g \in \mathcal{C}^{\infty}(\mathbb{R}; \mathbb{R})$,

$$(gD)' = g'D + gD'. \quad (3.2)$$

Proposition 3.18

For any $D \in \mathbb{D}$ and $g \in \mathcal{C}^{\infty}(\mathbb{R}; \mathbb{R})$, $gD \in \mathbb{D}$, and for any $f \in L_{\text{loc}}^1(\mathbb{R}; \mathbb{R})$, $gf_{\mathbb{D}} = (gf)_{\mathbb{D}}$, [78, 131].

Definition 3.19

The support of a distribution $D \in \mathbb{D}$ is the smallest closed set outside of which the distribution D is zero; i.e.,

$$\text{supp } D := \mathbb{R} \setminus \bigcup \left\{ T_0 \subseteq \mathbb{R} \mid \begin{array}{l} T_0 \text{ is open, } \forall \varphi \in \mathcal{C}_0^{\infty}(\mathbb{R}; \mathbb{R}) : \\ \text{supp } \varphi \subseteq T_0 \Rightarrow D(\varphi) = 0 \end{array} \right\}.$$

The set of all distributions with support in $M \subseteq \mathbb{R}$ is

$$\mathbb{D}_M := \{D \in \mathbb{D} \mid \text{supp } D \subseteq M\}.$$

Similarly, the set of all distributions with point support at $\tau \in \mathbb{R}$ is

$$\mathbb{D}_{\{\tau\}} = \{D \in \mathbb{D} \mid \text{supp } D \subseteq \{\tau\}\}.$$

Theorem 3.20

Note that a distribution D_τ has point support $\{\tau\}$ if and only if there exist $c_0, \dots, c_{d_\tau} \in \mathbb{R}$, $d_\tau \in \mathbb{N}$ such that

$$D_\tau = \sum_{i=0}^{d_\tau} c_i \delta_\tau^{(i)}, \quad (3.3)$$

where $\delta_\tau^{(k)}$ is the k -th derivative of the Dirac impulse δ_τ at $\tau \in T$, [30].

3.4 The space $\mathbb{D}_{\text{pw}C^\infty}(T)$ of piecewise smooth distributions**Definition 3.21: Piecewise-smooth functions**

Let $T \subseteq \mathbb{R}$ be an open set. A function $\alpha : T \rightarrow \mathbb{R}$ is called piecewise-smooth if and only if

$$\alpha = \sum_{i \in \mathbb{Z}} (\alpha_i)_{[\tau_i, \tau_{i+1})}, \quad (3.4)$$

where the functions $\alpha_i : T \rightarrow \mathbb{R}$, $i \in \mathbb{Z}$, are (globally) smooth and the set $\{\tau_i \in T \mid i \in \mathbb{Z}\}$ is an ordered discrete set, i.e. $\tau_i < \tau_{i+1}$ for all $i \in \mathbb{Z}$ and the intersection with any compact subset of T only contains finitely many points. The set of all piecewise-smooth functions is denoted by $C_{\text{pw}}^\infty(T; \mathbb{R})$.

Definition 3.22: Piecewise-smooth distributions, [130]

A distribution $D \in \mathbb{D}(T)$ is called *piecewise-smooth* if

$$D = \alpha_{\mathbb{D}} + \sum_{\tau \in \Delta} D_\tau, \quad (3.5)$$

where $\alpha \in C_{\text{pw}}^\infty(T; \mathbb{R})$, $\Delta \subseteq T$ is a finite discrete set, $T \subseteq \mathbb{R}$ is an open set and D_τ has a point support; i.e., $\text{supp} D_\tau \subseteq \{\tau\}$ for all $\tau \in \Delta$. The space of all piecewise-smooth distributions is denoted by $\mathbb{D}_{\text{pw}C^\infty}(T)$.

In Figure 3.1, an illustration of a piecewise-smooth distribution with the representation (3.5) is shown.

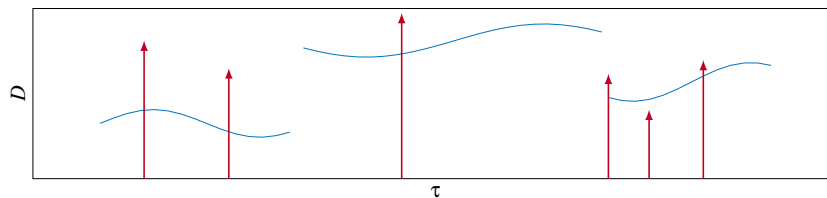


FIGURE 3.1: A visualisation of a distribution $D \in \mathbb{D}_{\text{pw}C^\infty}(T)$ having the representation $D = \alpha_{\mathbb{D}} + \sum_{\tau \in \Delta} D_\tau$ with different magnitudes of Dirac impulses (red arrows) and a piecewise-smooth function α (blue).

It is easily seen that the space of piecewise-smooth distributions $\mathbb{D}_{\text{pw}C^\infty}(T)$ is closed with respect to differentiation and contains the space of piecewise-smooth functions $C_{\text{pw}}^\infty(T; \mathbb{R})$ as a subspace.

Definition 3.23: Pointwise evaluation, [130]

For $D \in \mathbb{D}_{\text{pw}C^\infty}(T)$, where D is of the form (3.5), the *left* and *right sided evaluations* at $\tau \in \mathbb{R}$ are

$$D(\tau^-) := \lim_{\varepsilon \rightarrow 0} \alpha(\tau - \varepsilon), \quad D(\tau^+) := \lim_{\varepsilon \rightarrow 0} \alpha(\tau + \varepsilon),$$

where $\varepsilon > 0$.

Definition 3.24: Impulsive and regular parts, [130]

For any piecewise-smooth distribution $D \in \mathbb{D}_{\text{pw}C^\infty}(T)$ of the form (3.5), the *impulsive part of D at τ* and *impulsive part of D* are defined as, [130],

$$D[\tau] := \begin{cases} D_\tau, & \tau \in \Delta, \\ 0, & \tau \notin \Delta, \end{cases}$$

and

$$D[\cdot] := \sum_{\tau \in \Delta} D[\tau] = \sum_{\tau \in \Delta} D_\tau,$$

respectively. The *regular part of D* is defined as

$$D_{\text{reg}} := \alpha_{\mathbb{D}} = D - D[\cdot].$$

Remark 3.25

For a distribution $D \in \mathbb{D}_{\text{pw}C^\infty}(T)$, Definition 3.23 and 3.24 for left- and right-sided evaluations and impulsive part are well-defined, [130]. To see this, consider $D^1, D^2 \in \mathbb{D}_{\text{pw}C^\infty}(T)$ with

$$D^1 = (\alpha^1)_{\mathbb{D}} + \sum_{\tau \in \Delta_1} D_\tau^1 \quad \text{and} \quad D^2 = (\alpha^2)_{\mathbb{D}} + \sum_{\tau \in \Delta_2} D_\tau^2.$$

Then the following holds

$$D^1 = D^2 \iff \begin{cases} \alpha^1 = \alpha^2, \\ D_\tau^1 = D_\tau^2, & \forall \tau \in \Delta_1 \cap \Delta_2, \\ D_\tau^1 = 0, & \forall \tau \in \Delta_1 \setminus \Delta_2, \\ D_\tau^2 = 0, & \forall \tau \in \Delta_2 \setminus \Delta_1, \end{cases}$$

which justifies the claims.

Proposition 3.26: Derivative of piecewise-smooth distributions, [131]

For $D \in \mathbb{D}_{\text{pw}C^\infty}(T)$ of the form

$$D = \alpha_{\mathbb{D}} + \sum_{\tau \in \Delta} D_\tau, \quad \text{with} \quad \alpha = \sum_{i \in \mathbb{Z}} (\alpha_i)_{[\tau_i, \tau_{i+1})}, \quad (3.6)$$

the derivative of D is

$$D' = \left(\sum_{i \in \mathbb{Z}} (\alpha'_i)_{[\tau_i, \tau_{i+1})} \right)_{\mathbb{D}} + \sum_{i \in \mathbb{Z}} (D(\tau_i^+) - D(\tau_i^-)) \delta_{\tau_i} + D[\cdot]'$$

If $D \in \mathbb{D}_{\text{pw}C^\infty}(T)$, then $D' \in \mathbb{D}_{\text{pw}C^\infty}(T)$.

Proposition 3.27

Piecewise-smooth distributions have unique antiderivatives in $\mathbb{D}_{\text{pw}C^\infty}(T)$, [78, 131],

$$F = \int_{\tau_0} D, \text{ where } D \in \mathbb{D}_{\text{pw}C^\infty}(T), \tau_0 \in \mathbb{R},$$

such that $F' = D$ and $F(\tau_0^-) = 0$.

A distribution is piecewise-smooth if and only if locally it is equal to a finite derivative of a piecewise-smooth function, [130], in other words, for all $D \in \mathbb{D}_{\text{pw}C^\infty}(T)$ and all compact subsets $K \subseteq T \subseteq \mathbb{R}$ there exist $k \in \mathbb{N}$ and $\alpha \in C_{\text{pw}}^\infty(T; \mathbb{R})$ such that

$$D(\varphi) = (\alpha_{\mathbb{D}})^{(k)}(\varphi) \quad \forall \varphi \in C_0^\infty(T; \mathbb{R}) \text{ with } \text{supp } \varphi \subseteq K.$$

Definition 3.28: Distributional restriction

Let $D \in \mathbb{D}_{\text{pw}C^\infty}(T)$, as in Definition 3.22 and $M \subseteq \mathbb{R}$ an interval. The *distributional restriction* D_M of D on M is defined as, [131],

$$D_M := (\alpha_M)_{\mathbb{D}} + \sum_{\tau \in \Delta \cap M} D_\tau. \quad (3.7)$$

Hence, $\alpha_M \in C_{\text{pw}}^\infty(T; \mathbb{R})$. Furthermore, $\Delta \cap M$ is a finite discrete set; thus, D_M is a well-defined distribution. Distributional restriction D_M satisfies the following properties

(R-1): $D_M \subseteq (\mathbb{D}_{\text{pw}C^\infty}(T))_{\text{cl}M}$, for each $D \in \mathbb{D}_{\text{pw}C^\infty}(T)$ and is a projection for any fixed M .

(R-2): For $f \in C_{\text{pw}}^\infty(T; \mathbb{R})$, it holds that

$$(f_M)_{\mathbb{D}} = (f_{\mathbb{D}})_M.$$

(R-3): For every $\varphi \in C_0^\infty(T; \mathbb{R})$, $D \in \mathbb{D}_{\text{pw}C^\infty}(T)$ and $M \subseteq \mathbb{R}$,

$$\begin{aligned} \text{supp } \varphi \subseteq M &\Rightarrow D_M(\varphi) = D(\varphi), \\ \text{supp } \varphi \cap M = \emptyset &\Rightarrow D_M(\varphi) = 0. \end{aligned}$$

(R-4): For any $D \in \mathbb{D}_{\text{pw}C^\infty}(T)$,

$$D_M = \sum_{i \in \mathbb{N}} D_{M_i},$$

where M_i , for $i \in \mathbb{N}$, are pairwise disjoint union of a countable family of intervals such that $M := \bigcup_{i \in \mathbb{N}} M_i$. Moreover, for any pairwise disjoint sets $M_i, M_j \subseteq \mathbb{R}$,

with $i \neq j$, it holds that

$$(D_{M_i})_{M_j} = 0.$$

Corollary 3.29: Restrictions and derivatives, [131]

Let $T \subseteq \mathbb{R}$. For any $D \in \mathbb{D}_{\text{pw}C^\infty}(T)$

$$\begin{aligned} (D_{[\tau_1, \tau_2]})' &= (D')_{[\tau_1, \tau_2]} + D(\tau_1^-)\delta_{\tau_1} - D(\tau_2^-)\delta_{\tau_2}, \\ (D_{(\tau_1, \tau_2)})' &= (D')_{(\tau_1, \tau_2)} + D(\tau_1^+)\delta_{\tau_1} - D(\tau_2^-)\delta_{\tau_2}, \\ (D_{(\tau_1, \tau_2]})' &= (D')_{(\tau_1, \tau_2]} + D(\tau_1^+)\delta_{\tau_1} - D(\tau_2^+)\delta_{\tau_2}, \\ (D_{[\tau_1, \tau_2)})' &= (D')_{[\tau_1, \tau_2)} + D(\tau_1^-)\delta_{\tau_1} - D(\tau_2^+)\delta_{\tau_2}, \end{aligned}$$

where $\tau_1, \tau_2 \in [-\infty, \infty]$ and $\delta_{\mp\infty} = 0$.

Theorem 3.30

Properties **(R-1)**-**(R-4)** cannot be satisfied simultaneously by arbitrary distributions in \mathbb{D} , [130].

Example 3.31

Let $D \in \mathbb{D}$ given by

$$D : \varphi \mapsto \sum_{i=0}^{\infty} d_n \varphi(d_n),$$

where $d_n := \frac{(-1)^n}{n+1}$, $n \in \mathbb{N}$. The restriction of D to $(0, \infty)$ is not well-defined as the sum does not converge, although the distribution D is well-defined. See [130] for details and proof of Theorem 3.30.

Remark 3.32

It is impossible to define multiplication of any distributions within the space of distributions \mathbb{D} , [109]. Even if the distributions are induced by locally integrable functions, the product of these functions does not necessarily have to be locally integrable. For example, consider the function $f(\tau) = \frac{1}{\sqrt{|\tau|}} \in L^1_{\text{loc}}$ whose multiplication with itself $f^2(\tau) = \frac{1}{|\tau|} \notin L^1_{\text{loc}}$. On the other hand, within the space $\mathbb{D}_{\text{pw}C^\infty}(T)$, an associative multiplication of two distributions is defined by the *Fuchsteiner multiplication*, [13, 52, 130], yet this multiplication is not commutative.

Definition 3.33

Assume $D, E \in \mathbb{D}_{\text{pw}C^\infty}(T)$, with the representations

$$D = \alpha_{\mathbb{D}} + \sum_{\tau \in \Delta_D} D[\tau], \quad E = \beta_{\mathbb{D}} + \sum_{\tau \in \Delta_E} E[\tau],$$

as in Definition 3.22. Using (3.3) and (3.9), the multiplication of D and E is given by, [131],

$$DE = (\alpha\beta)_{\mathbb{D}} + \sum_{\tau \in \Delta_E} \alpha_{\mathbb{D}} E[\tau] + \sum_{\tau \in \Delta_D} D[\tau] \beta_{\mathbb{D}}.$$

Proposition 3.34: Multiplication and restriction, [130]

For any $D, E \in \mathbb{D}_{\text{pw}\mathcal{C}^\infty}(T)$, $\tau_1 \leq \tau_2 \in \mathbb{R} \cup \{\mp\infty\}$, $\varepsilon > 0$

$$\begin{aligned} (DE)_{(\tau_1, \tau_2)} &= D_{(\tau_1, \tau_2)} E_{(\tau_1, \tau_2)}, \\ (DE)_{[\tau_1, \tau_2]} &= D_{[\tau_1, \tau_2]} E_{[\tau_1, \tau_2]} + D[\tau_1] E_{(\tau_1 - \varepsilon, \tau_1)}, \\ (DE)_{(\tau_1, \tau_2]} &= D_{(\tau_1, \tau_2]} E_{(\tau_1, \tau_2]} + D_{(\tau_2, \tau_2 + \varepsilon)} E[\tau_2], \\ (DE)_{[\tau_1, \tau_2]} &= D_{[\tau_1, \tau_2]} E_{[\tau_1, \tau_2]} + D_{(\tau_2, \tau_2 + \varepsilon)} E[\tau_2] + D[\tau_1] E_{(\tau_1 - \varepsilon, \tau_1)}, \end{aligned}$$

with $D[\mp\infty] = 0$, $E[\mp\infty] = 0$.

Definition 3.35: Multiplication of a distribution with the Dirac impulse, [131]

Let $D \in \mathbb{D}_{\text{pw}\mathcal{C}^\infty}(T)$ with the representation (3.5) and $\tau \in \Delta$. The multiplication of D with δ_τ from the left and right are defined by

$$\begin{aligned} \delta_\tau D &:= D(\tau^-) \delta_\tau, \\ D \delta_\tau &:= D(\tau^+) \delta_\tau, \end{aligned} \tag{3.9}$$

and, exploiting (3.2), the following relations can be deduced inductively

$$\begin{aligned} \delta_\tau^{(k+1)} D &:= \left(\delta_\tau^{(k)} D \right)' - \delta_\tau^{(k)} D', \quad \forall k \in \mathbb{N}, \\ D \delta_\tau^{(k+1)} &:= \left(D \delta_\tau^{(k)} \right)' - D' \delta_\tau^{(k)}, \quad \forall k \in \mathbb{N}. \end{aligned}$$

Remark 3.36

The multiplication with distributions does not commute; i.e., $DE \neq ED$, for $D, E \in \mathbb{D}_{\text{pw}\mathcal{C}^\infty}(T)$, [130].

Example 3.37

Consider the multiplication of the Heaviside function $(H_\tau)_{\mathbb{D}}$ with the Dirac impulse δ_τ

$$\delta_\tau (H_\tau)_{\mathbb{D}} = 0 \neq \delta_\tau = (H_\tau)_{\mathbb{D}} \delta_\tau.$$

Chapter 4

Switched differential algebraic equations

Differential equations are appropriate tools to model dynamical systems of physical mechanisms. However, if the physical system to be modeled has any constraints, such as conservation laws, then the mathematical model of the process admits algebraic constraints, as well. Such systems are called *differential algebraic equations* (DAEs), which have a general form

$$\mathbf{F}(t, \dot{\mathbf{w}}, \mathbf{w}) = \mathbf{0}, \quad (4.1)$$

where \mathbf{w} is the unknown to be determined of the system, $\mathbf{F} : \mathbb{R} \times \mathbb{R}^m \times \mathbb{R}^m \rightarrow \mathbb{R}^n$, $m, n \in \mathbb{N}$.

DAE systems with a switching signal governing the transitions between these systems lead to switched DAEs (swDAEs). Switched DAEs are used to model electrical networks [89, 124], complementary metal-oxide-semiconductor ring oscillator [92], power systems [134], lumped parameter models [99], gas supply networks [66], water flow networks [77, 114] and district heating systems [65]. For physical processes are fundamentally nonlinear and time-variant, certain simplifications are typically imposed while modelling these systems. Nevertheless, the simplified model needs to serve sufficiently accurate performance to properly exhibit actual behaviors of the physical system while maintaining essential properties of the system. In this chapter, a brief overview on linear switched differential algebraic equations is provided where the considered swDAE is of the form

$$\mathbf{E}_\sigma \dot{\mathbf{w}} = \mathbf{H}_\sigma \mathbf{w} + \mathbf{f}_\sigma, \quad (4.2)$$

where $\mathbf{E}_\xi, \mathbf{H}_\xi \in \mathbb{R}^{n \times m}$, $\mathbf{f}_\xi : \mathbb{R} \rightarrow \mathbb{R}^n$ for $\xi = 1, 2, \dots, N$ and the switching signal $\sigma : \mathbb{R} \rightarrow \{1, 2, \dots, N\}$, $N \in \mathbb{N}$, denotes switches between DAE systems. Moreover, the matrix \mathbf{E}_ξ can be singular. On the other hand, if the matrix \mathbf{E}_ξ is invertible for every ξ , then one obtains a switched ODE system by multiplying Equation (4.2) with the inverse of \mathbf{E}_ξ ; i.e., \mathbf{E}_ξ^{-1} , on the left.

4.1 Mathematical structure

Consider the swDAE of the form

$$\mathbf{E}_\sigma \dot{\mathbf{w}}(t) = \mathbf{H}_\sigma \mathbf{w}(t) + \mathbf{B}_\sigma \mathbf{q}(t) + \mathbf{f}(t), \quad (4.3)$$

with the output $\mathbf{y}_D(t) := \mathbf{C}_{D_{\sigma(t)}} \mathbf{w}(t)$, where $\mathbf{w} : [t_0, \infty) \rightarrow \mathbb{R}^m$, $m \in \mathbb{N}$ is the state variable of the system, $\sigma : \mathbb{R} \rightarrow \{1, 2, \dots, N\}$, $N \in \mathbb{N}$, is a piecewise constant switching signal with a locally finite set of jump points and is right-continuous, $\mathbf{E}_\xi, \mathbf{H}_\xi \in \mathbb{R}^{n \times m}$ for each $\xi \in \{1, 2, \dots, N\}$ and $\mathbf{f} : [t_0, \infty) \rightarrow \mathbb{R}^m$ is some inhomogeneity, $\mathbf{B}_\xi \in \mathbb{R}^{m \times v}$, $\mathbf{q} : [t_0, \infty) \rightarrow \mathbb{R}^v$ is the input, $\mathbf{y}_D :$

$[t_0, \infty) \rightarrow \mathbb{R}^{m_1}$, $m_1 \in \mathbb{N}$, $\mathbf{C}_{D_\xi} \in \mathbb{R}^{m_1 \times m}$. Note that the matrix \mathbf{E}_ξ is not assumed to be non-singular.

Definition 4.1: Classical solution

Let $\mathbf{w} \in \mathbf{C}((t_0, \infty); \mathbb{R}^m)$ be any differentiable function. If \mathbf{w} satisfies the system (4.3) for all $t > t_0$, it is called a *classical solution*.

For the existence and uniqueness of solutions to (4.3), the following definition of regularity of matrix pairs will be employed.

Definition 4.2: Regularity of a matrix pair

The matrix pencil $s\mathbf{E}_\xi - \mathbf{H}_\xi \in \mathbb{R}^{n \times m}[s]$, $\xi \in \{1, 2, \dots, N\}$, $N \in \mathbb{N}$, is called *regular* if and only if $n = m$ and $\det(s\mathbf{E}_\xi - \mathbf{H}_\xi)$ is not the zero polynomial. The matrix pair $(\mathbf{E}_\xi, \mathbf{H}_\xi)$ and the corresponding mode ξ for the swDAE (4.3) are called regular if $s\mathbf{E}_\xi - \mathbf{H}_\xi$ is regular.

Definition 4.3: Nilpotency index, [81]

Let $\mathbf{N} \in \mathbb{R}^{m \times m}$ be any matrix. The nilpotency index $\nu \in \mathbb{N}$ of the matrix \mathbf{N} is the minimum value such that $\mathbf{N}^\nu = \mathbf{0}$.

Definition 4.4: Index of DAEs, [8]

Consider the following DAE

$$\mathbf{E}\dot{\mathbf{w}} = \mathbf{H}\mathbf{w} + \mathbf{f}, \quad (4.4)$$

where $\mathbf{E}, \mathbf{H} \in \mathbb{R}^{m \times m}$, $\mathbf{f} \in \mathbb{R}^m$ and (\mathbf{E}, \mathbf{H}) is regular. The *index* of the DAE (4.4) is the smallest number of the steps taken to analytically differentiate the DAE in order to have an explicit ODE system for every unknown of the DAE.

Note that switched DAEs are formulated by using DAEs without switches of the form (4.4) for each mode. In the following, the explicit solution formula for the DAEs will be presented. To this end, following [14, 55, 132, 135], quasi-Weierstrass form of a regular matrix pair (\mathbf{E}, \mathbf{H}) and its consistency projector, differential and impulse selectors are defined.

Theorem 4.5: Quasi-Weierstrass form, [14, 135]

Assume $(\mathbf{E}, \mathbf{H}) \in \mathbb{R}^{m \times m}$ is a regular matrix pair. There exist invertible matrices $\mathbf{S} \in \mathbb{R}^{m \times m}$ and $\mathbf{T} \in \mathbb{R}^{m \times m}$ which forms the matrix pair (\mathbf{E}, \mathbf{H}) into the *quasi-Weierstrass form*

$$(\mathbf{SET}, \mathbf{SHT}) = \left(\begin{bmatrix} \mathbf{I} & \mathbf{0} \\ \mathbf{0} & \mathbf{N} \end{bmatrix}, \begin{bmatrix} \mathbf{J} & \mathbf{0} \\ \mathbf{0} & \mathbf{I} \end{bmatrix} \right), \quad (4.5)$$

where $\mathbf{J} \in \mathbb{R}^{p \times p}$, $p \in \mathbb{N}$, $\mathbf{N} \in \mathbb{R}^{k \times k}$ is nilpotent, and $k = m - p$.

For later use, let $\mathbf{S}_1 \in \mathbb{R}^{p \times m}$ and $\mathbf{S}_2 \in \mathbb{R}^{k \times m}$ such that

$$\begin{pmatrix} \mathbf{S}_1 \\ \mathbf{S}_2 \end{pmatrix} = \mathbf{S}, \quad (4.6)$$

where \mathbf{S} is the invertible matrix given as in Theorem 4.5. To evaluate the invertible matrices $\mathbf{S}, \mathbf{T} \in \mathbb{R}^{m \times m}$ in Theorem 4.5, *Wong sequences* can be employed, [14, 140], as described in the following theorem.

Theorem 4.6: Wong sequences, [14, 140]

Let (\mathbf{E}, \mathbf{H}) be a regular matrix pair. The Wong sequences $\mathcal{V}_k, \mathcal{W}_k$ are defined as

$$\begin{aligned} \mathcal{V}_0 &:= \mathbb{R}^m, & \mathcal{V}_{i+1} &:= \mathbf{H}^{-1}(\mathbf{E}\mathcal{V}_i), & i &= 0, 1, 2, \dots, \\ \mathcal{W}_0 &:= \{0\}, & \mathcal{W}_{j+1} &:= \mathbf{E}^{-1}(\mathbf{H}\mathcal{W}_j), & j &= 0, 1, 2, \dots \end{aligned} \quad (4.7)$$

From (4.7), it can be concluded that $\mathcal{V}_{i+1} \subseteq \mathcal{V}_i, \mathcal{W}_{j+1} \supseteq \mathcal{W}_j$ and there exist $i^*, j^* \in \{0, 1, \dots, N\}$ such that

$$\mathcal{V}^* := \bigcap_{i \in \mathbb{N}} \mathcal{V}_i = \mathcal{V}_{i^*}, \quad \mathcal{W}^* := \bigcup_{j \in \mathbb{N}} \mathcal{W}_j = \mathcal{W}_{j^*}.$$

Let \mathbf{V}, \mathbf{W} be any full rank matrices such that $\text{im}\mathbf{V} = \mathcal{V}^*$ and $\text{im}\mathbf{W} = \mathcal{W}^*$. By defining $\mathbf{T} := [\mathbf{V}, \mathbf{W}]$ and $\mathbf{S} := [\mathbf{E}\mathbf{V}, \mathbf{H}\mathbf{W}]^{-1}$, for which both \mathbf{T}^{-1} and \mathbf{S}^{-1} exist, the quasi-Weierstrass form of (\mathbf{E}, \mathbf{H}) can be achieved.

Remark 4.7

By applying the quasi-Weierstrass form, the DAE (4.4) is decoupled into an ODE and a pure DAE part

$$\begin{aligned} \text{ODE: } \quad \dot{\mathbf{w}}_1 &= \mathbf{J}\mathbf{w}_1 + \mathbf{f}_1, \\ \text{DAE: } \quad \mathbf{N}\dot{\mathbf{w}}_2 &= \mathbf{w}_2 + \mathbf{f}_2, \end{aligned}$$

where \mathbf{N} is nilpotent, $\mathbf{T}^{-1}\mathbf{w} = (\mathbf{w}_1^\top, \mathbf{w}_2^\top)^\top$ and $\mathbf{S}\mathbf{f} = (\mathbf{f}_1^\top, \mathbf{f}_2^\top)^\top$.

Definition 4.8: Consistency projector, differential and impulse selectors, [121, 138]

For a regular matrix pair (\mathbf{E}, \mathbf{H}) with $\mathbf{E}, \mathbf{H} \in \mathbb{R}^{m \times m}$, its *consistency projector*, *differential* and *impulse selectors* are respectively defined as

$$\begin{aligned} \Pi_{(\mathbf{E}, \mathbf{H})} &:= \mathbf{T} \begin{bmatrix} \mathbf{I}_{p \times p} & \mathbf{0} \\ \mathbf{0} & \mathbf{0} \end{bmatrix} \mathbf{T}^{-1}, \\ \Pi_{(\mathbf{E}, \mathbf{H})}^{\text{diff}} &:= \mathbf{T} \begin{bmatrix} \mathbf{I}_{p \times p} & \mathbf{0} \\ \mathbf{0} & \mathbf{0} \end{bmatrix} \mathbf{S}, \quad \Pi_{(\mathbf{E}, \mathbf{H})}^{\text{imp}} := \mathbf{T} \begin{bmatrix} \mathbf{0} & \mathbf{0} \\ \mathbf{0} & \mathbf{I}_{k \times k} \end{bmatrix} \mathbf{S}, \end{aligned} \quad (4.8)$$

where $p + k = m$ and $\mathbf{S}, \mathbf{T} \in \mathbb{R}^{m \times m}$ are transformation matrices of the matrix pair (\mathbf{E}, \mathbf{H}) in order to obtain its quasi-Weierstrass form which can be obtained from Wong sequences.

Remark 4.9

The consistency projector, differential and impulse selectors defined in (4.8) do not depend on the choice of \mathbf{S} or \mathbf{T} , [130].

Theorem 4.10: Explicit solution formula, [132]

All (classical) solutions to (4.4) with a regular matrix pair (\mathbf{E}, \mathbf{H}) , for sufficiently smooth \mathbf{f} and for some $\bar{\mathbf{w}}_0 \in \mathbb{R}^m$ have the form

$$\begin{aligned} \mathbf{w}(t) = & e^{\mathbf{H}^{\text{diff}}(t-t_0)} \Pi_{(\mathbf{E}, \mathbf{H})} \bar{\mathbf{w}}_0 + \int_{t_0}^t e^{\mathbf{H}^{\text{diff}}(t-s)} \Pi_{(\mathbf{E}, \mathbf{H})}^{\text{diff}} \mathbf{f}(s) ds \\ & - \sum_{i=0}^{n-1} (\mathbf{E}^{\text{imp}})^i \Pi_{(\mathbf{E}, \mathbf{H})}^{\text{imp}} \mathbf{f}^{(i)}(t), \end{aligned} \quad (4.9)$$

where $\Pi_{(\mathbf{E}, \mathbf{H})}$ is the consistency projector, $\Pi_{(\mathbf{E}, \mathbf{H})}^{\text{diff}}$, $\Pi_{(\mathbf{E}, \mathbf{H})}^{\text{imp}}$ are differential and impulse selectors of (\mathbf{E}, \mathbf{H}) as in (4.8) and

$$\mathbf{H}^{\text{diff}} = \Pi_{(\mathbf{E}, \mathbf{H})}^{\text{diff}} \mathbf{H}, \quad \mathbf{E}^{\text{imp}} = \Pi_{(\mathbf{E}, \mathbf{H})}^{\text{imp}} \mathbf{E}, \quad (4.10)$$

and for every $\bar{\mathbf{w}}_0$, the initial value $\mathbf{w}(t_0) \in \mathbb{R}^m$ of the DAE (4.4) is given by

$$\mathbf{w}(t_0) = \Pi_{(\mathbf{E}, \mathbf{H})} \bar{\mathbf{w}}_0 - \sum_{i=0}^{n-1} (\mathbf{E}^{\text{imp}})^i \Pi_{(\mathbf{E}, \mathbf{H})}^{\text{imp}} \mathbf{f}^{(i)}(t_0),$$

where the solution \mathbf{w} is given by the formula (4.9).

Note that if the inhomogeneity $\mathbf{f} \in (\mathbb{D}_{\text{pw}C^\infty}(T))^m$ includes jumps or Dirac impulses, the antiderivative \mathbf{F} of the term $\phi(\cdot, t_0)_{\mathbb{D}}^{-1} \Pi_{(\mathbf{E}, \mathbf{H})}^{\text{diff}} \mathbf{f}$, where $\phi(\cdot, t_0) = e^{\mathbf{H}^{\text{diff}}(\cdot - t_0)}$, has to be defined such that

$$\mathbf{F} = \int_{t_0} \phi(\cdot, t_0)_{\mathbb{D}}^{-1} \Pi_{(\mathbf{E}, \mathbf{H})}^{\text{diff}} \mathbf{f},$$

where $\phi(\cdot, t_0)^{-1} := \phi(t_0, \cdot)$ and

$$\mathbf{F}' = \phi(\cdot, t_0)_{\mathbb{D}}^{-1} \Pi_{(\mathbf{E}, \mathbf{H})}^{\text{diff}} \mathbf{f} \quad \text{and} \quad \mathbf{F}(t_0^-) = 0,$$

so that the solution formula (4.9) is still valid.

4.2 Distributional swDAEs

As can be seen from the solution formula (4.9), the initial value $\mathbf{w}(t_0)$ for the DAE (4.4) cannot be prescribed arbitrarily. Therefore, prescribed initial conditions might be inconsistent for the DAE system description. Systems that have such *inconsistent initial values* may contain jumps and Dirac impulses in the solution. Furthermore, swDAEs might also lead to inconsistent initial values for its DAE subsystems within the system while changing its modes. However, to find solutions to inconsistent initial value problems within the space \mathbb{R}^m is not feasible. Therefore, the solution space must be carefully chosen so that it contains distributions. Indeed, a proper solution space which allows to include distributions is the space of piecewise-smooth distributions $\mathbb{D}_{\text{pw}C^\infty}(T)$ given in Definition 3.22. So, the unknown \mathbf{w} and the inhomogeneity \mathbf{f}_σ in (4.3) are vectors of distributions in $\mathbb{D}_{\text{pw}C^\infty}(T)$; i.e., $\mathbf{w}, \mathbf{f}_\sigma \in (\mathbb{D}_{\text{pw}C^\infty}(T))^m$. On the other hand, conceptually, it does not suffice merely to change the solution space, as neither might classical nor distributional solutions exist, for distributions cannot be evaluated at a certain point. In other words, from a distributional point of view $\mathbf{w}(t_0) = \mathbf{w}_0$ has no meaning. Even if distributions could be evaluated at initial times,

inconsistent initial values would not be allowed. To illustrate, consider the following DAE

$$\mathbf{E}\dot{\mathbf{w}} = \mathbf{H}\mathbf{w} + \mathbf{f}$$

with $\mathbf{E} = \mathbf{0}$, $\mathbf{H} = \mathbf{I}$ and $\mathbf{f} = \mathbf{0}$. The only (distributional) solution is $\mathbf{w} = \mathbf{0}$. Hence, any non-zero initial value will not yield a solution. Thus, the notion of a solution to such inconsistent initial value problems needs to be developed so that a distributional solution exists in the space $\mathbb{D}_{\text{pw}\mathcal{C}^\infty}(T)$. The idea of how to describe distributional solutions to inconsistent initial value problems in a proper way is that: Assume that the considered DAE gets activated at $t_0 \in \mathbb{R}$, and before t_0 the DAE can be inactive or governed by different conditions. There cannot exist any inconsistent initial values at any t_μ after t_0 . To this end, the so-called initial trajectory problem (ITP) arises

$$\begin{aligned} \mathbf{w}_{(-\infty, t_0)} &= \mathbf{w}_{(-\infty, t_0)}^{t_0}, \\ (\mathbf{E}\dot{\mathbf{w}})_{[t_0, \infty)} &= (\mathbf{H}\mathbf{w} + \mathbf{f})_{[t_0, \infty)}, \end{aligned} \quad (4.11)$$

where $\mathbf{w}^{t_0} : (-\infty, t_0) \rightarrow \mathbb{R}^m$ is an initial trajectory. However, if the initial value $\mathbf{w}^{t_0}(t_0)$ is inconsistent for the ITP, the solution will be in $\mathbb{D}_{\text{pw}\mathcal{C}^\infty}(T)$, and so are the components of the ITP (4.11) and initial trajectory.

Theorem 4.11: Unique solution to the ITP, [130]

Consider the ITP (4.11) with a regular matrix pair (\mathbf{E}, \mathbf{H}) . Let the quasi-Weierstrass form of (\mathbf{E}, \mathbf{H}) be given by (4.5), where the matrix \mathbf{N} has the nilpotency index $\nu \in \mathbb{N}$. Then for any initial trajectory $\mathbf{w}^{t_0} \in (\mathbb{D}_{\text{pw}\mathcal{C}^\infty}(T))^m$ and any inhomogeneity $\mathbf{f} \in (\mathbb{D}_{\text{pw}\mathcal{C}^\infty}(T))^m$ there exists a unique solution to the ITP. Assume that the inhomogeneity \mathbf{f} is $\nu - 1$ times differentiable on (t_0, ∞) and $\mathbf{f}_{(-\infty, t_0)} = \mathbf{0}$. The unique solution $\mathbf{w} \in (\mathbb{D}_{\text{pw}\mathcal{C}^\infty}(T))^m$ on (t_0, ∞) is given by the formula (4.9). Furthermore, the impulse at t_0 is

$$\mathbf{w}[t_0] = \sum_{i=0}^{\nu-2} (\mathbf{E}^{\text{imp}})^{i+1} (\mathbf{w}(t_0^+) - \mathbf{w}^{t_0}(t_0^-)) \delta^{(i)}$$

where

$$\mathbf{w}(t_0^+) = \Pi_{(\mathbf{E}, \mathbf{H})} \mathbf{w}^{t_0}(t_0^-) - \sum_{i=0}^{\nu-2} (\mathbf{E}^{\text{imp}})^i \Pi_{(\mathbf{E}, \mathbf{H})}^{\text{imp}} \mathbf{f}^{(i)}(t_0^+),$$

where \mathbf{E}^{imp} is given as in Equation (4.10) and Π^{imp} is the impulse selector.

The following existence and uniqueness result follows from the fact that swDAEs are considered as a set of ITPs which get activated successively.

Theorem 4.12: Existence and uniqueness, [130]

Consider the switched DAE given in (4.3) with regular matrix pairs $(\mathbf{E}_\xi, \mathbf{H}_\xi)$ for $\xi \in \{1, 2, \dots, N\}$ and assume for the switching signal σ

$$\sigma \in \left\{ \sigma : \mathbb{R} \rightarrow \{1, 2, \dots, N\} \left| \begin{array}{l} \sigma \text{ has locally finitely} \\ \text{many switches,} \\ \sigma_{(-\infty, t_0)} \text{ is constant} \end{array} \right. \right\}, \quad (4.12)$$

where the switching times are the initial times for the ITP (4.11). Then, for every initial trajectory $\mathbf{w}^{t_0} \in (\mathbb{D}_{\text{pw}\mathcal{C}^\infty}(T))^m$ with the initial time $t_0 \in \mathbb{R}$ and any inhomogeneity

$\mathbf{f} \in (\mathbb{D}_{\text{pw}C^\infty}(T))^m$, there exists a globally defined solution $\mathbf{w} \in (\mathbb{D}_{\text{pw}C^\infty}(T))^m$ which is uniquely given by $\mathbf{w}^{t_0}(t_0^-)$.

Remark 4.13

The condition in (4.12) that σ has locally finitely many switches is significant. Consider a swDAE (4.3) whose switching signal does not fulfill the condition that it has locally finitely many switches. Assume $\mathbf{w} \in (\mathbb{D}_{\text{pw}C^\infty}(T))^m$ with a point support is the solution to the considered swDAE. However, the infinite sum of \mathbf{w} might diverge. Or even if it is a well-defined distribution, its restriction to an interval may fail to be well-defined. This remark is also the reasoning behind the idea that Δ in Definition 3.22 is a finite discrete set.

Chapter 5

Coupling hyperbolic balance laws with switched DAEs of index one

In this chapter, the well-posedness of coupled switched systems consisting of semi-linear hyperbolic balance laws and switched DAEs is studied. Since solutions to DAEs whose index is more than one are in general distributions, they do not have the minimum regularity that nonlinear source terms of hyperbolic PDEs require. Therefore, only the special case of swDAEs of index one is considered. By employing an iterative converging procedure that is based on the solutions to PDEs and DAEs, the well-posedness of such systems is proven. Broad solutions, [24], which are based on the concept of characteristic curves, will be of use concerning hyperbolic balance laws. Then, the well-posedness of the coupled system is shown.

5.1 Coupled system

In this section, the following coupled system is considered, where a semi-linear hyperbolic balance law on a bounded interval has the form

$$\partial_t \mathbf{u}(t, x) + \mathbf{A}_\sigma(t, x) \partial_x \mathbf{u}(t, x) = \mathbf{s}_\sigma(t, x, \mathbf{u}(t, x)), \quad (5.1a)$$

where $\mathbf{u} : [0, T] \times [0, 1] \rightarrow \mathbb{R}^n$, $n \in \mathbb{N}$, is the n -dimensional vector of unknowns of the PDE, $\mathbf{A}_\xi : [0, T] \times [0, 1] \rightarrow \mathbb{R}^{n \times n}$, $\xi = 1, 2, \dots, N$, $\mathbf{s}_\xi \in \mathbb{R}^n$ is a source term, the switching signal $\sigma : \mathbb{R} \rightarrow \{1, 2, \dots, N\}$, $N \in \mathbb{N}$ denotes the switches. The boundary conditions of the PDE have the form

$$\mathbf{P}_\sigma(t) \begin{pmatrix} \mathbf{u}(t, 0^+) \\ \mathbf{u}(t, 1^-) \end{pmatrix} = \mathbf{P}_{\mathbf{w}, \sigma}(t) \mathbf{w}(t) + \mathbf{p}_\sigma(t), \quad (5.1b)$$

where $\mathbf{P}_\xi : [0, T] \rightarrow \mathbb{R}^{n \times 2n}$, $\mathbf{P}_{\mathbf{w}, \xi} : [0, T] \rightarrow \mathbb{R}^{n \times m}$, $\mathbf{p}_\xi : [0, T] \rightarrow \mathbb{R}^n$ constitute the boundary or coupling conditions and the initial condition is given as

$$\mathbf{u}(0, x) = \bar{\mathbf{u}}(x), \quad \bar{\mathbf{u}} : [0, 1] \rightarrow \mathbb{R}^n.$$

The switched DAE of the coupled system is given as follows

$$\mathbf{E}_\sigma \dot{\mathbf{w}} = \mathbf{H}_\sigma \mathbf{w} + \mathbf{K}_{0, \sigma}(t) \mathbf{u}(t, 0^+) + \mathbf{K}_{1, \sigma}(t) \mathbf{u}(t, 1^-) + \mathbf{f}(t), \quad t \geq 0, \quad (5.1c)$$

where $\mathbf{w} : [0, T] \rightarrow \mathbb{R}^m$ is the solution to the swDAE, $\mathbf{E}_\xi, \mathbf{H}_\xi \in \mathbb{R}^{m \times m}$, $\mathbf{K}_{0, \xi}, \mathbf{K}_{1, \xi} : [0, T] \rightarrow \mathbb{R}^{m \times n}$, $\mathbf{f} : [0, T] \rightarrow \mathbb{R}^m$ and whose initial condition is

$$\mathbf{w}(0) = \bar{\mathbf{w}}, \quad \bar{\mathbf{w}} \in \mathbb{R}^m.$$

In this chapter, the analysis of the coupled system (5.1) is restricted to the case of a swDAE system with index $\nu = 1$.

Note that (5.1b) is an algebraic equation and (5.1c) contains algebraic equations. Therefore, the coupled problem cannot be addressed simply as a combination of the two separate subsystems. Relations (5.1b) and (5.1c) have to be chosen such that the PDE provides only information via the outgoing characteristics and sufficient data is given as boundary conditions, as the following trivial example illustrates. In the following example, two simple DAE and PDE systems are coupled, where both have unique solutions and it is shown that the resulting coupled system has no solution as the DAE loses its regularity.

Example 5.1

Consider the scalar advection equation with characteristic speed equal to 1 and the initial condition given as

$$\begin{aligned} \partial_t v(t, x) + \partial_x v(t, x) &= 0, & t \in [0, 1], \quad x \in [0, \infty), \\ v(0, x) &= v_0(x), \end{aligned} \quad (5.2)$$

and with the boundary condition $b(t) := v(t, 0^+)$. Hence, its solution is completely determined by the initial data and the left boundary data. Let the output of the advection equation $y_P(t) := v(t, 0)$. From the classical PDE theory, it is known that there exists a unique solution to (5.2). And assume the following DAE with a regular matrix pair (\mathbf{E}, \mathbf{H})

$$\underbrace{\begin{bmatrix} 1 & 0 \\ 0 & 0 \end{bmatrix}}_{\mathbf{E}} \underbrace{\begin{bmatrix} \dot{w} \\ \dot{z} \end{bmatrix}}_{\mathbf{w}} = \underbrace{\begin{bmatrix} 1 & 0 \\ 0 & 1 \end{bmatrix}}_{\mathbf{H}} \underbrace{\begin{bmatrix} w \\ z \end{bmatrix}}_{\mathbf{z}} - \underbrace{\begin{bmatrix} 0 \\ 1 \end{bmatrix}}_{\mathbf{P}} q, \quad (5.3)$$

where q is an input. Let the output of the swDAE (5.3) be

$$y_D(t) := \begin{bmatrix} 0 & 1 \end{bmatrix} \begin{bmatrix} w \\ z \end{bmatrix}.$$

Similarly, from the classical DAE theory, [130], it is known that there exists a unique solution to (5.3). Now let the advection equation (5.2) be coupled with the DAE (5.3) at $x = 0$ of the PDE domain. The coupling between these systems is achieved via $b(t) = y_D(t)$ and $q(t) = y_P(t)$. Since $v(t, 0^+)$ is the incoming wave for (5.2), the term $\mathbf{P}q$ has to be written in a way that it is contained in $\mathbf{H}w$

$$\begin{bmatrix} 1 & 0 \\ 0 & 0 \end{bmatrix} \begin{bmatrix} \dot{w} \\ \dot{z} \end{bmatrix} = \begin{bmatrix} 1 & 0 \\ 0 & 0 \end{bmatrix} \begin{bmatrix} w \\ z \end{bmatrix}.$$

However, this kind of coupling rule yields the matrix pair

$$(\mathbf{E}, \mathbf{H}) = \left(\begin{bmatrix} 1 & 0 \\ 0 & 0 \end{bmatrix}, \begin{bmatrix} 1 & 0 \\ 0 & 0 \end{bmatrix} \right),$$

which is no more regular; i.e., $\det(s\mathbf{E} - \mathbf{H}) = 0$. In this example, the differential algebraic equation is unable to select the boundary data, since the DAE and the boundary conditions coincide. In other words, the boundary condition does not contain any information; thus, the transport equation has infinitely many solutions.

To avoid settings as in Example 5.1, the PDE is rewritten into its characteristic variables

and the DAE is decomposed into pure algebraic part and pure ODE part as in Remark 4.7. The resulting system then has the form

$$\begin{aligned}
\partial_t \mathbf{v} + \Lambda(t, x) \partial \mathbf{v} &= \mathbf{h}(t, x, \mathbf{v}), \\
\begin{pmatrix} \mathbf{v}_+(t, 0^+) \\ \mathbf{v}_-(t, 1^-) \end{pmatrix} &= \begin{pmatrix} \mathbf{P}_{\mathbf{w}_1, 0}(t) & \mathbf{P}_{\mathbf{w}_2, 0}(t) \\ \mathbf{P}_{\mathbf{w}_1, 1}(t) & \mathbf{P}_{\mathbf{w}_2, 1}(t) \end{pmatrix} \begin{pmatrix} \mathbf{w}_1(t) \\ \mathbf{w}_2(t) \end{pmatrix} + \begin{pmatrix} \mathbf{p}_0(t) \\ \mathbf{p}_1(t) \end{pmatrix} + \begin{pmatrix} \mathbf{N}^-(t) \\ \mathbf{N}^+(t) \end{pmatrix} \begin{pmatrix} \mathbf{v}_-(t, 0) \\ \mathbf{v}_+(t, 1) \end{pmatrix}, \\
\mathbf{v}(0, x) &= \bar{\mathbf{v}}(x), \\
\dot{\mathbf{w}}_1(t) &= \mathbf{J}\mathbf{w}_1(t) + \mathbf{S}_1 \mathbf{K}_0(t) \mathbf{R}(t, 0) \begin{pmatrix} \mathbf{v}_-(t, 0^+) \\ \mathbf{v}_+(t, 0^+) \end{pmatrix} \\
&\quad + \mathbf{S}_1 \mathbf{K}_1(t) \mathbf{R}(t, 1) \begin{pmatrix} \mathbf{v}_-(t, 1^-) \\ \mathbf{v}_+(t, 1^-) \end{pmatrix} + \mathbf{S}_1 \mathbf{f}(t), \\
\mathbf{w}_2(t) &= -\mathbf{S}_2 \mathbf{K}_0(t) \mathbf{R}(t, 0) \begin{pmatrix} \mathbf{v}_-(t, 0^+) \\ \mathbf{v}_+(t, 0^+) \end{pmatrix} \\
&\quad - \mathbf{S}_2 \mathbf{K}_1(t) \mathbf{R}(t, 1) \begin{pmatrix} \mathbf{v}_-(t, 1^-) \\ \mathbf{v}_+(t, 1^-) \end{pmatrix} - \mathbf{S}_2 \mathbf{f}(t), \\
\mathbf{w}_1(0) &= \bar{\mathbf{w}}_1.
\end{aligned} \tag{5.4}$$

The algebraic conditions do not conflict with the boundary conditions, provided that

(C-1): For the coupled system (5.1)

$$\mathbf{S}_2 \mathbf{K}_0(t) \mathbf{R}^+(t, 0) = \mathbf{0} \quad \text{and} \quad \mathbf{S}_2 \mathbf{K}_1(t) \mathbf{R}^-(t, 1) = \mathbf{0},$$

hold, where \mathbf{S}_2 is chosen as in (4.6). Furthermore, $\mathbf{S}_1 \mathbf{K}_0(t)$, $\mathbf{S}_1 \mathbf{K}_1(t)$ and $\mathbf{f}(t)$ are measurable in time.

Remark 5.2

Note that if this condition is not satisfied, it might be possible to transfer these algebraic relations into the formulation of the coupling conditions.

With Condition **(C-1)**, one can decouple the algebraic equations and replace \mathbf{w}_2 in the boundary conditions so that the new system reads

$$\begin{aligned}
\partial_t \mathbf{v} + \Lambda(t, x) \partial \mathbf{v} &= \mathbf{h}(t, x, \mathbf{v}), \\
\begin{pmatrix} \mathbf{v}_+(t, 0^+) \\ \mathbf{v}_-(t, 1^-) \end{pmatrix} &= \begin{pmatrix} \mathbf{P}_{\mathbf{w}_1, 0}(t) \\ \mathbf{P}_{\mathbf{w}_1, 1}(t) \end{pmatrix} \mathbf{w}_1(t) + \begin{pmatrix} \tilde{\mathbf{p}}_0(t) \\ \tilde{\mathbf{p}}_1(t) \end{pmatrix} + \begin{pmatrix} \tilde{\mathbf{N}}^-(t) \\ \tilde{\mathbf{N}}^+(t) \end{pmatrix} \begin{pmatrix} \mathbf{v}_-(t, 0) \\ \mathbf{v}_+(t, 1) \end{pmatrix} \\
\mathbf{v}(0, x) &= \bar{\mathbf{v}}(x), \\
\dot{\mathbf{w}}_1(t) &= \mathbf{J}\mathbf{w}_1(t) + \mathbf{S}_1 \mathbf{K}_0(t) \mathbf{R}(t, 0) \begin{pmatrix} \mathbf{v}_-(t, 0^+) \\ \mathbf{v}_+(t, 0^+) \end{pmatrix} \\
&\quad + \mathbf{S}_1 \mathbf{K}_1(t) \mathbf{R}(t, 1) \begin{pmatrix} \mathbf{v}_-(t, 1^-) \\ \mathbf{v}_+(t, 1^-) \end{pmatrix} + \mathbf{S}_1 \mathbf{f}(t).
\end{aligned} \tag{5.5}$$

Note that the terms $\tilde{\mathbf{N}}^-$ and $\tilde{\mathbf{N}}^+$ in (5.5) can be different from zero, even if in (5.4) $\mathbf{N}^- = \mathbf{0}$ and $\mathbf{N}^+ = \mathbf{0}$. Moreover, the dependencies on $\mathbf{v}_+(t, 0^+)$ and $\mathbf{v}_-(t, 1^-)$ in the ODE can be replaced with boundary conditions.

The system (5.5) can be rewritten in a more compact form as follows

$$\begin{aligned}
\partial_t \mathbf{u}(t, x) + \mathbf{A}(t, x) \partial_x \mathbf{u}(t, x) &= \mathbf{s}(t, x, \mathbf{u}(t, x)), \\
\mathbf{B}(t) \begin{pmatrix} \mathbf{u}(t, 0^+) \\ \mathbf{u}(t, 1^-) \end{pmatrix} &= \mathbf{B}_{\mathbf{w}_1}(t) \mathbf{w}_1(t) + \mathbf{b}(t), \\
\mathbf{u}(0, x) &= \bar{\mathbf{u}}(x), \\
\dot{\mathbf{w}}_1(t) &= \mathbf{J} \mathbf{w}_1(t) + (\mathbf{G}_0 \quad \mathbf{G}_1) \begin{pmatrix} \mathbf{u}(t, 0^+) \\ \mathbf{u}(t, 1^-) \end{pmatrix} + \mathbf{g}(t), \\
\mathbf{w}_1(0) &= \bar{\mathbf{w}}_1,
\end{aligned} \tag{5.6}$$

with the choices

$$\mathbf{B}(t) = \begin{pmatrix} -\tilde{\mathbf{N}}_0^- & \mathbf{I} & \mathbf{0} & -\tilde{\mathbf{N}}_1^- \\ -\tilde{\mathbf{N}}_0^+ & \mathbf{0} & \mathbf{I} & -\tilde{\mathbf{N}}_1^+ \end{pmatrix}, \quad \mathbf{B}_{\mathbf{w}_1} = \begin{pmatrix} \mathbf{P}_{\mathbf{w}_1, 0}(t) \\ \mathbf{P}_{\mathbf{w}_1, 1}(t) \end{pmatrix}, \quad \mathbf{b} = \begin{pmatrix} \tilde{\mathbf{p}}_0(t) \\ \tilde{\mathbf{p}}_1(t) \end{pmatrix},$$

and $\mathbf{G}_0 = \mathbf{S}_1 \mathbf{K}_0$, $\mathbf{G}_1 = \mathbf{S}_1 \mathbf{K}_1$, $\mathbf{g} = \mathbf{S}_1 \mathbf{f}$. System (5.6) is equivalent to (5.1) due to Condition (C-1). For this system, the analytical results are provided below.

Definition 5.3

Fix $T > 0$. A pair $(\mathbf{u}, \mathbf{w}_1)$ is a solution to (5.6) on the time interval $[0, T]$ if the following conditions hold.

(1): \mathbf{u} is a broad solution on $[0, T]$ to the system

$$\begin{cases} \partial_t \mathbf{u} + \mathbf{A}(t, x) \partial_x \mathbf{u} = \mathbf{s}(t, x, \mathbf{u}), \\ \mathbf{B}(t) \begin{pmatrix} \mathbf{u}(t, 0^+) \\ \mathbf{u}(t, 1^-) \end{pmatrix} = \mathbf{B}_{\mathbf{w}_1}(t) \mathbf{w}_1(t) + \mathbf{b}(t), \\ \mathbf{u}(0, x) = \bar{\mathbf{u}}, \end{cases}$$

in the sense of Definition 2.7.

(2): $\mathbf{w}_1 \in \mathbf{C}^0([0, T]; \mathbb{R}^p)$ satisfies

$$\mathbf{w}_1(t) = \bar{\mathbf{w}}_1 + \int_0^t (\mathbf{J} \mathbf{w}_1(s) + \mathbf{G}(s)) ds,$$

for every $t \in [0, T]$, where

$$\mathbf{G}(t) = \mathbf{G}_0(t) \mathbf{u}(t, 0^+) + \mathbf{G}_1(t) \mathbf{u}(t, 1^-) + \mathbf{g}(t),$$

for a.e. $t \in [0, T]$.

The following lemma from [19] will be employed to prove well-posedness of the solution to the coupled system (5.6).

Lemma 5.4: Lemma 4.2 from [19]

Assume that the sequence $h_n \in \mathbf{C}^0([0, T]; \mathbb{R}^+)$ satisfies

$$h_n(t) \leq \alpha + \beta \int_0^t h_{n-2}(\tau) d\tau, \quad \text{with } h_0(t) \in [0, H] \quad \text{and} \quad h_1(t) \in [0, H],$$

for positive numbers α, β and H . Then for all $n \geq 1$,

$$\max \{h_{2n}(t), h_{2n+1}(t)\} \leq \alpha \sum_{i=0}^{n-1} \frac{\beta^i t^i}{i!} + H \frac{\beta^n t^n}{n!}.$$

Theorem 5.5

Assume that $(\mathbf{E}_\xi, \mathbf{H}_\xi)$ is regular for each $\xi = 1, 2, \dots, N$ and that Condition **(C-1)**, hypotheses **(H-1)**-**(H-5)** hold. Then, for every $T > 0$, there exists a semigroup

$$\mathcal{S} : [0, T] \times \mathcal{D} \longrightarrow \mathcal{D},$$

where

$$\mathcal{D} = \{(\bar{\mathbf{u}}, \bar{\mathbf{w}}_1) \in \mathbf{L}^1((0, 1); \mathbb{R}^n) \times \mathbb{R}^p : \mathbf{TV}(\bar{\mathbf{u}}) < +\infty\},$$

satisfying the following conditions

(1): $(\mathbf{u}(t, x), \mathbf{w}_1(t)) = \mathcal{S}(t, \bar{\mathbf{u}}, \bar{\mathbf{w}}_1)(x)$, for every $(\bar{\mathbf{u}}, \bar{\mathbf{w}}_1) \in \mathcal{D}$, is the solution to the coupled system (5.1) (or to the alternative form (5.6)) in the sense of Definition 5.3.

(2): $\mathcal{S}(0, \bar{\mathbf{u}}, \bar{\mathbf{w}}_1) = (\bar{\mathbf{u}}, \bar{\mathbf{w}}_1)$ for every $(\bar{\mathbf{u}}, \bar{\mathbf{w}}_1) \in \mathcal{D}$.

(3): For every $0 \leq t_1 \leq t_2 \leq T$ and $(\bar{\mathbf{u}}, \bar{\mathbf{w}}_1) \in \mathcal{D}$, it holds:

$$\mathcal{S}(t_2, \bar{\mathbf{u}}, \bar{\mathbf{w}}_1) = \mathcal{S}(t_2 - t_1, \mathcal{S}(t_1, \bar{\mathbf{u}}, \bar{\mathbf{w}}_1)).$$

(4): There exists $L > 0$ such that

$$\|\mathcal{S}(t, \bar{\mathbf{u}}, \bar{\mathbf{w}}_1) - \mathcal{S}(t, \tilde{\mathbf{u}}, \tilde{\mathbf{w}}_1)\|_{\mathbf{L}^1(0,1)} \leq L \left[\|\bar{\mathbf{u}} - \tilde{\mathbf{u}}\|_{\mathbf{L}^1(0,1)} + \|\bar{\mathbf{w}}_1 - \tilde{\mathbf{w}}_1\|_{\mathbf{L}^1(0,t)} \right] \quad (5.7)$$

for a.e. $t \in [0, T]$ and for all $(\bar{\mathbf{u}}, \bar{\mathbf{w}}_1) \in \mathcal{D}$ and $(\tilde{\mathbf{u}}, \tilde{\mathbf{w}}_1) \in \mathcal{D}$.

Proof. The solution to the system (5.6) is constructed by passing to the limit of a sequence of approximate solutions. The proof is divided into several steps.

Construction of approximate solutions. Set $\mathbf{u}_0(t, x) \equiv \bar{\mathbf{u}}(x)$ and $\mathbf{w}_{1_0}(t) \equiv \bar{\mathbf{w}}_1$. For every $k \geq 1$, given \mathbf{u}_{k-1} and $\mathbf{w}_{1_{k-1}}$, recursively define \mathbf{u}_k as the solution to

$$\begin{cases} \partial_t \mathbf{u}_k(t, x) + \mathbf{A}(t, x) \partial_x \mathbf{u}_k(t, x) = \mathbf{s}(t, x, \mathbf{u}_k), \\ \mathbf{B}(t) \begin{pmatrix} \mathbf{u}_k(t, 0^+) \\ \mathbf{u}_k(t, 1^-) \end{pmatrix} = \mathbf{B}_{\mathbf{w}_1}(t) \mathbf{w}_{1_{k-1}}(t) + \mathbf{b}(t), \\ \mathbf{u}_k(0, x) = \bar{\mathbf{u}}. \end{cases} \quad (5.8)$$

Note that Theorem 2.9 applies to the system (5.8) hence the solution \mathbf{u}_k exists and is unique. Moreover define $\mathbf{w}_{1_k} \in \mathbf{C}^0([0, T]; \mathbb{R}^p)$ as the solution to the linear non homogeneous system

$$\begin{cases} \dot{\mathbf{w}}_{1_k}(t) = \mathbf{J} \mathbf{w}_{1_k}(t) + \mathbf{G}_0(t) \mathbf{u}_{k-1}(t, 0^+) + \mathbf{G}_1(t) \mathbf{u}_{k-1}(t, 1^-) + \mathbf{g}(t), \\ \mathbf{w}_{1_k}(0) = \bar{\mathbf{w}}_1. \end{cases} \quad (5.9)$$

Classical theory of ODEs implies that the previous system admits a unique solution, since, by Theorem 2.9 and Condition (C-1), the function

$$t \longmapsto \mathbf{G}_0(t)\mathbf{u}_{k-1}(t, 0^+) + \mathbf{G}_1(t)\mathbf{u}_{k-1}(t, 1^-) + \mathbf{g}(t)$$

is measurable; see [25, Theorem 3.1].

\mathbf{w}_{1_k} is a Cauchy sequence. For $k \geq 2$ and $t \in [0, T]$, by using (5.9), one obtains

$$\begin{aligned} |\mathbf{w}_{1_k}(t) - \mathbf{w}_{1_{k-1}}(t)| &\leq \int_0^t |\mathbf{J}(\mathbf{w}_{1_k}(s) - \mathbf{w}_{1_{k-1}}(s))| \, ds \\ &\quad + \int_0^t |\mathbf{G}_0(s)(\mathbf{u}_{k-1}(s, 0) - \mathbf{u}_{k-2}(s, 0))| \, ds \\ &\quad + \int_0^t |\mathbf{G}_1(s)(\mathbf{u}_{k-1}(s, 1) - \mathbf{u}_{k-2}(s, 1))| \, ds \\ &\leq \|\mathbf{J}\| \int_0^t |\mathbf{w}_{1_k}(s) - \mathbf{w}_{1_{k-1}}(s)| \, ds \\ &\quad + L_G \int_0^t |\mathbf{u}_{k-1}(s, 0) - \mathbf{u}_{k-2}(s, 0)| \, ds \\ &\quad + L_G \int_0^t |\mathbf{u}_{k-1}(s, 1) - \mathbf{u}_{k-2}(s, 1)| \, ds, \end{aligned}$$

where $L_G := \max \left\{ \sup_{t \in [0, T]} \|\mathbf{G}_0(t)\|, \sup_{t \in [0, T]} \|\mathbf{G}_1(t)\| \right\}$. By Gronwall Lemma, for $k \geq 2$ and $t \in [0, T]$, the following is obtained

$$\begin{aligned} |\mathbf{w}_{1_k}(t) - \mathbf{w}_{1_{k-1}}(t)| &\leq e^{\|\mathbf{J}\|t} L_G \|\mathbf{u}_{k-1}(\cdot, 0) - \mathbf{u}_{k-2}(\cdot, 0)\|_{\mathbf{L}^1(0, t)} \\ &\quad + e^{\|\mathbf{J}\|t} L_G \|\mathbf{u}_{k-1}(\cdot, 1) - \mathbf{u}_{k-2}(\cdot, 1)\|_{\mathbf{L}^1(0, t)}. \end{aligned} \quad (5.10)$$

By using (2.25) and (2.26), one obtains that, for $k \geq 3$,

$$\begin{aligned} |\mathbf{w}_{1_k}(t) - \mathbf{w}_{1_{k-1}}(t)| &\leq e^{\|\mathbf{J}\|t} L_G L \|\mathbf{B}_{\mathbf{w}_1}(\mathbf{w}_{1_{k-2}} - \mathbf{w}_{1_{k-3}})\|_{\mathbf{L}^1(0, t)} \\ &\leq e^{\|\mathbf{J}\|t} L_G L \|\mathbf{B}_{\mathbf{w}_1}\| \int_0^t |\mathbf{w}_{1_{k-2}}(s) - \mathbf{w}_{1_{k-3}}(s)| \, ds. \end{aligned}$$

By applying Lemma 5.4, [19, Lemma 4.2], with $\alpha = 0$, $\beta = e^{\|\mathbf{J}\|t} L_G L \|\mathbf{B}_{\mathbf{w}_1}\|$ and $\mathbf{h}_k(t) = |\mathbf{w}_{1_k}(t) - \mathbf{w}_{1_{k-1}}(t)|$ to the inequality

$$\mathbf{h}_n(t) \leq \alpha + \beta \int_0^t \mathbf{h}_{n-2}(\tau) \, d\tau,$$

one obtains for all $n \geq 1$

$$\max\{\mathbf{h}_{2n}(t), \mathbf{h}_{2n+1}(t)\} \leq \alpha \sum_{i=0}^{n-1} \frac{\beta^i t^i}{i!} + Y \frac{\beta^n t^n}{n!},$$

where $Y \geq \max\{\|\mathbf{h}_0\|, \|\mathbf{h}_1\|\}$.

Thus, there exists a positive constant C_1 such that

$$\|\mathbf{w}_{1_k} - \mathbf{w}_{1_{k-1}}\|_{\mathbf{C}^0([0, T])} \leq C_1 \frac{(e^{\|\mathbf{J}\|T} L_G L \|\mathbf{B}_{\mathbf{w}_1}\|)^k T^k}{k!},$$

for every $k \geq 3$. Therefore, for every $k > j \geq 3$,

$$\begin{aligned} \|\mathbf{w}_{1_k} - \mathbf{w}_{1_j}\|_{\mathbf{C}^0([0,T])} &\leq \sum_{i=j+1}^k \|\mathbf{w}_{1_i} - \mathbf{w}_{1_{i-1}}\|_{\mathbf{C}^0([0,T])} \\ &\leq C_1 \sum_{i=j+1}^k \frac{(e^{\|\mathbf{J}\|T} L_G L \|\mathbf{B}_{\mathbf{w}_1}\|)^i T^i}{i!}, \end{aligned}$$

which proves that \mathbf{w}_{1_k} is a Cauchy sequence in $\mathbf{C}^0([0,T])$. Thus, there exists $\mathbf{w}_1^* \in \mathbf{C}^0([0,T])$ such that \mathbf{w}_{1_k} converges to \mathbf{w}_1^* in $\mathbf{C}^0([0,T])$ as $k \rightarrow +\infty$.

\mathbf{u}_k is a Cauchy sequence. By using (2.23), one obtains the existence of a constant $C > 0$ such that, for every k and k' , the estimate

$$\begin{aligned} \|\mathbf{u}_k(t, \cdot) - \mathbf{u}_{k'}(t, \cdot)\|_{\mathbf{L}^1(0,1)} &\leq C \|\mathbf{w}_{1_{k-1}} - \mathbf{w}_{1_{k'-1}}\|_{\mathbf{L}^1(0,T)} \\ &\leq CT \|\mathbf{w}_{1_{k-1}} - \mathbf{w}_{1_{k'-1}}\|_{\mathbf{C}^0([0,T])} \end{aligned}$$

holds for every $t \in [0, T]$. Thus \mathbf{u}_k is a Cauchy sequence in $\mathbf{C}^0([0, T]; \mathbf{L}^1(0, 1))$, proving the existence of $\mathbf{u}^* \in \mathbf{C}^0([0, T]; \mathbf{L}^1(0, 1))$ such that \mathbf{u}_k converges to \mathbf{u}^* in $\mathbf{C}^0([0, T]; \mathbf{L}^1(0, 1))$ as $k \rightarrow +\infty$.

The couple $(\mathbf{u}^*, \mathbf{w}_1^*)$ is a solution to (5.6). First, it is shown that \mathbf{w}_1^* is the solution to the ODE with the input from \mathbf{u}^* . Due to (5.9), one has, for every $t \in [0, T]$,

$$\mathbf{w}_{1_k}(t) = \bar{\mathbf{w}}_1 + \int_0^t \mathbf{J} \mathbf{w}_{1_k}(s) ds + \int_0^t [\mathbf{G}_0(s) \mathbf{u}_{k-1}(s, 0^+) + \mathbf{G}_1(s) \mathbf{u}_{k-1}(s, 1^-) + \mathbf{g}(s)] ds.$$

By using again (2.25) and (2.26), it holds that both the sequences $\mathbf{u}_k(\cdot, 0^+)$ and $\mathbf{u}_k(\cdot, 1^-)$ are Cauchy sequences in $\mathbf{L}^1(0, T)$ and the limits are $\mathbf{u}^*(\cdot, 0^+)$ and $\mathbf{u}^*(\cdot, 1^-)$, respectively, since the non-characteristic condition (H-4) holds, see [2]. By passing to the limit $k \rightarrow \infty$, one thus obtains

$$\mathbf{w}_1^*(t) = \bar{\mathbf{w}}_1 + \int_0^t \mathbf{J} \mathbf{w}_1^*(s) ds + \int_0^t [\mathbf{G}_0(s) \mathbf{u}^*(s, 0^+) + \mathbf{G}_1(s) \mathbf{u}^*(s, 1^-) + \mathbf{g}(s)] ds,$$

proving that \mathbf{w}_1^* satisfies Condition (2) of Definition 5.3.

Conversely, define $\tilde{\mathbf{u}}$ as the solution to the hyperbolic system

$$\begin{cases} \partial_t \tilde{\mathbf{u}}(t, x) + \mathbf{A}(t, x) \partial_x \tilde{\mathbf{u}}(t, x) = \mathbf{s}(t, x, \tilde{\mathbf{u}}), \\ \mathbf{B}(t) \begin{pmatrix} \tilde{\mathbf{u}}(t, 0^+) \\ \tilde{\mathbf{u}}(t, 1^-) \end{pmatrix} = \mathbf{B}_{\mathbf{w}_1}(t) \mathbf{w}_1^*(t) + \mathbf{b}(t), \\ \tilde{\mathbf{u}}(0, x) = \bar{\mathbf{u}}. \end{cases}$$

Due to (2.23), for $t \in [0, T]$ and $k \geq 1$, one has

$$\|\tilde{\mathbf{u}}(t) - \mathbf{u}_k(t)\|_{\mathbf{L}^1(0,1)} \leq L \|\mathbf{w}_1^* - \mathbf{w}_{1_{k-1}}\|_{\mathbf{L}^1(0,t)},$$

for some positive constant L . Since \mathbf{w}_{1_k} is a Cauchy sequence and \mathbf{u}_k converges to \mathbf{u}^* in $\mathbf{C}^0([0, T]; \mathbf{L}^1(0, 1))$, it holds $\tilde{\mathbf{u}} = \mathbf{u}^*$ in $\mathbf{C}^0([0, T]; \mathbf{L}^1(0, 1))$, proving that \mathbf{u}^* satisfies Condition (1) of Definition 5.3.

Well-posedness estimate. Consider two initial conditions, namely $(\bar{\mathbf{u}}, \bar{\mathbf{w}}_1)$ and $(\tilde{\mathbf{u}}, \tilde{\mathbf{w}}_1)$ with $\mathbf{TV}(\bar{\mathbf{u}}) + \mathbf{TV}(\tilde{\mathbf{u}}) < +\infty$. Denote with $(\bar{\mathbf{u}}_k, \bar{\mathbf{w}}_{1_k})$ and with $(\tilde{\mathbf{u}}_k, \tilde{\mathbf{w}}_{1_k})$ the sequences constructed

as in the first part of the proof for the initial conditions given by $(\bar{\mathbf{u}}, \bar{\mathbf{w}}_1)$ and, respectively, by $(\tilde{\mathbf{u}}, \tilde{\mathbf{w}}_1)$. By (2.23), there exists a constant $C_1 > 0$ such that

$$\|\bar{\mathbf{u}}_k(t) - \tilde{\mathbf{u}}_k(t)\|_{\mathbf{L}^1(0,1)} \leq C_1 \|\bar{\mathbf{u}} - \tilde{\mathbf{u}}\|_{\mathbf{L}^1(0,1)} + C_1 \int_0^t |\bar{\mathbf{w}}_{1_k}(s) - \tilde{\mathbf{w}}_{1_k}(s)| \, ds, \quad (5.11)$$

for a.e. $t \in [0, T]$. Moreover, there exists $C_2 > 0$ such that, for every $t \in [0, T]$,

$$\begin{aligned} |\bar{\mathbf{w}}_{1_k}(t) - \tilde{\mathbf{w}}_{1_k}(t)| &\leq |\bar{\mathbf{w}}_1 - \tilde{\mathbf{w}}_1| + C_2 \int_0^t |\bar{\mathbf{w}}_{1_k}(s) - \tilde{\mathbf{w}}_{1_k}(s)| \, ds \\ &\quad + C_2 \int_0^t |\bar{\mathbf{u}}_k(s, 0) - \tilde{\mathbf{u}}_k(s, 0)| \, ds \\ &\quad + C_2 \int_0^t |\bar{\mathbf{u}}_k(s, 1) - \tilde{\mathbf{u}}_k(s, 1)| \, ds. \end{aligned} \quad (5.12)$$

By using (2.25) and (2.26) in (5.12), one obtains that there exists $C_3 > 0$ such that

$$|\bar{\mathbf{w}}_{1_k}(t) - \tilde{\mathbf{w}}_{1_k}(t)| \leq |\bar{\mathbf{w}}_1 - \tilde{\mathbf{w}}_1| + C_2 \int_0^t |\bar{\mathbf{w}}_{1_k}(s) - \tilde{\mathbf{w}}_{1_k}(s)| \, ds + C_3 \|\bar{\mathbf{u}} - \tilde{\mathbf{u}}\|_{\mathbf{L}^1(0,1)}, \quad (5.13)$$

for every $t \in [0, T]$, and hence, by Gronwall Lemma,

$$\begin{aligned} |\bar{\mathbf{w}}_{1_k}(t) - \tilde{\mathbf{w}}_{1_k}(t)| &\leq \left[|\bar{\mathbf{w}}_1 - \tilde{\mathbf{w}}_1| + C_3 \|\bar{\mathbf{u}} - \tilde{\mathbf{u}}\|_{\mathbf{L}^1(0,1)} \right] e^{C_2 t} \\ &\leq \left[|\bar{\mathbf{w}}_1 - \tilde{\mathbf{w}}_1| + C_3 \|\bar{\mathbf{u}} - \tilde{\mathbf{u}}\|_{\mathbf{L}^1(0,1)} \right] e^{C_2 T}, \end{aligned} \quad (5.14)$$

for every $t \in [0, T]$. Inserting (5.14) in (5.11), one obtains, for a.e. $t \in [0, T]$,

$$\begin{aligned} \|\bar{\mathbf{u}}_k(t) - \tilde{\mathbf{u}}_k(t)\|_{\mathbf{L}^1(0,1)} &\leq \left(C_1 + \frac{C_3}{C_2} (e^{C_2 T} - 1) \right) \|\bar{\mathbf{u}} - \tilde{\mathbf{u}}\|_{\mathbf{L}^1(0,1)} \\ &\quad + \frac{C_1}{C_2} |\bar{\mathbf{w}}_1 - \tilde{\mathbf{w}}_1| (e^{C_2 T} - 1). \end{aligned} \quad (5.15)$$

By passing to the limit as $k \rightarrow +\infty$ in (5.14) and in (5.15), it follows that (5.7) holds. \square

Corollary 5.6

Let $T > 0$ and $\sigma: [0, T] \rightarrow \mathbb{N}$ be a given switching signal with finitely many switching points. Then, under the above hypotheses, system (5.1) has a unique solution (\mathbf{u}, \mathbf{w}) on $[0, T]$.

A proof can be obtained by iteratively applying Theorem 5.5.

Chapter 6

Theory of distributions in time and space

In Section 2.2.1, the classical solution to linear hyperbolic PDEs has been reviewed. However, considering a coupling with switched DAEs of arbitrary index, the boundary data for the PDE is given by piecewise smooth distributions. Thus, the solutions to the PDEs need to be extended in the distributional sense, including Dirac impulses and derivatives of Dirac impulses. In other words, impulsive boundary conditions for the PDEs need to be allowed. However, if one considers distributions on $\mathbb{R} \times \mathbb{R}$, the necessary properties of solutions would not be captured in this space. The reason is that the traces at initial time and the boundaries are still need to be evaluated. In this space, it would not be possible to capture the information at the PDE boundaries or in the initial condition. Therefore, an appropriate solution space called the space of *piecewise-smooth distributions in time and space* is constructed. In this chapter, this new space, which is denoted by $\mathbb{D}_{\text{pw}C^\infty}(T \times X)$, is established and properties of distributions that belong to this space are demonstrated.

In this chapter, the tools which are defined in Section 3.1 are employed. In order to work with distributions in time and space domains, the mathematical structures in Section 3.1 are adapted for $d = 2$.

6.1 Distributions in time and space domains

In this section, test functions are considered in $C_0^\infty(\mathbb{R} \times \mathbb{R}; \mathbb{R})$ and distributions acting on those test functions are studied.

Definition 6.1: Distributions in $\mathbb{R} \times \mathbb{R}$

A continuous linear functional $D : C_0^\infty(\mathbb{R} \times \mathbb{R}; \mathbb{R}) \rightarrow \mathbb{R}$ is called a *distribution* in time and space. It is linear if

$$D(a\varphi + b\vartheta) = c_1D(\varphi) + c_2D(\vartheta),$$

for all $a, b \in \mathbb{R}$ and $\varphi, \vartheta \in C_0^\infty(\mathbb{R} \times \mathbb{R}; \mathbb{R})$, and it is continuous if $\{\varphi_n\}_{n \in \mathbb{N}}$ converges to φ in $C_0^\infty(\mathbb{R} \times \mathbb{R}; \mathbb{R})$, then

$$\lim_{n \rightarrow \infty} D(\varphi_n) = D(\varphi).$$

The space of distributions in time and space is denoted by $\mathbb{D}(C_0^\infty(\mathbb{R} \times \mathbb{R}; \mathbb{R}); \mathbb{R})$, which is the dual space of $C_0^\infty(\mathbb{R} \times \mathbb{R}; \mathbb{R})$.

In the sequel, instead of writing $\mathbb{D}(C_0^\infty(\mathbb{R} \times \mathbb{R}; \mathbb{R}); \mathbb{R})$, in short hand notation \mathbb{D} (or $\mathbb{D}(\mathbb{R} \times \mathbb{R})$) is used to denote the space of distributions in $(\mathbb{R} \times \mathbb{R})$, which will not mean the same space of distributions in time domain as defined and used in Chapter 3 unless specified.

Lemma 6.2: Regular distributions

Let $f \in L^1_{\text{loc}}(\mathbb{R} \times \mathbb{R}; \mathbb{R})$, that is, on every compact set $K \subset \mathbb{R} \times \mathbb{R}$, the Lebesgue integral of f is finite. Then the *regular distribution* $f_{\mathbb{D}}$ induced by f is given by

$$\begin{aligned} f_{\mathbb{D}} : C_0^\infty(\mathbb{R} \times \mathbb{R}) &\rightarrow \mathbb{R} \\ \varphi &\mapsto \int_{\mathbb{R}} \int_{\mathbb{R}} \varphi f, \end{aligned} \quad (6.1)$$

and the space of regular distributions is denoted by \mathbb{D}_{reg}

$$\mathbb{D}_{\text{reg}} = \{f_{\mathbb{D}} \mid f \in L^1_{\text{loc}}(\mathbb{R} \times \mathbb{R}; \mathbb{R})\}.$$

Regular distributions in $\mathbb{R} \times \mathbb{R}$ are distributions.

Proof. The proof is similar to the proof of Lemma 3.6, therefore, it is omitted here. \square

Proposition 6.3

The space of regular distributions $\mathbb{D}_{\text{reg}}(\mathbb{R} \times \mathbb{R})$ is a proper subset of the space of distributions $\mathbb{D}(\mathbb{R} \times \mathbb{R})$, [79].

Proposition 6.4

Let $f, g \in L^1_{\text{loc}}(\mathbb{R} \times \mathbb{R}; \mathbb{R})$ be any two functions. The regular distributions $f_{\mathbb{D}}, g_{\mathbb{D}}$ induced by f, g satisfies $f_{\mathbb{D}} = g_{\mathbb{D}}$ if and only if $f = g$ almost everywhere, [78].

Derivatives of distributions Let $f \in L^1_{\text{loc}}(\mathbb{R} \times \mathbb{R}; \mathbb{R})$ such that its partial derivatives $\partial_t f$ and $\partial_x f$ exist and are in $L^1_{\text{loc}}(\mathbb{R} \times \mathbb{R}; \mathbb{R})$. The distributional partial derivatives of the distribution $f_{\mathbb{D}}$ induced by f are

$$\begin{aligned} \partial_t f_{\mathbb{D}} &= \int_{\mathbb{R}} \int_{\mathbb{R}} \partial_t f \varphi & \partial_x f_{\mathbb{D}} &= \int_{\mathbb{R}} \int_{\mathbb{R}} \partial_x f \varphi \\ &= - \int_{\mathbb{R}} \int_{\mathbb{R}} f \partial_t \varphi & &= - \int_{\mathbb{R}} \int_{\mathbb{R}} f \partial_x \varphi \\ &= -f_{\mathbb{D}}(\partial_t \varphi), & &= -f_{\mathbb{D}}(\partial_x \varphi), \end{aligned}$$

for every $\varphi \in C_0^\infty(\mathbb{R} \times \mathbb{R}; \mathbb{R})$ where φ vanishes at $\mp\infty$ as it has a bounded support. Hence, the distributional partial derivatives of any distribution in $\mathbb{D}(\mathbb{R} \times \mathbb{R})$ can also be defined similarly.

Definition 6.5: Distributional partial derivatives

The *distributional partial derivatives* of a distribution $D \in \mathbb{D}(\mathbb{R} \times \mathbb{R})$ are

$$\begin{aligned} D_t &:= \partial_t D := \frac{\partial_{\mathbb{D}}}{\partial t} D : \mathbb{D} \rightarrow \mathbb{D} \\ &D \mapsto -D(\partial_t \varphi), \\ D_x &:= \partial_x D := \frac{\partial_{\mathbb{D}}}{\partial x} D : \mathbb{D} \rightarrow \mathbb{D} \\ &D \mapsto -D(\partial_x \varphi), \end{aligned} \quad \text{where } \varphi \in C_0^\infty(\mathbb{R} \times \mathbb{R}; \mathbb{R}).$$

Corollary 6.6

The space $\mathbb{D}(\mathbb{R} \times \mathbb{R})$ is closed under differentiation; i.e., $D_t, D_x \in \mathbb{D}(\mathbb{R} \times \mathbb{R})$ for any distribution $D \in \mathbb{D}(\mathbb{R} \times \mathbb{R})$.

Proof. Let $\varphi \in C_{\text{pw}}^\infty(\mathbb{R} \times \mathbb{R}; \mathbb{R})$. As $D \in \mathbb{D}$ is well-defined, the distributional partial derivatives $D_t = -D(\partial_t \varphi)$, $D_x = -D(\partial_x \varphi)$ are also well-defined. Linearity and continuity of D_t, D_x follow from those of D , as well. \square

Corollary 6.7

Higher order distributional partial derivatives of a distribution $D \in \mathbb{D}(\mathbb{R} \times \mathbb{R})$ are given by

$$\begin{aligned} \left(\frac{\partial \mathbb{D}}{\partial t}\right)^{(k)} : \mathbb{D} &\rightarrow \mathbb{D}, & D &\mapsto (-1)^{(k)} D \left(\left(\frac{\partial}{\partial t}\right)^{(k)} \varphi \right), \\ \left(\frac{\partial \mathbb{D}}{\partial x}\right)^{(k)} : \mathbb{D} &\rightarrow \mathbb{D}, & D &\mapsto (-1)^{(k)} D \left(\left(\frac{\partial}{\partial x}\right)^{(k)} \varphi \right), \end{aligned}$$

for $k \in \mathbb{N}$ and $\varphi \in C_0^\infty(\mathbb{R} \times \mathbb{R}; \mathbb{R})$.

Lemma 6.8: Multiplication with smooth functions

For any $D \in \mathbb{D}(\mathbb{R} \times \mathbb{R})$ and $g \in C^\infty(\mathbb{R} \times \mathbb{R}; \mathbb{R})$, the multiplication gD is defined by

$$\begin{aligned} gD : C^\infty(\mathbb{R} \times \mathbb{R}; \mathbb{R}) &\rightarrow \mathbb{R} \\ \varphi &\mapsto D(g\varphi). \end{aligned}$$

Furthermore, multiplication of a distribution with a smooth function is a well-defined distribution; i.e., $gD \in \mathbb{D}(\mathbb{R} \times \mathbb{R})$ and

$$\partial_t(gD) = (\partial_t g)D + g(\partial_t D), \quad \partial_x(gD) = (\partial_x g)D + g(\partial_x D).$$

Proof. Linearity of gD is obvious. As $g \in C^\infty(\mathbb{R} \times \mathbb{R})$ and $\varphi \in C_{\text{pw}}^\infty(\mathbb{R} \times \mathbb{R})$, the product $g\varphi \in C_{\text{pw}}^\infty(\mathbb{R} \times \mathbb{R})$. Thus, continuity of $D(g\varphi)$ follows, so does gD . Moreover,

$$\begin{aligned} \partial_t(gD) &= -gD(\partial_t \varphi) \\ &= -D(g\partial_t \varphi + \partial_t g\varphi) + D(\partial_t g\varphi) \\ &= (\partial_t g)D + g(\partial_t D) \end{aligned}$$

which yields the last property. \square

Definition 6.9: Support of a distribution

The *support* of a distribution $D \in \mathbb{D}$ is

$$\text{supp } D := (\mathbb{R} \times \mathbb{R}) \setminus \bigcup \left\{ T_o \times X_o \subseteq \mathbb{R} \times \mathbb{R} \mid \begin{array}{l} T_o \times X_o \text{ open sets, } \forall \varphi \in C_{\text{pw}}^\infty : \\ \text{supp } \varphi \subseteq T_o \times X_o \Rightarrow D(\varphi) = 0 \end{array} \right\}.$$

Proposition 6.10

For every $f \in L^1_{\text{loc}}(\mathbb{R} \times \mathbb{R}; \mathbb{R})$, $\text{supp } f_{\mathbb{D}}$ has measure zero if and only if $f_{\mathbb{D}} = 0$.

Proof. Let $S = \text{supp } f_{\mathbb{D}}$, then by definition $S^c := \mathbb{R} \times \mathbb{R} \setminus S$ is open and for all $\varphi \in C_0^\infty(\mathbb{R} \times \mathbb{R}; \mathbb{R})$ with $\text{supp } \varphi \subseteq S^c$ it holds $f_{\mathbb{D}}(\varphi) = 0$. Let

$$\mathcal{B}_{\rho_i}(t_i, x_i) = \left\{ (t, x) \mid \sqrt{(t-t_i)^2 + (x-x_i)^2} < \rho_i \right\}$$

denote an open ball with rational numbers t_i, x_i as well as $\rho_i > 0$ such that (t_i, x_i) is its center with $\rho > 0$ its radius. Then, every open set in $\mathbb{R} \times \mathbb{R}$ is a countable union of such open balls $\mathcal{B}_{\rho_i}(t_i, x_i)$ with $t_i, x_i \in \mathbb{Q}$ and $\rho_i \in \mathbb{Q}^+$, $i \in \mathbb{N}$, [142], such that

$$S^c = \bigcup_{i \in \mathbb{N}} \mathcal{B}_{\rho_i}(t_i, x_i).$$

Let $\varphi \in C_0^\infty(\mathbb{R} \times \mathbb{R}; \mathbb{R})$. For $t_i, x_i \in \mathbb{R}$, $\rho_i \in \mathbb{R}^+$, let $\sigma \in \mathbb{R}^+$ and $\phi_{\mathcal{B}_{\rho_i}}^\sigma \in C_0^\infty(\mathbb{R} \times \mathbb{R}; \mathbb{R})$ such that

$$\phi_{\mathcal{B}_{\rho_i}}^\sigma(t, x) = \begin{cases} 1, & \text{if } (t, x) \in \overline{\mathcal{B}_{\rho_i}(t_i, x_i)}, \\ 0, & \text{if } (t, x) \notin \mathcal{B}_{\rho_i + \sigma}(t_i, x_i), \end{cases}$$

and $0 \leq \phi_{\mathcal{B}_{\rho_i}}^\sigma(t, x) \leq 1$ for every $(t, x) \in \mathbb{R} \times \mathbb{R}$. For $\varepsilon > 0$, choose $\varepsilon_i > 0$, $i \in \mathbb{N}$, such that

$$\varepsilon_i < \min \left\{ \frac{\varepsilon}{2^{i+2}}, \frac{\rho_i}{4} \right\}.$$

Let

$$\varphi_\varepsilon := \varphi \prod_i \left(1 - \phi_{\mathcal{B}_{\rho_i - \varepsilon_i}}^{\varepsilon_i} \right).$$

Then, $\varphi_\varepsilon \in C_0^\infty(\mathbb{R} \times \mathbb{R}; \mathbb{R})$ and $\text{supp}(\varphi - \varphi_\varepsilon) \subseteq S^c$. Thus, $f_{\mathbb{D}}(\varphi) = f_{\mathbb{D}}(\varphi_\varepsilon)$. Moreover,

$$\text{supp } \varphi_\varepsilon \subseteq S \cup S_\varepsilon^c,$$

where

$$S_\varepsilon^c := \bigcup_{i \in \mathbb{N}} \left(\mathcal{B}_{\rho_i} \setminus \overline{\mathcal{B}_{\rho_i - 2\varepsilon_i}} \right). \quad (6.2)$$

Taking into consideration that $|\varphi_\varepsilon(t, x)| \leq |\varphi(t, x)|$, $\varphi_\varepsilon(t, x) = 0$ on $S^c \setminus S_\varepsilon^c$ and S has measure zero, (6.2) yields

$$\begin{aligned} |f_{\mathbb{D}}(\varphi)| &= |f_{\mathbb{D}}(\varphi_\varepsilon)| \\ &\leq \int_{\mathbb{R}} \int_{\mathbb{R}} |\varphi_\varepsilon| |f| \\ &= \int_S |\varphi_\varepsilon| |f| + \int_{S_\varepsilon^c} |\varphi_\varepsilon| |f| + \int_{S^c \setminus S_\varepsilon^c} |\varphi_\varepsilon| |f| \\ &= \int_{S_\varepsilon^c} |\varphi_\varepsilon| |f| \end{aligned}$$

$$= \|\varphi\|_{L^\infty} \int_{S_\varepsilon^c} |f|.$$

The Lebesgue measure $\mu(S_\varepsilon^c)$ of S_ε^c is

$$\mu(S_\varepsilon^c) = \sum_{i \in \mathbb{N}} 4\pi\varepsilon_i^2 < \sum_{i \in \mathbb{N}} \pi \frac{\varepsilon^2}{2^{2i}} = \pi\varepsilon^2,$$

thus, $\int_{S_\varepsilon^c} |f| \rightarrow 0$ as $\varepsilon \rightarrow 0$. Hence, $f_{\mathbb{D}} = 0$ since φ is chosen arbitrarily. \square

6.2 The space $\mathbb{D}_{\text{pw}C^\infty}(T \times X)$ of piecewise smooth distributions

Definition 6.11: Polyhedral partition

Denote by $T \subseteq \mathbb{R}$ (time) and $X \subseteq \mathbb{R}$ (space) *open* sets. A family of subsets $(P_i)_{i \in I}$ of $T \times X$ for some index set I is said to be a *polyhedral partition* of $T \times X$ if and only if P_i are polyhedral sets; i.e., the intersection of finitely many (open or closed) half-spaces in $T \times X$ which are pairwise disjoint and $\bigcup_{i \in I} P_i = T \times X$.

Definition 6.12: Piecewise-smooth functions in time and space

Let $T \subseteq \mathbb{R}$ and $X \subseteq \mathbb{R}$ be open sets. A function $\beta : T \times X \rightarrow \mathbb{R}$ is called (*polyhedral*) *piecewise-smooth* if and only if there exists a locally finite polyhedral partition $\bigcup_{i \in I} P_i$ of $T \times X$; that is, the intersection of $\{P_i \mid i \in I\}$ with any compact subset of $T \times X$ only contains finitely many elements of the polyhedral partition; and a family of smooth functions $\beta_i : T \times X \rightarrow \mathbb{R}$, $i \in I$ such that

$$\beta = \sum_{i \in I} \chi_{P_i} \beta_i, \quad (6.3)$$

where χ_{P_i} is the characteristic function of the set $P_i \subseteq T \times X$. The space of piecewise-smooth functions in time and space is denoted by $C_{\text{pw}}^\infty(T \times X; \mathbb{R})$.

For a piecewise smooth function $\beta : T \times X \rightarrow \mathbb{R}$, it is easily seen that for any $t \in T$ and $x \in X$, the functions $\beta(t, \cdot)$ and $\beta(\cdot, x)$ are scalar piecewise-smooth functions as in Definition 3.21.

Definition 6.13: Dirac segment, [85, 120, 141]

Let $L \subseteq T \times X$ be a line segment; i.e., there exists $t_0, t_1 \in T$, $x_0, x_1 \in X$ such that

$$L = \{(t_0 + \alpha(t_1 - t_0), x_0 + \alpha(x_1 - x_0)) \mid \alpha \in [0, 1]\}. \quad (6.4)$$

Then the *Dirac segment* on L is

$$\begin{aligned} \delta_L : C_0^\infty(T \times X; \mathbb{R}) &\rightarrow \mathbb{R} \\ \varphi &\mapsto \int_L \varphi, \end{aligned} \quad (6.5)$$

where $\int_L \varphi$ is the usual line integral given by

$$\int_L \varphi = \int_0^1 \varphi(t_0 + \alpha(t_1 - t_0), x_0 + \alpha(x_1 - x_0)) \sqrt{\Delta t^2 + \Delta x^2} d\alpha,$$

where $\Delta t = t_1 - t_0$ and $\Delta x = x_1 - x_0$, see Figure 6.1. Furthermore, for unbounded lines; i.e., $\alpha \in \mathbb{R}$ in (6.4) and for some $\Delta t \geq 0$, $\Delta x \geq 0$ with the condition $\Delta t^2 + \Delta x^2 > 0$, the line integral is of the form

$$\int_L \varphi = \int_{-\infty}^{\infty} \varphi(t_0 + \alpha\Delta t, x_0 + \alpha\Delta x) \sqrt{\Delta t^2 + \Delta x^2} d\alpha.$$

Note that if $\Delta t \neq 0$ then, the parametrization of the line can be formulated as

$$L = \left\{ \left(t, x_0 + \frac{\Delta x}{\Delta t}(t - t_0) \right) \mid t \in \mathbb{R} \right\}$$

and the Dirac segment on L

$$\int_L \varphi = \int_{t_0}^{t_1} \varphi\left(t, x_0 + \frac{\Delta x}{\Delta t}(t - t_0)\right) \sqrt{1 + \frac{\Delta x^2}{\Delta t^2}} dt, \quad (6.6)$$

and, similarly, if $\Delta x \neq 0$ then, the parametrization of the line can be written as

$$L = \left\{ \left(t_0 + \frac{\Delta t}{\Delta x}(x - x_0), x \right) \mid x \in \mathbb{R} \right\}$$

and the Dirac segment on L

$$\int_L \varphi = \int_{x_0}^{x_1} \varphi\left(t_0 + \frac{\Delta t}{\Delta x}(x - x_0), x\right) \sqrt{1 + \frac{\Delta t^2}{\Delta x^2}} dx. \quad (6.7)$$

Conjecture 6.14

Let $T \subseteq \mathbb{R}$, $X \subseteq \mathbb{R}$ be open, $L \subseteq T \times X$ be some parametrized line and $D \in \mathbb{D}(T \times X)$ be a distribution whose support is the line L . Then D can be written as a linear combination of Dirac segments on L

$$D = \sum_{i=0}^m \sum_{j=0}^n a_{i,j} \partial_t^{(i)} \partial_x^{(j)} \delta_L \quad \text{where } m, n \in \mathbb{N}.$$

Proposition 6.15

For any $g \in C^\infty(\mathbb{R} \times \mathbb{R}; \mathbb{R})$, and any $m, n \in \mathbb{N}$, the product of the smooth function g with the partial derivatives of Dirac segment δ_L on L is

$$g \partial_t^{(m)} \partial_x^{(n)} \delta_L = \sum_{i=0}^m \sum_{j=0}^n (-1)^{i+j} \binom{m}{i} \binom{n}{j} \partial_t^{(i)} \partial_x^{(j)} g|_L \cdot \partial_t^{(m-i)} \partial_x^{(n-j)} \delta_L, \quad (6.8)$$

where L is some parametrized line and $g|_L$ is given by

$$g|_L := g\phi_{L,\varepsilon}, \quad (6.9)$$

where an arbitrarily small $\varepsilon > 0$ and $\phi_{L,\varepsilon} \in C_c^\infty(T \times X; \mathbb{R})$, with $T, X \subseteq \mathbb{R}$, such that

$$\phi_{L,\varepsilon}(t,x) = \begin{cases} 1, & \text{if } \bigcup_{(t_L, x_L) \in L} \mathcal{B}_{\varepsilon/2}(t_L, x_L), \\ 0, & \text{if } (T \times X) \setminus \bigcup_{(t_L, x_L) \in L} \mathcal{B}_{\varepsilon/2}(t_L, x_L) \end{cases}$$

where

$$\mathcal{B}_r(\tilde{t}, \tilde{x}) = \left\{ (t, x) \mid \sqrt{(\tilde{t} - t)^2 + (\tilde{x} - x)^2} < r, r \in \mathbb{R}^+ \cup \{0\} \right\}.$$

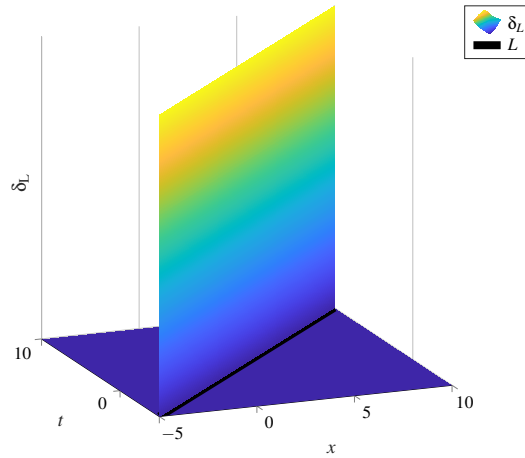


FIGURE 6.1: The Dirac segment δ_L on some line segment L .

Proof. Let $T, X \subseteq \mathbb{R}$ and $L = \{(t_0 + \alpha\Delta t, x_0 + \alpha\Delta x) \mid \alpha \in \mathbb{R}\}$ a parametrized line where $t_0 \in T$, $x_0 \in X$. Let $\phi_{L,\varepsilon} \in C_c^\infty(T \times X; \mathbb{R})$ such that $\phi_{L,\varepsilon}(t,x) = 1$ on $\bigcup \mathcal{B}_{\varepsilon/2}(t_L, x_L)$ where $(t_L, x_L) \in L$ and $\phi_{L,\varepsilon}(t,x) = 0$ on $(T \times X) \setminus \bigcup \mathcal{B}_{\varepsilon/2}(t_L, x_L)$. If $\varepsilon \in (0, 1]$, for any $\varphi \in C_c^\infty(T \times X; \mathbb{R})$, the following holds

$$\varphi(t,x) = \varphi(t,x)\phi_{L,\varepsilon}\left(\frac{t}{\varepsilon}, \frac{x}{\varepsilon}\right) \quad \text{for } (t,x) \in \mathcal{B}_{\varepsilon/2}(t_L, x_L) \quad \forall (t_L, x_L) \in L.$$

Then, for $m = 0 = n$, one obtains

$$\begin{aligned} g\delta_L &= \delta_L(g\varphi) \\ &= \int_L g\varphi \\ &= \int_L g\varphi\phi_{L,\varepsilon} \\ &= (g\phi_{L,\varepsilon})\delta_L =: g|_L \cdot \delta_L, \end{aligned}$$

where $g\phi_{L,\varepsilon} = g$ for $(t,x) \in \mathcal{B}_{\varepsilon/2}(t_L, x_L)$ and 0 otherwise.

For $m = 1 = n$, it holds

$$\begin{aligned} g\partial_t\partial_x\delta_L &= \partial_t\partial_x\delta_L(g\varphi) \\ &= \int_L \partial_t\partial_x g|_L \cdot \varphi + \int_L \partial_x g|_L \cdot \partial_t\varphi + \int_L \partial_t g|_L \cdot \partial_x\varphi + \int_L g|_L \cdot \partial_t\partial_x\varphi \\ &= \partial_t\partial_x g|_L \cdot \delta_L - \partial_x g|_L \cdot \partial_t\delta_L - \partial_t g|_L \cdot \partial_x\delta_L + g|_L \cdot \partial_t\partial_x\delta_L \end{aligned}$$

$$= \sum_{i=0}^1 \sum_{j=0}^1 (-1)^{i+j} \binom{1}{i} \binom{1}{j} \partial_t^{(i)} \partial_x^{(j)} g|_L \cdot \partial_t^{(1-i)} \partial_x^{(1-j)} \delta_L.$$

Assume, the claim holds for $m \geq 1$. For $m+1$, $n=1$, one obtains the following

$$\begin{aligned} g \partial_t^{(m+1)} \partial_x \delta_L &= \partial_t^{(m+1)} \partial_x \delta_L (g\varphi) \\ &= (-1) \partial_t (-1)^{m+1} \partial_t^{(m)} \partial_x \int_L g \varphi \\ &= (-1) \partial_t \sum_{i=0}^m \sum_{j=0}^1 (-1)^{i+j} \binom{m}{i} \binom{1}{j} \partial_t^{(i)} \partial_x^{(j)} g|_L \cdot \partial_t^{(m-i)} \partial_x^{(1-j)} \delta_L \\ &= \sum_{i=0}^{m+1} \sum_{j=0}^1 (-1)^{i+j} \binom{m+1}{i} \binom{1}{j} \partial_t^{(i)} \partial_x^{(j)} g|_L \cdot \partial_t^{(m+1-i)} \partial_x^{(1-j)} \delta_L. \end{aligned}$$

It follows in a similar fashion for the case $n+1$, $m=1$ by assuming the claim holds for $n \geq 1$, $m=1$. Therefore, by induction on m and n , the claim (6.8) holds true. \square

Remark 6.16

The product $g\phi_{L,\varepsilon} = g|_L$ in (6.9) can be considered to be the *evaluation of g on the line L* as $\phi_{L,\varepsilon}$ has a support that is in ε -neighborhood of L for arbitrarily small $\varepsilon > 0$.

Lemma 6.17

Assume that $T = \mathbb{R}$, $X = \mathbb{R}$ and consider the unbounded line given by

$$L = \{(t_0 + \alpha\Delta t, x_0 + \alpha\Delta x) \mid \alpha \in \mathbb{R}\}$$

for some $t_0 \in T$, $x_0 \in X$ and $\Delta t > 0, \Delta x > 0$. For the step function along L , see Figure 6.2, given by

$$H_L(t, x) = \begin{cases} 1, & t - t_0 \geq \frac{\Delta t}{\Delta x}(x - x_0), \\ 0, & \text{otherwise,} \end{cases} = \begin{cases} 1, & x - x_0 \leq \frac{\Delta x}{\Delta t}(t - t_0), \\ 0, & \text{otherwise,} \end{cases}$$

it holds

$$\partial_t H_{L_{\mathbb{D}}} = \frac{1}{\sqrt{1 + \left(\frac{\Delta t}{\Delta x}\right)^2}} \delta_L, \quad \partial_x H_{L_{\mathbb{D}}} = -\frac{1}{\sqrt{1 + \left(\frac{\Delta x}{\Delta t}\right)^2}} \delta_L,$$

in particular,

$$\partial_t H_{L_{\mathbb{D}}} = -\frac{\Delta x}{\Delta t} \partial_x H_{L_{\mathbb{D}}}.$$

Proof. Recall the general definition of the partial derivative of a distribution D on $T \times X$:

$$(\partial_t D)(\varphi) = -D(\partial_t \varphi) \quad \text{and} \quad (\partial_x D)(\varphi) = -D(\partial_x \varphi).$$

Hence, the following holds

$$\begin{aligned}
 (\partial_t H_{L_{\mathbb{D}}})(\varphi) &= - \int_X \int_T H_L(t, x) \partial_t \varphi(t, x) dt dx \\
 &= - \int_{-\infty}^{\infty} \int_{t_0 + \frac{\Delta t}{\Delta x}(x - x_0)}^{\infty} \partial_t \varphi(t, x) dt dx \\
 &= \int_{-\infty}^{\infty} \varphi(t_0 + \frac{\Delta t}{\Delta x}(x - x_0), x) dx = \frac{1}{\sqrt{1 + (\frac{\Delta t}{\Delta x})^2}} \int_L \varphi,
 \end{aligned} \tag{6.10}$$

$$\begin{aligned}
 (\partial_x H_{L_{\mathbb{D}}})(\varphi) &= - \int_T \int_X H_L(t, x) \partial_x \varphi(t, x) dx dt \\
 &= - \int_{-\infty}^{\infty} \int_{-\infty}^{x_0 + \frac{\Delta x}{\Delta t}(t - t_0)} \partial_x \varphi(t, x) dx dt \\
 &= - \int_{-\infty}^{\infty} \varphi(t, x_0 + \frac{\Delta x}{\Delta t}(t - t_0)) dt = - \frac{1}{\sqrt{1 + (\frac{\Delta x}{\Delta t})^2}} \int_L \varphi.
 \end{aligned} \tag{6.11}$$

Hence, the claims follow. \square

Corollary 6.18

Let $T \subseteq \mathbb{R}$, $X \subseteq \mathbb{R}$ and $P \subseteq T \times X$ be a polyhedral set with the line segments L_1, L_2, \dots, L_p as its boundaries. Then the partial derivatives of $\chi_{P_{\mathbb{D}}}$ is a linear combination of Dirac segments $\delta_{L_1}, \delta_{L_2}, \dots, \delta_{L_p}$

$$\left(\partial_t^{(m)} \partial_x^{(n)} \chi_{P_{\mathbb{D}}} \right) (\varphi) = \sum_{i=1}^p \xi_i \partial_t^{(m-1)} \partial_x^{(n-1)} \delta_{L_i} \tag{6.12}$$

where $\xi_i \in \mathbb{R}$.

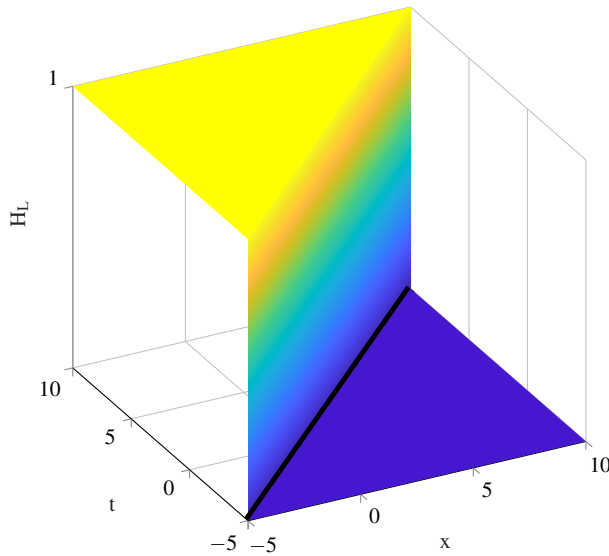


FIGURE 6.2: An illustration of the step function in time and space along some parametrized line L (in black).

Proof. Consider the characteristic function χ_P of a polyhedral set P given by

$$\chi_P(t, x) = \begin{cases} 1, & \text{if } (t, x) \in P, \\ 0, & \text{else,} \end{cases}$$

and assume the boundary Γ of the set P consists of lines and/or line segments L_1, L_2, \dots, L_p , $p \in \mathbb{N} \setminus \{0\}$ that are parametrized as

$$\begin{aligned} L_i &= \{ (t_0^i + \alpha \Delta_i t, x_0^i + \alpha \Delta_i x) \mid \alpha \in [0, \infty) \}, \\ L_i &= \{ (t_0^i + \alpha \Delta_i t, x_0^i + \alpha \Delta_i x) \mid \alpha \in [0, 1] \}, \end{aligned} \quad \text{for } i = 1, \dots, p.$$

Then, one obtains

$$\begin{aligned} (\partial_t \chi_{P_{\mathbb{D}}})(\varphi) &= - \int_P \chi_P(t, x) \partial_t \varphi(t, x) dP \\ &= \int_{\Gamma} \varphi(t, x) d\Gamma = \sum_{i=1}^p \frac{1}{\sqrt{1 + \left(\frac{\Delta_i t}{\Delta_i x}\right)^2}} \int_{L_i} \varphi(t, x) \\ &= \sum_{i=1}^p a_i \delta_{L_i}, \end{aligned}$$

where $a_i \in \mathbb{R}$. Similarly,

$$\begin{aligned} (\partial_x \chi_{P_{\mathbb{D}}})(\varphi) &= - \int_P \chi_P(t, x) \partial_x \varphi(t, x) dP \\ &= - \int_{\Gamma} \varphi(t, x) d\Gamma = - \sum_{i=1}^p \frac{1}{\sqrt{1 + \left(\frac{\Delta_i x}{\Delta_i t}\right)^2}} \int_{L_i} \varphi(t, x) \\ &= \sum_{i=1}^p b_i \delta_{L_i}, \end{aligned}$$

where $b_i \in \mathbb{R}$. Assume for $m \geq 1$, $n = 1$ the following holds

$$\left(\partial_t^{(m)} \partial_x \chi_{P_{\mathbb{D}}} \right) (\varphi) = \sum_{i=1}^p \xi_i \partial_t^{(m-1)} \delta_{L_i},$$

where $\xi_i \in \mathbb{R}$. For $m + 1$, $n = 1$, one obtains

$$\begin{aligned} \left(\partial_t^{(m+1)} \partial_x \chi_{P_{\mathbb{D}}} \right) (\varphi) &= \left(\partial_t \partial_t^{(m)} \partial_x \chi_{P_{\mathbb{D}}} \right) (\varphi) \\ &= \partial_t \sum_{i=1}^p \xi_i \partial_t^{(m-1)} \delta_{L_i} = \sum_{i=1}^p \xi_i \partial_t^{(m)} \delta_{L_i}. \end{aligned}$$

Similar steps can be conducted to prove the result for $n + 1$, $m = 1$ assuming it holds for $n \geq 1$ and $m = 1$. Hence, by induction on m and n , the claim follows as in (6.12). \square

Definition 6.19: Piecewise-smooth distributions in time and space

A distribution $D : C_0^\infty(T \times X; \mathbb{R}) \rightarrow \mathbb{R}$ is called piecewise smooth if and only if there

exists a piecewise smooth function $\beta : T \times X \rightarrow \mathbb{R}$ and a locally finite family of line segments $(L_j)_{j \in J}$ in $T \times X$ and coefficients $\alpha_j^{k,\ell} \in \mathbb{R}$, $k = 0, 1, \dots, n_j^t$, $n_j^t \in \mathbb{N}$, $\ell = 0, 1, \dots, n_j^x$, $n_j^x \in \mathbb{N}$ such that

$$D = \beta_{\mathbb{D}} + \sum_{j \in J} \sum_{k,\ell} \alpha_j^{k,\ell} \partial_t^{(k)} \partial_x^{(\ell)} \delta_{L_j}. \quad (6.13)$$

The space of piecewise-smooth distributions in $T \times X$ is denoted by $\mathbb{D}_{\text{pwC}^\infty}(T \times X)$.

In Figure 6.3, a visualisation of a piecewise-smooth distribution in time and space can be seen where polyhedral partition of the considered domain, Dirac segments and piecewise-smooth functions over polyhedral sets are presented.

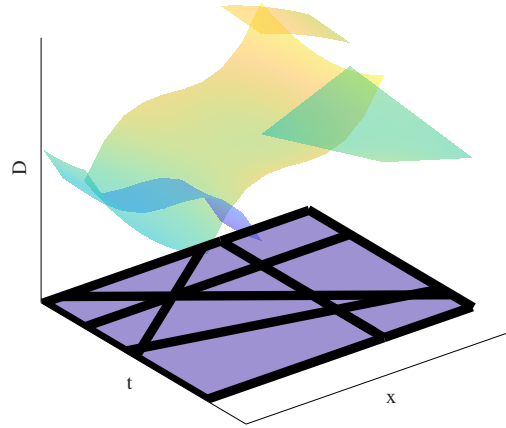


FIGURE 6.3: A 3D illustration of a distribution D in $\mathbb{D}_{\text{pwC}^\infty}(T \times X)$ consisting of four polyhedral sets. The blue region is polyhedral partition of $T \times X$, four polyhedral piecewise-smooth functions are defined over each polyhedral set, on each black line there is a Dirac segment. Magnitudes of Dirac segments are kept small for the ease of visualisation.

Proposition 6.20

Let $D \in \mathbb{D}_{\text{pwC}^\infty}(T \times X)$ given by (6.13) and (6.3), then

$$\partial_t D \in \mathbb{D}_{\text{pwC}^\infty}(T \times X) \quad \text{and} \quad \partial_x D \in \mathbb{D}_{\text{pwC}^\infty}(T \times X),$$

where ∂_t and ∂_x indicate distributional partial derivatives.

Proof. It suffices to show that the (partial) derivative of (the induced distribution by) a piecewise-smooth function (in the sense of Definition 6.12) is a piecewise-smooth function. Since the sum in (6.3) is locally finite, it furthermore suffices to consider only a single summand and since the multiplication with a smooth function is well-defined for general distributions, it suffices to show that the partial derivatives of the indicator function χ_P for any polyhedral set $P \subseteq T \times X$ is a piecewise-smooth distribution, which was already established in Corollary 6.18. Consider the piecewise-smooth function β given as (6.3), for each $i \in I$,

$$\begin{aligned} \frac{\partial_{\mathbb{D}}}{\partial t} (\chi_{P_i} \cdot \beta_i)_{\mathbb{D}} &= \frac{\partial_{\mathbb{D}}}{\partial t} (\beta_i \cdot (\chi_{P_i})_{\mathbb{D}}) \\ &= \partial_t \beta_i \cdot (\chi_{P_i})_{\mathbb{D}} + \beta_i \frac{\partial_{\mathbb{D}}}{\partial t} (\chi_{P_i})_{\mathbb{D}} \\ &= (\chi_{P_i} \partial_t \beta_i)_{\mathbb{D}} + \beta_i \sum_{i=1}^{p_i^*} a_i \delta_{L_i}, \end{aligned}$$

where $a_i \in \mathbb{R}$, $p_i^* \in \mathbb{N}$ is the number of lines that form the boundaries of the polyhedral set $P_i \subseteq T \times X$, hence finite. As a result, if $D \in \mathbb{D}_{\text{pw}\mathcal{C}^\infty}(T \times X)$, then $\partial_t D \in \mathbb{D}_{\text{pw}\mathcal{C}^\infty}(T \times X)$. \square

Lemma 6.21

Let $D \in \mathbb{D}_{\text{pw}\mathcal{C}^\infty}(T \times X)$ given by (6.13) and (6.3), then the restriction of D to any polyhedral set $P \subseteq T \times X$ given by

$$D_P := \left(\sum_{i \in I} \chi_{P_i \cap P} \beta_i \right)_{\mathbb{D}} + \sum_{j \in \mathcal{J}} \sum_{k, \ell} \alpha_j^{k, \ell} \partial_t^{(k)} \partial_x^{(\ell)} \delta_{L_j \cap P} \quad (6.14)$$

is well-defined and a piecewise-smooth distribution.

Proof. First note that the intersection of two polyhedral sets is again a polyhedral set, hence $\sum_{i \in I} \chi_{P_i \cap P} \beta_i$ is a piecewise-smooth function and $(\sum_{i \in I} \chi_{P_i \cap P} \beta_i)_{\mathbb{D}}$ is a well-defined piecewise-smooth distribution with support contained in the closure \bar{P} of P . Furthermore, the intersection of a line segment with a polyhedral set is again a line segment (or empty), for any test function $\varphi \in \mathcal{C}_0^\infty(T \times X)$, the summand

$$\sum_{j \in \mathcal{J}} \sum_{k, \ell} \alpha_j^{k, \ell} \partial_t^{(k)} \partial_x^{(\ell)} \delta_{L_j \cap P}$$

is also a finite sum and hence well-defined with the support contained in \bar{P} . Therefore, D_P as in (6.14) defines a distribution. Moreover, for each $\varphi \in \mathcal{C}_0^\infty(T \times X)$, $D \in \mathbb{D}_{\text{pw}\mathcal{C}^\infty}(T \times X)$ and $P \subseteq T \times X$, if $\text{supp } \varphi \subseteq P$, then $D_P(\varphi) = D(\varphi)$ and if $\text{supp } \varphi \cap P = \emptyset$, then any k -th order partial derivative of φ is zero for every $k \in \mathbb{N}$ and for all $(t, x) \in \bar{P}$; thus, $\varphi = 0$ and $D_P(\varphi) = 0$ (since any derivative of any order of test functions have zero value on a compact set). For any pairwise disjoint polyhedral sets \tilde{P}_i such that $P = \bigcup_{i \in \mathbb{N}} \tilde{P}_i$ it also holds $D_P = \sum_{i \in \mathbb{N}} D_{\tilde{P}_i}$ considering the aforementioned arguments. Hence D_P as in (6.14) is again a well-defined piecewise-smooth distribution. \square

In the following, for any $(t, x) \in T \times X$, the *partial evaluations* $D(t^+, \cdot)$, $D(t^-, \cdot)$, $D(\cdot, x^-)$, $D(\cdot, x^+)$ are defined such that they are piecewise-smooth distributions in X or T , respectively, and such that (partial) differentiation commutes with the partial evaluation; i.e.,

$$(\partial_x D)(t^\pm, \cdot) = D(t^\pm, \cdot)' \quad \text{and} \quad (\partial_t D)(\cdot, x^\pm) = D(\cdot, x^\pm)',$$

where $(\cdot)'$ denotes the (scalar) differentiation in $\mathbb{D}_{\text{pw}\mathcal{C}^\infty}(X)$ or $\mathbb{D}_{\text{pw}\mathcal{C}^\infty}(T)$, respectively. Considering the representation (6.13), it is obvious that for piecewise-smooth functions such an evaluation is trivially defined as

$$\begin{aligned} \beta(t^+, \cdot)_{\mathbb{D}} &:= \lim_{\varepsilon \searrow 0} \beta(t + \varepsilon, \cdot) = \beta(t, \cdot), & \beta(\cdot, x^+)_{\mathbb{D}} &:= \lim_{\varepsilon \searrow 0} \beta(\cdot, x + \varepsilon) = \beta(\cdot, x), \\ \beta(t^-, \cdot)_{\mathbb{D}} &:= \lim_{\varepsilon \searrow 0} \beta(t - \varepsilon, \cdot) = \beta(t, \cdot), & \beta(\cdot, x^-)_{\mathbb{D}} &:= \lim_{\varepsilon \searrow 0} \beta(\cdot, x - \varepsilon) = \beta(\cdot, x), \end{aligned} \quad (6.15)$$

where $\varepsilon > 0$. To define partial evaluations of Dirac segments, consider, for instance,

$$(\partial_t H_{L_{\mathbb{D}}})(\cdot, x^-) = H_{L_{\mathbb{D}}}(\cdot, x^-)',$$

where $H_{L_{\mathbb{D}}}(\cdot, x^-) \in \mathbb{D}_{\text{pw}\mathcal{C}^\infty}(T)$ whose scalar differentiation is the one dimensional Dirac impulse $\delta_{t_0 + \frac{\Delta t}{\Delta x}(x - x_0)}$ and $(\partial_t H_{L_{\mathbb{D}}})$ expressed as in (6.10). Therefore, due to commutativity requirement concerning differentiation and evaluation, and taking Lemma 6.17 into consideration, there is only one possible choice to define partial evaluations of Dirac segments as

$$\begin{aligned}
\delta_L(t^+, \cdot) &:= \begin{cases} \sqrt{1 + \frac{\Delta x^2}{\Delta t^2}} \delta_{x_0 + \frac{\Delta x}{\Delta t}(t-t_0)}, & t \in [t_0, t_1], \\ 0, & \text{otherwise,} \end{cases} \\
\delta_L(t^-, \cdot) &:= \begin{cases} \sqrt{1 + \frac{\Delta x^2}{\Delta t^2}} \delta_{x_0 + \frac{\Delta x}{\Delta t}(t-t_0)}, & t \in (t_0, t_1], \\ 0, & \text{otherwise,} \end{cases} \\
\delta_L(\cdot, x^+) &:= \begin{cases} \sqrt{1 + \frac{\Delta t^2}{\Delta x^2}} \delta_{t_0 + \frac{\Delta t}{\Delta x}(x-x_0)}, & x \in [x_0, x_1], \\ 0, & \text{otherwise,} \end{cases} \\
\delta_L(\cdot, x^-) &:= \begin{cases} \sqrt{1 + \frac{\Delta t^2}{\Delta x^2}} \delta_{t_0 + \frac{\Delta t}{\Delta x}(x-x_0)}, & x \in (x_0, x_1], \\ 0, & \text{otherwise.} \end{cases}
\end{aligned} \tag{6.16}$$

Remark 6.22

The factors in front of δ distributions in (6.16) are due to the parametrization of the line L which yields transformation of axes, such as rotation, reflection and translation, which is also the case in Lemma 6.17 when differentiating the step function. Therefore, it is easy to see the connection of the step functions; and hence Dirac impulses, in one- and two-dimension. Given the parametrized line L , if sufficient transformations of axes are carried out to obtain such a coordinate system whose x -axis is the line L , then at some specific x , the Heaviside step function $\mathbb{1}_{[t, \infty)}$ in 1D is obtained.

Definition 6.23

Let $D \in \mathbb{D}_{\text{pw}C^\infty}(T \times X)$ given by (6.13) and (6.3). Then for any $(t, x) \in T \times X$, *partial evaluations* of D are given by

$$\begin{aligned}
D(t^\pm, \cdot) &:= \beta(t^\pm, \cdot)_{\mathbb{D}} + \sum_{j \in \mathcal{J}} \sum_{k, \ell} \alpha_j^{k, \ell} \partial_t^{(k)} \partial_x^{(\ell)} (\delta_{L_j}(t^\pm, \cdot)), \\
D(\cdot, x^\pm) &:= \beta(\cdot, x^\pm)_{\mathbb{D}} + \sum_{j \in \mathcal{J}} \sum_{k, \ell} \alpha_j^{k, \ell} \partial_t^{(k)} \partial_x^{(\ell)} (\delta_{L_j}(\cdot, x^\pm)),
\end{aligned}$$

where $\beta(t^\pm, \cdot)_{\mathbb{D}}$, $\beta(\cdot, x^\pm)_{\mathbb{D}}$ and $\delta_L(t^\pm, \cdot)$, $\delta_L(\cdot, x^\pm)$ are given as in (6.15) and (6.16), respectively.

Corollary 6.24

For this choice of evaluation, it holds that for $\varepsilon > 0$, $t \in T$ and $x \in X$

$$\begin{aligned}
D(t^+, \cdot)(\varphi(t, \cdot)) &= \lim_{\varepsilon \searrow 0} \frac{1}{\varepsilon} D_{(t, t+\varepsilon) \times X}(\varphi), \\
D(\cdot, x^+)(\varphi(\cdot, x)) &= \lim_{\varepsilon \searrow 0} \frac{1}{\varepsilon} D_{T \times (x, x+\varepsilon)}(\varphi), \\
D(t^-, \cdot)(\varphi(t, \cdot)) &= \lim_{\varepsilon \searrow 0} \frac{1}{\varepsilon} D_{(t-\varepsilon, t) \times X}(\varphi), \\
D(\cdot, x^-)(\varphi(\cdot, x)) &= \lim_{\varepsilon \searrow 0} \frac{1}{\varepsilon} D_{T \times (x-\varepsilon, x)}(\varphi),
\end{aligned}$$

where $D \in \mathbb{D}_{\text{pw}C^\infty}(T \times X)$.

Proof. The first relation is proved as the rest is akin. Let $D \in \mathbb{D}_{\text{pw}C^\infty}(T \times X)$ with the representation (6.13) and $L_j = \left\{ \left(t, x_{0j} + \frac{\Delta x_j}{\Delta t_j} (t - t_{0j}) \right) \mid t \in \mathbb{R}, \Delta t_j = 0 \right\}$ be the parametrized line for $j \in \mathcal{J}$. This parametrization yields $\delta_{L_j}(t^+, \cdot) = 0$ and also $L_j \cap ((t, t + \varepsilon) \times X) = \emptyset$ for $t \in \mathbb{R}$, where $L_j = \{(t_0, x) \mid x \in X\}$. Now let the parametrized line L_j be given by $L_j = \left\{ \left(t, x_{0j} + \frac{\Delta x_j}{\Delta t_j} (t - t_{0j}) \right) \mid t \in \mathbb{R}, \Delta t_j > 0 \right\}$ for $j \in \mathcal{J}$. Then

$$\begin{aligned}
\lim_{\varepsilon \searrow 0} \frac{1}{\varepsilon} D_{(t, t+\varepsilon) \times X}(\varphi) &= \lim_{\varepsilon \searrow 0} \frac{1}{\varepsilon} \left(\sum_{i \in I} \chi_{P_i \cap ((t, t+\varepsilon) \times X)} \beta_i \right)_{\mathbb{D}}(\varphi) \\
&\quad + \lim_{\varepsilon \searrow 0} \frac{1}{\varepsilon} \sum_{j \in \mathcal{J}} \sum_{k, \ell} \alpha_j^{k, \ell} \partial_t^{(k)} \partial_x^{(\ell)} \delta_{L_j \cap ((t, t+\varepsilon) \times X)}(\varphi) \\
&= \lim_{\varepsilon \searrow 0} \frac{1}{\varepsilon} \left(\int_t^{t+\varepsilon} \int_X \sum_{i \in I} \chi_{P_i} \beta_i \varphi \right) \\
&\quad + \sum_{j \in \mathcal{J}} \sum_{k, \ell} (-1)^k \alpha_j^{k, \ell} \partial_x^{(\ell)} \lim_{\varepsilon \searrow 0} \frac{1}{\varepsilon} \int_t^{t+\varepsilon} \partial_t^{(k)} \varphi \left(\tau, x_{0j} + \frac{\Delta x_j}{\Delta t_j} (\tau - t_{0j}) \right) \sqrt{1 + \frac{\Delta x_j^2}{\Delta t_j^2}} d\tau \\
&= \left(\sum_{i \in I} \beta_i(t, \cdot) (\varphi(t, \cdot)) \right) \\
&\quad + \sum_{j \in \mathcal{J}} \sum_{k, \ell} (-1)^k \alpha_j^{k, \ell} \partial_x^{(\ell)} \partial_t^{(k)} \varphi \left(t, x_{0j} + \frac{\Delta x_j}{\Delta t_j} (t - t_{0j}) \right) \sqrt{1 + \frac{\Delta x_j^2}{\Delta t_j^2}} \\
&= \beta(t, \cdot) (\varphi(t, \cdot)) + \sum_{j \in \mathcal{J}} \sum_{k, \ell} \alpha_j^{k, \ell} \partial_x^{(\ell)} \partial_t^{(k)} \delta_{x_{0j} + \frac{\Delta x_j}{\Delta t_j} (t - t_{0j})} (\varphi(t, \cdot)) \sqrt{1 + \frac{\Delta x_j^2}{\Delta t_j^2}} \\
&= \beta(t^+, \cdot)_{\mathbb{D}} (\varphi(t, \cdot)) + \sum_{j \in \mathcal{J}} \sum_{k, \ell} \alpha_j^{k, \ell} \partial_t^{(k)} \partial_x^{(\ell)} (\delta_{L_j}(t^\pm, \cdot)) (\varphi(t, \cdot)) \\
&= D(t^+, \cdot) (\varphi(t, \cdot)),
\end{aligned}$$

where $\varepsilon > 0$ and Equation (6.6) (as $\Delta t_j \neq 0$) and the mean value theorem are employed. Note that $\Delta x_j / \Delta t_j$ is independent of ε for each $j \in \mathcal{J}$ as the slopes of parametrized lines remain the same. \square

Remark 6.25

Note that due to Lemma 6.17, when $\Delta t = 0$ the partial evaluations $\delta_L(t^\pm, \cdot)$ are defined as 0. Similarly, for $\Delta x = 0$ the partial evaluations $\delta_L(\cdot, x^\pm) = 0$.

Proof. This is a consequence of Lemma 6.17; i.e., the relations between partial derivatives of the step function and Dirac segments. For the temporal partial derivative in (6.10), the line L , on which the Dirac segment is taken, is parametrized such that $\{(t_0 + \frac{\Delta t}{\Delta x}(x - x_0), x \mid x \in R\}$ where $\Delta x \neq 0$. And for the spatial partial derivative in (6.11), the line L is parametrized such that $\{t, (x_0 + \frac{\Delta x}{\Delta t}(t - t_0)) \mid t \in R\}$ where $\Delta t \neq 0$. \square

Chapter 7

Distributional solutions for linear hyperbolic PDEs

In this chapter, the solutions of linear hyperbolic PDEs in the space of piecewise-smooth distributions in time and space $\mathbb{D}_{\text{pw}C^\infty}(T \times X)$ are studied. The solutions are interpreted in the distributional sense, therefore, thanks to this solution framework, they can have jumps, Dirac impulses and arbitrary high order of their derivatives. The space $\mathbb{D}_{\text{pw}C^\infty}(T \times X)$ allows the trace evaluation on the boundaries of PDEs which is required for coupling PDEs with swDAEs as solutions to swDAEs can include jumps and Dirac impulses. Hence, the solution space for PDEs must be chosen suitably according to solutions of swDAEs. Furthermore, an explicit distributional solution formula to linear hyperbolic PDEs is provided and then the uniqueness result for the constructed solution is shown.

7.1 Scalar advection equation

Before addressing linear systems, the following scalar advection equation is studied

$$\partial_t v + \lambda \partial_x v = 0, \quad (7.1)$$

where $\lambda \in \mathbb{R}$ is the wave speed and the initial condition is prescribed as

$$\text{I.C.} \quad v(t_0^+, \cdot) = v^0, \quad (7.2)$$

where $v^0 \in \mathbb{D}_{\text{pw}C^\infty}((a, b))$ and the boundary condition given by

$$\text{B.C.} \quad \begin{cases} v(\cdot, a^+) = v^L, & \text{if } \lambda > 0, \\ v(\cdot, b^-) = v^R, & \text{if } \lambda < 0, \end{cases} \quad (7.3)$$

where $v^L, v^R \in \mathbb{D}_{\text{pw}C^\infty}((t_0, \infty))$.

Now the definition of the shift operator for continuous functions in Definition 2.10 is expanded to distributions.

Definition 7.1: 2D shift operators for Dirac impulses

Let $T, X \subseteq \mathbb{R}$ be open sets. The *distributional time shift operator* of a Dirac impulse $\delta_{t^*} \in \mathbb{D}_{\text{pw}C^\infty}(T)$ at $t^* \in T$ with speed $\lambda \neq 0$ and initial position x_0 is given by

$$S_{\text{time}}^{\lambda, x_0} \delta_{t^*} := \frac{1}{\sqrt{1 + \frac{1}{\lambda^2}}} \delta_{L_{\text{time}}^{\lambda, (t^*, x_0)}},$$

where $L_{\text{time}}^{\lambda, (t^*, x_0)} := \{(t, x_0 + \lambda(t - t^*)) \mid t \in T\} \cap (T \times X)$. Moreover, the *distributional space shift operator* of a Dirac impulse $\delta_{x^*} \in \mathbb{D}_{\text{pw}C^\infty}(X)$ at $x^* \in X$ with speed λ and initial time t_0 is given by

$$\mathcal{S}_{\text{space}}^{\lambda, t_0} \delta_{x^*} := \frac{1}{\sqrt{1 + \lambda^2}} \delta_{L_{\text{space}}^{\lambda, (t_0, x^*)}},$$

where $L_{\text{space}}^{\lambda, (t_0, x^*)} := \{(t_0 + \frac{1}{\lambda}(x - x^*), x) \mid x \in X\} \cap (T \times X)$.

Note that the factors $1/\sqrt{1 + 1/\lambda^2}$ and $1/\sqrt{1 + \lambda^2}$ in the definition of the shift operator for Dirac impulses are necessary to obtain the following equalities

$$\left(\mathcal{S}_{\text{time}}^{\lambda, x_0} \delta_{t^*}\right)(\cdot, x^\pm) = \delta_{t^* + \frac{1}{\lambda}(x - x_0)} \quad \text{and} \quad \left(\mathcal{S}_{\text{space}}^{\lambda, t_0} \delta_{x^*}\right)(t^\pm, \cdot) = \delta_{x^* + \lambda(t - t_0)}.$$

In particular,

$$\left(\mathcal{S}_{\text{time}}^{\lambda, x_0} \delta_{t^*}\right)(\cdot, x_0^\pm) = \delta_{t^*} \quad \text{and} \quad \left(\mathcal{S}_{\text{space}}^{\lambda, t_0} \delta_{x^*}\right)(t_0^\pm, \cdot) = \delta_{x^*}.$$

An illustration of the time- and space shift of Dirac impulses can also be found in Figure 7.1.

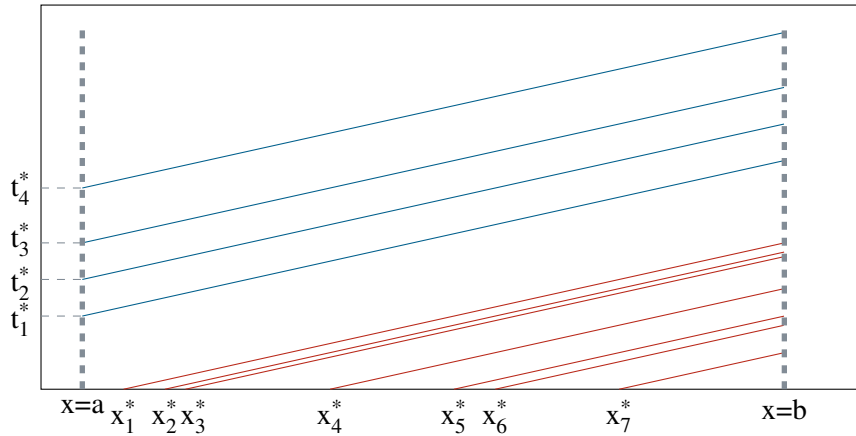


FIGURE 7.1: PDE domain $(t_0, \infty) \times (a, b)$, $\lambda > 0$. An example of Dirac impulses prescribed in initial and boundary conditions at certain locations in space, x_m^* , $m = \{1, 2, \dots, 7\}$, and time domains, t_i^* , $i = \{1, 2, 3, 4\}$, respectively. The blue and red lines correspond to the Dirac segments on these lines and show how Dirac impulses are shifted within the domain.

Definition 7.2: 2D shift operators for piecewise-smooth distributions

Let $T \subseteq \mathbb{R}$, $X \subseteq \mathbb{R}$ be open sets. Let $D^T \in \mathbb{D}_{\text{pw}C^\infty}(T)$ and $D^X \in \mathbb{D}_{\text{pw}C^\infty}(X)$ be given by

$$D^T = d_{\mathbb{D}}^T + \sum_{t^* \in T^*} D_{t^*}^T \quad \text{and} \quad D^X = d_{\mathbb{D}}^X + \sum_{x^* \in X^*} D_{x^*}^X, \quad (7.4)$$

where $d^T \in C_{\text{pw}}^\infty(T)$, $d^X \in C_{\text{pw}}^\infty(X)$, $T^* \subset T$ and $X^* \subset X$ are locally finite sets, and for each $t^* \in T^*$ and $x^* \in X^*$, there exist $n^{t^*} \in \mathbb{N}$ and $n^{x^*} \in \mathbb{N}$, $c_i^{t^*} \in \mathbb{R}$, $i = 0, 1, \dots, n^{t^*}$ and

$c_j^{x^*} \in \mathbb{R}$, $j = 0, 1, \dots, n^{x^*}$ such that

$$D_{t^*}^T = \sum_{i=0}^{n^{t^*}} c_i^{t^*} \partial_t^{(i)} \delta_{t^*} \quad \text{and} \quad D_{x^*}^X = \sum_{j=0}^{n^{x^*}} c_j^{x^*} \partial_x^{(j)} \delta_{x^*}.$$

Then the distributional time shift of D^T with speed λ and initial position x_0 is given by

$$\mathcal{S}_{\text{time}}^{\lambda, x_0} D^T := (\mathcal{S}_{\text{time}}^{\lambda, x_0} d^T)_{\mathbb{D}} + \sum_{t^* \in T^*} \sum_{i=0}^{n^{t^*}} c_i^{t^*} \partial_t^{(i)} \mathcal{S}_{\text{time}}^{\lambda, x_0} \delta_{t^*},$$

and the distributional space shift of D^X with speed λ and initial time t_0 is given by

$$\mathcal{S}_{\text{space}}^{\lambda, t_0} D^X := (\mathcal{S}_{\text{space}}^{\lambda, t_0} d^X)_{\mathbb{D}} + \sum_{x^* \in X^*} \sum_{j=0}^{n^{x^*}} c_j^{x^*} \partial_x^{(j)} \mathcal{S}_{\text{space}}^{\lambda, t_0} \delta_{x^*}.$$

Corollary 7.3

2D distributional time and shift operators, $\mathcal{S}_{\text{time}}^{\lambda, x_0}$, $\mathcal{S}_{\text{space}}^{\lambda, t_0}$, where λ , t_0 , $x_0 \in \mathbb{R}$, commute with distributional partial derivative operators $\partial_t^{(n)}$, $\partial_x^{(n)}$ for $n \in \mathbb{N}$.

Proof. Below, the claim is proven for the Dirac impulse/segment as for piecewise-smooth functions it has been proven in Chapter 2. Let $\delta_{t^*} \in \mathbb{D}_{\text{pw}C^\infty}(T)$ for some $t^* \in \mathbb{R}$. Then for $n = 1$

$$\begin{aligned} \partial_t \mathcal{S}_{\text{time}}^{\lambda, x_0} \delta_{t^*} &= \partial_t \delta_{L_{\text{time}}^{\lambda, (t^*, x_0)}} \\ &= -\delta_{L_{\text{time}}^{\lambda, (t^*, x_0)}} (\partial_t \varphi) \\ &= - \int_{L_{\text{time}}^{\lambda, (t^*, x_0)}} \partial_t \varphi \\ &= -\partial_t \int_{L_{\text{time}}^{\lambda, (t^*, x_0)}} \varphi \\ &= \partial_t \mathcal{S}_{\text{time}}^{\lambda, x_0} \delta_{t^*}. \end{aligned}$$

Assume the claim holds for $n \geq 1$. Then, for $n + 1$, the following is obtained

$$\begin{aligned} \mathcal{S}_{\text{time}}^{\lambda, x_0} \partial_t^{(n+1)} \delta_{t^*} &= \mathcal{S}_{\text{time}}^{\lambda, x_0} \partial_t^{(n)} \partial_t \delta_{t^*} \\ &= \partial_t^{(n)} \mathcal{S}_{\text{time}}^{\lambda, x_0} \partial_t \delta_{t^*} \\ &= \partial_t^{(n+1)} \mathcal{S}_{\text{time}}^{\lambda, x_0} \delta_{t^*}. \end{aligned}$$

Thus, by induction, the claim follows. Analogously, the above steps are followed to prove the commutativity of $\mathcal{S}_{\text{space}}^{\lambda, t_0}$ and $\partial_x^{(n)}$. \square

Assume $\lambda > 0$ and let v^{t_0} and v^L be given as in (7.2) and (7.3) with the representations as in (7.4). With the distributions v^{t_0} , v^L , below the *distributional solution* to Equation (7.1) in terms of the distributional space/time shift operators $\mathcal{S}_{\text{space}}^{\lambda, t_0}$, $\mathcal{S}_{\text{time}}^{\lambda, a}$ is formulated. As seen in

Section 2.2.1, since the solution is constant along the characteristics, exploiting the distributional space and time shift operators given in Definition 7.2, it can be written as

$$v = \left(\left(\mathbb{1}_{\{x-a \geq \lambda(t-t_0)\}} \right)_{\mathbb{D}} \mathcal{S}_{\text{space}}^{\lambda, t_0} v^{t_0} + \left(\mathbb{1}_{\{x-a < \lambda(t-t_0)\}} \right)_{\mathbb{D}} \mathcal{S}_{\text{time}}^{\lambda, a} v^L \right). \quad (7.5)$$

Then, the *distributional solution* to the differential equation (7.1) at the right boundary with $\lambda > 0$ takes the form

$$v(\cdot, b^-) = \left(\left(\mathbb{1}_{\left(t_0, t_0 + \frac{b-a}{\lambda}\right)} \right)_{\mathbb{D}} \mathcal{S}_{\text{space}}^{\lambda, t_0} v^{t_0} + \left(\mathbb{1}_{\left(t_0 + \frac{b-a}{\lambda}, \infty\right)} \right)_{\mathbb{D}} \mathcal{S}_{\text{time}}^{\lambda, a} v^L \right)(\cdot, b^-),$$

which can be put in the form

$$v(\cdot, b^-) = \left(\mathcal{S}_{\text{time}}^{\lambda, a} v^L \right)(\cdot, b^-),$$

where

$$\left(\mathcal{S}_{\text{time}}^{\lambda, a} v^L \right)(\cdot, b^-) := \left(\mathcal{S}_{\text{space}}^{\lambda, t_0} v^{t_0} \right)(\cdot, b^-), \quad \text{on } \left(t_0, t_0 + \frac{b-a}{\lambda} \right).$$

Now assume $\lambda < 0$ and let v^{t_0} and v^R be given as in (7.2) and (7.3) with the representations as in (7.4). The solution formulae to Equation (7.1) with $\lambda < 0$ are now of the form

$$v = \left(\left(\mathbb{1}_{\{x-b \leq \lambda(t-t_0)\}} \right)_{\mathbb{D}} \mathcal{S}_{\text{space}}^{\lambda, t_0} v^{t_0} + \left(\mathbb{1}_{\{x-b > \lambda(t-t_0)\}} \right)_{\mathbb{D}} \mathcal{S}_{\text{time}}^{\lambda, b} v^R \right),$$

Similarly, the *distributional solution* to the differential equation (7.1) with $\lambda < 0$ at the left boundary can be written as

$$v(\cdot, a^+) = \left(\left(\mathbb{1}_{\left(t_0, t_0 + \frac{b-a}{-\lambda}\right)} \right)_{\mathbb{D}} \mathcal{S}_{\text{space}}^{\lambda, t_0} v^{t_0} + \left(\mathbb{1}_{\left(t_0 + \frac{b-a}{-\lambda}, \infty\right)} \right)_{\mathbb{D}} \mathcal{S}_{\text{time}}^{\lambda, b} v^R \right)(\cdot, a^+),$$

which is then of the form

$$v(\cdot, a^+) = \mathcal{S}_{\text{time}}^{\lambda, b} v^R(\cdot, a^+),$$

where

$$\left(\mathcal{S}_{\text{time}}^{\lambda, b} v^R \right)(\cdot, a^+) := \left(\mathcal{S}_{\text{space}}^{\lambda, t_0} v^{t_0} \right)(\cdot, a^+), \quad \text{on } \left(t_0, t_0 + \frac{b-a}{-\lambda} \right).$$

7.2 Linear systems of partial differential equations

As a system of PDEs with boundary conditions, the following system is considered

$$\partial_t \mathbf{u} + \mathbf{A} \partial_x \mathbf{u} = \mathbf{0}, \quad (7.6a)$$

$$\text{I.C.} \quad \mathbf{u}(t_0^+, \cdot) = \mathbf{u}^{t_0}, \quad (7.6b)$$

$$\text{B.C.} \quad \mathbf{P}_a \mathbf{u}(\cdot, a^+) = \mathbf{b}^a, \quad \text{and} \quad \mathbf{P}_b \mathbf{u}(\cdot, b^-) = \mathbf{b}^b, \quad (7.6c)$$

with the unknown $\mathbf{u} \in (\mathbb{D}_{\text{pw}C^\infty}((t_0, \infty) \times (a, b)))^n$ and initial condition $\mathbf{u}^{t_0} \in (\mathbb{D}_{\text{pw}C^\infty}(a, b))^n$ and $\mathbf{b}^a \in (\mathbb{D}_{\text{pw}C^\infty}((t_0, \infty)))^{n-\ell}$, $\mathbf{b}^b \in (\mathbb{D}_{\text{pw}C^\infty}((t_0, \infty)))^\ell$ are left and right boundary conditions with $\mathbf{P}_a \in \mathbb{R}^{(n-\ell) \times n}$, and $\mathbf{P}_b \in \mathbb{R}^{\ell \times n}$.

As in Section 2.2.1 with Assumption **(H-3)**, the system is decomposed into its *distributional characteristic variables* $\mathbf{v} \in (\mathbb{D}_{\text{pwC}^\infty}((t_0, \infty) \times (a, b)))^n$ with the initial condition

$$\mathbf{v}(t_0^+, \cdot) = \begin{pmatrix} \mathbf{v}_-(t_0^+, \cdot) \\ \mathbf{v}_+(t_0^+, \cdot) \end{pmatrix} =: \begin{pmatrix} \mathbf{v}_-^{t_0} \\ \mathbf{v}_+^{t_0} \end{pmatrix}, \quad (7.7)$$

where $\mathbf{v}_-^{t_0} \in (\mathbb{D}_{\text{pwC}^\infty}(a, b))^\ell$, $\mathbf{v}_+^{t_0} \in (\mathbb{D}_{\text{pwC}^\infty}(a, b))^{n-\ell}$ and the boundary conditions take the form

$$\mathbf{M}\mathbf{v}(\cdot, a^+) = \mathbf{b}^a, \quad \text{and} \quad \mathbf{N}\mathbf{v}(\cdot, b^-) = \mathbf{b}^b,$$

where the boundary conditions for the right- and left-going waves can be expressed as

$$\mathbf{v}_+(\cdot, a^+) = \tilde{\mathbf{b}}_a, \quad (7.8a)$$

$$\mathbf{v}_-(\cdot, b^-) = \tilde{\mathbf{b}}_b, \quad (7.8b)$$

where boundary conditions $\tilde{\mathbf{b}}_a \in (\mathbb{D}_{\text{pwC}^\infty}(T))^{n-\ell}$, $\tilde{\mathbf{b}}_b \in (\mathbb{D}_{\text{pwC}^\infty}(T))^\ell$, $\mathbf{v} = (\mathbf{v}_-^\top, \mathbf{v}_+^\top)^\top$ and $\mathbf{v}^{t_0} = (\mathbf{v}_-^{t_0\top}, \mathbf{v}_+^{t_0\top})^\top$ where $\mathbf{v}_- \in (\mathbb{D}_{\text{pwC}^\infty}((t_0, \infty) \times (a, b)))^\ell$ stands for the left-going waves, whilst $\mathbf{v}_+ \in (\mathbb{D}_{\text{pwC}^\infty}((t_0, \infty) \times (a, b)))^{n-\ell}$ for the right-going waves.

The *distributional solution* \mathbf{v} to the decomposed system of (7.6a), as was done similarly to (2.5), with the initial condition (7.7) and boundary conditions (7.8a)-(7.8b) can be written in terms of the solutions of the left- and right-going waves

$$\begin{aligned} \mathbf{v} &= \sum_{i \in K^-} \begin{bmatrix} \text{diag}(\mathbf{e}_i) \\ \mathbf{0}_{n-\ell, \ell} \end{bmatrix} \left((\mathbb{1}_{\{x-b \leq \lambda_i(t-t_0)\}})_{\mathbb{D}} \mathcal{S}_{\text{space}}^{\lambda_i, t_0} \mathbf{v}_-^{t_0} + (\mathbb{1}_{\{x-b > \lambda_i(t-t_0)\}})_{\mathbb{D}} \mathcal{S}_{\text{time}}^{\lambda_i, b} \tilde{\mathbf{b}}^b \right) \\ &+ \sum_{j \in K^+} \begin{bmatrix} \mathbf{0}_{\ell, n-\ell} \\ \text{diag}(\mathbf{e}_j) \end{bmatrix} \left((\mathbb{1}_{\{x-a \geq \lambda_j(t-t_0)\}})_{\mathbb{D}} \mathcal{S}_{\text{space}}^{\lambda_j, t_0} \mathbf{v}_+^{t_0} + (\mathbb{1}_{\{x-a < \lambda_j(t-t_0)\}})_{\mathbb{D}} \mathcal{S}_{\text{time}}^{\lambda_j, a} \tilde{\mathbf{b}}^a \right), \end{aligned} \quad (7.9)$$

where $K^- := \{1, \dots, \ell\}$ and $K^+ := \{\ell + 1, \dots, n\}$ and $\mathbf{e}_i \in \mathbb{R}^\ell$ and $\mathbf{e}_j \in \mathbb{R}^{n-\ell}$ are the i -th and j -th directional unit vectors, respectively.

The distributional solution \mathbf{u} to the IBVP (7.6) is now formulated via inversion of the distributional characteristic variables $\mathbf{u} = \mathbf{R}\mathbf{v}$. Let $\Pi_p := \mathbf{R} \text{diag}(\mathbf{e}_p) \mathbf{R}^{-1}$ with $\mathbf{e}_p \in \mathbb{R}^n$ the p -th directional unit vector. The solution is

$$\begin{aligned} \mathbf{u} &= \sum_{i \in K^-} \Pi_i \left((\mathbb{1}_{\{x-b \leq \lambda_i(t-t_0)\}})_{\mathbb{D}} \mathcal{S}_{\text{space}}^{\lambda_i, t_0} \mathbf{u}^{t_0} + (\mathbb{1}_{\{x-b > \lambda_i(t-t_0)\}})_{\mathbb{D}} \mathcal{S}_{\text{time}}^{\lambda_i, b} \mathbf{u}^R \right) \\ &+ \sum_{j \in K^+} \Pi_j \left((\mathbb{1}_{\{x-a \geq \lambda_j(t-t_0)\}})_{\mathbb{D}} \mathcal{S}_{\text{space}}^{\lambda_j, t_0} \mathbf{u}^{t_0} + (\mathbb{1}_{\{x-a < \lambda_j(t-t_0)\}})_{\mathbb{D}} \mathcal{S}_{\text{time}}^{\lambda_j, a} \mathbf{u}^L \right), \end{aligned}$$

or, in the compact form

$$\mathbf{u} = \sum_{i \in K^-} \Pi_i \left(\mathcal{S}_{\text{time}}^{\lambda_i, b} \mathbf{u}^R \right) + \sum_{j \in K^+} \Pi_j \left(\mathcal{S}_{\text{time}}^{\lambda_j, a} \mathbf{u}^L \right), \quad (7.10)$$

with

$$\begin{aligned} \left(\mathcal{S}_{\text{time}}^{\Lambda^-, \mathbf{I}, b} \mathbf{u}^R \right) &:= \sum_{i \in K^-} \Pi_i \left(\mathcal{S}_{\text{space}}^{\lambda_i, t_0} \mathbf{u}^{t_0} \right), \quad \text{on} \quad \left(t_0, t_0 + \frac{b-x}{-\lambda_i} \right), \\ \left(\mathcal{S}_{\text{time}}^{\Lambda^+, \mathbf{I}, a} \mathbf{u}^L \right) &:= \sum_{i \in K^+} \Pi_i \left(\mathcal{S}_{\text{space}}^{\lambda_i, t_0} \mathbf{u}^{t_0} \right), \quad \text{on} \quad \left(t_0, t_0 + \frac{x-a}{\lambda_i} \right). \end{aligned}$$

At the left- and right-end of the spatial domain, the distributional solution \mathbf{u} is as follows

$$\begin{aligned}\mathbf{u}(\cdot, a^+) &= \mathbf{R} \begin{bmatrix} \mathbf{0}_{\ell, n-\ell} \\ \mathbf{M}_2^{-1} \end{bmatrix} \mathbf{b}^a(\cdot) \\ &\quad + \mathbf{R} \begin{bmatrix} \mathbf{I}_{\ell, \ell} & \mathbf{0}_{\ell, n-\ell} \\ -\mathbf{M}_2^{-1} \mathbf{M}_1 & \mathbf{0}_{n-\ell, n-\ell} \end{bmatrix} \mathbf{R}^{-1} \sum_{i \in K^-} \Pi_i \left(\mathcal{S}_{\text{time}}^{\lambda_i, b} \mathbf{u}^R \right) (\cdot, a^+), \\ \mathbf{u}(\cdot, b^-) &= \mathbf{R} \begin{bmatrix} \mathbf{N}_1^{-1} \\ \mathbf{0}_{n-\ell, \ell} \end{bmatrix} \mathbf{b}^b(\cdot) \\ &\quad + \mathbf{R} \begin{bmatrix} \mathbf{0}_{\ell, \ell} & -\mathbf{N}_1^{-1} \mathbf{N}_2 \\ \mathbf{0}_{n-\ell, \ell} & \mathbf{I}_{n-\ell, n-\ell} \end{bmatrix} \mathbf{R}^{-1} \sum_{j \in K^+} \Pi_j \left(\mathcal{S}_{\text{time}}^{\lambda_j, a} \mathbf{u}^L \right) (\cdot, b^-),\end{aligned}\tag{7.11}$$

where $\mathbf{u}^L := \mathbf{u}(\cdot, a^+)$, $\mathbf{u}^R := \mathbf{u}(\cdot, b^-)$ and with

$$\begin{aligned}\left(\mathcal{S}_{\text{time}}^{\Lambda^-, \mathbf{I}, b} \mathbf{u}^R \right) (\cdot, a^+) &:= \sum_{i \in K^-} \Pi_i \left(\mathcal{S}_{\text{space}}^{\lambda_i, t_0} \mathbf{u}^{t_0} \right) (\cdot, a^+), \quad \text{on } \left(t_0, t_0 + \frac{b-a}{-\lambda_i} \right), \\ \left(\mathcal{S}_{\text{time}}^{\Lambda^+, \mathbf{I}, a} \mathbf{u}^L \right) (\cdot, b^-) &:= \sum_{i \in K^+} \Pi_i \left(\mathcal{S}_{\text{space}}^{\lambda_i, t_0} \mathbf{u}^{t_0} \right) (\cdot, b^-), \quad \text{on } \left(t_0, t_0 + \frac{b-a}{\lambda_i} \right).\end{aligned}\tag{7.12}$$

Similar to the 1D time shift defined in Definition 2.17, below the 1D distributional time shift $\mathcal{S}_{\text{time}}^\tau$ for Dirac impulses and piecewise-smooth distributions $D \in \mathbb{D}_{\text{pw}C^\infty}(T)$ is defined.

Definition 7.4: 1D distributional time shift operator for Dirac impulses

Let $T \subseteq \mathbb{R}$ be an open set. The 1D distributional time shift operator $\mathcal{S}_{\text{time}}^\tau$ with $\tau \in \mathbb{R}$ of a Dirac impulse $\delta_{t^*} \in \mathbb{D}_{\text{pw}C^\infty}(T)$ at $t^* \in T$ is defined by

$$\mathcal{S}_{\text{time}}^\tau \delta_{t^*} := \delta_{t^* + \tau}.$$

Definition 7.5: 1D distributional time shift operator for piecewise-smooth distributions

Let $T \subseteq \mathbb{R}$ be an open set. Let $D \in \mathbb{D}_{\text{pw}C^\infty}(T)$ be given by

$$D = d_{\mathbb{D}} + \sum_{t^* \in T^*} D_{t^*},$$

where $d \in C_{\text{pw}}^\infty(T)$, $T^* \subset T$ is a locally finite set, and for each $t^* \in T^*$, there exist $n^{t^*} \in \mathbb{N}$, $c_i^{t^*} \in \mathbb{R}$, $i = 0, 1, \dots, n^{t^*}$ such that

$$D_{t^*} = \sum_{i=0}^{n^{t^*}} c_i^{t^*} \partial_t^{(i)} \delta_{t^*}.$$

Then the 1D distributional time shift of D is given by

$$\mathcal{S}_{\text{time}}^\tau D := (\mathcal{S}_{\text{time}}^\tau d)_{\mathbb{D}} + \sum_{t^* \in T^*} \sum_{i=0}^{n^{t^*}} c_i^{t^*} \partial_t^{(i)} \mathcal{S}_{\text{time}}^\tau \delta_{t^*}.$$

Remark 7.6

Similar to Corollary 7.3, 1D distributional time shift operator $\mathcal{S}_{\text{time}}^\tau$ for $\tau \in \mathbb{R}$ commutes with the distributional derivative operator $\frac{d}{dt}$.

Remark 7.7

Let $\mathbf{u}_{ab} := \left(\mathbf{u}^{L^\top}, \mathbf{u}^{R^\top} \right)^\top \in (\mathbb{D}_{\text{pw}C^\infty}(T))^{2n}$, where \mathbf{u}^L and \mathbf{u}^R are defined in (7.11). Below, \mathbf{u}_{ab} is expressed in a compressed form in terms of the 1D distributional time shift operator $\mathcal{S}_{\text{time}}^\tau$

$$\mathbf{u}_{ab} = \mathbf{F} \begin{bmatrix} \mathbf{b}^a \\ \mathbf{b}^b \end{bmatrix} + \sum_{k=1}^n \mathbf{D}_k \mathcal{S}_{\text{time}}^{\tau_k} \mathbf{u}_{ab}, \quad (7.13)$$

where

$$\mathbf{F} = \begin{bmatrix} \mathbf{F}_a & \mathbf{0}_{n,\ell} \\ \mathbf{0}_{n,n-\ell} & \mathbf{F}_b \end{bmatrix}, \quad \mathbf{D}_k = \begin{bmatrix} \mathbf{0}_{n,n} & \mathbf{D}_k^{ab} \\ \mathbf{D}_k^{ba} & \mathbf{0}_{n,n} \end{bmatrix},$$

$$\tau_k = \frac{b-a}{\text{sgn}(\lambda_k)\lambda_k}, \quad k = 1, 2, \dots, n,$$

where the matrices $\mathbf{F}_a, \mathbf{F}_b, \mathbf{D}_k^{ab}, \mathbf{D}_k^{ba}$ are given in (2.67)-(2.68). The extensions of initial conditions as boundary conditions for $t \leq t_0 + \frac{b-a}{\text{sgn}(\lambda_k)\lambda_k}$ are adapted from (7.12). Hence, the equality (7.13) follows from the equations in (7.11).

So far, a piecewise-smooth distributional solution to the IBVP (7.6) has been constructed. In the following theorem, the uniqueness of the constructed solution is shown.

Theorem 7.8: Uniqueness of the distributional solution

For all initial and boundary conditions, the IBVP (7.6) has a solution in the space of piecewise-smooth distributions $\mathbb{D}_{\text{pw}C^\infty}$. Moreover, for each initial and boundary condition, there is only one solution given by Equation (7.10).

Proof. As the considered PDE is linear, it is sufficient to show that the i -th characteristic component $v_i \equiv 0$ is the only solution to the problem with zero initial and boundary conditions. Let $T \subseteq \mathbb{R}$, $X \subseteq \mathbb{R}$ be open sets and δ_L is the Dirac segment on the line segment $L \subseteq T \times X$. First, it is verified that δ_L is a solution to the i -th characteristic component of the PDE, if the line segment L has slope $1/\lambda_i$, where $\lambda_i \in \mathbb{R} \setminus \{0\}$ and crosses the boundaries of the domain. Let $\varphi \in C_{\text{pw}}^\infty(T \times X; \mathbb{R})$ be a test function with $\text{supp } \varphi \subset T \times X$ and the parametrization of the line segment L be given by $L = \left\{ (t, x_0 + \frac{\Delta x}{\Delta t}(t - t_0)) \mid t \in \mathbb{R} \right\}$ where $t_0 \in \mathbb{R}$, $\Delta t \neq 0$, $\Delta x \neq 0$. Recall the partial derivatives of the Dirac segment δ_L are

$$(\partial_t \delta_L)(\varphi) = - \int_{t_0}^{t_1} \partial_1 \varphi \left(t, x_0 + \frac{\Delta x}{\Delta t}(t - t_0) \right) \sqrt{1 + \frac{\Delta x^2}{\Delta t^2}} dt,$$

$$(\partial_x \delta_L)(\varphi) = - \int_{t_0}^{t_1} \partial_2 \varphi \left(t, x_0 + \frac{\Delta x}{\Delta t}(t - t_0) \right) \sqrt{1 + \frac{\Delta x^2}{\Delta t^2}} dt,$$

where ∂_1 and ∂_2 represent partial derivatives with respect to the first and second components. Using the chain rule

$$\frac{d}{dt}\varphi = \frac{\partial\varphi}{\partial x}\frac{dx}{dt} + \frac{\partial\varphi}{\partial t}\frac{dt}{dt},$$

the following is obtained

$$\begin{aligned} \partial_t\delta_L + \lambda_i\partial_x\delta_L &= \partial_t\left(\sum_{k,\ell}\alpha_{k,\ell}\partial_t^{(k)}\partial_x^{(\ell)}\delta_L\right)(\varphi) \\ &\quad + \lambda_i\partial_x\left(\sum_{k,\ell}\alpha_{k,\ell}\partial_t^{(k)}\partial_x^{(\ell)}\delta_L\right)(\varphi) \\ &\quad - \sum_{k,\ell}\alpha_{k,\ell}\partial_t^{(k)}\partial_x^{(\ell)}\sqrt{1+\frac{\Delta x^2}{\Delta t^2}}\left(\int_{t_0}^{t_1}\left[\partial_1\varphi\left(t,x_0+\frac{\Delta x}{\Delta t}(t-t_0)\right)\right.\right. \\ &\quad \left.\left.+ \lambda_i\partial_2\varphi\left(t,x_0+\frac{\Delta x}{\Delta t}(t-t_0)\right)\right]dt\right) \\ &\quad - \sum_{k,\ell}\alpha_{k,\ell}\partial_t^{(k)}\partial_x^{(\ell)}\sqrt{1+\frac{\Delta x^2}{\Delta t^2}}\left(\int_{t_0}^{t_1}\left[\frac{d}{dt}\varphi\left(t,x_0+\frac{\Delta x}{\Delta t}(t-t_0)\right)\right.\right. \\ &\quad \left.\left.+ \left(\lambda_i-\frac{\Delta x}{\Delta t}\right)\partial_2\varphi\left(t,x_0+\frac{\Delta x}{\Delta t}(t-t_0)\right)\right]dt\right) \\ &\quad - \sum_{k,\ell}\alpha_{k,\ell}\partial_t^{(k)}\partial_x^{(\ell)}\left(\varphi\left(t_1,x_0+\frac{\Delta x}{\Delta t}(t_1-t_0)\right)+\varphi(t_0,x_0)\right. \\ &\quad \left.-\sqrt{1+\frac{\Delta x^2}{\Delta t^2}}\left(\lambda_i-\frac{\Delta x}{\Delta t}\right)\int_{t_0}^{t_1}\partial_2\varphi\left(t,x_0+\frac{\Delta x}{\Delta t}(t-t_0)\right)dt\right). \end{aligned}$$

This expression is zero for all $\varphi \in C_{pw}^\infty(T \times X; \mathbb{R})$, if $\lambda_i = \frac{\Delta x}{\Delta t}$, $(t_0, x_0) \notin \text{supp } \varphi$, and $(t_1, x_1) \notin \text{supp } \varphi$. Thus, the slope $\Delta t/\Delta x$ of the line segment L is the multiplicative inverse of the characteristic speed λ_i and the line segment L has to fully cross the considered domain. But at the points, where the line segment L hits the initial time or the boundaries of the domain, the solution has to satisfy the imposed conditions. Therefore, the strength of the Dirac segment is equal to zero; i.e., the factor $\alpha_{k,\ell}$ is zero. Due to the linearity of the considered PDE, the above computation can be extended directly to any combination of spacial and temporal derivatives of δ_L ; and hence, the uniqueness of the solution to the IBVP (7.6) follows. \square

Remark 7.9

The proof of Theorem 7.8 states that there cannot exist any Dirac segments which appear and/or disappear only within the domain without having any connections to the boundaries of the considered domain.

Chapter 8

Coupling linear PDE systems with switched DAE systems

In this chapter, a linear hyperbolic partial differential equation is coupled with a switched differential algebraic equation via boundary conditions, see Figure 8.1. The closed loop setting illustrated in Figure 8.1 can include general network structures. In this coupled system the values of the switched DAE provide the boundary conditions for the PDE and the values of the PDE serve as input to the DAE. After a detailed description of the coupled system including examples of a simple power network and a part of a simplified circulatory system, an existence and uniqueness result for general switched delay DAEs is established and the existence and uniqueness of solutions of the coupled system is concluded. At the end of this chapter, numerical results for the power grid and circulatory system examples are explained and illustrated.

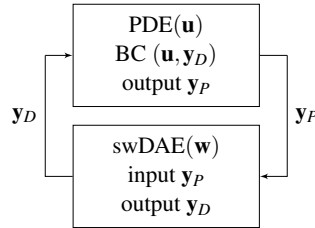


FIGURE 8.1: Coupling of a PDE with a switched DAE via boundary conditions.

8.1 System class

In this section, linear hyperbolic PDEs on a bounded interval, which have the following form, are considered

$$\partial_t \mathbf{u}(t, x) + \mathbf{A} \partial_x \mathbf{u}(t, x) = 0, \quad x \in [a, b], t \geq t_0, \quad (8.1a)$$

$$\mathbf{y}_P(t) = \mathbf{C}_P \mathbf{u}_{ab}(t), \quad t \geq t_0 \quad (8.1b)$$

where $a, b, t_0 \in \mathbb{R}$ with $a < b$, $\mathbf{u} : [t_0, \infty) \times [a, b] \rightarrow \mathbb{R}^n$, $n \in \mathbb{N}$, is the n -dimensional vector of unknowns of the PDE, $\mathbf{A} \in \mathbb{R}^{n \times n}$ and $\mathbf{y}_P : [t_0, \infty) \rightarrow \mathbb{R}^v$, $v \in \mathbb{N}$ is the v -dimensional output of the PDE depending on $\mathbf{u}_{ab}(t) := (\mathbf{u}(t, a)^\top, \mathbf{u}(t, b)^\top)^\top \in \mathbb{R}^{2n}$ and $\mathbf{C}_P \in \mathbb{R}^{v \times 2n}$. The boundary conditions of the PDE have the form

$$\mathbf{P} \mathbf{u}_{ab}(t) = \mathbf{y}_D(t), \quad t > t_0, \quad (8.1c)$$

where $\mathbf{P} \in \mathbb{R}^{n \times 2n}$ and $\mathbf{y}_D : [t_0, \infty) \rightarrow \mathbb{R}^n$ is the output of the switched DAE

$$\mathbf{E}_\sigma \dot{\mathbf{w}}(t) = \mathbf{H}_\sigma \mathbf{w}(t) + \mathbf{B}_\sigma \mathbf{y}_P(t) + \mathbf{f}_\sigma(t), \quad t \geq t_0, \quad (8.1d)$$

$$\mathbf{y}_D(t) = \mathbf{C}_{D\sigma} \mathbf{w}(t), \quad t \geq t_0, \quad (8.1e)$$

with the m -dimensional vector of unknowns $\mathbf{w} : [t_0, \infty) \rightarrow \mathbb{R}^m$, $m \in \mathbb{N}$, the switching signal $\sigma : \mathbb{R} \rightarrow \{1, 2, \dots, N\}$, $N \in \mathbb{N}$, and $\mathbf{E}_\xi, \mathbf{H}_\xi \in \mathbb{R}^{m \times m}$, $\mathbf{B}_\xi \in \mathbb{R}^{m \times v}$, $\mathbf{f}_\xi : [t_0, \infty) \rightarrow \mathbb{R}^m$, $\mathbf{C}_{D\xi} \in \mathbb{R}^{m \times n}$ for each $\xi \in \{1, 2, \dots, N\}$.

The coupled system (8.1) has to be equipped with initial conditions

$$\mathbf{u}(t_0, x) = \mathbf{u}^{t_0}(x), \quad x \in [a, b], \quad (8.2a)$$

$$\mathbf{w}(t_0) = \mathbf{w}^{t_0}, \quad (8.2b)$$

where $\mathbf{u}^{t_0} : [a, b] \rightarrow \mathbb{R}^n$ and $\mathbf{w}^{t_0} \in \mathbb{R}^m$.

Remark 8.1

The coupling structure in (8.1) is quite general, in fact, arbitrary networks whose edges represent PDEs and whose nodes represent (switched) DAEs which couple different PDEs are covered. Consider for example a network as illustrated in Figure 8.2a, where on each edge \mathcal{E}_i , $i = 1, \dots, 5$, the quantity $\mathbf{u}^{\mathcal{E}_i}$ is governed by a linear PDE $\mathbf{u}_t^{\mathcal{E}_i} + \mathbf{A}\mathbf{u}_x^{\mathcal{E}_i} = 0$. At each node \mathcal{N}_j , $j = 1, \dots, 4$, algebraic and/or differential conditions combine possible internal states $\mathbf{w}^{\mathcal{N}_j}$ with certain boundary values $\mathbf{q}^{\mathcal{N}_j}$ from the connected $\mathbf{u}^{\mathcal{E}_i}$; i.e., $\mathbf{E}_\sigma^{\mathcal{N}_j} \dot{\mathbf{w}}^{\mathcal{N}_j} = \mathbf{H}_\sigma^{\mathcal{N}_j} \mathbf{w}^{\mathcal{N}_j} + \mathbf{B}_\sigma^{\mathcal{N}_j} \mathbf{y}_P^{\mathcal{N}_j} + \mathbf{f}_\sigma^{\mathcal{N}_j}$. This setup can be rewritten in the form (8.1) by first rescaling the spatial domain (which simply modifies the coefficient matrices $\mathbf{A}^{\mathcal{E}_i}$ by a constant multiple) so that all PDEs are defined on the same interval and can be viewed as a single PDE where the new unknown \mathbf{u} consists of the unknowns $\mathbf{u}^{\mathcal{E}_i}$ of each edge \mathcal{E}_i stacked over each other (the \mathbf{A} -matrix is then a block diagonal matrix). In a similar way, the unknowns $\mathbf{w}^{\mathcal{N}_j}$ and inhomogeneities $\mathbf{f}_\sigma^{\mathcal{N}_j}$ of switched DAEs for each node \mathcal{N}_j can be stacked over each other leading to the new vector variable \mathbf{w} and inhomogeneity \mathbf{f}_σ . Furthermore, arranging the corresponding coefficient matrices of each swDAE in such a way that resulting coefficient matrices form block diagonal matrices results a single swDAE together with the unknown \mathbf{w} and inhomogeneity \mathbf{f} , see Figure 8.2b. Hence, by rearranging PDEs and swDAEs, a network (loop) consisting of a single node and a single edge is obtained, see Figure 8.2c. A similar reduction is used in [72]. In the sequel, this method is employed for the specific examples of a simple power grid with a switching transformer and a simplified part of the circulatory system in a human body.

8.1.1 Power grid example

In this section, the simple electrical power grid with a switching transformer is considered, which is illustrated in Figure 8.3.

Each line \mathcal{E}_i , $i = 1, \dots, 4$, is modeled by the telegrapher's equations given by

$$\begin{aligned} \partial_t I_i(t, x) + \frac{1}{L_i} \partial_x V_i(t, x) &= 0, \\ \partial_t V_i(t, x) + \frac{1}{C_i} \partial_x I_i(t, x) &= 0, \end{aligned} \quad (8.3)$$

where $x \in [a_i, b_i]$, $b_i > a_i$, I_i and V_i stand for the current and voltage, respectively, and the constants L_i and C_i are inductance and capacitance, respectively. In particular, each line \mathcal{E}_i has a position-dependent current I_i and voltage V_i . By appropriate scaling of the spatial

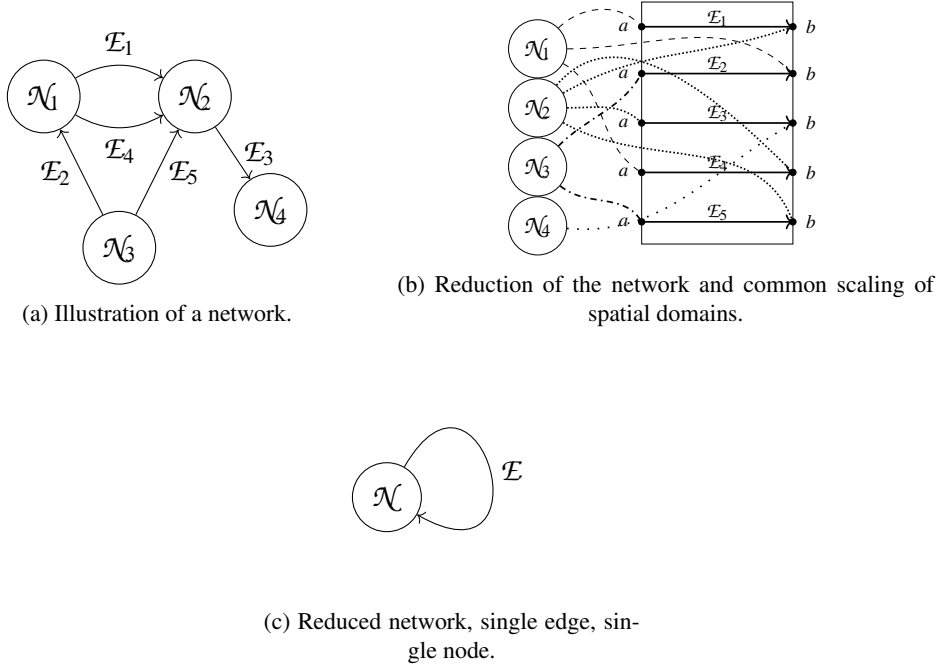


FIGURE 8.2: An example of a network consisting of four nodes and five connecting edges and how to reduce it to one node and one edge (loop) network which still has all the features of the original network.

domains of each edge for the telegrapher's equations, it can be assumed that all PDEs are defined on the common domain $T \times X = [0, \infty) \times [a, b]$. At the nodes there is a coupling between corresponding boundary values, where the "outputs" of the telegrapher's equations are the boundary currents I_i for each line \mathcal{E}_i . A generator is located at the first node, where an externally given voltage is assumed. This algebraic constraint is modeled by the algebraic relations

$$\begin{aligned} 0 &= z_1 - v_G, \\ y_D^1 &= z_1, \end{aligned} \tag{8.4}$$

where $v_G : [0, \infty) \rightarrow \mathbb{R}$ is the externally given time-varying voltage of the generator together with the boundary condition $V_1(\cdot, a^+) = y_D^1$. On the consumption nodes, all voltages are assumed to be equal and it is assumed that the consumption is modeled as a simple Ohm's resistance; i.e., the sum of the (directed) currents at the boundary of the lines is proportional to the voltage at the node, which is modeled by the DAE

$$\begin{aligned} 0 &= z_{24} - R_{24}(I_4(\cdot, a^+) - I_2(\cdot, b^-)), & y_D^{24} &= z_{24}, \\ 0 &= z_{34} - R_{34}(I_3(\cdot, b^-) + I_4(\cdot, b^-)), & y_D^{34} &= z_{34}, \end{aligned} \tag{8.5}$$

where $R_{24}, R_{34} > 0$ are the resistive loads. Furthermore, the following boundary conditions are imposed

$$\begin{aligned} V_2(\cdot, b^-) &= y_D^{24}, & V_3(\cdot, b^-) &= y_D^{34}, \\ V_4(\cdot, a^+) &= y_D^{24}, & V_4(\cdot, b^-) &= y_D^{34}. \end{aligned}$$

Finally, the switching transformer node is governed by the electric circuit given in Figure 8.4.

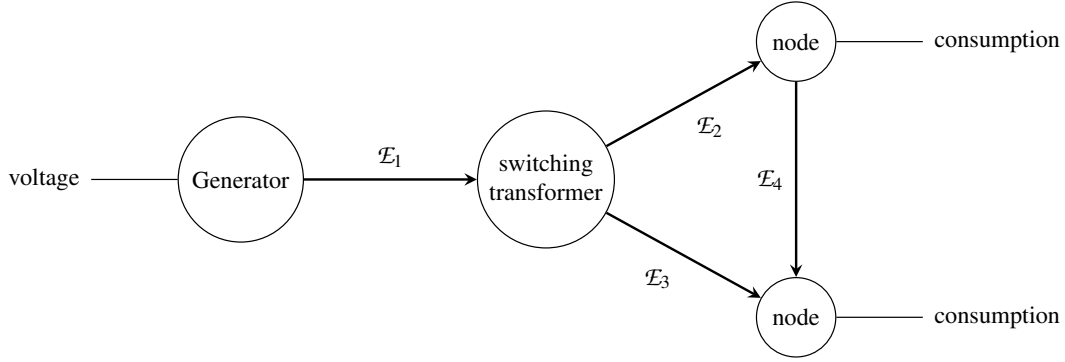


FIGURE 8.3: Simple electrical power grid with one generator node, one switching transformer node and two consumption nodes.

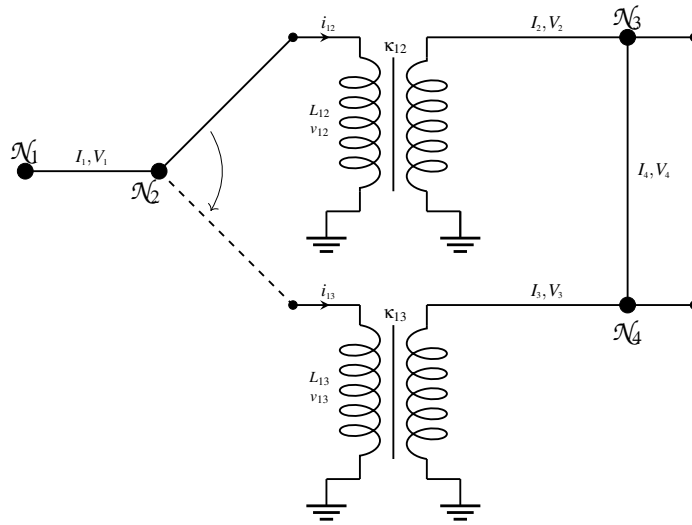


FIGURE 8.4: A node connecting three power lines with a switching transformer.

The switch independent equations governing this switching transformer node are as follows

$$\begin{aligned} L_{12} \frac{d}{dt} i_{12} &= v_{12}, & L_{13} \frac{d}{dt} i_{13} &= v_{13}, \\ V_2(\cdot, a^+) &= \kappa_{12} v_{12}, & V_3(\cdot, a^+) &= \kappa_{13} v_{13}, \end{aligned} \quad (8.6)$$

where $\kappa_{12}, \kappa_{13} > 0$ are amplifiers. Note that, in this example, amplifiers are used only for the voltage values, so the power grid example is a simplified model.

If the switch connects \mathcal{E}_1 and \mathcal{E}_2 , then the following three algebraic constraints hold

$$0 = i_{12} - I_1, \quad i_{13} = 0, \quad V_1(\cdot, b^-) = v_{12},$$

and, otherwise,

$$i_{12} = 0, \quad 0 = i_{13} - I_1, \quad V_1(\cdot, b^-) = v_{13}.$$

Let $\tilde{\mathbf{w}} = (i_{12}, i_{13}, v_{12}, v_{13})^\top$ be the state vector, then the rules governing the switching transformer node can be compactly written as a switched DAE

$$\begin{aligned} \tilde{\mathbf{E}}_\sigma \tilde{\mathbf{w}} &= \tilde{\mathbf{H}}_\sigma \tilde{\mathbf{w}} + \tilde{\mathbf{B}}_\sigma \tilde{\mathbf{y}}_P \\ \tilde{\mathbf{y}}_D &= \tilde{\mathbf{C}}_{D_\sigma} \tilde{\mathbf{w}}, \end{aligned}$$

where

$$\begin{aligned}\tilde{\mathbf{E}}_1 = \tilde{\mathbf{E}}_2 &= \begin{bmatrix} L_{12} & 0 & 0 & 0 \\ 0 & L_{13} & 0 & 0 \\ 0 & 0 & 0 & 0 \\ 0 & 0 & 0 & 0 \end{bmatrix}, & \tilde{\mathbf{H}}_1 = \tilde{\mathbf{H}}_2 &= \begin{bmatrix} 0 & 0 & 1 & 0 \\ 0 & 0 & 0 & 1 \\ 1 & 0 & 0 & 0 \\ 0 & 1 & 0 & 0 \end{bmatrix}, \\ \tilde{\mathbf{B}}_1 &= \begin{bmatrix} 0 & 0 & 0 & 0 \\ 0 & 0 & 0 & 0 \\ -1 & 0 & 0 & 0 \\ 0 & 0 & 0 & 0 \end{bmatrix} =: [\tilde{\mathbf{B}}_1^1, \mathbf{0}, \mathbf{0}], & \tilde{\mathbf{B}}_2 &= \begin{bmatrix} 0 & 0 & 0 & 0 \\ 0 & 0 & 0 & 0 \\ 0 & 0 & 0 & 0 \\ -1 & 0 & 0 & 0 \end{bmatrix} =: [\tilde{\mathbf{B}}_2^1, \mathbf{0}, \mathbf{0}], \\ \tilde{\mathbf{C}}_1 &= \begin{bmatrix} 0 & 0 & 1 & 0 \\ 0 & 0 & \kappa_{12} & 0 \\ 0 & 0 & 0 & \kappa_{13} \end{bmatrix}, & \tilde{\mathbf{C}}_2 &= \begin{bmatrix} 0 & 0 & 0 & 1 \\ 0 & 0 & \kappa_{12} & 0 \\ 0 & 0 & 0 & \kappa_{13} \end{bmatrix},\end{aligned}$$

and the coupling via the boundaries of \mathcal{E}_1 , \mathcal{E}_2 and \mathcal{E}_3 are as follows

$$\tilde{\mathbf{y}}_P = (I_1(\cdot, b^-), I_2(\cdot, a^+), I_3(\cdot, a^+))^\top, \quad \tilde{\mathbf{y}}_D = (V_1(\cdot, b^-), V_2(\cdot, a^+), V_3(\cdot, a^+))^\top.$$

Thus, the overall coupled system has the form (8.1) with

$$\mathbf{A} = \begin{bmatrix} \mathbf{A}_1 & 0 & 0 & 0 \\ 0 & \mathbf{A}_2 & 0 & 0 \\ 0 & 0 & \mathbf{A}_3 & 0 \\ 0 & 0 & 0 & \mathbf{A}_4 \end{bmatrix} \quad \text{where } \mathbf{A}_i = \begin{bmatrix} 0 & \frac{1}{(b_i - a_i)L_i} \\ \frac{1}{(b_i - a_i)C_i} & 0 \end{bmatrix} \quad \forall i = 1, \dots, 4, \quad (8.7)$$

$\mathbf{u} = (\mathbf{u}_1^\top, \mathbf{u}_2^\top, \mathbf{u}_3^\top, \mathbf{u}_4^\top)^\top$ with $\mathbf{u}_i = (I_i, V_i)^\top$, the output of the PDE (used as an input to the switched DAE) are all currents at the boundaries of the power lines; i.e., the coefficient matrix for the output is

$$\mathbf{C}_P = \begin{bmatrix} 1 & 0 & 0 & 0 & 0 & 0 & 0 & 0 & 0 & 0 & 0 & 0 & 0 & 0 & 0 & 0 & 0 & 0 & 0 & 0 \\ 0 & 0 & 1 & 0 & 0 & 0 & 0 & 0 & 0 & 0 & 0 & 0 & 0 & 0 & 0 & 0 & 0 & 0 & 0 & 0 \\ 0 & 0 & 0 & 0 & 1 & 0 & 0 & 0 & 0 & 0 & 0 & 0 & 0 & 0 & 0 & 0 & 0 & 0 & 0 & 0 \\ 0 & 0 & 0 & 0 & 0 & 0 & 1 & 0 & 0 & 0 & 0 & 0 & 0 & 0 & 0 & 0 & 0 & 0 & 0 & 0 \\ 0 & 0 & 0 & 0 & 0 & 0 & 0 & 0 & 1 & 0 & 0 & 0 & 0 & 0 & 0 & 0 & 0 & 0 & 0 & 0 \\ 0 & 0 & 0 & 0 & 0 & 0 & 0 & 0 & 0 & 0 & 1 & 0 & 0 & 0 & 0 & 0 & 0 & 0 & 0 & 0 \\ 0 & 0 & 0 & 0 & 0 & 0 & 0 & 0 & 0 & 0 & 0 & 0 & 1 & 0 & 0 & 0 & 0 & 0 & 0 & 0 \\ 0 & 0 & 0 & 0 & 0 & 0 & 0 & 0 & 0 & 0 & 0 & 0 & 0 & 0 & 1 & 0 & 0 & 0 & 0 & 0 \end{bmatrix},$$

the switched DAE has the state vector $\mathbf{w} = (z_1, i_{12}, i_{13}, v_{12}, v_{13}, z_{24}, z_{34})^\top$ and the following coefficient matrices

$$\begin{aligned}\mathbf{E}_k &= \begin{bmatrix} 0 & 0 & 0 & 0 \\ 0 & \tilde{\mathbf{E}}_k & 0 & 0 \\ 0 & 0 & 0 & 0 \\ 0 & 0 & 0 & 0 \end{bmatrix}, & \mathbf{H}_k &= \begin{bmatrix} 1 & 0 & 0 & 0 \\ 0 & \tilde{\mathbf{H}}_k & 0 & 0 \\ 0 & 0 & 1 & 0 \\ 0 & 0 & 0 & 1 \end{bmatrix}, \\ \mathbf{B}_k &= \begin{bmatrix} 0 & 0 & 0 & 0 & 0 & 0 & 0 \\ 0 & 0 & 0 & \tilde{\mathbf{B}}_k^1 & 0 & 0 & 0 \\ 0 & 0 & 0 & -R_{24} & R_{24} & 0 & 0 \\ 0 & 0 & 0 & 0 & 0 & -R_{34} & -R_{34} \end{bmatrix}, & & (8.8) \\ \mathbf{C}_{Dk} &= \begin{bmatrix} 1 & 0 & 0 & 0 \\ 0 & [0,1,0] & 0 & 0 \\ 0 & [0,0,1] & 0 & 0 \\ 0 & 0 & 1 & 0 \\ 0 & [1,0,0] & 0 & 0 \\ 0 & 0 & 1 & 0 \\ 0 & 0 & 0 & 1 \\ 0 & 0 & 0 & 1 \end{bmatrix} \cdot \begin{bmatrix} 1 & 0 & 0 & 0 \\ 0 & \tilde{\mathbf{C}}_k & 0 & 0 \\ 0 & 0 & 1 & 0 \\ 0 & 0 & 0 & 1 \end{bmatrix}, & \mathbf{f}_k &= \begin{bmatrix} -v_G \\ 0 \\ 0 \\ 0 \\ 0 \\ 0 \end{bmatrix},\end{aligned}$$

where $k = 1, 2$ stands for the different modes of the swDAE and the coupling matrix $\mathbf{P} = \begin{bmatrix} \mathbf{P}_a \\ \mathbf{P}_b \end{bmatrix}$ for the boundary values of the PDE is given by

$$\mathbf{P}_a = \mathbf{P}_b = \begin{bmatrix} 0 & 1 & 0 & 0 & 0 & 0 & 0 & 0 \\ 0 & 0 & 0 & 1 & 0 & 0 & 0 & 0 \\ 0 & 0 & 0 & 0 & 0 & 1 & 0 & 0 \\ 0 & 0 & 0 & 0 & 0 & 0 & 0 & 1 \end{bmatrix}.$$

8.1.2 Multi-scale blood flow modelling

In this section, a representative modelling of pulmonary circulation, heart and systemic circulation is given. The wave propagation in pulmonary venous and ascending aorta is expressed

in terms of PDEs while the dynamics of the left heart is modeled using swDAEs. First, it is explained how these models are derived and then how they are coupled with each other.

1D Blood Flow Model

One-dimensional blood flow models for vessels are derived from the incompressible Navier-Stokes equations, [15, 51],

$$\begin{aligned} \mathbf{u}_t + \mathbf{u} \cdot \nabla \mathbf{u} - \Delta \mathbf{u} + \nabla P &= 0, \\ \operatorname{div} \mathbf{u} &= 0, \end{aligned} \quad t > 0,$$

under some simplifying assumptions on a cylindrical domain Ω which is considered as a portion of a vessel, which changes in time because blood vessels contract and expand depending on changes in volume and pressure.

For brevity, the vessels are assumed to be straight cylinders with circular cross-sectional areas, [50, 101].

Integrating the Navier-Stokes equations over the circular cross-sectional area results in the following one-dimensional blood flow PDEs for vessels, [48, 86, 94, 101],

$$\begin{aligned} \partial_t A(t, x) + \partial_x Q(t, x) &= 0, \\ \partial_t Q(t, x) + \partial_x \left(\alpha \frac{Q(t, x)^2}{A(t, x)} \right) + \frac{A(t, x)}{\rho} \partial_x P(t, x) &= -f_{\text{fr}}(t, x) \frac{Q(t, x)}{A(t, x)}, \end{aligned} \quad (8.9)$$

where $t > 0$, $x \in [a, b]$ with $b > a$, $A : \mathbb{R}^+ \times [a, b] \rightarrow \mathbb{R}^+$ cross-sectional area of the vessel, $Q : \mathbb{R}^+ \times [a, b] \rightarrow \mathbb{R}$ flow rate, $P : \mathbb{R}^+ \times [a, b] \rightarrow \mathbb{R}^+$ mean internal pressure over the cross-sectional area, $f_{\text{fr}} : \mathbb{R}^+ \times [a, b] \rightarrow \mathbb{R}^+$ friction force on blood that is exerted by vessel walls, $\rho \in \mathbb{R}^+$ density of the blood, α a dimensionless momentum-flux correction factor, called Boussinesq coefficient, depending on velocity profile, since the velocity across a section is not always *uniform*, [27]. However, arterial blood flow has been proven to have a uniform velocity profile in general, [46]. Therefore, the momentum-flux correction term is considered $\alpha = 1$, [86, 94].

The unknowns of the system (8.9) are A, Q and P , whereas the system has only two equations. Therefore, to close the system (8.9), the following pressure law is employed, [49, 94],

$$P(t, x) = P_{\text{ext}}(t, x) + \Psi(A; A_0, K, P_0), \quad (8.10)$$

where $P_{\text{ext}}(t, x)$ is the external pressure which is assumed to be constant $P_{\text{ext}} = 0$, and $\Phi(t, x)$ is the transmural pressure¹ given by

$$\Psi(A(t, x); A_0(x), K(x), P_0) = K(x) \phi(A(t, x); A_0(x)) + P_0,$$

where A_0 and P_0 are the reference cross-sectional area and reference pressure and assumed to be constant; and $K(x)$ is a function given by

$$K(x) = \frac{h(x)E(x)}{(1 - \sigma^2)R_0}, \quad K(x) > 0,$$

where $E(x)$ is the Young modulus, $h(x)$ is the wall elasticity, σ is the Poisson ratio, and R_0 is the reference vessel radius. For incompressible fluids, $\sigma = 1/2$. In the literature, there are different approaches to link the pressure P and cross-sectional area A , see [82, 129].

¹Transmural pressure is the pressure difference between the internal; i.e., pressure in the vessel, and external pressure.

For simplicity, K is assumed to be constant. The function $\phi(A(t, x), A_0)$ is given by

$$\phi(A(t, x), A_0) = \left(\frac{A}{A_0}\right)^m - \left(\frac{A}{A_0}\right)^n,$$

where m and n are constants which are related to mechanical and geometrical properties of vessels, [126]. It is assumed $m = 0.5$ and $n = 0$, [93, 94]. From the relation between pressure P and cross-sectional area A (8.10), the following is obtained

$$\partial_x P = \partial_A P \partial_x A = \frac{K}{2A_0} \frac{1}{\sqrt{A}} \partial_x A,$$

which yields the nonconservative form of the system (8.9) in (P, Q) variables

$$\partial_t \begin{pmatrix} P \\ Q \end{pmatrix} + \begin{pmatrix} 0 & \partial_A P \\ -\frac{Q^2}{A^2} \partial_P A + \frac{A}{\rho} & 2\frac{Q}{A} \end{pmatrix} \partial_x \begin{pmatrix} P \\ Q \end{pmatrix} = \begin{pmatrix} 0 & 0 \\ 0 & -\frac{f_{fr}}{A} \end{pmatrix} \begin{pmatrix} P \\ Q \end{pmatrix}, \quad (8.11)$$

with suitable boundary conditions.

The system (8.9) can also be formulated without the pressure term P as a balance law

$$\partial_t \mathbf{u}(t, x) + \partial_x \mathbf{f}(\mathbf{u}(t, x)) = \mathbf{g}(x, t, \mathbf{u}(t, x)), \quad (8.12)$$

where

$$\mathbf{u} = \begin{pmatrix} A \\ Q \end{pmatrix}, \quad \mathbf{f}(\mathbf{u}) = \begin{pmatrix} Q \\ \frac{Q^2}{A} + \frac{K}{3\rho A_0} A^{3/2} \end{pmatrix}, \quad \mathbf{g} = \begin{pmatrix} 0 \\ -f_{fr} \frac{Q}{A} \end{pmatrix},$$

with \mathbf{u} being the unknown vector, \mathbf{f} corresponding flux function, and \mathbf{g} source term. The Jacobian \mathbf{J} of the flux function \mathbf{f} is computed as

$$\nabla_{\mathbf{u}} \mathbf{f}(\mathbf{u}) = \mathbf{J}(\mathbf{u}) = \begin{pmatrix} 0 & 1 \\ -\left(\frac{Q}{A}\right)^2 + \frac{K}{2\rho A_0} \sqrt{A} & 2\frac{Q}{A} \end{pmatrix}, \quad (8.13)$$

where $V = Q/A$ is the mean velocity of the blood through the cross-sectional area A and let

$$c := \sqrt{\frac{K}{\rho} A \frac{\partial P}{\partial A}} = \sqrt{\frac{K}{2\rho A_0}} \sqrt{A},$$

which is the propagation speed of waves.

The Jacobian matrix \mathbf{J} has two real and distinct eigenvalues λ_1 and λ_2 , which can be computed by solving $\det(\mathbf{J} - \lambda \mathbf{I}) = 0$ for λ ,

$$\det \begin{pmatrix} -\lambda & 1 \\ \frac{K}{2\rho A_0} \sqrt{A} - V^2 & 2V - \lambda \end{pmatrix} = 0,$$

for which the eigenvectors λ_1 and λ_2 are found as

$$\lambda_1 = V - \sqrt{\frac{K}{2\rho A_0}} \sqrt{A} = V - c, \quad \text{and} \quad \lambda_2 = V + \sqrt{\frac{K}{2\rho A_0}} \sqrt{A} = V + c,$$

with a complete set of right-eigenvectors \mathbf{r}_1 and \mathbf{r}_2 corresponding to the eigenvalues λ_1 and λ_2 given by

$$\mathbf{r}_1 = \begin{pmatrix} 1 \\ V - c \end{pmatrix}, \quad \text{and} \quad \mathbf{r}_2 = \begin{pmatrix} 1 \\ V + c \end{pmatrix},$$

respectively.

Definition 8.2: Sub- and supercritical flow, [69, 112]

The flow is said to be *subcritical* if the velocity of the flow is smaller than the wave speed. If the flow speed is larger than the wave speed, then the flow is called *supercritical*.

Remark 8.3

Under physiological conditions, the wave speed c for arterial blood flow is much greater than the flow speed, [59, 110, 112, 139]. As a result, $\lambda_1 < 0$ and $\lambda_2 > 0$; hence, the blood flow is subcritical for arterial blood flow.

Linearization of the blood flow model

If the small perturbations are considered, a linear PDE system can be obtained by linearizing the system (8.12). Furthermore, as pointed out in [43, 111], under physiological conditions, the equations that model the blood flow are only weakly nonlinear. As a result, linearizing the system (8.12) can grasp the features of the blood flow.

Below the system (8.12) is linearized around the equilibrium point $\mathbf{u}_s = (A_s, Q_s)^\top$, where $A_s > 0$, by a Taylor series expansion

$$\mathbf{u}(t, x) = \mathbf{u}_s + \varepsilon \mathbf{w}(t, x) + O(\varepsilon), \quad (8.14)$$

where \mathbf{u}_s is constant in x and t , and $\varepsilon > 0$ is *small*. Higher order terms $O(\varepsilon)$ in (8.14) are very close to zero for (A_s, Q_s) sufficiently close to (A, Q) , and hence, they can be dropped out to attain the approximation $\mathbf{u}(t, x) = \mathbf{u}_s + \varepsilon \mathbf{w}(t, x)$. Inserting this approximation $\mathbf{u}(t, x)$ into the nonlinear system (8.12) yields

$$\begin{aligned} \varepsilon \partial_t \mathbf{w}(t, x) + \partial_x f(\mathbf{u}_s + \varepsilon \mathbf{w}(t, x)) &= \mathbf{g}(x, t, \mathbf{u}_s, \mathbf{w}), \\ \partial_t \mathbf{w}(t, x) + \nabla_{\mathbf{u}_s} f(\mathbf{u}_s) \partial_x \mathbf{w}(t, x) &= \frac{1}{\varepsilon} \mathbf{g}(x, t, \mathbf{u}_s, \mathbf{w}), \end{aligned}$$

evaluating $\nabla_{\mathbf{u}_s} \mathbf{f}(\mathbf{u}_s)$ results in the following linearized system

$$\partial_t \begin{pmatrix} A \\ Q \end{pmatrix} + \partial_x \begin{pmatrix} 0 & 1 \\ -\left(\frac{Q_s}{A_s}\right)^2 + \frac{K}{2\rho A_0} \sqrt{A_s} & 2\frac{Q_s}{A_s} \end{pmatrix} \partial_x \begin{pmatrix} A \\ Q \end{pmatrix} = \begin{pmatrix} 0 \\ \frac{-f_{fr}}{A_s} Q \end{pmatrix},$$

or, similarly,

$$\partial_t \begin{pmatrix} A \\ Q \end{pmatrix} + \begin{pmatrix} 0 & 1 \\ c_s^2 - V_s^2 & 2V_s \end{pmatrix} \partial_x \begin{pmatrix} A \\ Q \end{pmatrix} = \begin{pmatrix} 0 \\ \frac{-f_{fr}}{A_s} Q \end{pmatrix}, \quad (8.15)$$

where $c_s = \sqrt{\frac{K}{2\rho A_0} \sqrt{A_s}}$ and $V_s = Q_s/A_s$ are constant.

Let \mathbf{J}_s be the constant coefficient matrix in (8.15); i.e.,

$$\mathbf{J}_s = \begin{pmatrix} 0 & 1 \\ c_s^2 - V_s^2 & 2V_s \end{pmatrix},$$

whose eigenvalues $\lambda_1 = V_s - c_s$ and $\lambda_2 = V_s + c_s$ are distinct and real with the corresponding eigenvectors $\mathbf{r}_1 = (1, V_s - c_s)^\top$ and $\mathbf{r}_2 = (1, V_s + c_s)^\top$, respectively. Hence, the waves move at characteristic speeds λ_1 and λ_2 . Therefore, the constant coefficient matrix \mathbf{J}_s is \mathbb{R} diagonalizable

$$\mathbf{J}_s = \mathbf{R}\mathbf{\Lambda}\mathbf{R}^{-1},$$

where

$$\mathbf{R} = \begin{pmatrix} 1 & 1 \\ V_s - c_s & V_s + c_s \end{pmatrix}, \quad \mathbf{\Lambda} = \begin{pmatrix} V_s - c_s & 0 \\ 0 & V_s + c_s \end{pmatrix}. \quad (8.16)$$

It is assumed that $A_s = A_0$ and $V_s = 0$ and in a similar fashion, the nonlinear system (8.11) can be linearized around an equilibrium point $(A_0, 0)$ as

$$\partial_t \begin{pmatrix} P \\ Q \end{pmatrix} + \begin{pmatrix} 0 & \frac{K}{2A_0\sqrt{A_0}} \\ \frac{A_0}{\rho} & 0 \end{pmatrix} \partial_x \begin{pmatrix} P \\ Q \end{pmatrix} = \begin{pmatrix} 0 \\ -\frac{f_{ix}}{A_0} Q \end{pmatrix}. \quad (8.17)$$

In the case that the source term $\mathbf{g} = \mathbf{0}$, by applying the coordinate transformation $\mathbf{v} = \mathbf{R}^{-1}\mathbf{u}$, the system (8.17) is decoupled into a system of scalar PDEs

$$\partial_t \mathbf{v} + \mathbf{\Lambda} \partial_x \mathbf{v} = \mathbf{0}, \quad (8.18)$$

where the characteristic variable \mathbf{v} , the diagonal matrix of eigenvalues $\mathbf{\Lambda}$ and the matrix of right eigenvectors \mathbf{R} are as follows

$$\mathbf{v}(\mathbf{u}(t, x)) = \begin{pmatrix} v_-(\mathbf{u}(t, x)) \\ v_+(\mathbf{u}(t, x)) \end{pmatrix} = \frac{1}{2c_0} \begin{pmatrix} -Q(t, x) + c_0 P(t, x) \\ Q(t, x) + c_0 P(t, x) \end{pmatrix}, \quad (8.19)$$

$$\mathbf{\Lambda} = \begin{pmatrix} -c_0 & 0 \\ 0 & c_0 \end{pmatrix}, \quad \mathbf{R} = \begin{pmatrix} 1 & 1 \\ -c_0 & c_0 \end{pmatrix},$$

with $c_0 = c(A_0) = \sqrt{\frac{K}{2\rho A_0}} \sqrt{A_0}$.

Along the characteristics λ_1, λ_2 , changes in pressure and mean velocity move backward and forward in x -direction, respectively. Therefore, at each boundary of the spatial domain, one boundary condition has to be prescribed such as

$$\begin{aligned} \mathbf{P}_a \mathbf{u}(t, a^+) &= b_a(t), \\ \mathbf{P}_b \mathbf{u}(t, b^-) &= b_b(t), \end{aligned}$$

where $\mathbf{P}_a, \mathbf{P}_b \in \mathbb{R}^{1 \times 2}$, $b_a : [0, \infty) \rightarrow \mathbb{R}$ and $b_b : [0, \infty) \rightarrow \mathbb{R}$.

Deriving the lumped parameter models from 1D models

In the previous section, the 1D blood flow equations for elastic vessels derived from Navier-Stokes equations have been studied. On the other hand, blood flow in the heart and in smaller vessels; namely arteriols, capillaries and venules, is modeled via *lumped parameter models*. To obtain the lumped parameter models for the blood flow equations from 1D blood flow equations, the linearized 1D equations (8.17) are integrated over the spatial domain, with some assumptions.

The system (8.17) can be written in a simpler form as

$$\begin{aligned} \bar{C} \partial_t P + \partial_x Q &= 0, \\ \bar{L} \partial_t Q + \partial_x P &= -\bar{R} Q, \end{aligned} \quad (8.20)$$

where

$$\bar{C} = \frac{2A_0\sqrt{A_0}}{K}, \quad \bar{L} = \frac{\rho}{A_0}, \quad \bar{R} = \frac{\rho f_{fr}}{A_0^2}.$$

Integrating both equations in (8.20) over x yields

$$\begin{aligned} C \frac{d}{dt} \bar{P} + Q_R - Q_L &= 0, \\ L \frac{d}{dt} \bar{Q} + P_R - P_L &= -RQ, \end{aligned} \quad (8.21)$$

where $Q_L(t) = Q(a, t)$, $Q_R(t) = Q(b, t)$, $P_L(t) = P(a, t)$, $P_R(t) = P(b, t)$, $C = b\bar{C}$, $L = b\bar{L}$, $R = b\bar{R}$, and \bar{P} and \bar{Q} represent the average pressure and flow rate

$$\bar{P} = \frac{1}{b-a} \int_a^b P(t, x) dx \quad \text{and} \quad \bar{Q} = \frac{1}{b-a} \int_a^b Q(t, x) dx.$$

Given two boundary conditions to the system (8.17), let P_L and Q_R be given to close the system (8.21), it is assumed

$$\bar{P} \approx P_R \quad \text{and} \quad \bar{Q} \approx Q_L,$$

as the pulse wave velocity is between the values 3.12 – 13.4 meter/second, [39]; that is, waves move very fast, relating the mean values \bar{P}, \bar{Q} to pointwise values P, Q is physiologically reasonable. Then the lumped parameter model can be written as

$$\begin{aligned} C \frac{d}{dt} P_R + Q_R - Q_0 &= 0, \\ L \frac{d}{dt} Q_0 + P_R - P_0 &= -RQ. \end{aligned}$$

The blood flow models can be related to electrical circuits including a resistor, capacitor and inductance. Using this analogy, blood flow rate and pressure are expressed by Kirchhoff's law in the next section. The analogous representation is shown in Table 8.1. Vessel compliance C is the volume of blood that the vessel can store in response to transmural pressure. Vascular resistance R opposes to blood flow and corresponds to the electrical resistance that opposes to the current. And the momentum of the blood is the inertia L .

TABLE 8.1: Analogy of electrical circuits and circulatory system.

Circulatory system	Symbol	Electrical circuit	Symbol
Blood pressure	P	Potential difference	V
Flow rate	Q	Current	I
Vascular resistance	R	Electrical resistance	R
Inertia of blood	L	Inductance	L
Vessel compliance	C	Capacitance	C

Modeling the left heart as a system of switched DAEs

The dynamics of the cardiac chambers are described by the time-varying elastance model given as in [116, 117, 118] by

$$E_{la}(t) = E_{laa} e_{la}(t) + E_{lab}, \quad (8.22a)$$

$$E_{lv}(t) = E_{lva} e_{lv}(t) + E_{lvb}, \quad (8.22b)$$

where E_{laa}, E_{lva} are active elastances; i.e, systolic elastance coefficients, while E_{lab}, E_{lvb} are passive elastances; i.e., diastolic elastance coefficients. Moreover, e_{la}, e_{lv} are normalized time-varying elastances for left ventricle and left atrium, respectively, given by, as in [86, 94],

$$e_{la} = \begin{cases} 0.5 \left(1 + \cos \left(\frac{\pi(t+T_0-t_{rla})}{T_{rpla}} \right) \right), & \text{if } 0 \leq t \leq t_{rla} + T_{rpla} - T_0, \\ 0, & \text{if } t_{rla} + T_{rpla} - T_0 < t \leq t_{cla}, \\ 0.5 \left(1 - \cos \left(\frac{\pi(t-t_{cla})}{T_{cpla}} \right) \right), & \text{if } t_{cla} < t \leq t_{cla} + T_{cpla}, \\ 0.5 \left(1 + \cos \left(\frac{\pi(t-t_{rla})}{T_{rpla}} \right) \right), & \text{if } t_{cla} + T_{cpla} < t \leq T_0, \end{cases} \quad (8.23)$$

$$e_{lv} = \begin{cases} 0.5 \left(1 - \cos \left(\frac{\pi t}{T_{cplv}} \right) \right), & \text{if } 0 \leq t \leq T_{cplv}, \\ 0.5 \left(1 + \cos \left(\frac{\pi(t-T_{cplv})}{T_{rplv}} \right) \right), & \text{if } T_{cplv} < t \leq T_{cplv} + T_{rplv}, \\ 0, & \text{if } T_{cplv} + T_{rplv} < t \leq T_0, \end{cases}$$

where $T_{cplv}, T_{cpla}, T_{rplv}, T_{rpla}$ stand for durations of left ventricular contraction, left atrial contraction, left ventricular relaxation, left atrial relaxation, t_{cla} and t_{rla} are the times when the left atria starts contracting and relaxing, respectively, and T_0 represents the length of one complete cardiac cycle.

The time variation of chamber volumes v_{ch} is formulated in terms of incoming and outgoing blood flow

$$\frac{d}{dt} v_{ch} = q_{in} - q_{cv}, \quad (8.24)$$

where q_{in} is the blood flowing into the heart chamber.

Moreover, time varying blood pressure-volume relations in each cardiac cycle are given by, [94],

$$p_{la}(t) = p_{la,e} + E_{la}(t) (v_{la} - v_{la,0}) + S_{la} \frac{d}{dt} v_{la},$$

$$p_{lv}(t) = p_{lv,e} + E_{lv}(t) (v_{lv} - v_{lv,0}) + S_{lv} \frac{d}{dt} v_{lv},$$

where $p_{la,e}, p_{lv,e}$ are external pressures and S_{la}, S_{lv} are viscoelasticity coefficients of the cardiac walls of left atrium and left ventricle, respectively; $v_{la,0}, v_{lv,0}$ are dead chamber volumes of the corresponding heart chambers. The external pressures and dead volumes of chambers of the heart are assumed to be zero.

The time variation of flow rate through cardiac valve is described by the relation, [86, 94],

$$\frac{d}{dt} q_{cv} = \frac{\Delta p_{cv} - R_{cv} q_{cv} - B_{cv} q_{cv} |q_{cv}|}{L_{cv}}, \quad (8.26)$$

where Δp_{cv} stands for the pressure difference on its both sides cardiac valve, L_{cv} ($\text{mmHg} \cdot \text{s}^2 \cdot \text{ml}^{-1}$), R_{cv} ($\text{mmHg} \cdot \text{s}^2 \cdot \text{ml}^{-1}$) and B_{cv} ($\text{mmHg} \cdot \text{s}^2 \cdot \text{ml}^{-2}$) represent inertance, resistance, and Bernoulli's resistance, respectively.

The swDAE model for the volume of the cardiac chamber and flow rate through the valve assumes the state variable $(v_{ch}, q_{cv})^\top$, where the time variation of the volume v_{ch} is given by (8.24) and q_{cv} is modified as in [1, 99]. When the valve is open, it is expressed as

$$\frac{d}{dt} q_{cv} = \frac{\Delta p_{cv} - R_{cv} q_{cv}}{L_{cv}},$$

and when the valve is closed, the flow rate through cardiac valve is set to zero

$$q_{cv} = 0,$$

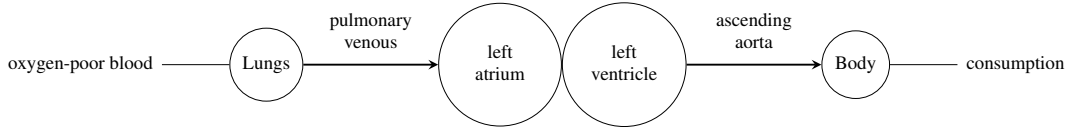


FIGURE 8.5: A simple illustration of the left heart with lungs, left atrium, left ventricle, a consumption node (body). Blood flows in the direction of arrows. Cardiac valves are located between left atrium-left ventricle and between left ventricle-ascending aorta.

which contributes to the algebraic constraint in the system.

8.1.3 Coupled circulatory system

In this section, the blood flow PDE model is coupled with swDAE model where both systems are explained in previous sections, see Figure 8.5. The blood flows through pulmonary venous into the left atrium then through the mitral valve into the left ventricle, and then through the aortic valve to the ascending aorta.

The flow through pulmonary venous and ascending aorta are modeled as a linear system of conservation laws, respectively, given as

$$\begin{cases} \partial_t A_{pv} + \partial_x Q_{pv} = 0, \\ \partial_t Q_{pv} + \frac{K}{2\rho\sqrt{(A_0)_{pv}}}\partial_x A = 0, \end{cases} \quad (8.27)$$

$$\begin{cases} \partial_t A_{aa} + \partial_x Q_{aa} = 0, \\ \partial_t Q_{aa} + \frac{K}{2\rho\sqrt{(A_0)_{aa}}}\partial_x A = 0, \end{cases}$$

where $x \in [a_j, b_j]$ with $b_j > a_j$, for $j = 1$ for pulmonary venous and $j = 2$ for ascending aorta, $A_{pv} : \mathbb{R}^+ \times [a_1, b_1] \rightarrow \mathbb{R}^+$, $Q_{pv} : \mathbb{R}^+ \times [a_1, b_1] \rightarrow \mathbb{R}$ and $P_{pv} : \mathbb{R}^+ \times [a_1, b_1] \rightarrow \mathbb{R}^+$ are cross sectional area, flow rate and internal pressure of pulmonary venous, respectively, with the pressure law given by (8.10). Similarly, $A_{aa} : \mathbb{R}^+ \times [a_2, b_2] \rightarrow \mathbb{R}^+$, $Q_{aa} : \mathbb{R}^+ \times [a_2, b_2] \rightarrow \mathbb{R}$ and $P_{aa} : \mathbb{R}^+ \times [a_2, b_2] \rightarrow \mathbb{R}^+$ cross sectional area, flow rate and internal pressure of ascending aorta, respectively. Let $\mathbf{u}_{pv} = (A_{pv}, Q_{pv})^\top$ and $\mathbf{u}_{aa} = (A_{aa}, Q_{aa})^\top$ denote the unknowns in (8.27). It is assumed that the following initial and boundary conditions are prescribed for the systems in (8.27)

$$\begin{aligned} \mathbf{u}_{pv}(0, x) &= \mathbf{u}_{pv}^0(x), & \mathbf{u}_{aa}(0, x) &= \mathbf{u}_{aa}^0(x), \\ [0 \quad 1] \mathbf{u}_{pv}(t, 0^+) &= Q_G(t), & [1 \quad 0] \mathbf{u}_{pv}(t, b_1^-) &= b_P(t), \\ [0 \quad 1] \mathbf{u}_{aa}(t, 0^+) &= b_Q(t), & [1 \quad 0] \mathbf{u}_{aa}(t, b_2^-) &= P_G(t), \end{aligned}$$

where $\mathbf{u}_{pv}^0 : [a_1, b_1] \rightarrow \mathbb{R}^2$, $\mathbf{u}_{aa}^0 : [a_2, b_2] \rightarrow \mathbb{R}^2$, and $Q_G : [0, \infty) \rightarrow \mathbb{R}$, $P_G : [0, \infty) \rightarrow \mathbb{R}^+$ are boundary conditions for the flow rate at the left end of the spatial domain of the pulmonary venous and for the pressure values at the right end of the spatial domain of the ascending aorta whereas $b_P : [0, \infty) \rightarrow \mathbb{R}^+$, $b_Q : [0, \infty) \rightarrow \mathbb{R}$ are boundary conditions for pressure and flow rate of pulmonary venous and ascending aorta, respectively, that are assigned to the PDE system by the switched DAE system. So, conservation rules determine its inputs as a function of outputs of the swDAE.

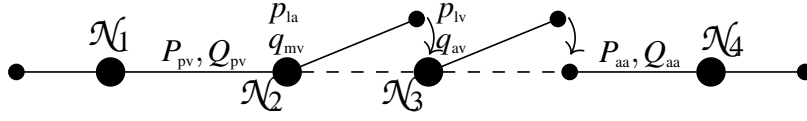


FIGURE 8.6: Mitral and aortic valves allowing blood flow from left atrium to left ventricle and from left ventricle to aorta, depicted as switches.

The switched DAE model for the left atrium is given as

$$\begin{cases} \frac{d}{dt} v_{la} = \tilde{Q} - q_{mv} \\ \frac{d}{dt} q_{mv} = \frac{E_{la} v_{la} + R_{la} \frac{d}{dt} v_{la} - E_{lv} v_{lv} - R_{lv} \frac{d}{dt} v_{lv} - R_{la} q_{mv}}{L_{mv}}, & \text{if } p_{la} - p_{lv} > 0, \\ q_{mv} = 0, & \text{if } p_{la} - p_{lv} \leq 0, \end{cases} \quad (8.28)$$

where $v_{la} : [0, \infty) \rightarrow \mathbb{R}^+$, $v_{lv} : [0, \infty) \rightarrow \mathbb{R}^+$, $q_{mv} : [0, \infty) \rightarrow \mathbb{R}$, $p_{la}, p_{lv} : [0, \infty) \rightarrow \mathbb{R}^+$ are volume of the left atrium and left ventricle, blood flow rate through the mitral valve, and pressures of the left atrium and ventricle, respectively. $E_{la} \in \mathbb{R}^+$ stands for the elastance of the left atrium, $R_{la} \in \mathbb{R}^+$ resistance of the left atrium and $L_{mv} \in \mathbb{R}^+$ inductance of the mitral valve, $\tilde{Q} : [0, \infty) \rightarrow \mathbb{R}$ is the external blood flow coming from pulmonary circulation.

In a similar fashion, switched DAE model for the left ventricle is

$$\begin{cases} \frac{d}{dt} v_{lv} = q_{mv} - q_{av} \\ \frac{d}{dt} q_{av} = \frac{E_{lv} v_{lv} + R_{lv} \frac{d}{dt} v_{lv} - \tilde{P} - R_{aa} C_{aa} \frac{d}{dt} \tilde{P} - R_{lv} q_{av}}{L_{av}}, & \text{if } p_{lv} - \tilde{P} > 0, \\ q_{av} = 0, & \text{if } p_{lv} - \tilde{P} \leq 0, \end{cases} \quad (8.29)$$

where $q_{av} : [0, \infty) \rightarrow \mathbb{R}$ is the blood flow rate through the aortic valve. $E_{lv} \in \mathbb{R}^+$, $R_{lv} \in \mathbb{R}^+$ stand for the elastance and resistance of the left ventricle, respectively, and $L_{av} \in \mathbb{R}^+$ inductance of the aortic valve, $\tilde{P} : [0, \infty) \rightarrow \mathbb{R}^+$ is the external blood pressure of the ascending aorta.

The dynamics of the valves is governed by the pressure gradient, see Figure 8.6. Below, the switch independent equations governing motions of cardiac valves in the left heart are gathered

$$\begin{aligned} \frac{d}{dt} v_{la} = \tilde{Q} - q_{mv}, & \quad \frac{d}{dt} v_{lv} = q_{mv} - q_{av}, & \quad R_{la} \frac{d}{dt} v_{la} = p_{la} - E_{la} v_{la}, \\ & \quad b_Q = q_{av}, & \quad b_P = p_{la}. \end{aligned}$$

If the mitral valve opens and aortic valve shuts, then the following equations hold

$$\begin{aligned} L_{mv} \frac{d}{dt} q_{mv} - R_{la} \frac{d}{dt} v_{la} + R_{lv} \frac{d}{dt} v_{lv} &= E_{la} v_{la} - E_{lv} v_{lv} - R_{la} q_{mv}, \\ q_{av} &= 0, \end{aligned}$$

if the mitral valve closes and aortic valve opens

$$\begin{aligned} q_{mv} &= 0, \\ L_{av} \frac{d}{dt} q_{av} - R_{lv} \frac{d}{dt} v_{lv} &= E_{lv} v_{lv} - \tilde{P} - R_{aa} C_{aa} \frac{d}{dt} \tilde{P} - R_{lv} q_{av}, \end{aligned}$$

where E_{1a}, E_{1v} are given by (8.22a)-(8.22b), and if both valves shut, then the following holds

$$\begin{aligned} q_{mv} &= 0, \\ q_{av} &= 0. \end{aligned}$$

Remark 8.4

It is physiologically not possible that both the mitral and aortic valves are open at once for a healthy heart, [45].

Let $\tilde{\mathbf{w}} = (v_{1a}, q_{mv}, v_{1v}, q_{av}, p_{1a})^\top$ be the state vector, then the switched DAE equations governing transitions of valves can be written as follows

$$\begin{aligned} \tilde{\mathbf{E}}_\sigma \dot{\tilde{\mathbf{w}}} &= \tilde{\mathbf{H}}_\sigma \tilde{\mathbf{w}} + \tilde{\mathbf{B}}_\sigma \tilde{\mathbf{y}}_P, \\ \tilde{\mathbf{y}}_D &= \tilde{\mathbf{C}}_{D_\sigma} \tilde{\mathbf{w}}, \end{aligned}$$

where the coefficient matrices are

$$\begin{aligned} \tilde{\mathbf{E}}_1 &= \begin{bmatrix} 1 & 0 & 0 & 0 & 0 \\ -R_{1a} & L_{mv} & R_{1v} & 0 & 0 \\ 0 & 0 & 1 & 0 & 0 \\ 0 & 0 & 0 & 0 & 0 \\ R_{1a} & 0 & 0 & 0 & 0 \end{bmatrix}, & \tilde{\mathbf{H}}_1 &= \begin{bmatrix} 0 & -1 & 0 & 0 & 0 \\ E_{1a} & -R_{1a} & -E_{1v} & 0 & 0 \\ 0 & 1 & 0 & -1 & 0 \\ 0 & 0 & 0 & 1 & 0 \\ -E_{1a} & 0 & 0 & 0 & 1 \end{bmatrix}, & \tilde{\mathbf{B}}_1 &= \begin{bmatrix} 0 & 0 & 1 \\ 0 & 0 & 0 \\ 0 & 0 & 0 \\ 0 & 0 & 0 \\ 0 & 0 & 0 \end{bmatrix}, \\ \tilde{\mathbf{E}}_2 &= \begin{bmatrix} 1 & 0 & 0 & 0 & 0 \\ 0 & 0 & 0 & 0 & 0 \\ 0 & 0 & 1 & 0 & 0 \\ 0 & 0 & -R_{1v} & L_{av} & 0 \\ R_{1a} & 0 & 0 & 0 & 0 \end{bmatrix}, & \tilde{\mathbf{H}}_2 &= \begin{bmatrix} 0 & -1 & 0 & 0 & 0 \\ 0 & 1 & 0 & 0 & 0 \\ 0 & 1 & 0 & -1 & 0 \\ 0 & 0 & E_{1v} & -R_{1v} & 0 \\ -E_{1a} & 0 & 0 & 0 & 1 \end{bmatrix}, & \tilde{\mathbf{B}}_2 &= \begin{bmatrix} 0 & 0 & 1 \\ 0 & 0 & 0 \\ 0 & 0 & 0 \\ -1 & -R_{aa} C_{aa} & 0 \\ 0 & 0 & 0 \end{bmatrix}, \\ \tilde{\mathbf{E}}_3 &= \begin{bmatrix} 1 & 0 & 0 & 0 & 0 \\ 0 & 0 & 0 & 0 & 0 \\ 0 & 0 & 1 & 0 & 0 \\ 0 & 0 & 0 & 0 & 0 \\ R_{1a} & 0 & 0 & 0 & 0 \end{bmatrix}, & \tilde{\mathbf{H}}_3 &= \begin{bmatrix} 0 & -1 & 0 & 0 & 0 \\ 0 & 1 & 0 & 0 & 0 \\ 0 & 1 & 0 & -1 & 0 \\ 0 & 0 & 0 & 1 & 0 \\ -E_{1a} & 0 & 0 & 0 & 1 \end{bmatrix}, & \tilde{\mathbf{B}}_3 &= \tilde{\mathbf{B}}_1, \\ \tilde{\mathbf{C}}_{D_1} &= \begin{bmatrix} 0 & 0 & 0 & 1 & 0 \\ 0 & 0 & 0 & 0 & 1 \end{bmatrix}, & \tilde{\mathbf{C}}_{D_2} &= \tilde{\mathbf{C}}_{D_1}, & \tilde{\mathbf{C}}_{D_3} &= \tilde{\mathbf{C}}_{D_1}, \end{aligned}$$

where $R_{1a}, L_{mv}, R_{1v}, L_{av}, R_{aa}, C_{aa}$ are physiological constants given in Table 8.3 and the coupling via boundaries of pulmonary venous and ascending aorta are given by

$$\tilde{\mathbf{y}}_P = (P_{aa}(\cdot, a_2^+), \frac{d}{dt} P_{aa}(\cdot, a_2^+), Q_{pv}(\cdot, b_1^-))^\top, \quad \tilde{\mathbf{y}}_D = (Q_{aa}(\cdot, a_2^+), P_{pv}(\cdot, b_1^-))^\top,$$

where $\tilde{P} := P_{aa}(\cdot, a_2^+)$ and $\tilde{Q} := Q_{pv}(\cdot, b_1^-)$.

For the complete coupled model, an externally given blood flow is assumed, where blood flows in from lungs at the first node \mathcal{N}_1 in Figure 8.6. The algebraic relations are

$$\begin{aligned} 0 &= q_L - Q_G, \\ y_D^1 &= q_L, \end{aligned}$$

where $Q_G : [0, \infty) \rightarrow \mathbb{R}$ is the externally given blood flow from lungs with the boundary condition $Q_{pv}(\cdot, a_1^+) = y_D^1$. Moreover, at the last node \mathcal{N}_4 in Figure 8.6, an externally given blood pressure is assumed, for which the algebraic relations are

$$\begin{aligned} 0 &= p_B - P_G, \\ y_D^4 &= p_B, \end{aligned}$$

where $P_G : [0, \infty) \rightarrow \mathbb{R}^+$ is the externally given blood pressure with the boundary condition $P_{aa}(\cdot, b_2^-) = y_D^4$.

The complete coupled system is then of the form (8.1) where

$$\mathbf{A} = \begin{bmatrix} \mathbf{A}_1 & 0 \\ 0 & \mathbf{A}_2 \end{bmatrix} \quad \text{with } \mathbf{A}_j = \begin{bmatrix} 0 & \frac{1}{b_j - a_j} \\ \frac{1}{b_j - a_j} c_j^2 & 0 \end{bmatrix} \quad \text{for } j = 1, 2, \quad \mathbf{u} = \begin{pmatrix} \mathbf{u}_{pv} \\ \mathbf{u}_{aa} \end{pmatrix},$$

and the output of the PDE is

$$\mathbf{y}_P = (Q_{pv}(\cdot, a_1^+), Q_{aa}(\cdot, a_2^+), P_{pv}(\cdot, b_1^-), P_{aa}(\cdot, b_2^-))^\top,$$

with the following coefficient matrix

$$\mathbf{C}_p = \begin{bmatrix} 1 & 0 & 0 & 0 & 0 & 0 & 0 & 0 \\ 0 & 0 & 1 & 0 & 0 & 0 & 0 & 0 \\ 0 & 0 & 0 & 0 & 0 & 1 & 0 & 0 \\ 0 & 0 & 0 & 0 & 0 & 0 & 0 & 1 \end{bmatrix},$$

and the switched DAE now has the state vector $\mathbf{w} = (q_L, v_{1a}, q_{mv}, v_{1v}, q_{av}, p_{1a}, p_B)^\top$, and coefficient matrices

$$\mathbf{E}_k = \begin{bmatrix} 0 & 0 & 0 \\ 0 & \tilde{\mathbf{E}}_k & 0 \\ 0 & 0 & 0 \end{bmatrix}, \quad \mathbf{H}_k = \begin{bmatrix} 1 & 0 & 0 \\ 0 & \tilde{\mathbf{H}}_k & 0 \\ 0 & 0 & 1 \end{bmatrix}, \quad \mathbf{B}_k = \begin{bmatrix} 0 & 0 & 0 \\ 0 & \tilde{\mathbf{B}}_k & 0 \\ 0 & 0 & 0 \end{bmatrix},$$

$$\mathbf{C}_{D_k} = \begin{bmatrix} 1 & 0 & 0 \\ 0 & \tilde{\mathbf{C}}_k & 0 \\ 0 & 0 & 1 \end{bmatrix}, \quad \mathbf{f}_k = \begin{bmatrix} -Q_G \\ 0 \\ 0 \\ 0 \\ 0 \\ 0 \\ -P_G \end{bmatrix},$$

for $k = 1, 2$ and the coupling matrix $\mathbf{P} = \begin{bmatrix} \mathbf{P}_a \\ \mathbf{P}_b \end{bmatrix}$ is

$$\mathbf{P}_a = \begin{bmatrix} 0 & 1 & 0 & 0 \\ 0 & 0 & 0 & 1 \end{bmatrix}, \quad \mathbf{P}_b = \begin{bmatrix} 1 & 0 & 0 & 0 \\ 0 & 0 & 1 & 0 \end{bmatrix}.$$

Parameter values for the blood flow example are given in Tables 8.2 and 8.3.

TABLE 8.2: Parameter values depending on medical data for the left heart chambers and cardiac valves, [86, 94, 99].

E_{1aa}	E_{1ab}	E_{1va}	E_{1vb}	T_{cplv}	T_{cpla}	T_{rplv}	T_{rpla}	t_{cla}	t_{rla}	T_0
0.070	0.090	2.750	0.080	0.300	0.170	0.150	0.170	0.800	0.970	1

TABLE 8.3: Modified parameter values for the left heart cardiac valves and pulmonary circulation, [86, 94, 99, 117].

L_{mv}	L_{av}	R_{1a}	R_{1v}	L_{pv}	R_{pv}	C_{aa}	R_{aa}	S_{1a}	S_{1v}
0.0002	0.0005	0.001	0.003	0.0005	0.005	0.1	0.01	$0.0005p_{1a}$	$0.0005p_{1v}$

8.2 The coupled system

In this section, the distributional solution framework for linear hyperbolic PDEs introduced in Chapter 6 is used to establish a link between the coupled system of PDE-swDAE and the solutions of a switched *delay* DAE. Then, the existence and uniqueness result for general switched delay DAEs is demonstrated and the main result about the existence and uniqueness of solutions of the coupled system can be concluded.

8.2.1 Existence and uniqueness of solutions of the coupled system

In the following, the switched DAE (8.1d) with output \mathbf{y}_D given by (8.1e) together with the boundary behavior $\mathbf{u}_{ab} := (\mathbf{u}(\cdot, a)^\top, \mathbf{u}(\cdot, b)^\top)^\top$ of the PDE (8.1a) is studied. Based on the results from Chapter 6, the solution \mathbf{w} and \mathbf{u}_{ab} of the coupled system can now be related one-to-one with the solution of a switched delay DAE as follows.

Theorem 8.5

Consider the coupled system (8.1) satisfying Assumptions (H-3), (H'-5) and (H'-6). Then $\mathbf{z} := (\mathbf{w}^\top, \mathbf{u}_{ab}^\top)^\top$ is a solution of the coupled system if and only if \mathbf{z} solves the switched delay DAE (swDDAE)

$$\begin{bmatrix} \mathbf{E}_\sigma & \mathbf{0} \\ \mathbf{0} & \mathbf{0} \end{bmatrix} \dot{\mathbf{z}} = \begin{bmatrix} \mathbf{H}_\sigma & \mathbf{B}_\sigma \mathbf{C}_P \\ \mathbf{F} \mathbf{C}_{D\sigma} & -\mathbf{I} \end{bmatrix} \mathbf{z} + \sum_{k=1}^d \left(\begin{bmatrix} \mathbf{0} & \mathbf{0} \\ \mathbf{0} & \mathbf{D}_k \end{bmatrix} \mathcal{S}_{\text{time}}^{\tau_k} \mathbf{z} \right) + \begin{bmatrix} \mathbf{f}_\sigma \\ \mathbf{0} \end{bmatrix}, \quad (8.30)$$

where τ_k , \mathbf{u}_{ab} and the matrices \mathbf{F} and \mathbf{D}_k are given as in Remark 7.7 and its components as in Equations (2.67)-(2.68).

Proof. (\Leftarrow) Assume that $\mathbf{z} = (\mathbf{w}^\top, \mathbf{u}_{ab}^\top)^\top$ solves the swDDAE (8.30). From Equation (8.30), the following swDAE is obtained

$$\mathbf{E}_\sigma \dot{\mathbf{w}} = \mathbf{H}_\sigma \mathbf{w} + \mathbf{B}_\sigma \mathbf{C}_P \mathbf{u}_{ab} + \mathbf{f}_\sigma,$$

where \mathbf{w} is the solution with the input $\mathbf{y}_P = \mathbf{C}_P \mathbf{u}_{ab}$ as shown in Theorem 4.12. And also, from the swDDAE (8.30), the traces at the boundaries of the PDE are obtained as

$$\begin{aligned} \mathbf{u}(\cdot, a^+) &= \mathbf{F}_a \mathbf{b}^a + \sum_{i=1}^n \mathbf{D}_k^{ab} \left(\mathcal{S}_{\text{time}}^{\tau_k} \mathbf{u}^b \right) \\ &= \mathbf{F}_a \mathbf{b}^a + \sum_{i=1}^n \mathbf{D}_k^{ab} \left(\mathcal{S}_{\text{time}}^{\lambda_k, b} \mathbf{u}^b \right) (\cdot, a^+), \\ \mathbf{u}(\cdot, b^-) &= \mathbf{F}_b \mathbf{b}^b + \sum_{i=1}^n \mathbf{D}_k^{ba} \left(\mathcal{S}_{\text{time}}^{\tau_k} \mathbf{u}^a \right) \\ &= \mathbf{F}_b \mathbf{b}^b + \sum_{i=1}^n \mathbf{D}_k^{ba} \left(\mathcal{S}_{\text{time}}^{\lambda_k, a} \mathbf{u}^a \right) (\cdot, b^-), \end{aligned}$$

where $\begin{bmatrix} \mathbf{b}^a \\ \mathbf{b}^b \end{bmatrix} = \mathbf{C}_{D\sigma} \mathbf{w}$, which together yield the solution \mathbf{u}

$$\mathbf{u} = \sum_{i \in K^-} \Pi_i \left(\mathcal{S}_{\text{time}}^{\lambda_i, b} \mathbf{u}^b \right) + \sum_{j \in K^+} \Pi_j \left(\mathcal{S}_{\text{time}}^{\lambda_j, a} \mathbf{u}^a \right),$$

where

$$\begin{aligned} \left(\mathcal{S}_{\text{time}}^{\Lambda^-, \mathbf{I}, b} \mathbf{u}^b \right) &:= \sum_{i \in K^-} \Pi_i \left(\mathcal{S}_{\text{space}}^{\lambda_i, t_0} \mathbf{u}^{t_0} \right), \quad \text{on } \left(t_0, t_0 + \frac{b-x}{-\lambda_i} \right), \\ \left(\mathcal{S}_{\text{time}}^{\Lambda^+, \mathbf{I}, a} \mathbf{u}^a \right) &:= \sum_{j \in K^+} \Pi_j \left(\mathcal{S}_{\text{space}}^{\lambda_j, t_0} \mathbf{u}^{t_0} \right), \quad \text{on } \left(t_0, t_0 + \frac{x-a}{\lambda_j} \right), \end{aligned}$$

where $\Pi_p := \mathbf{R} \text{diag}(\mathbf{e}_p) \mathbf{R}^{-1}$ with $\mathbf{e}_p \in \mathbb{R}^n$ is the p -th directional unit vector.

(\Rightarrow) Assume that \mathbf{w} is the solution to the swDAE (8.1d)

$$\mathbf{E}_\sigma \dot{\mathbf{w}} = \mathbf{H}_\sigma \mathbf{w} + \mathbf{B}_\sigma \mathbf{y}_P + \mathbf{f}_\sigma,$$

where $\mathbf{y}_P = \mathbf{C}_P \mathbf{u}_{ab}$ and that \mathbf{u} is the solution to the PDE (8.1a) given as in Equation (7.10). Then \mathbf{u}_{ab} is of the form

$$\mathbf{u}_{ab}(t) = \mathbf{F} \mathbf{C}_{D_\sigma} \mathbf{w} + \sum_{k=1}^n \mathbf{D}_k \mathcal{S}_{\text{time}}^{\tau_k} \mathbf{u}_{ab},$$

where $\begin{bmatrix} \mathbf{b}^a \\ \mathbf{b}^b \end{bmatrix} = \mathbf{C}_{D_\sigma} \mathbf{w}$. Hence, $\mathbf{z} = (\mathbf{w}^\top, \mathbf{u}_{ab}^\top)^\top$ solves the swDDAE (8.30). \square

Since the solution of the coupled system on the whole domain can be recovered via Equation (7.10), it has been shown that the solution properties of the coupled system can equivalently be characterized by the swDDAE (8.30).

The following result establishes conditions for existence and uniqueness of solutions for general swDDAEs.

Theorem 8.6: Existence and uniqueness of solutions for swDDAEs

Consider the following switched delay differential algebraic equations having $d \in \mathbb{N}$ delays such that $0 < \tau_1 < \tau_2 < \dots < \tau_d$

$$\mathcal{E}_\sigma \dot{\mathbf{z}} = \mathcal{H}_\sigma \mathbf{z} + \sum_{j=1}^d \mathcal{D}_j \mathcal{S}_{\text{time}}^{\tau_j} \mathbf{z} + \mathbf{g}_\sigma, \quad (8.31)$$

with $\sigma : \mathbb{R} \rightarrow \{1, 2, \dots, N\}$, $N \in \mathbb{N}$, $\mathcal{E}_\xi, \mathcal{H}_\xi, \mathcal{D}_1, \dots, \mathcal{D}_d \in \mathbb{R}^{m \times m}$ for each $\xi \in \{1, 2, \dots, N\}$. Assume that $(\mathcal{E}_\xi, \mathcal{H}_\xi)$ is regular for each $\xi \in \{1, 2, \dots, N\}$, then for any initial trajectory $\mathbf{z}^0 \in (\mathbb{D}_{\text{pw}C^\infty})^m$ and any inhomogeneity $\mathbf{g}_\xi \in (\mathbb{D}_{\text{pw}C^\infty})^m$, the corresponding initial trajectory problem has a unique solution.

Proof. The result is a simple consequence from the ‘‘method of steps’’ and the details for DDAEs with a single delay $d = 1$ can be found in [133]. In the following proof, the *prime* notation (\prime) is adapted to indicate the derivative of distributions in addition to the *dot* notation $(\dot{})$ since the derivative of a distribution restricted to an interval and restricting a derivative of a distribution to an interval do not have the same meaning. In other words, the operations restriction to an interval and differentiation of a distribution do not commute.

Let τ be the smallest delay within the set $\{\tau_1, \dots, \tau_d\}$. Then the solution to the swDDAE system (8.31) is shown to be expressed as

$$\mathbf{z} = \mathbf{z}_{(-\infty, t_0)}^{t_0} + \sum_{k=1}^{\infty} \mathbf{z}_{[\tilde{t}_{k-1}, \tilde{t}_k]}^k, \quad (8.32)$$

where $\tilde{t}_k := t_0 + k\tau$, $k \in \mathbb{N}$, $\tilde{t}_0 := t_0$, and $\mathbf{z}^k \in (\mathbb{D}_{\text{pw}C^\infty})^m$ is the unique solution to the non-delay swDAE, (Theorem 4.12),

$$\begin{aligned} \mathbf{z}_{(-\infty, \tilde{t}_{k-1})}^k &= \mathbf{z}_{(-\infty, \tilde{t}_{k-1})}^{k-1} \\ \left(\mathcal{E}_\sigma \dot{\mathbf{z}}^k \right)_{[\tilde{t}_{k-1}, \infty)} &= \left(\mathcal{H}_\sigma \mathbf{z}^k + \mathbf{g}_\sigma \right)_{[\tilde{t}_{k-1}, \infty)}, \end{aligned} \quad (8.33)$$

where $\tilde{\mathbf{g}}_\sigma := \left(\sum_{j=1}^d \mathcal{D}_j \mathcal{S}_{\text{time}}^{\tau_j} \mathbf{z}^{k-1} + \mathbf{g}_\sigma \right)$. Let $T \subseteq \mathbb{R}$ and $X \subseteq \mathbb{R}$ be open sets. For all $\phi \in C_{\text{pw}}^\infty(T \times X; \mathbb{R})$, $\mathbf{z}(\phi)$ is a well-defined distribution as test functions ϕ have compact supports and, hence, the sum in (8.32) is taken over locally finite sets. Therefore, the sum is finite for each $\phi \in C_{\text{pw}}^\infty(T \times X; \mathbb{R})$. Moreover, $\mathbf{z} \in (\mathbb{D}_{\text{pw}C^\infty})^m$ since it is a linear combination of

piecewise-smooth distributions. For any $k \geq 1$,

$$\begin{aligned}
(\mathcal{E}_\sigma \dot{\mathbf{z}})_{[\tilde{t}_{k-1}, \tilde{t}_k]} &= \mathcal{E}_\sigma \left(\left(\mathbf{z}_{(-\infty, t_0)}^{t_0} \right)' + \sum_{p=1}^{\infty} \left(\mathbf{z}_{[\tilde{t}_{p-1}, \tilde{t}_p]}^p \right)' \right)_{[\tilde{t}_{k-1}, \tilde{t}_k]} \\
&= \mathcal{E}_\sigma \left(\dot{\mathbf{z}}_{(-\infty, t_0)}^0 - \mathbf{z}^{t_0}(t_0^-) \delta_{t_0} \right. \\
&\quad \left. + \sum_{p=1}^{\infty} \left(\dot{\mathbf{z}}_{[\tilde{t}_{p-1}, \tilde{t}_p]}^p + \mathbf{z}^p(\tilde{t}_{p-1}^-) \delta_{\tilde{t}_{p-1}} - \mathbf{z}^p(\tilde{t}_p^-) \delta_{\tilde{t}_p} \right) \right)_{[\tilde{t}_{k-1}, \tilde{t}_k]} \\
&= \left(\mathcal{E}_\sigma \dot{\mathbf{z}}^k \right)_{[\tilde{t}_{k-1}, \tilde{t}_k]} \\
&= \left(\mathcal{H}_\sigma \mathbf{z}^k + \mathbf{g}_\sigma \right)_{[\tilde{t}_{k-1}, \tilde{t}_k]} \\
&= \mathcal{H}_\sigma \mathbf{z}_{[\tilde{t}_{k-1}, \tilde{t}_k]} + \sum_{j=1}^d \mathcal{D}_j \left(\mathcal{S}_{\text{time}}^{\tau_j} \mathbf{z}^{k-1} \right)_{[\tilde{t}_{k-1}, \tilde{t}_k]} + \mathbf{g}_{\sigma_{[\tilde{t}_{k-1}, \tilde{t}_k]}} \\
&= \left(\mathcal{H}_\sigma \mathbf{z} + \sum_{j=1}^d \mathcal{D}_j \mathcal{S}_{\text{time}}^{\tau_j} \mathbf{z} + \mathbf{g}_\sigma \right)_{[\tilde{t}_{k-1}, \tilde{t}_k]},
\end{aligned}$$

where the relations in Corollary 3.29 are exploited. Hence, \mathbf{z} given in (8.32) is the unique solution to (8.31). \square

Remark 8.7

The existence and uniqueness result in Theorem 8.6 can easily be extended to the case that the delay coefficient matrices \mathcal{D}_j , $j = 1, 2, \dots, d$ in (8.31) are switch dependent; i.e., Equation (8.31) becomes

$$\mathcal{E}_\sigma \dot{\mathbf{z}} = \mathcal{H}_\sigma \mathbf{z} + \sum_{j=1}^d \mathcal{D}_{j,\sigma} \mathcal{S}_{\text{time}}^{\tau_j} \mathbf{z} + \mathbf{g}_\sigma.$$

However, for this case, technical details are omitted as such switch dependent delay terms do not occur in the applications studied in this thesis.

The main result about existence and uniqueness of solutions of the coupled system can now be stated.

Corollary 8.8

Consider the coupled system (8.1) with a hyperbolic PDE (Assumption (H-3)) and suitable boundary conditions (Assumption (H'-5)-(H'-6)). Furthermore, assume that for all $\xi \in \{1, \dots, N\}$ the matrix pairs $(\mathbf{E}_\xi, \mathbf{H}_\xi + \mathbf{B}_\xi \mathbf{C}_P \mathbf{F} \mathbf{C}_{D\xi})$ with \mathbf{F} as in Remark 7.7 are *regular*. Then for any initial value $\mathbf{u}^{t_0} \in \mathbb{D}_{\text{pw}C^\infty}(X)^n$, $\mathbf{w}^{t_0} \in \mathbb{R}^m$ and external inhomogeneities $\mathbf{f}_\xi \in \mathbb{D}_{\text{pw}C^\infty}(T)^m$, there exists a unique solution $(\mathbf{u}, \mathbf{w}) \in \mathbb{D}_{\text{pw}C^\infty}(T \times X)^n \times \mathbb{D}_{\text{pw}C^\infty}(T)^m$ of the coupled system.

Proof. This is a consequence of Theorems 8.5 and 8.6 and the fact that $\det(s\mathcal{E}_\xi - \mathcal{H}_\xi) = \det(s\mathbf{E}_\xi - (\mathbf{H}_\xi + \mathbf{B}_\xi \mathbf{C}_P \mathbf{F} \mathbf{C}_{D\xi}))$. \square

Remark 8.9

In Corollary 8.8, the condition on the regularity of matrix pairs $(\mathbf{E}_\xi, \mathbf{H}_\xi + \mathbf{B}_\xi \mathbf{C}_P \mathbf{F} \mathbf{C}_{D\xi})$ for all $\xi \in \{1, \dots, N\}$ ensures that the coupling rules define a well-defined coupled system. In other words, only outgoing characteristics of the PDE can provide information to the swDAE.

8.3 Numerical results

In this section, it is explained how the examples of power grid and circulatory system described in Sections 8.1.1 and 8.1.3 are solved numerically, and the numerical results are illustrated.

8.3.1 General setup for the PDE discretization

Each spatial domain is considered $I = [a, b]$, $b > a$. To discretize the spatial domain I into $N \in \mathbb{N}$ computing cells, multiple grid cells $I_i = [x_{i-1/2}, x_{i+1/2}]$ are considered such that the interiors of cells are pairwise disjoint and the union of all cells covers the domain. Denote by $\Delta x = x_{i+1/2} - x_{i-1/2}$ cell length, which is assumed to be constant; i.e., $\Delta x = (b - a)/N$. Thus, all boundaries of cells are of the form $x_{i+1/2} = i\Delta x$. The center of each cell I_i is $x_i = (i - 1/2)\Delta x$. Furthermore, boundary conditions at $x = a$ and $x = b$ are required to define the values at the interfaces $x_{1/2}$ and $x_{N+1/2}$ so that the numerical scheme can update the very left and very right cells I_1 and I_N of the discretized domain for the next time step t^{n+1} . Ghost cells $I_0 = [a - \Delta x, a]$ and $I_{N+1} = [b, b + \Delta x]$ are placed at boundaries. In other words, *imaginary data* are created in these ghost cells, see Figure 8.7. Moreover, at $x_{1/2}$ and $x_{N+1/2}$, *intermediate states* are obtained. The discretization of the time variable is done in accordance with time step size $\Delta t = t_{n+1} - t_n$, such that the Courant-Friedrichs-Lewy (CFL) number \mathcal{C} , [60, 84], for the numerical scheme is smaller than 1

$$\Delta t = \mathcal{C} \frac{\Delta x}{|\lambda|_{\max}},$$

where $|\lambda|_{\max}$ is the largest wave speed in amplitude of the system.

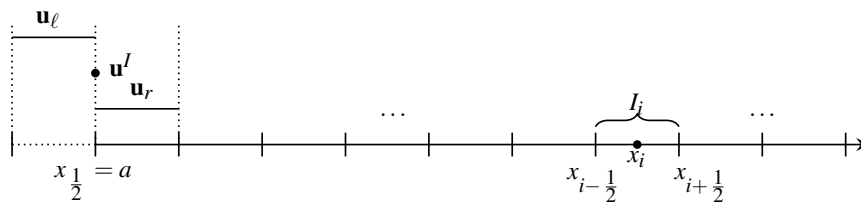


FIGURE 8.7: Imaginary, intermediate and right states, $\mathbf{u}_l, \mathbf{u}^l, \mathbf{u}_r$, at the left end of the domain $x_{1/2} = a$ are shown. Furthermore, a general cell structure is depicted with the cell I_i , cell center x_i and boundaries of the cell I_i , namely $x_{i-1/2}$ and $x_{i+1/2}$.

8.3.2 The power grid

Note that the matrix pairs $(\mathcal{E}_\sigma, \mathcal{H}_\sigma)$ in the power grid example are regular. Denote by $\mathcal{E} := \{\mathcal{E}_1, \mathcal{E}_2, \mathcal{E}_3, \mathcal{E}_4\}$ the set of edges in the coupled network, over which the PDE is discretized. For discretizing the spatial domain $[a, b]$, consider $x_k = (k - 1/2)\Delta x$, $k = 1, \dots, N$,

$\Delta x = (b-a)/N$, where N is the number of cells in the mesh. Then two ghost cells I_0 and I_{N+1} are inserted at both ends of the computational domain which are treated as boundaries. The CFL number is assumed to be $\mathcal{C}_l = 1$ and denote by $\mathbf{u}_j^n = \mathbf{u}(x_j, t^n)$ the approximated solution at time t^n and position x_j . Denote by $(\mathbf{u}_k)_j^n = ((u_k^1)_j^n, (u_k^2)_j^n)^\top$ to have a suitable representation for the unknowns for every edge $k \in \mathfrak{E}$. Before the initialization to solve the coupled system at each time, first, the discretized PDE over each edge $k \in \mathfrak{E}$ is decomposed into its characteristic variables $(\mathbf{v}_k)_j^n$ as left-going, $(v_k^-)_j^n$, and right-going characteristic waves, $(v_k^+)_j^n$, where $(u_k^1)_j^n = (v_k^-)_j^n + (v_k^+)_j^n$ and $(u_k^2)_j^n = -(v_k^-)_j^n + (v_k^+)_j^n$. To solve the decomposed PDE numerically, the upwind scheme is used, [61, 83, 97, 127, 125], and implicit Euler method, [125], for the swDAE. At each time iteration, the decomposed PDE is solved numerically, then, $(\mathbf{u}_k)_j^{n+1}$ is updated via inverse coordinate change $(\mathbf{u}_k)_j^{n+1} = \mathbf{R}_k(\mathbf{v}_k)_j^{n+1}$, where $(\mathbf{v}_k)_j^n = ((v_k^-)_j^n, (v_k^+)_j^n)^\top$ and $\mathbf{A}_k = \mathbf{R}_k \Lambda_k \mathbf{R}_k^{-1}$ for $k \in \mathfrak{E}$, where \mathbf{A}_k is the coefficient matrix given as in (8.7). The equations in (8.5) together result in coupling conditions in terms of the characteristic variables as follows

$$\begin{aligned} (v_2^-)_{N+1}^n &= 2(v_4^-)_{-1}^n - (v_2^+)_{N+1}^n, & (v_4^-)_{N+1}^n &= -\frac{2}{3}(v_3^+)_{N+1}^n + \frac{1}{3}(v_4^+)_{N+1}^n, \\ (v_4^+)_{-1}^n &= 2(v_2^+)_{N+1}^n - (v_4^-)_{-1}^n, & (v_3^-)_{N+1}^n &= \frac{1}{3}(v_3^+)_{N+1}^n - \frac{2}{3}(v_4^+)_{N+1}^n, \end{aligned}$$

which are four out of eight of boundary conditions for the decoupled PDE, and hence, they build up the inputs to the swDAE as

$$\begin{aligned} (u_4^1)_0^n &= (v_4^-)_{-1}^n + (v_4^+)_{-1}^n, & (u_2^1)_N^n &= (v_2^-)_{N+1}^n + (v_2^+)_{N+1}^n, \\ (u_3^1)_N^n &= (v_3^-)_{N+1}^n + (v_3^+)_{N+1}^n, & (u_4^1)_N^n &= (v_4^-)_{N+1}^n + (v_4^+)_{N+1}^n. \end{aligned}$$

The remaining four inputs to the swDAE are given in terms of characteristic variables $(v_1^-)_{-1}^n$, $(v_1^+)_{N+1}^n$, $(v_2^-)_{-1}^n$ and $(v_3^-)_{-1}^n$. Then, at each time step, the swDAE is solved and the boundary conditions $(v_1^+)_{-1}^n$, $(v_1^-)_{N+1}^n$, $(v_2^+)_{-1}^n$ and $(v_3^+)_{-1}^n$ are obtained. At \mathcal{N}_1 in Figure 8.4, the boundary condition is assigned as $(u_1^2)_0^n = v_G$, where v_G is the prescribed constant voltage source, and hence, the boundary condition for the characteristics $(v_1^+)_{-1}^n = v_G + (v_1^-)_{-1}^n$. At \mathcal{N}_2 over \mathfrak{E}_1 , the input to the swDAE is $(u_1^1)_N^n = (v_1^-)_N^n + (v_1^+)_{N+1}^n$ and the boundary condition for the characteristic variable is $(u_1^2)_N^n = -(v_1^-)_N^n + (v_1^+)_{N+1}^n$. The swDAE assigns this boundary condition according to (8.6)

$$\left. \begin{aligned} i_{1\eta}^{n+1} &= (u_1^1)_N^n \\ v_{1\eta}^{n+1} &= \frac{d}{dt} i_{1\eta}^{n+1} \\ (u_1^2)_N^n &= v_{1\eta}^{n+1} \end{aligned} \right\} \Leftrightarrow \begin{cases} i_{1\eta}^{n+1} = 2(v_1^+)_{N+1}^n - v_{1\eta}^{n+1} \\ \frac{d}{dt} \left(2(v_1^+)_{N+1}^n - v_{1\eta}^{n+1} \right) = v_{1\eta}^{n+1} \\ (v_1^-)_{N+1}^n = (v_1^+)_{N+1}^n - v_{1\eta}^{n+1}, \end{cases}$$

where $\eta = 2$ or $\eta = 3$ depending on to which edge the switching transformer connects \mathfrak{E}_1 and $i_{12}^n, i_{13}^n, v_{12}^n, v_{13}^n$ are discretized state variables for the swDAE at time t^n . If $\eta = 2$, v_{12}^{n+1} is computed as above, then the boundary condition $(v_1^-)_{N+1}^n = (v_1^+)_{N+1}^n - v_{12}^{n+1}$ is assigned, hence, $i_{12}^{n+1} = (v_1^+)_{N+1}^n + (v_1^-)_{N+1}^n$. Furthermore, $i_{13}^{n+1} = 0$ and

$$\begin{aligned} v_{13}^{n+1} &= \frac{d}{dt} i_{13}^{n+1} \\ &= \frac{i_{13}^{n+1} - i_{13}^n}{\Delta t}. \end{aligned} \tag{8.36}$$

If $\eta = 3$, then $i_{12}^{n+1} = 0$ and v_{12}^{n+1} is found similarly as in (8.36). Then, the boundary conditions $(u_2^2)_0^n = \kappa_{12} v_{12}^n$ and $(u_3^2)_0^n = \kappa_{13} v_{13}^n$ are assigned, thus, the boundary conditions in characteristic variables $(v_2^+)_{-1}^n = (v_2^-)_{-1}^n + (u_2^2)_0^n$ and $(v_3^+)_{-1}^n = (v_3^-)_{-1}^n + (u_3^2)_0^n$ are assigned. Then, the solution for $(\mathbf{u}_k)_j^{n+1}$ is updated, for all $k \in \mathfrak{E}$ by using the eigenvector matrix \mathbf{R}_k

and $(v_k^-)_{\eta}^{n+1}$, $\eta = 0, 1, \dots, N$ and $(v_k^+)_{\gamma}^{n+1}$, $\gamma = 1, 2, \dots, N+1$. Until the prescribed final time is reached, the time is updated; i.e., $t^{n+1} = t^n + \Delta t$, and the above steps are repeated.

If, instead of solving for $(\mathbf{v}_k)_j^n$, one attempts to solve for $(\mathbf{u}_k)_j^n$ and assigns inputs/outputs without considering them in characteristic variables, oscillations might occur at boundaries at each time step. The method described in this section covers the Dirac impulses and ensures that such oscillations do not take place. Therefore, the numerical steps defined above should be carried out in characteristic variables and then the original unknown variables $(\mathbf{u}_k)_j^n$ should be updated accordingly.

Remark 8.10

In numerical simulations, the amplitude of the Dirac delta becomes larger as the width of the grid cell becomes smaller. In other words, the Dirac delta is spread over the numerical cells in the numerical examples.

Discontinuous initial condition

The computational domain is considered $[a, b] = [0, 0.5]$, initial time $t_0 = 0$, and final time $t_{\max} = 1.5$, the number of cells $N = 150$, $\Delta x = 3.3 \times 10^{-3}$. The constant voltage at \mathcal{N}_1 is $v_G = 0.5$. The constants are assumed to be $L_{12} = 1$, $L_{13} = 1$, $\kappa_{12} = 1$, $\kappa_{13} = 1$, $R_{24} = 1$, $R_{34} = 1$, $L_k = 1$ and $C_k = 1$ for each $k \in \mathcal{E}$. The initial conditions for the PDE are $I_1(0, x) = 0$, $x \in [0, 0.5]$, $V_1(0, x) = 0$ for $x \in [0, 0.3)$ and $V_1(0, x) = 1$ for $x \in [0.3, 0.5]$, $I_k(0, x) = 0$ and $V_k(0, x) = 0$, $x \in [0, 0.5]$, for $k = 2, 3, 4$, see Figure 8.8. The switching transformer initially connects the edges 1 and 2 for $t \in [0, 0.4)$ and then connects the edges 1 and 3 for $t \in [0.4, 0.7)$. For $t \in [0.7, 1.5]$, it connects the edges 1 and 2 again. In Figure 8.9, the plots for all edges are shown at $t = 0.5$. After the first switch at $t = 0.4$, a Dirac impulse occurs on \mathcal{E}_2 . In Figure 8.10, the plots for all edges at $t = 0.8$ are shown. After the second switch at $t = 0.7$, there happens another Dirac impulse on \mathcal{E}_3 . And in Figure 8.11, the solution over the whole domain $(t, x) \in [0, 1.5] \times [0, 0.5]$ is shown for all edges where the lines in the plot of the solution for the edges \mathcal{E}_2 , \mathcal{E}_3 and \mathcal{E}_4 show how Dirac impulses move in the domain.

Dirac impulse as initial condition

The setup of this example is the same as the previous example. The only difference from the previous example is that the initial condition on the first edge \mathcal{E}_1 is given zero everywhere for both the voltage and current values except at $x = 0.3$ the voltage has a Dirac impulse, as seen in Figure 8.12. Initial conditions for \mathcal{E}_2 , \mathcal{E}_3 , \mathcal{E}_4 are prescribed as zero for both currents and voltages. The switch initially connects the edges 1 and 2 for $t \in [0, 0.4)$ and then connects the edges 1 and 3 for $t \in [0.4, 0.7)$. For $t \in [0.7, 1.5]$, it connects the edges 1 and 2 again. In Figure 8.13, the plots for all edges are shown at $t = 0.25$. Dirac impulse on \mathcal{E}_1 moves along \mathcal{E}_1 and then to \mathcal{E}_2 . In Figure 8.14, the results at $t = 0.6$ are shown. After the first switch at $t = 0.4$, a Dirac impulse occurs on \mathcal{E}_2 . And on \mathcal{E}_3 , the information from \mathcal{E}_1 enters the domain. In Figure 8.15, the plots for all edges at $t = 0.8$ are shown. After the second switch at $t = 0.7$, there happens another Dirac impulse on \mathcal{E}_3 . In Figure 8.16, the solution over the whole domain $(t, x) \in [0, 1.5] \times [0, 0.5]$ is shown for all edges where the lines on \mathcal{E}_1 , \mathcal{E}_2 , \mathcal{E}_3 and \mathcal{E}_4 show how Dirac impulses move in the domain.

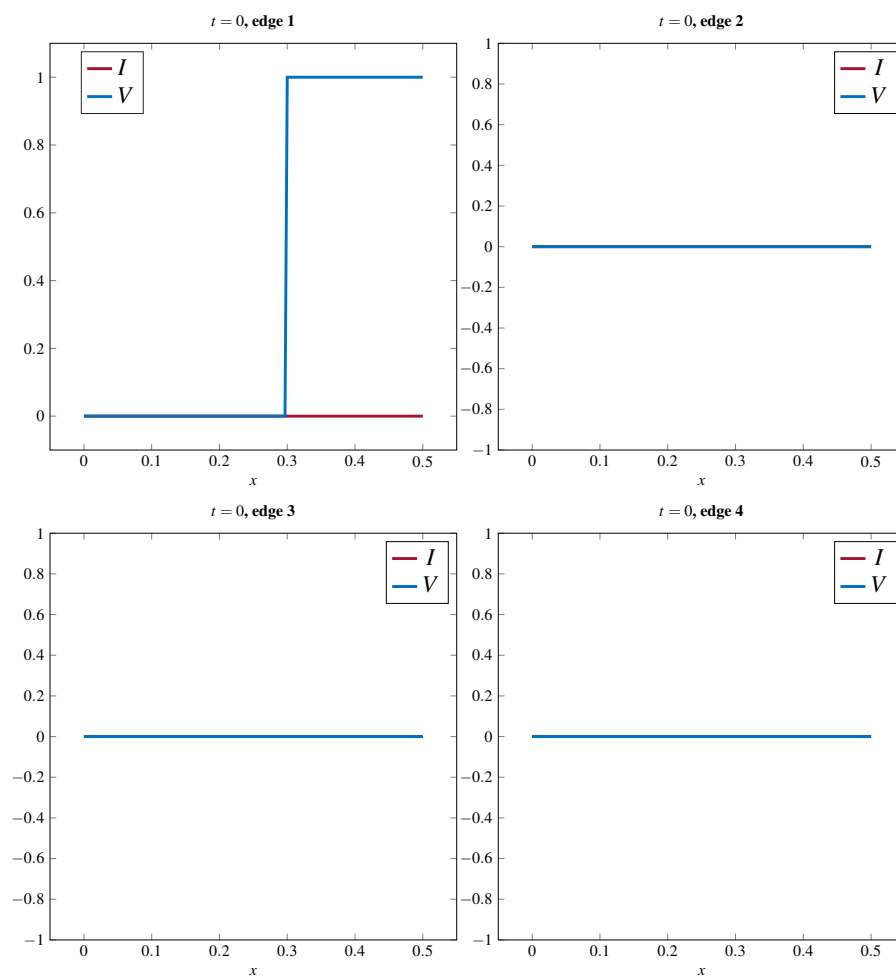


FIGURE 8.8: Initial conditions for the power grid example.

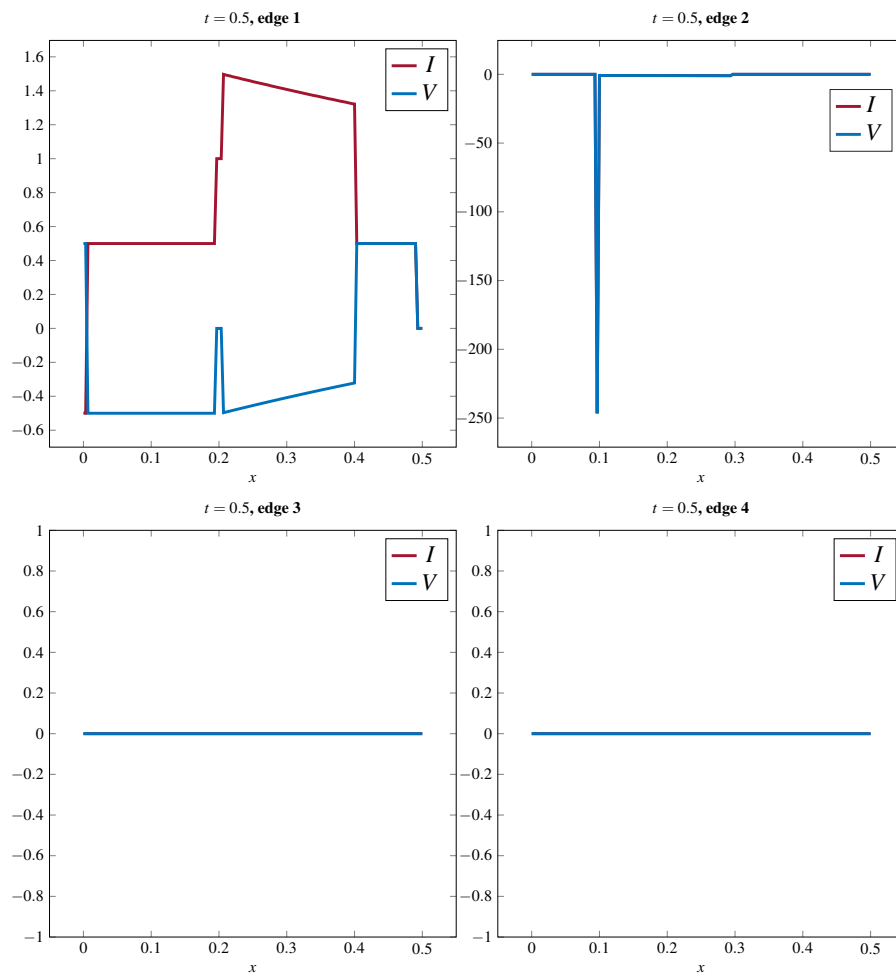


FIGURE 8.9: $t = 0.5$. After the first switch at $t = 0.4$, the peak on \mathcal{E}_2 occurs when \mathcal{E}_1 and \mathcal{E}_2 are disconnected. On \mathcal{E}_3 and \mathcal{E}_4 edges, no changes have happened yet.

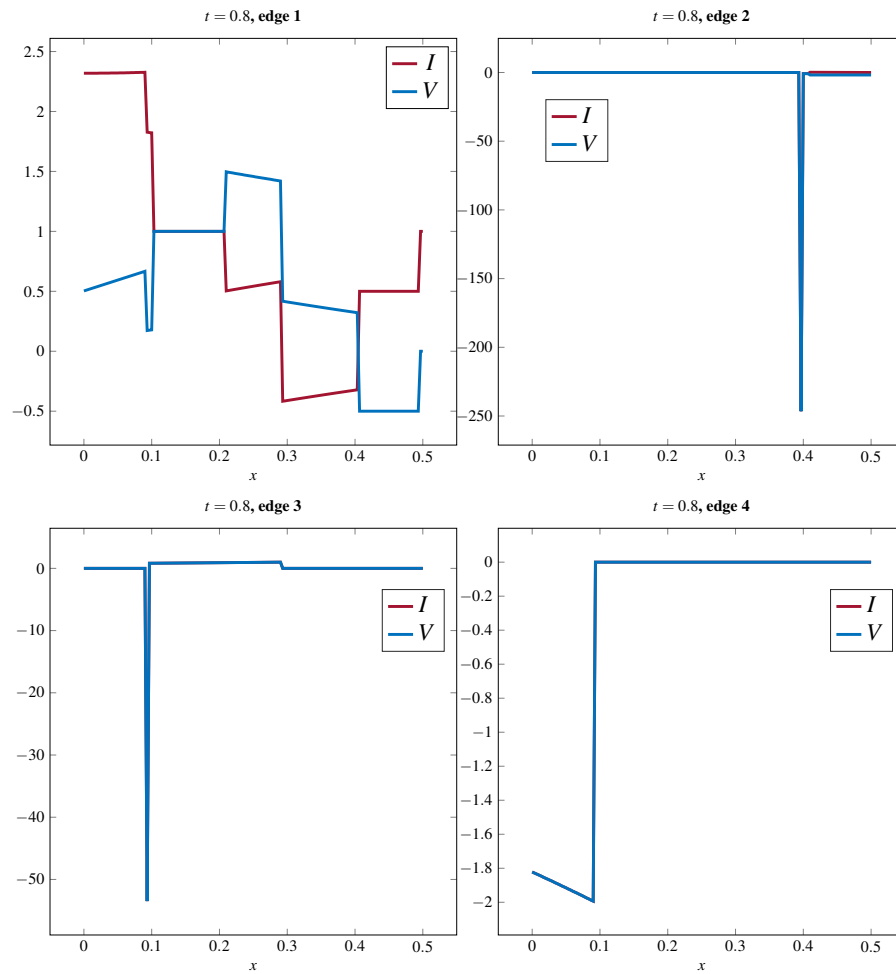


FIGURE 8.10: $t = 0.8$. After the second switch at $t = 0.7$, switching transformer disconnects \mathcal{E}_1 and \mathcal{E}_3 , therefore, peak on \mathcal{E}_3 occurs.

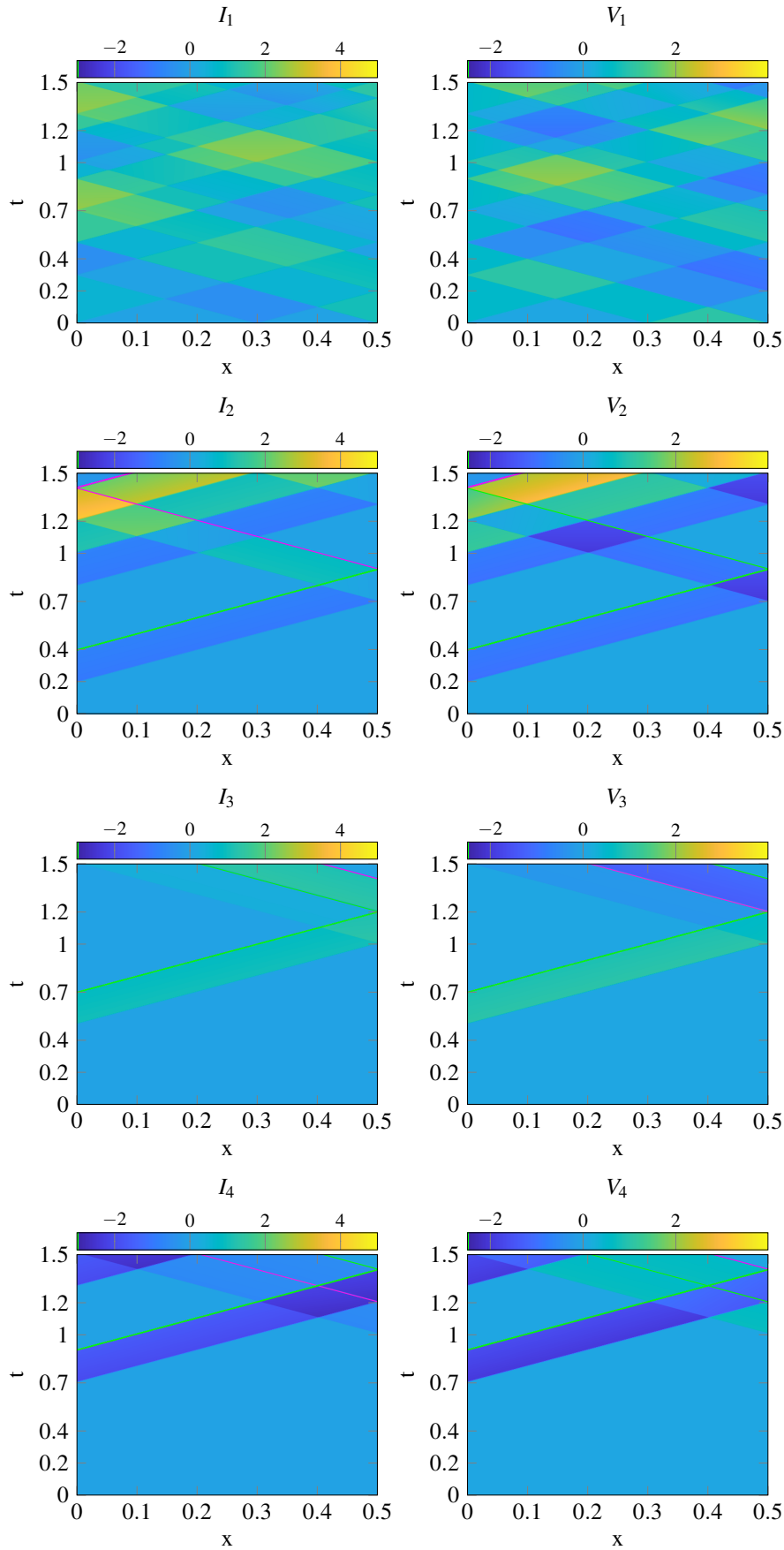
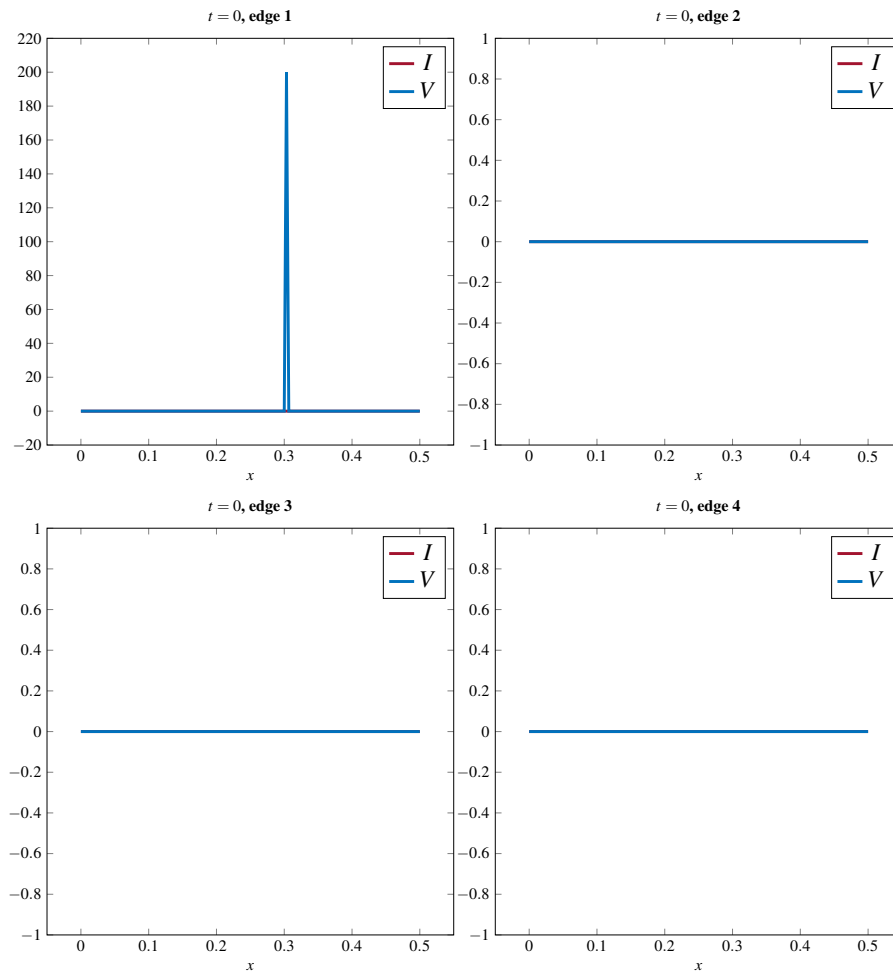


FIGURE 8.11: PDE solutions for the power grid example with initial condition having a discontinuity on \mathfrak{E}_1 , on edges for the domain $(t,x) \in [0,1.5] \times [0,0.5]$. The switching times at $t = 0.4$ and $t = 0.7$. The plots on the left show values for I_k whereas on the right for V_k for the edges \mathfrak{E}_k , $k = 1, 2, 3, 4$, ($I_k = (u_k^2)$, $V_k = (u_k^1)$ in discretized variables).

FIGURE 8.12: The initial conditions for edges $\mathfrak{E}_1, \mathfrak{E}_2, \mathfrak{E}_3, \mathfrak{E}_4$ at time $t = 0$.

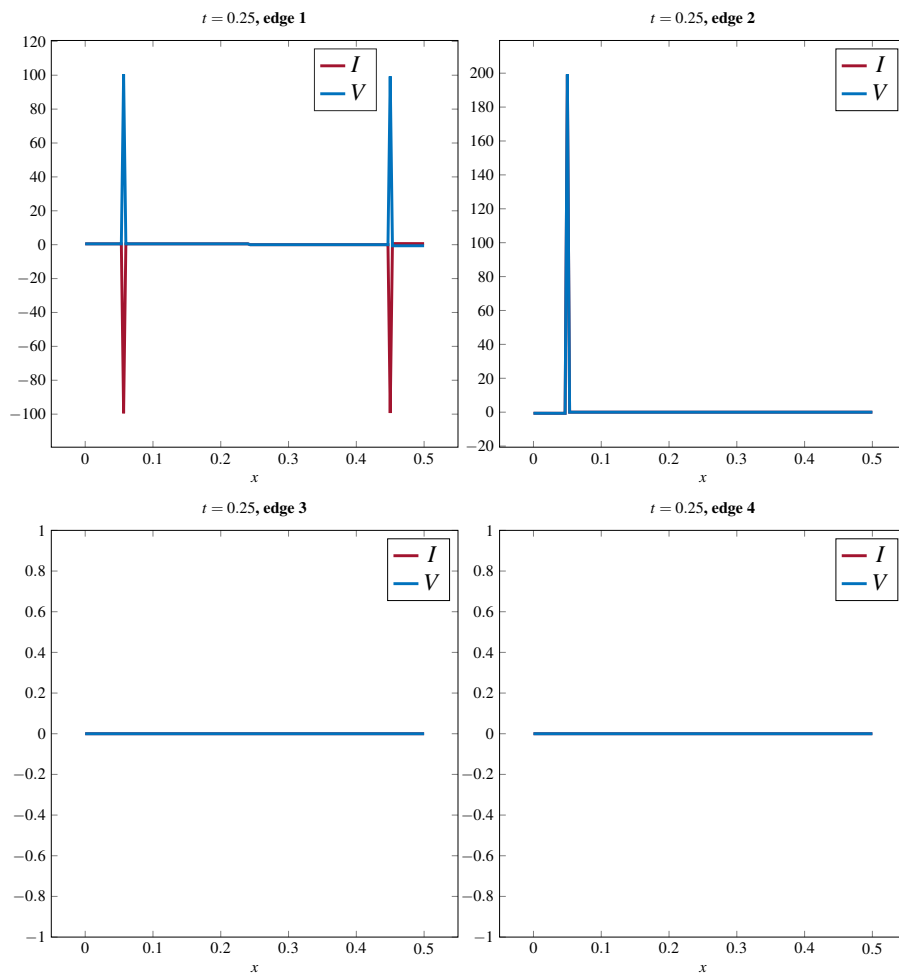


FIGURE 8.13: At time $t = 0.25$. Switching has not happened yet, Dirac impulse on \mathcal{E}_2 is due to the initial condition on \mathcal{E}_1 . On \mathcal{E}_3 and \mathcal{E}_4 there occurs no change as the information from \mathcal{E}_1 or \mathcal{E}_2 has not reached there yet.

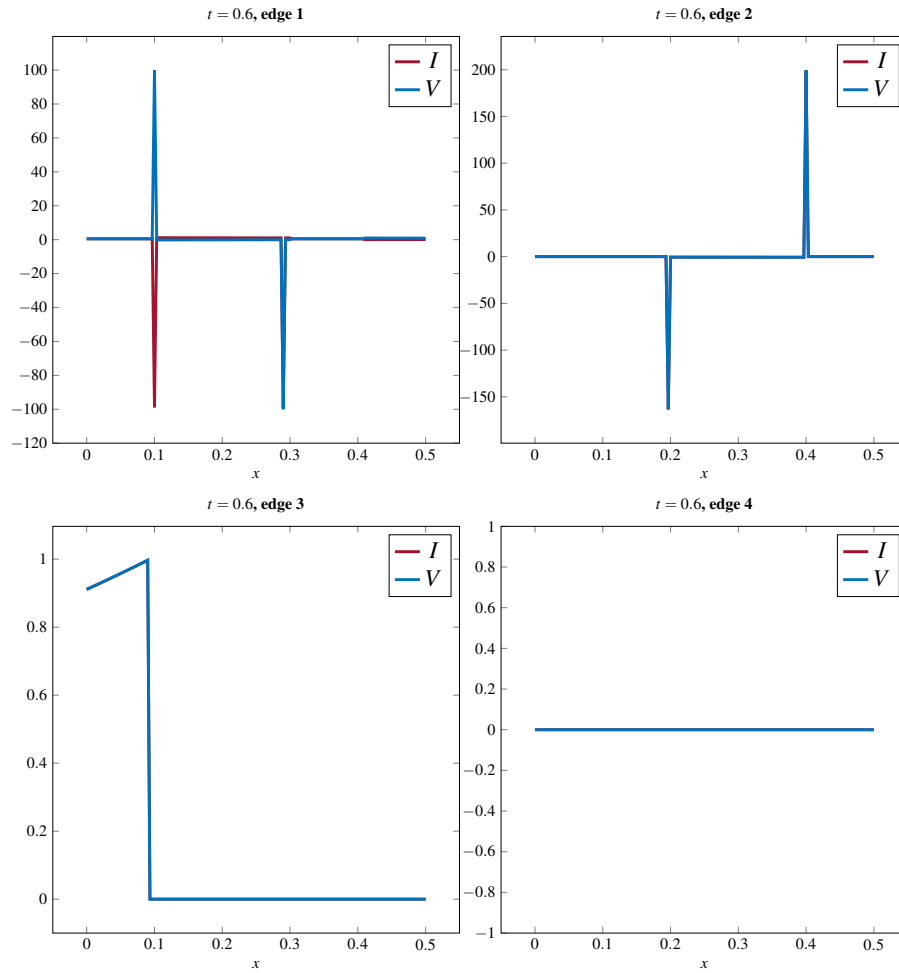


FIGURE 8.14: At time $t = 0.6$. After the first switch at $t = 0.4$, the Dirac impulses on \mathcal{E}_2 brought about by the initial condition and switch are shown. Along \mathcal{E}_3 , the information coming from \mathcal{E}_1 travels in after the switch.

8.3.3 The simplified circulatory system

In this section, the numerical methods are shown to numerically solve the coupled PDE system (8.27) with the switched DAE (8.28) and (8.29) for the nonlinear blood flow example by applying the Roe scheme to the PDE, [107, 125, 127], and explicit Euler method to the swDAE. Even though this example includes a nonlinear system of equations, the same results hold as in the linear case due to the linearization of the scheme. Moreover, the numerical results obtained by MATLAB are demonstrated.

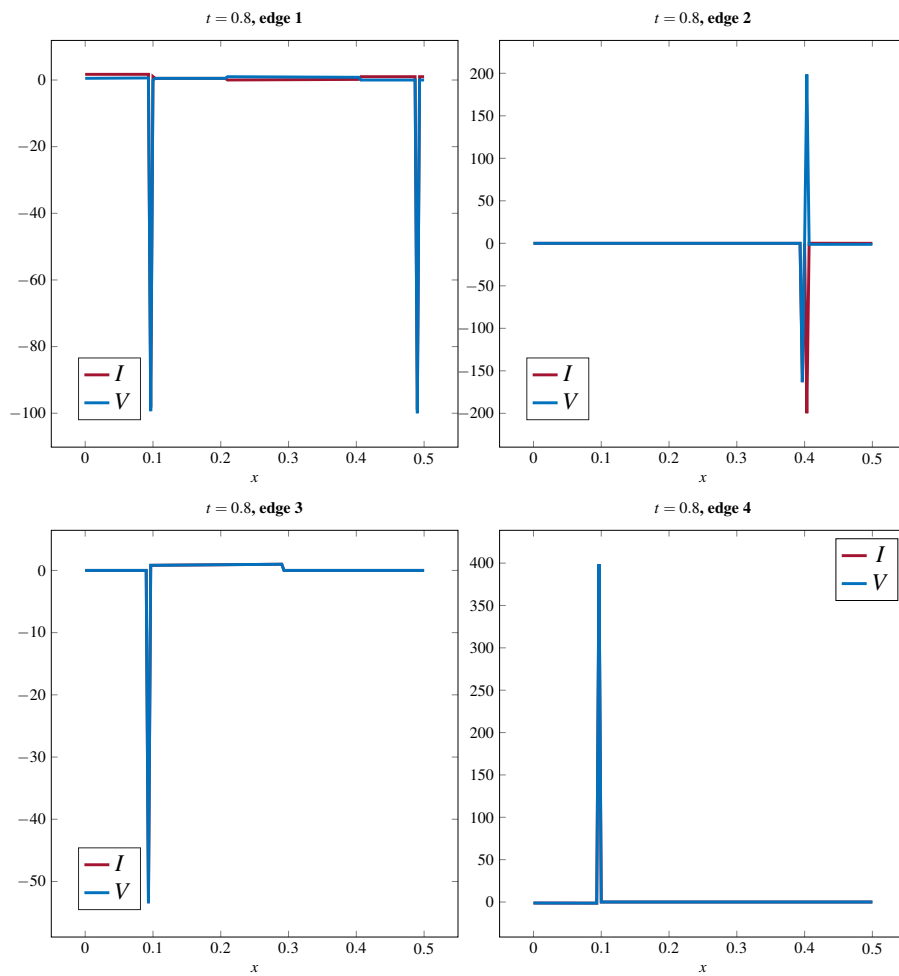


FIGURE 8.15: At time $t = 0.8$. After the second switch at $t = 0.7$, on \mathcal{E}_3 Dirac impulse is caused by the second switch and on \mathcal{E}_4 Dirac impulse is due to \mathcal{E}_2 .

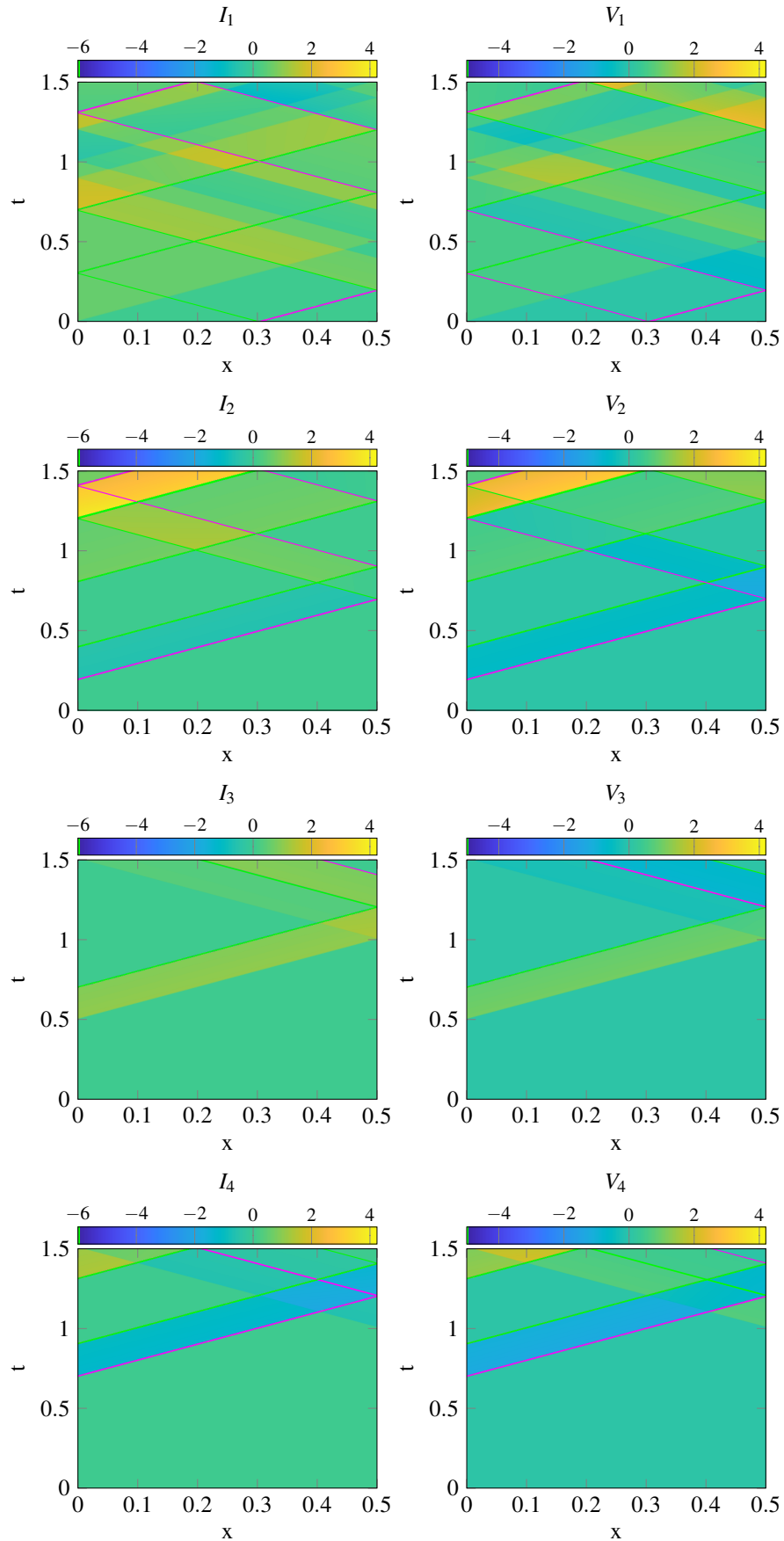


FIGURE 8.16: PDE solutions for the power grid example with initial condition having a Dirac impulse on \mathcal{E}_1 , on edges for the domain $(t,x) \in [0, 1.5] \times [0, 0.5]$. The switching times at $t = 0.4$ and $t = 0.7$. The plots on the left show values for I_k whereas on the right for V_k for the edges $k = 1, 2, 3, 4$, ($I_k = (u_k^2)$, $V_k = (u_k^1)$ in discretized variables).

Roe approximation

First, the matrix (8.13) is linearized and intermediate states that satisfy coupling conditions at coupling points are evaluated. To replace the Jacobian matrix of $\mathbf{f}(\mathbf{u})$ given in (8.13) with a Roe matrix $\mathbf{A}_{i+1/2}$, Roe's linearization method is employed, [107, 125, 128]. The averaged Roe state variables $A_{i+1/2}$ and $V_{i+1/2}$ are given by, [128],

$$A_{i+1/2} = \frac{A_i + A_{i+1}}{2}, \quad \text{and} \quad V_{i+1/2} = \frac{V_i \sqrt{A_i} + V_{i+1} \sqrt{A_{i+1}}}{\sqrt{A_i} + \sqrt{A_{i+1}}},$$

where A_i , V_i and A_{i+1} , V_{i+1} are variables in cells I_i and I_{i+1} , respectively. These averaged variables then yield the Roe matrix $\mathbf{A}_{i+1/2}$

$$\mathbf{A}_{i+1/2} = \begin{pmatrix} 0 & 1 \\ c_{i+1/2}^2 - V_{i+1/2}^2 & 2V_{i+1/2} \end{pmatrix}, \quad (8.37)$$

where $c_{i+1/2} = \sqrt{\frac{K}{2\rho A_0} \sqrt{A_{i+1/2}}}$. One of the properties that the Roe matrix (8.37) has, is being diagonalizable, cf. [107]. Hence,

$$\mathbf{A}_{i+1/2} = \mathbf{R}_{i+1/2} \cdot \Lambda_{i+1/2} \cdot \mathbf{R}_{i+1/2}^{-1},$$

where $\Lambda_{i+1/2}$ is the diagonal matrix whose entries are the eigenvalues of the Roe matrix $\mathbf{A}_{i+1/2}$ and $\mathbf{R}_{i+1/2}$ is the matrix whose columns are the corresponding right eigenvectors to those eigenvalues of the Roe matrix $\mathbf{A}_{i+1/2}$. From the Roe flux $\mathbf{F}_{i+1/2}$, [84, 136], left fluctuations are defined as

$$\begin{aligned} \mathbf{D}_{i+1/2}^-(\mathbf{u}_i, \mathbf{u}_{i+1}) &:= \mathbf{F}_{i+1/2}(\mathbf{u}_i, \mathbf{u}_{i+1}) - \mathbf{f}(\mathbf{u}_i) \\ &= \sum_{\lambda_i < 0} \alpha_i \lambda_i \mathbf{r}^{(i)} \\ &= \mathbf{R}_{i+1/2} \Lambda_{i+1/2}^- \mathbf{R}_{i+1/2}^{-1} (\mathbf{u}_{i+1} - \mathbf{u}_i) \\ &= \mathbf{R}_{i+1/2} \Lambda_{i+1/2}^- \tilde{\alpha}_{i+1/2}^- \end{aligned}$$

where $\tilde{\alpha}_{i+1/2}^-$ is the wave strength, $\Lambda_{i+1/2}^-$ represents the diagonal matrix whose entries are zeros and negative eigenvalues of the Roe matrix $\mathbf{A}_{i+1/2}$ and $\mathbf{R}_{i+1/2}$ is the matrix whose columns are the corresponding right eigenvectors. Similarly, right fluctuations are defined as

$$\begin{aligned} \mathbf{D}_{i+1/2}^+(\mathbf{u}_i, \mathbf{u}_{i+1}) &:= \mathbf{f}(\mathbf{u}_{i+1}) - \mathbf{F}_{i+1/2}(\mathbf{u}_i, \mathbf{u}_{i+1}) \\ &= \sum_{\lambda_i > 0} \alpha_i \lambda_i \mathbf{r}^{(i)} \\ &= \mathbf{R}_{i+1/2} \Lambda_{i+1/2}^+ \mathbf{R}_{i+1/2}^{-1} (\mathbf{u}_{i+1} - \mathbf{u}_i) \\ &= \mathbf{R}_{i+1/2} \Lambda_{i+1/2}^+ \tilde{\alpha}_{i+1/2}^+ \end{aligned}$$

with $\Lambda_{i+1/2}^+$ diagonal matrix whose entries are zeros and positive eigenvalues of $\mathbf{A}_{i+1/2}$ and $\mathbf{R}_{i+1/2}$ is the matrix whose columns are the corresponding right eigenvectors. Assuming that over the spatial domain x , the direction where x increases is considered positive, the term $\mathbf{D}_{i+1/2}^-$ contains all contributions of left-going waves at the interface $x_{i+1/2}$, whereas $\mathbf{D}_{i+1/2}^+$ includes all right-going waves at $x_{i+1/2}$.

To find the intermediate states $\mathbf{u}_{pv}^I, \mathbf{u}_{aa}^I$ at the coupling points, see Figure 8.7, the following numerical conditions are imposed

$$\mathbf{D}_{N+1/2}^-(\mathbf{u}_N, \mathbf{u}_{N+1}) = \mathbf{F}_{1/2}(\mathbf{u}_N, \mathbf{u}_{N+1}) - \mathbf{f}(\mathbf{u}_N) \stackrel{!}{=} 0, \quad (8.38a)$$

$$\mathbf{D}_{1/2}^-(\mathbf{u}_0, \mathbf{u}_1) = \mathbf{F}_{1/2}(\mathbf{u}_0, \mathbf{u}_1) - \mathbf{f}(\mathbf{u}_0) \stackrel{!}{=} 0, \quad (8.38b)$$

which means that under the assumption that at the coupling points at $x = b$ and $x = a$ for $x \in [a, b]$, the backward flux must be equal to zero, as the backward-going waves cannot be tracked at $x = b$ and $x = a$. The state \mathbf{u}_0 in (8.38b) and \mathbf{u}_{N+1} in (8.38a) can be considered imaginary states. The intermediate states \mathbf{u}_{pv}^I and \mathbf{u}_{aa}^I can be connected to the right state \mathbf{u}_{N+1} from (8.38a) and \mathbf{u}_1 from (8.38b) by the waves that are inward direction to those coupling points. The conditions $\mathbf{D}_{N+1/2}^- = 0$ and $\mathbf{D}_{1/2}^- = 0$ mean $\alpha_1 = 0$, where $\vec{\alpha} = (\alpha_1, \alpha_2)^\top$. So, the wave strengths for the backward going waves are zero. Thus, regarding the conditions (8.38), backward going waves from coupling points contribute the numerical conditions.

Numerical results

The spatial domains I^{pv}, I^{aa} to be discretized are assumed to be $[0, 2]$. Equidistant mesh points $x_k = (k - 1/2)\Delta x$, $k = 1, \dots, N$, with $\Delta x = (b - a)/N$, where $N = 50$. Two ghost cells for each domain, $I_0^{pv}, I_{N+1}^{pv}, I_0^{aa}$ and I_{N+1}^{aa} , are placed at left and right ends of the computational domains I^{pv}, I^{aa} . As the scheme used is explicit, the CFL condition has to be satisfied. Thus, $\mathcal{C} = 0.9$. Furthermore, the time step Δt is calculated according to \mathcal{C} , and then the time variable is updated; i.e., $t^{n+1} = t^n + \Delta t$. The approximated solution of the PDE at time t^n and position x_j is denoted by $\mathbf{u}_j^n = \mathbf{u}(x_j, t^n)$, where

$$\mathbf{u}_j^n = \left((\mathbf{u}_{pv}^\top)_j^n, (\mathbf{u}_{aa}^\top)_j^n \right)^\top \text{ with } \begin{cases} (\mathbf{u}_{pv})_j^n = \left((A_{pv})_j^n, (Q_{pv})_j^n, (V_{pv})_j^n, (P_{pv})_j^n \right)^\top, \\ (\mathbf{u}_{aa})_j^n = \left((A_{aa})_j^n, (Q_{aa})_j^n, (V_{aa})_j^n, (P_{aa})_j^n \right)^\top, \end{cases}$$

where A, Q, V and P stand for cross-sectional area, blood flow rate, velocity and pressure. The velocity V is expressed as $V = Q/A$. Similarly, the approximated solution of the swDAE at time t^n is denoted by $\mathbf{w}^n = \mathbf{w}(t^n)$, where $\mathbf{w}^n = (v_{la}^n, v_{lv}^n, q_{mv}^n, q_{av}^n, p_{la}^n, p_{lv}^n)$, where v, q and p represent volume, flow rate and pressure.

Depending on physiological parameters, [6, 28, 64], initial conditions for PDE are assigned as follows

$$\begin{aligned} (Q_{pv})_j^0 &= 150 \text{ ml/s}, & (P_{pv})_j^0 &= 666.65 \text{ Pa}, \\ (Q_{aa})_j^0 &= 50 \text{ ml/s}, & (P_{aa})_j^0 &= 1.3333 \times 10^4 \text{ Pa}, \end{aligned}$$

from which $(A_{pv})_j^0$ and $(A_{aa})_j^0$ are calculated

$$(A_{pv})_j^0 = A_0^v \left(\frac{(P_{pv})_j^0 - P_0^v - P_{\text{ext}}^v}{K_v} + 1 \right)^2, \quad (A_{aa})_j^0 = A_0^a \left(\frac{(P_{aa})_j^0 - P_0^a - P_{\text{ext}}^a}{K_a} + 1 \right)^2,$$

where $A_0^v = \pi(r_0^v)^2 \text{ cm}^2$ with reference vessel radius $r_0^v = 0.7 \text{ cm}$ stands for reference cross-sectional area for pulmonary venous, $A_0^a = \pi(r_0^a)^2 \text{ cm}^2$ with $r_0^a = 1.4 \text{ cm}$ reference cross-sectional area for ascending aorta, $P_0^v = 666.65 \text{ Pa}$ ($\approx 5 \text{ mmHg}$) reference pressure for pulmonary venous, $P_0^a = 1.3333 \times 10^4 \text{ Pa}$ ($\approx 100 \text{ mmHg}$) reference pressure for ascending aorta,

$P_{\text{ext}}^v = 0$, $P_{\text{ext}}^a = 0$ mmHg external pressures for pulmonary venous and ascending aorta, mechanical/geometrical constants $K_v = 2(c_0^v)^2 \rho$, $K_a = 2(c_0^a)^2 \rho$, $\rho = 1.05 \times 10^3$ kg/m³ density of the blood and reference wave speeds $c_0^v = 1.053$, $c_0^a = 5.11$ m/s, [94]. Similarly, regarding physical measurements of the heart, [115], initial conditions for swDAE are

$$\begin{aligned} v_{\text{la}} &= 50 \text{ ml}, & v_{\text{lv}} &= 80 \text{ ml}, \\ q_{\text{mv}} &= 50 \text{ ml/s}, & q_{\text{av}} &= 100 \text{ ml/s}, \\ p_{\text{la}} &= 10 \text{ mmHg}, & p_{\text{lv}} &= 100 \text{ mmHg}. \end{aligned}$$

Taking into account physiological values of the flow rate in vivo, which have been measured using Doppler² and two dimensional echocardiography³, [37, 54, 108], at the left end of the pulmonary venous, I_0^{pv} , the prescribed flow rate is taken as a sinusoidal wave, see Figure 8.17,

$$(Q_{\text{pv}})_0 = \max(0, \sin(2\pi(t - 0.15)))200 + \sin((t - 0.1)4\pi)130.$$

The boundary condition at the right end of the pulmonary venous (P_{pv}^n)_{N+1} is assigned by the state variable p_{la}^n of the swDAE as follows

$$(A_{\text{pv}}^I)^n = A_0^v \left(\frac{p_{\text{la}}^n - P_0^v - P_{\text{ext}}^v}{K_v} + 1 \right)^2, \quad (8.39)$$

where $(A_{\text{pv}}^I)^n$ is the cross-sectional area of the intermediate state \mathbf{u}_{pv}^I at $x_{N+1/2}$ between cells I_N^{pv} and I_{N+1}^{pv} , then $(A_{\text{pv}}^n)_{N+1}$ is updated as

$$(A_{\text{pv}}^n)_{N+1} = 2(A_{\text{pv}}^I)^n - (A_{\text{pv}}^n)_N,$$

and finally pressure law yields

$$(P_{\text{pv}}^n)_{N+1} = P_e^v + P_0^v + K_v \left(\frac{\sqrt{(A_{\text{pv}}^n)_{N+1}}}{\sqrt{A_0^v}} - 1 \right).$$

Then ghost cells for $(Q_{\text{pv}}^n)_{N+1}$ and $(V_{\text{pv}}^n)_{N+1}$ are filled

$$\begin{aligned} (Q_{\text{pv}}^n)_{N+1} &= (Q_{\text{pv}}^n)_N, \\ (V_{\text{pv}}^n)_{N+1} &= (Q_{\text{pv}}^n)_N / (A_{\text{pv}}^n)_N. \end{aligned}$$

To determine the output of the PDE over pulmonary venous $(Q_{\text{pv}}^I)^n$ at $x_{N+1/2}$, first define the intermediate value for velocity $(V_{\text{pv}}^I)^n$ as

$$(V_{\text{pv}}^I)^n = \frac{\sqrt{(A_{\text{pv}}^n)_N} (Q_{\text{pv}}^n)_{N+1} + \sqrt{(A_{\text{pv}}^n)_{N+1}} (Q_{\text{pv}}^n)_N}{(A_{\text{pv}}^n)_N \sqrt{(A_{\text{pv}}^n)_{N+1}} + (A_{\text{pv}}^n)_{N+1} \sqrt{(A_{\text{pv}}^n)_N}}, \quad (8.40)$$

²Doppler echocardiography is a technique using Doppler ultrasonography to analyse functions of the heart, [6]. Doppler ultrasonography is used to determine blood flow in vessels by measuring high-frequency sound waves that echo moving tissues or blood, [119].

³Echocardiography is a procedure employing sound waves to produce images of the heart[9].

which constitutes together with $(A_{pv}^I)^n$ given as in (8.39), the following Roe matrix

$$\mathbf{A}_{pv}^I = \begin{bmatrix} 0 & 1 \\ (c_v^I)^2 - ((V_{pv}^I)^n)^2 & 2(V_{pv}^I)^n \end{bmatrix}, \quad \text{where } c_v^I = \sqrt{\frac{K_v \sqrt{(A_{pv}^I)^n}}{2\rho \sqrt{A_0^v}}}, \quad (8.41)$$

so that wave strength $\vec{\alpha}_{pv}$ is defined as

$$\vec{\alpha}_{pv} := \begin{pmatrix} (\alpha_{pv})_1 \\ (\alpha_{pv})_2 \end{pmatrix} = \mathbf{R}_{pv}^{-1} ((\mathbf{u}_{pv})_{N+1}^n - (\mathbf{u}_{pv})_N^n),$$

where \mathbf{R}_{pv} is the matrix whose columns correspond to the eigenvalues of the matrix given in (8.41), denote by Λ_{pv} the diagonal matrix whose entries are those eigenvalues. Let $\Lambda_{pv}^- := \min(\mathbf{0}_{2 \times 2}, \Lambda_{pv})$. Then the left fluctuation matrix \mathbf{D}_{pv}^- at $x_{N+1/2}$ is defined as

$$\mathbf{D}_{pv}^- := \begin{pmatrix} (D_{pv})_1 \\ (D_{pv})_2 \end{pmatrix} = \mathbf{R}_{pv} \Lambda_{pv}^- \vec{\alpha}_{pv}.$$

Therefore, the numerical output $(Q_{pv}^I)^n$ at $x_{N+1/2}$ is formulated as

$$(Q_{pv}^I)^n = (Q_{pv})_N^n + (D_{pv})_1.$$

Over the ascending aorta, the right boundary is assigned by the solution of the PDE in the last physical cell

$$(P_{aa})_{N+1}^n = (P_{aa})_N^n,$$

while the left boundary condition $(Q_{aa})_0^n$ is determined by the swDAE according to the numerical coupling condition explained in the previous section. To this end, the MATLAB built-in function `fsolve` is employed which tries to find the solution $\mathbf{y} = (y_1, y_2)^\top$ with the given tolerance to the following problem: Let $(\mathbf{u}_{aa}^I)^n$ be the intermediate state at $x_{1/2}$ over ascending aorta and let $(A_{aa}^I)^n$, $(V_{aa}^I)^n$ be the components of $(\mathbf{u}_{aa}^I)^n$ that are

$$(A_{aa}^I)^n = \frac{y_1 + (A_{aa})_1^n}{2}, \quad \text{and} \quad (V_{aa}^I)^n = \frac{\sqrt{y_1} (Q_{aa})_1^n + \sqrt{(A_{aa})_1^n} y_2}{\sqrt{y_1} (A_{aa})_1^n + \sqrt{(A_{aa})_1^n} y_1},$$

which contribute to the following Roe matrix

$$\mathbf{A}_{aa}^I = \begin{bmatrix} 0 & 1 \\ (c_a^I)^2 - (V_{aa}^I)^2 & 2V_{aa}^I \end{bmatrix}, \quad \text{where } c_a^I = \sqrt{\frac{K_a \sqrt{(A_{aa}^I)^n}}{2\rho \sqrt{A_0^a}}}, \quad (8.42)$$

from which the wave strength $\vec{\alpha}_{aa}$ is determined

$$\vec{\alpha}_{aa} := \begin{pmatrix} (\alpha_{aa})_1 \\ (\alpha_{aa})_2 \end{pmatrix} = \mathbf{R}_{aa}^{-1} ((\mathbf{u}_{aa})_{N+1}^n - \mathbf{y}),$$

where \mathbf{R}_{aa} is the matrix whose columns correspond to the eigenvalues of the matrix given in (8.42), denote by Λ_{aa} the diagonal matrix whose entries are those eigenvalues. Let $\Lambda_{aa}^- := \min(\mathbf{0}_{2 \times 2}, \Lambda_{aa})$. Then left fluctuation matrix at $x_{1/2}$ is

$$\mathbf{D}_{aa}^- := \begin{pmatrix} (D_{aa})_1 \\ (D_{aa})_2 \end{pmatrix} = \mathbf{R}_{aa} \Lambda_{aa}^- \vec{\alpha}_{aa}.$$

As the numerical coupling condition imposes, the following has to be satisfied

$$\begin{aligned}(D_{aa})_1 + y_2 - q_{av}^{n+1} &\stackrel{!}{=} 0, \\ (\alpha_{aa})_1 &\stackrel{!}{=} 0.\end{aligned}$$

As `fsolve` finds the solution \mathbf{y} , ghost cells can be updated as follows

$$\begin{aligned}(A_{aa})_0^n &= y_1, \quad (Q_{aa})_0^n = y_2, \quad (V_{aa})_0^n = \frac{(Q_{aa})_0^n}{(A_{aa})_0^n}, \\ (P_{aa})_0^n &= P_{\text{ext}} + P_0^a + \beta_a \left(\frac{\sqrt{(A_{aa})_0^n}}{\sqrt{A_0^a}} - 1 \right), \\ (\mathbf{u}_{aa})_{N+1}^n &= (\mathbf{u}_{aa})_N^n.\end{aligned}$$

The output $(P_{aa}^I)^n$ over ascending aorta is then evaluated as

$$\begin{aligned}(A_{aa}^I)^n &= \frac{(A_{aa})_0^n + (A_{aa})_1^n}{2}, \\ (P_{aa}^I)^n &= P_{\text{ext}} + P_0^v + \beta_a \left(\frac{\sqrt{(A_{aa}^I)^n}}{\sqrt{A_0^a}} - 1 \right).\end{aligned}$$

Next, the time variable is updated according to the CFL number \mathcal{C} . Hence, $|\lambda|_{\max}$ of the PDE system has to be found at every iteration.

To update the PDE solution, the Roe scheme is used

$$\begin{aligned}(\mathbf{u}_\eta)_j^{n+1} &= (\mathbf{u}_\eta)_j^n - \frac{\Delta t}{\Delta x} \left((\mathbf{A}_{j-1/2}^\eta)^+ \left((\mathbf{u}_\eta)_j^n - (\mathbf{u}_\eta)_{j-1}^n \right) \right. \\ &\quad \left. + (\mathbf{A}_{j+1/2}^\eta)^- \left((\mathbf{u}_\eta)_{j+1}^n - (\mathbf{u}_\eta)_j^n \right) \right),\end{aligned}\tag{8.43}$$

with $\eta = \{\text{pv}, \text{aa}\}$ for $j = 1, \dots, N$, where $\mathbf{A}_{j+1/2}^\eta$ is assumed to be the Roe matrix of the PDE given by

$$\mathbf{A}_{j+1/2}^\eta = \begin{bmatrix} 0 & 1 \\ (c_\xi)_j^2 - \left((V_\eta^I)_j^n \right)^2 & 2(V_\eta^I)_j^n \end{bmatrix},\tag{8.44}$$

where

$$\begin{aligned}(A_\eta^I)_j^n &= \frac{(A_\eta)_j^n + (A_\eta)_{j+1}^n}{2}, \quad (c_\xi)_j = \sqrt{\frac{K_\xi \sqrt{(A_\eta)_j^n}}{2\rho \sqrt{A_0^\xi}}}, \\ (V_\eta^I)_j^n &= \frac{\sqrt{(A_\eta)_j^n} (Q_\eta)_{j+1}^n + \sqrt{(A_\eta)_{j+1}^n} (Q_\eta)_j^n}{(A_\eta)_j^n \sqrt{(A_\eta)_{j+1}^n} + (A_\eta)_{j+1}^n \sqrt{(A_\eta)_j^n}},\end{aligned}\quad j = 1, \dots, N-1,$$

for $\xi = \{v, a\}$. As a result, for each t^n , $|\lambda|_{\max}$ can be found as the eigenvalues of PDE at each interface can be calculated by using the matrix $\mathbf{A}_{j+1/2}^\eta$ where

$$\mathbf{A}_{j+1/2}^\eta = (\mathbf{R}_\eta)_{j+1/2} (\Lambda_\eta)_{j+1/2} (\mathbf{R}_\eta^{-1})_{j+1/2}.$$

Moreover, increments of the solution

$$(\mathbf{A}_{j+1/2}^\eta)^\pm \left((\mathbf{u}_\eta)_{j+1}^n - (\mathbf{u}_\eta)_j^n \right) = (\mathbf{R}_\eta)_{j+1/2} (\Lambda_\eta)_{j+1/2}^\pm (\mathbf{R}_\eta^{-1})_{j+1/2} \left((\mathbf{u}_\eta)_{j+1}^n - (\mathbf{u}_\eta)_j^n \right).$$

can be computed to update the numerical solution. After finding $|\lambda|_{\max}$, the solution is updated according to the Roe scheme (8.43) as Δt is determined.

With the necessary input and sufficient information which will pass to the swDAE, now the numerical method to solve the swDAE is explained. Given the time period $T_0 = 1$ of one cardiac cycle and time instances t^{n+1} , before solving swDAE, time-varying elastances of the left atrium E_{la} and left ventricle E_{lv} are calculated, at each iteration $t_*^{n+1} := \text{mod}(t^{n+1}, T_0)$, as

$$\begin{aligned} E_{la}^{n+1} &= E_{laa}e_{la}^{n+1} + E_{lab}, \\ E_{lv}^{n+1} &= E_{lva}e_{lv}^{n+1} + E_{lvb}, \end{aligned}$$

where normalized time-varying elastances e_{la}, e_{lv} are evaluated as in Formulae (8.23); and values of $E_{laa}, E_{lva}, E_{lab}, E_{lvb}$ are given as in Table 8.2. For the numerical results of E_{la} and E_{lv} , see Figure 8.18. After the values of elastances at t_*^{n+1} are calculated, swDAE is solved by passing the values $E_{la}^{n+1}, E_{lv}^{n+1}, (Q_{pv}^I)^n, (P_{aa}^I)^n$ and Δt

$$\begin{aligned} v_{la}^{n+1} &= v_{la}^n + \Delta t \left((Q_{pv}^I)^n - q_{mv}^n \right), \\ v_{lv}^{n+1} &= v_{lv}^n + \Delta t (q_{mv}^n - q_{av}^n), \\ p_{la}^{n+1} &= E_{la}^{n+1} v_{la}^{n+1}, \\ p_{lv}^{n+1} &= E_{lv}^{n+1} v_{lv}^{n+1}, \end{aligned}$$

if $p_{la}^{n+1} > p_{lv}^{n+1}$ holds

$$q_{mv}^{n+1} = q_{mv}^n + \Delta t \frac{E_{la}^{n+1} v_{la}^{n+1} + R_{la} p_{la}^{n+1} \left((Q_{pv}^I)^n - q_{mv}^n \right)}{L_{mv}} - \frac{E_{lv}^{n+1} v_{lv}^{n+1} + R_{lv} p_{lv}^{n+1} (q_{mv}^n - q_{av}^n) + R_{la} q_{mv}^n}{L_{mv}},$$

else $q_{mv}^{n+1} = 0$,

if $p_{lv}^{n+1} > (P_{aa}^I)^n$ holds

$$q_{av}^{n+1} = q_{av}^v + \Delta t \frac{E_{lv}^{n+1} v_{lv}^{n+1} + R_{lv} p_{lv}^{n+1} (q_{mv}^{n+1} - q_{av}^n)}{L_{av}} - \frac{R_{lv} q_{av}^n + (P_{aa}^I)^n + R_{aa} C_{aa} \left((P_{aa}^I)^n - (P_{aa}^I)^{n-1} \right)}{L_{av}}$$

else $q_{av}^{n+1} = 0$.

The scheme runs as explained above until t_{\max} . The results are shown in Figures 8.19, 8.20, 8.21, 8.22, 8.23, 8.24. In Figure 8.19, the numerical results for the volumes of the left atrium and ventricle are demonstrated while in Figure 8.20 for pressures of those are displayed. Once the value of the aortic pressure is exceeded by the value of the left ventricular pressure, blood starts being ejecting into the aorta by the left ventricle. Blood ejection continues until the pressure value of the aorta is higher than that of the left ventricle, see Figure 8.21. The scheme is able to produce the well-known feature of the aortic valve, which is blood flowing backwards while valve closure resulting from interactions between the pressure gradient and mechanical properties of tissues, see 8.21, [67]. In Figure 8.22, it is also reproduced that pressure increases at the closure of the aortic valve. In Figure 8.24, the negative flow in the pulmonary venous is caused by the atrial contraction. In the results for blood flow rate through aortic valve, an unusual and unphysical behavior is observed, which is a

kink immediately after closure of the aortic valve, see Figure 8.25. Once the aortic valve closes for the first time in one cardiac cycle, it instantaneously keeps opening and closing again. To address and analyse this problem, in the next section, a much simpler system is studied, which still has the same framework.

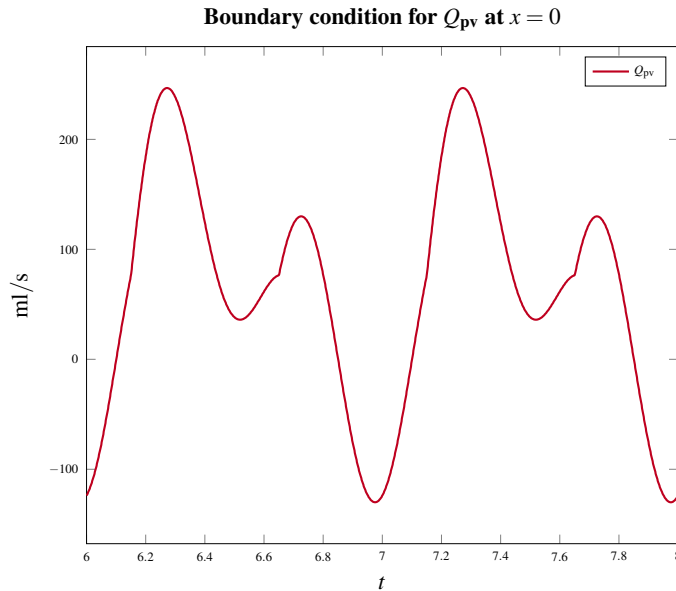


FIGURE 8.17: Prescribed left boundary data for the pulmonary venous, flow rate $(Q_{pv})_0^n$ at time t^n with initial time $t^0 = 0$ until $t_{\max} = 8$.

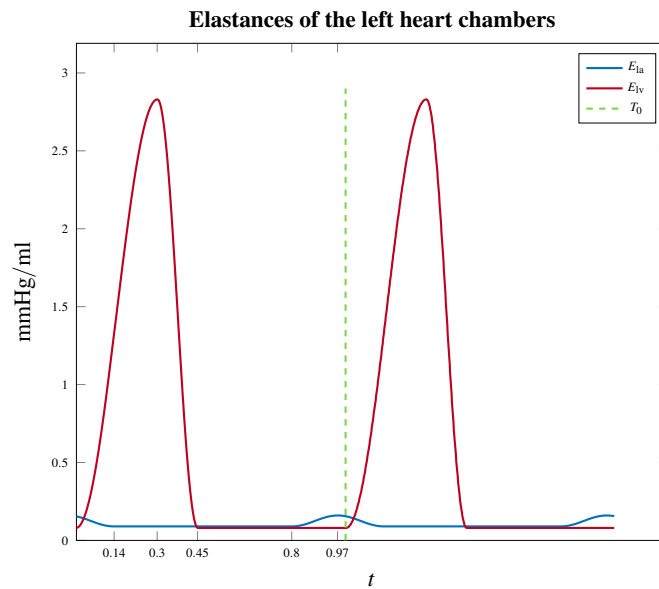


FIGURE 8.18: Elastances for the left atrium, E_{la} , and left ventricle, E_{lv} , over two cardiac cycles with cycle period $T_0 = 1$ second.

8.3.4 Coupling a simpler system

In this section, the reader is referred to Appendix to get an intuitive grasp of the reasoning of this section. In the numerical results of blood flow example in Section 8.3.3, certain behaviors, which resemble Zeno behavior as briefly explained in Appendix, have been observed.

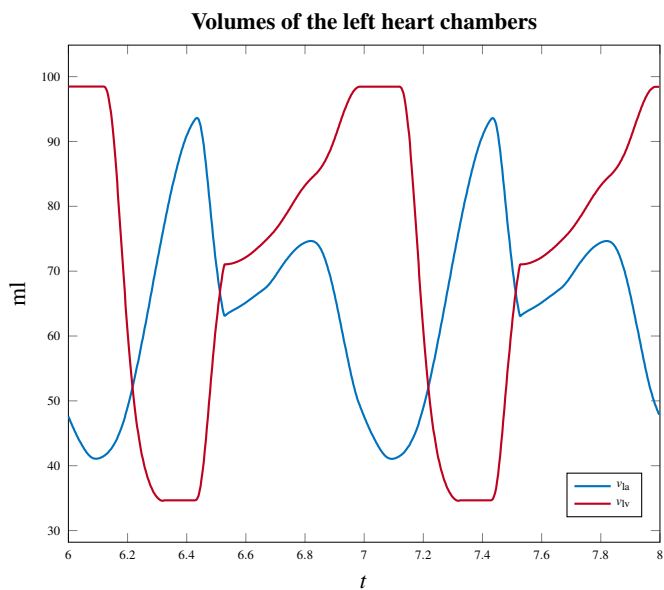


FIGURE 8.19: Volumes of the left atrium and left ventricle.

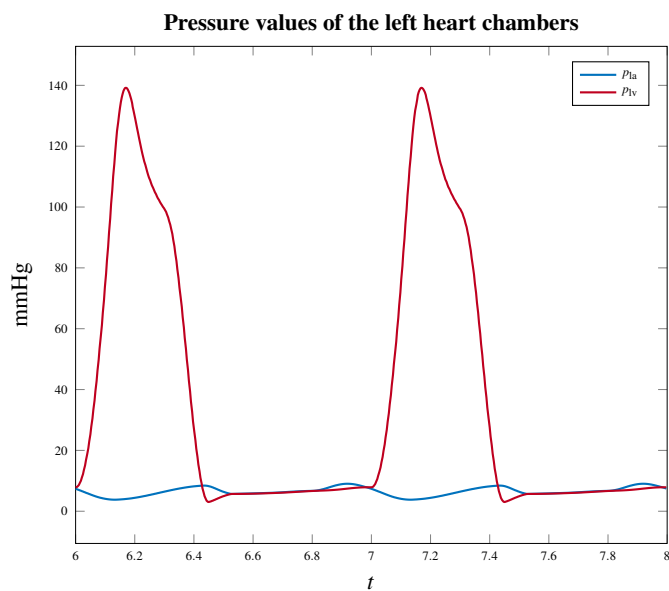


FIGURE 8.20: Pressure values of the left atrium and left ventricle.

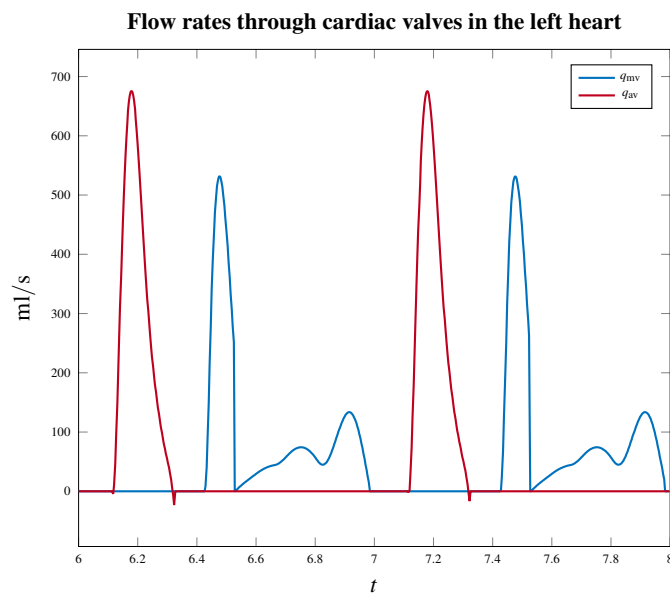


FIGURE 8.21: Blood flow rate through mitral valve and aortic valve. While one cardiac valve in the left heart is open, the other valve remains closed.

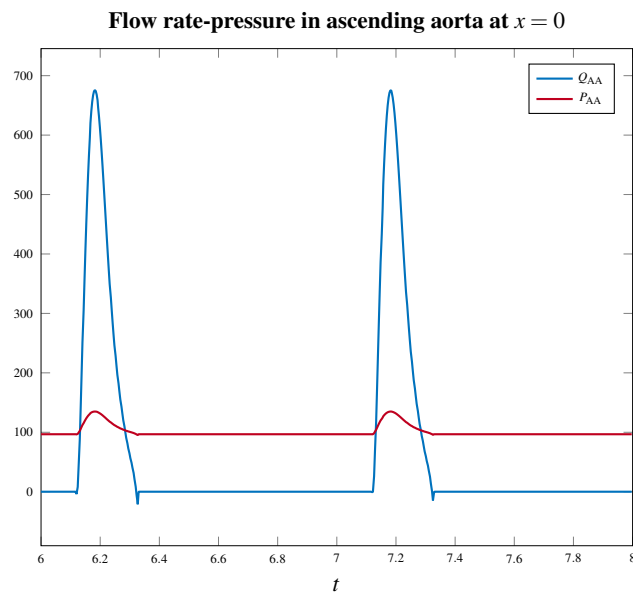


FIGURE 8.22: Pressure (mmHg) and flow rate (ml/s) values of the ascending aorta at its left end.

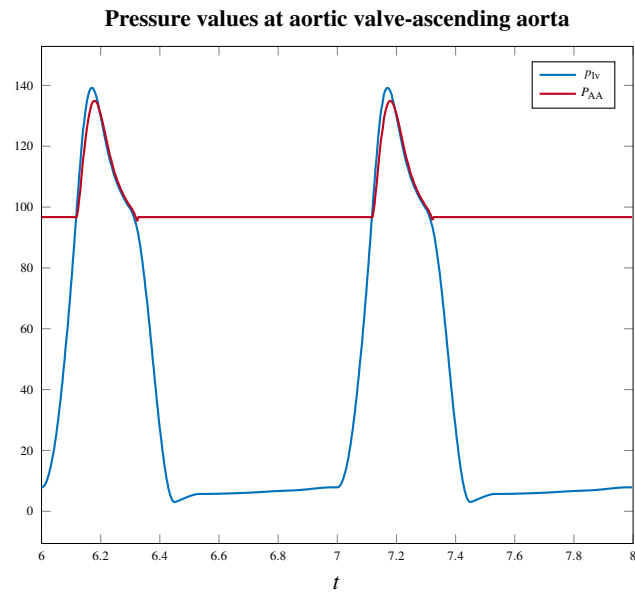


FIGURE 8.23: Pressure (mmHg) values of the left ventricle and ascending aorta at the coupling point.

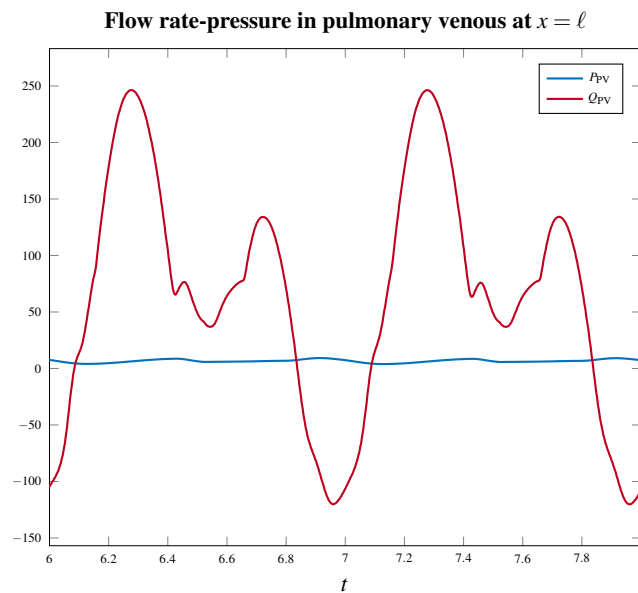


FIGURE 8.24: Pressure (mmHg) and flow rate (ml/s) values of the pulmonary venous at the coupling point.

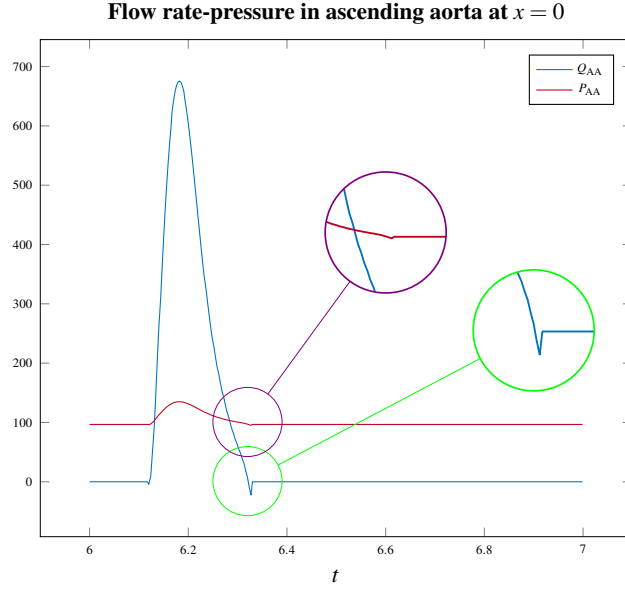


FIGURE 8.25: Unphysical behavior during cardiac cycle. After the aortic valve shuts, it keeps opening and closing instantaneously.

To investigate whether there is indeed such way of behaving in results of blood flow example, in this section, much simpler systems are coupled, which still have the same structure, inputs and outputs as blood flow model given in Section 8.1.3. Furthermore, there is one valve between these systems that opens and shuts according to the pressure difference on both sides.

Consider the following switched DAE

$$\mathbf{E}_\sigma \dot{\mathbf{w}}(t) = \mathbf{H}_\sigma \mathbf{w}(t) + \mathbf{B}_\sigma z(t), \quad t \geq t_0, \quad (8.45)$$

with two modes \mathbf{m}_1 and \mathbf{m}_2 where coefficient matrices are as follows

$$\begin{aligned} \mathbf{E}_1 &= \begin{bmatrix} 1 & 0 \\ 0 & 1 \end{bmatrix}, \quad \mathbf{H}_1 = \begin{bmatrix} 0 & -1 \\ 1 & 0 \end{bmatrix}, \quad \mathbf{B}_1 = \begin{bmatrix} 0 \\ -1 \end{bmatrix}, \\ \mathbf{E}_2 &= \begin{bmatrix} 1 & 0 \\ 0 & 0 \end{bmatrix}, \quad \mathbf{H}_2 = \begin{bmatrix} 0 & -1 \\ 0 & 1 \end{bmatrix}, \quad \mathbf{B}_2 = \begin{bmatrix} 0 \\ 0 \end{bmatrix}, \end{aligned} \quad (8.46)$$

respectively. The state vector and input of the system (8.45) are, respectively, $\mathbf{w} = (p, q)^\top$ and $z := \hat{P}$; with the initial condition $\bar{\mathbf{w}} := (\bar{p}, \bar{q})^\top = \mathbf{w}(t_0)$, and output of the system (8.45) $y_D := q$, is coupled to the PDE system

$$\mathbf{u}_t + \begin{pmatrix} 0 & 1 \\ 1 & 0 \end{pmatrix} \mathbf{u}_x = \mathbf{0}, \quad t \geq t_0, \quad x \in [a, \infty), \quad (8.47)$$

where $\mathbf{u} = (P, Q)^\top$, at its left boundary. Further, the output of (8.47) is $y_P := P(\cdot, a^+)$. For the swDAE (8.45), switching between modes \mathbf{m}_1 and \mathbf{m}_2 occurs according to the pressure difference; i.e., for $p > \hat{P}$, mode \mathbf{m}_1 is active and for $p \leq \hat{P}$, mode \mathbf{m}_2 is active. In other words, when $p > \hat{P}$, the valve is open; while $p \leq \hat{P}$ holds, the valve is closed.

From Assumption (H'-5), only one boundary condition has to be prescribed for (8.47)

$$\mathbf{P}_a \mathbf{u}(t, a^+) = b^a(t) \quad \text{where } \mathbf{P}_a \in \mathbb{R}^{1 \times 2}.$$

Assume $b^a(t) = Q(t, a^+)$; so, $\mathbf{P}_a = [0 \ 1]$. Hence, the coupling between swDAE and PDE systems is constructed via $b^a(t) = y_D$ and $q = y_P$.

In the following, the PDE system (8.47) is reduced to algebraic conditions by considering it in its characteristic variables (8.18) with (8.19) (where $c_0 = 1$) only at the coupling point $x = a$

$$\begin{aligned}\widehat{P}(t) &= v_1(t) + v_2(t), \\ \widehat{Q}(t) &= -v_1(t) + v_2(t),\end{aligned}\tag{8.48}$$

where $\widehat{P} := P(\cdot, a)$, $\widehat{Q} := Q(\cdot, a)$, $v_1 := v_-(\cdot, a)$ and $v_2 := v_+(\cdot, a)$ with v_- and v_+ representing left- and right going waves and the boundary condition in terms of characteristic variables is formulated as follows

$$\mathbf{M}\mathbf{v}(\cdot, a) = \begin{bmatrix} -1 & 1 \end{bmatrix} \begin{bmatrix} v_-(\cdot, a) \\ v_+(\cdot, a) \end{bmatrix} = Q(t, a),$$

where $\mathbf{M} = \mathbf{P}_a \mathbf{R}$ and \mathbf{R} is given in (8.19). In other words, the boundary condition can be found as

$$v_+(\cdot, a) = v_-(\cdot, a) + Q(\cdot, a).$$

Hence, the unknown \widehat{P} in (8.48) can be written in terms of the known variables as

$$\widehat{P} = 2v_1 + b^a,\tag{8.49}$$

where $b^a = y_D$.

By inserting the equality (8.49) into the swDAE system (8.45), the coefficient matrices \mathbf{H}_1 , \mathbf{B}_1 and the input z take the form

$$\mathbf{H}_1 = \begin{bmatrix} 0 & -1 \\ 1 & -1 \end{bmatrix}, \quad \mathbf{B}_1 = \begin{bmatrix} 0 \\ -2 \end{bmatrix}, \quad z = v_1,\tag{8.50}$$

whereas the rest of the system (8.45) stays as it is given in (8.46).

In the following, the solution to the ODE system from (8.45) with matrices $\mathbf{E}_1, \mathbf{H}_1, \mathbf{B}_1$ is given and the initial condition is assumed as $\bar{\mathbf{y}} = (\bar{p}, 0)$ since as $p \leq \widehat{P}$ holds, say at time t_s , the valve shuts and immediately $p(t_s^+) > \widehat{P}(t_s^+)$ follows again due to $\widehat{P}(t_s) > \widehat{P}(t_s^+)$. Hence, switching from \mathbf{m}_1 to \mathbf{m}_2 then back to \mathbf{m}_1 happens at a time instance.

The eigenvalues λ_1, λ_2 and corresponding eigenvectors $\mathbf{r}_1, \mathbf{r}_2$ of the matrix \mathbf{H}_1 in (8.50) are

$$\lambda_{1,2} = -\frac{1}{2} \mp i\frac{\sqrt{3}}{2}, \quad \mathbf{r}_1 = \begin{pmatrix} 1 \\ -\lambda_1 \end{pmatrix}, \quad \mathbf{r}_2 = \begin{pmatrix} 1 \\ -\lambda_2 \end{pmatrix}.$$

The solution $\tilde{\mathbf{w}}$ to the ODE system from (8.45) with matrices and input as in (8.50) is as follows

$$\begin{aligned}\tilde{\mathbf{w}}(t) &= \frac{2v_1}{i\sqrt{3}} \begin{pmatrix} \lambda_2(1 - e^{\lambda_1(t-t_0)}) - \lambda_1(1 - e^{\lambda_2(t-t_0)}) \\ e^{\lambda_1(t-t_0)} - e^{\lambda_2(t-t_0)} \end{pmatrix} - \frac{\bar{p}}{i\sqrt{3}} \begin{pmatrix} -\lambda_2 e^{\lambda_1(t-t_0)} + \lambda_1 e^{\lambda_2(t-t_0)} \\ e^{\lambda_1(t-t_0)} - e^{\lambda_2(t-t_0)} \end{pmatrix} \\ &= (\bar{p} - 2v_1) e^{-\frac{1}{2}(t-t_0)} \begin{pmatrix} \cos\left(\frac{\sqrt{3}}{2}(t-t_0)\right) + \frac{1}{\sqrt{3}} \sin\left(\frac{\sqrt{3}}{2}(t-t_0)\right) \\ \frac{2}{\sqrt{3}} \sin\left(\frac{\sqrt{3}}{2}(t-t_0)\right) \end{pmatrix} + 2v_1 \begin{pmatrix} 1 \\ 0 \end{pmatrix}.\end{aligned}$$

The times t_k^* , $k = 1, 2, \dots$, can now be found such that $p(t_k^*) = \widehat{P}(t_k^*)$ holds. From (8.49), $p(t_i^*) = 2v_1 + q(t_i^*)$ is solved, which gives $t_k^* = kt^*$ where $t^* = \frac{2\sqrt{3}\pi}{9}$. Therefore, there is no Zeno behavior as jump times t_k^* , $k = 1, 2, \dots$, remain the same and there is no accumulation. Each jump time kt^* , $k = 1, 2, \dots$, becomes an initial time $t_{0,k}$ for time intervals $[kt^*, (k+1)t^*]$ for the ODE system. Therefore, the solution $\tilde{\mathbf{w}}_k = (p_k, q_k)^\top$ to the ODE system for $t \in$

$[kt^*, (k+1)t^*]$, $k = 1, 2, \dots$, can be written as

$$\mathbf{y}_k(t) = (\bar{p}_k - 2v_1) e^{-\frac{1}{2}(t-t_{0,k})} \Gamma + 2v_1 \begin{pmatrix} 1 \\ 0 \end{pmatrix},$$

with

$$\Gamma := \begin{pmatrix} \cos\left(\frac{\sqrt{3}}{2}(t-t_{0,k})\right) + \frac{1}{\sqrt{3}} \sin\left(\frac{\sqrt{3}}{2}(t-t_{0,k})\right) \\ \frac{2}{\sqrt{3}} \sin\left(\frac{\sqrt{3}}{2}(t-t_{0,k})\right) \end{pmatrix},$$

where $\bar{p}_k = p_k(t_{0,k})$ for $t \in [kt^*, (k+1)t^*]$, $k = 1, 2, \dots$. To be more precise, $\bar{p}_0 := p_0(0) := p(0)$ is given and $\bar{p}_k = p_{k-1}(kt^*)$, $k = 1, 2, 3, \dots$. By induction, the value of the solution $\tilde{\mathbf{w}}_k((k+1)t^*)$ at jump times can be found as well

$$\begin{aligned} p_k((k+1)t^*) &= (\bar{p}_k - 2v_1) e^{-\frac{1}{2}t^*} + 2v_1, \\ q_k((k+1)t^*) &= (\bar{p}_k - 2v_1) e^{-\frac{1}{2}t^*}, \end{aligned}$$

with which, in the following, size of jumps, call it J_k , is evaluated in each time interval. By using iteration on \bar{p}_k , \bar{p}_k is rewritten in terms of \bar{p}_0

$$\begin{aligned} \bar{p}_k &= p_{k-1}(kt^*) \\ &= (\bar{p}_0 - 2v_1) e^{-\frac{k}{2}t^*} + 2v_1. \end{aligned}$$

Furthermore, with the formula for $\bar{p}_k(t)$ expressed in terms of \bar{p}_0 , $p_k(t)$ and $q_k(t)$ can be rewritten in terms of \bar{p}_0 as following

$$\begin{aligned} p_k(t) &= (\bar{p}_0 - 2v_1) e^{-\frac{1}{2}t} \left[\cos(\tau_t) + \frac{1}{\sqrt{3}} \sin(\tau_t) \right] + 2v_1, \\ q_k(t) &= \frac{2}{\sqrt{3}} (\bar{p}_0 - 2v_1) e^{-\frac{1}{2}t} \sin(\tau_t), \end{aligned}$$

where

$$\tau_t = \frac{\sqrt{3}}{2} (t - kt^*).$$

The total area under the solution plot in Figure 8.26a gives the total flux Q_{total} entering the PDE domain at $x = a$. Let $A_{q,k}$ denote the area under the graph over each time interval $[kt^*, (k+1)t^*]$, $k = 1, 2, \dots$. Then

$$A_{q,0} = (\bar{p}_0 - 2v_1) \left(1 - e^{-\frac{1}{2}t^*} \right).$$

Similarly, $A_{q,1}$ can be found as follows

$$A_{q,1} = (\bar{p}_0 - 2v_1) \left(1 - e^{-\frac{1}{2}t^*} \right) e^{-\frac{1}{2}t^*}.$$

As a result, $A_{q,k}$ can be formulated as

$$A_{q,k} = A_{q,0} e^{-\frac{1}{2}kt^*}.$$

The total flux flowing is then formulated as

$$\begin{aligned} Q_{\text{total}} &= \sum_{k=0}^{\infty} A_{q,k} \\ &= \bar{p}_0 - 2v_1. \end{aligned}$$

Hence, blood flow in the system is conserved.

The size of difference in pressure values, \mathcal{J}_0 , is evaluated in the first time interval $[0, t^*]$

$$\begin{aligned} \mathcal{J}_0 &= \bar{p}_0 - p_0(t^*) \\ &= (\bar{p}_0 - 2v_1) \left(1 - e^{-\frac{t^*}{2}} \right), \end{aligned} \quad (8.51)$$

where $t^* = \frac{2\sqrt{3}\pi}{9}$.

For the next time interval $[t^*, 2t^*]$, the difference of pressure values, \mathcal{J}_1 , is

$$\begin{aligned} \mathcal{J}_1 &= \bar{p}_1 - p_1(2t^*) \\ &= e^{-\frac{1}{2}t^*} \mathcal{J}_0, \end{aligned}$$

where \mathcal{J}_0 is given in (8.51). Similarly, for \mathcal{J}_2 , the expression is as follows

$$\begin{aligned} \mathcal{J}_2 &= \bar{p}_2 - p_2(3t^*) \\ &= e^{-\frac{1}{2}2t^*} \mathcal{J}_0, \end{aligned}$$

where \mathcal{J}_0 is given in (8.51).

By iteration on \mathcal{J}_k for $k = 1, 2, \dots$, a general formula for the jump size \mathcal{J}_k in $[kt^*, (k+1)t^*]$ is found in terms of \mathcal{J}_0 as

$$\mathcal{J}_k = e^{-\frac{1}{2}kt^*} \mathcal{J}_0, \quad (8.52)$$

where \mathcal{J}_0 is given in (8.51). From (8.52), difference of pressures on both sides of the valve converges to 0. As a result, the Zeno-like behavior in the numerical results for the blood flow example in Section 8.3.3 reflects the outcome of the Riemann problem, not the Zeno behavior, at every time instance when the valve shuts as the pressure value for the PDE system starts decreasing, which makes the pressure value for the switched DAE system get larger than the one of the PDE.

Remark 8.11

If, instead, one considers the ODE equations to model the opening and closure of valves, which are given below, the Zeno behaviour, which is present in the coupled nonlinear hyperbolic PDE-DAE model for the circulatory system, would be cured. The valve opening and closure rates are respectively determined by instantaneous pressure difference Δp on both sides of the valve and the state v of the valve as, [95],

$$\begin{aligned} \frac{d}{dt} v &= (1 - v) K_{\text{op}}(\Delta p - \Delta p_{\text{op}}), & \text{if } \Delta p > \Delta p_{\text{op}}, \\ \frac{d}{dt} v &= v K_{\text{cl}}(\Delta p - \Delta p_{\text{cl}}), & \text{if } \Delta p > \Delta p_{\text{cl}}, \end{aligned}$$

where $K_{\text{op}}, K_{\text{cl}}$ are the valve opening and closure coefficients and $\Delta p_{\text{op}}, \Delta p_{\text{cl}}$ are threshold pressure differences for opening and closing, respectively. With these ODEs, one can

model the lumped parameter model of the circulatory system as an ODE system instead of DAEs. This model including only ODEs for the valve motion suits the framework studied in [17].

Numerical results

In this section, it is explained how the coupled system in Section 8.3.4 is solved numerically for blood flow rate, Q_N , and difference in pressure values, ΔP_N , using MATLAB. The results for ΔP_N and Q_N are shown in Figure 8.25b and Figure 8.26b along with the analytic solutions of ΔP and Q in Figure 8.25a and Figure 8.26a, respectively.

The spatial domain $[a, b]$ for the PDE system is considered to be $I = [0, 1]$ and is partitioned into $N = 50$ computational cells. Furthermore, two ghost cells are placed at left- and right ends of the computational spatial domain I ; namely I_0 and I_{N+1} , respectively. The time variable t is discretized and updated as $t^{n+1} = t^n + \Delta t$ according to the CFL number \mathcal{C} which is chosen to be 1. Initial time $t_0 = 0$ and maximum time t_{\max} until which the numerical computations run is taken as 17. Denote by $\mathbf{u}_j^n = \mathbf{u}(x_j, t^n)$ the approximated solution at time t^n and position x_j of the PDE system (8.47) such that $\mathbf{u}_j^n = \begin{pmatrix} P_j^n \\ Q_j^n \end{pmatrix}^\top$. Furthermore, denote by $\mathbf{w}^n = \mathbf{w}(t^n)$ the approximated solution at time t^n of the switched DAE (8.45) with coefficient matrices given in (8.46) such that $\mathbf{w}^n = \begin{pmatrix} p^n \\ q^n \end{pmatrix}^\top$. At each time step, the discretized PDE system (8.47) is decomposed via change of coordinate $\mathbf{v}_j^n = \mathbf{R}^{-1} \mathbf{u}_j^n$, where

$$\mathbf{R} = \begin{pmatrix} 1 & 1 \\ -1 & 1 \end{pmatrix}, \text{ such that } \mathbf{A} = \mathbf{R} \mathbf{\Lambda} \mathbf{R}^{-1} \text{ with } \mathbf{A} = \begin{pmatrix} 0 & 1 \\ 1 & 0 \end{pmatrix},$$

into its characteristic variables $\mathbf{v}_j^n = \begin{pmatrix} (v^-)_j^n \\ (v^+)_j^n \end{pmatrix}^\top$ with left- and right going waves $(v^-)_j^n$ and $(v^+)_j^n$, respectively, where $P_j^n = (v^-)_j^n + (v^+)_j^n$ and $Q_j^n = -(v^-)_j^n + (v^+)_j^n$ and solve this decomposed PDE numerically for the next time step t^{n+1} . The decomposed PDE system is solved by using the upwind scheme,

$$\begin{aligned} (v^-)_j^{n+1} &= (v^-)_j^n + \frac{\Delta t}{\Delta x} \left((v^-)_{j+1}^n - (v^-)_j^n \right), \text{ for } j = 1, 2, \dots, N, \\ (v^+)_j^{n+1} &= (v^+)_j^n - \frac{\Delta t}{\Delta x} \left((v^+)_j^n - (v^+)_{j-1}^n \right), \text{ for } j = 1, 2, \dots, N, \end{aligned}$$

and the swDAE system is solved by using implicit Euler. After the PDE is solved for its characteristic variables \mathbf{v}_j^{n+1} , the unknown \mathbf{u}_j^{n+1} of the original PDE system is updated via inverse coordinate change $\mathbf{u}_j^{n+1} = \mathbf{R} \mathbf{v}_j^{n+1}$.

The initial conditions for the switched DAE and PDE are given as follows

$$\begin{aligned} (p_0, q_0) &= (1, 0), \\ (P_j^0, Q_j^0) &= (0, 0.9), \quad \forall j = 0, 1, \dots, N+1, \end{aligned}$$

respectively, so that the initial pressure value p_0 of the swDAE is larger than the initial pressure value P_0^0 of the PDE in order for the valve to open. If, as an initial condition, p_0 were smaller than P_0^0 , the valve between two systems would never open as it opens and shuts according to the pressure difference.

Boundary conditions at I_0 and I_{N+1} are assigned on characteristic variables $(v^+)_0^n$ and $(v^-)_{N+1}^n$, respectively, as

$$\begin{aligned} (v^+)_0^n &= q^n + (v^-)_1^n, \\ (v^-)_{N+1}^n &= (v^-)_N^n, \end{aligned}$$

where q^n is the output of the swDAE at time t^n .

To update solutions $(v^-)_{0}^{n+1}$ and $(v^+)_{N+1}^{n+1}$ in ghost cells I_0 and I_{N+1} , the following assignment is numerically performed

$$\begin{aligned} (v^-)_{0}^{n+1} &= (v^-)_{1}^{n+1}, \\ (v^+)_{N+1}^{n+1} &= (v^+)_{N}^{n+1}. \end{aligned}$$

At each iteration after the PDE is solved numerically, P_0^{n+1} is assigned to the swDAE as an input. Then, with the given input, the swDAE system is solved

$$\begin{aligned} p^{n+1} &= p^n + \Delta t (-q^n), \\ \begin{cases} q^{n+1} = q^n + \Delta t (p^{n+1} - P_0^{n+1}), & \text{if } p^{n+1} > P_0^{n+1}, \\ q^{n+1} = 0, & \text{if } p^{n+1} \leq P_0^{n+1}. \end{cases} \end{aligned}$$

Then the time variable t^n is updated for the next time step and iterated until the maximum time t_{\max} is reached.

The numerical results support the analytical ones for this simple system. It also explains why there occurs a kink in numerical results of flow rate in circulation system example.

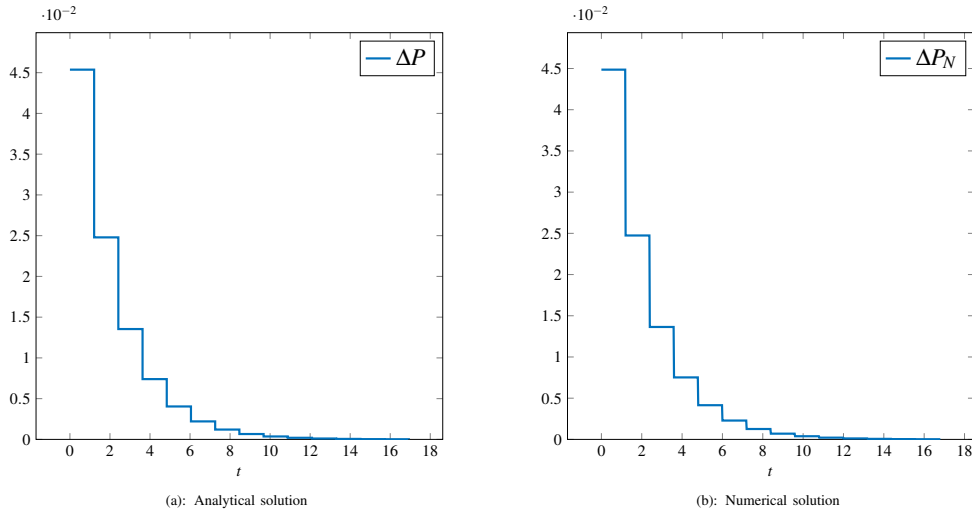


FIGURE 8.26: Analytical and numerical difference in pressure values with initial conditions $p(0) = 1$, $P(0,0) = 0.9$, $t_{\max} = 17$. Analytical and numerical results coincide with each other.

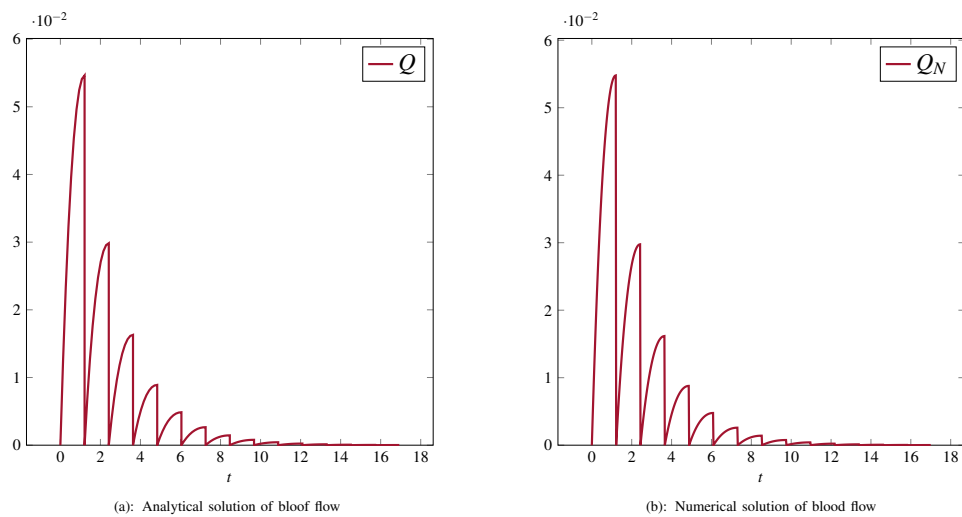


FIGURE 8.27: Analytical and numerical solution for blood flow $q(t)$, initial condition $q(0) = 0$, $t_{\max} = 17$. Analytical and numerical results coincide with each other.

Chapter 9

Appendix

9.1 Zeno behavior

In this section, the definitions of a hybrid system and Zeno behavior, which can arise in these systems, are briefly explained. In the last decade, Zeno behavior has been of great importance as its occurrence can be troublesome from analytical and numerical points of view, [4, 74, 113, 143].

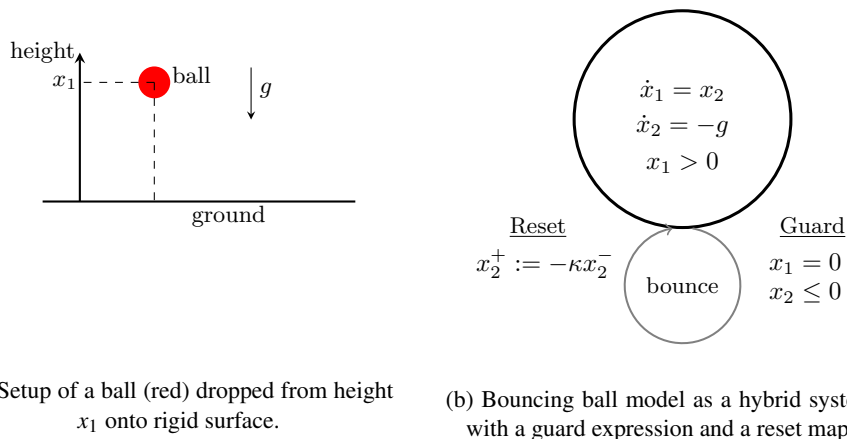


FIGURE 9.1: Bouncing ball on a rigid surface showing Zeno behavior.

If a continuous and discrete behavior interacts with each other in a dynamical system, then such systems are called *hybrid systems*, [68, 87]. Roughly speaking, physical systems that have modes, transitions and switches can be modeled as hybrid systems, [23, 26]. In hybrid systems, if discrete transitions occur infinitely many times in finite time, this notion is called *Zeno behavior*, [26, 87]. However, in physical world it is infeasible that any system has Zeno behavior. The following is a classical example of this Zeno behavior.

Example 9.1: Bouncing ball

A ball which is dropped from some height onto the rigid surface with or without velocity shows the Zeno behavior. In Figure 9.1a, the setup of of the ball dropped from height x_1 is shown. Denote by x_2 and g velocity of the ball and gravity of Earth, respectively. The hybrid system for bouncing ball model, see Figure 9.1b, is

$$\begin{aligned} \dot{\mathbf{x}} &= \mathbf{Ax} + \mathbf{B}, \\ \mathbf{y} &= \mathbf{Cx}, \end{aligned} \tag{9.1}$$

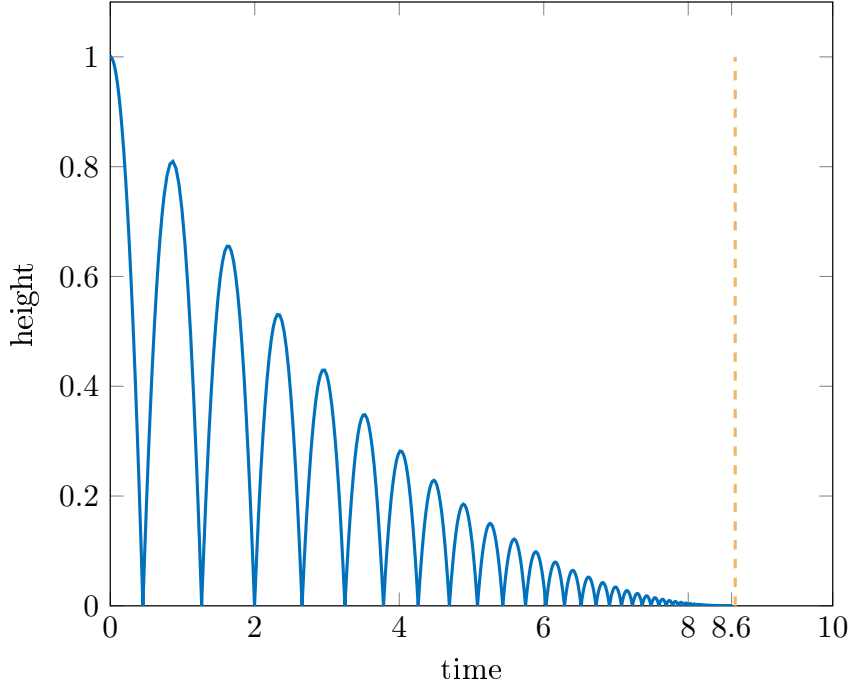


FIGURE 9.2: Simulation of the bouncing ball that is dropped from height $x_1 = 1$ onto a rigid surface, the Zeno-time $\tau_\infty = 8.5833$.

where \mathbf{x} is the unknown vector and \mathbf{y} is output of the system

$$\mathbf{x} = \begin{bmatrix} x_1 \\ x_2 \end{bmatrix}, \quad \mathbf{A} = \begin{bmatrix} 0 & 1 \\ 0 & 0 \end{bmatrix}, \quad \mathbf{B} = \begin{bmatrix} 0 \\ -g \end{bmatrix}, \quad \mathbf{C} = [1 \quad 0],$$

with the guard expression

$$[1 \quad 0] \mathbf{x} = 0 \quad \wedge \quad [0 \quad 1] \mathbf{x} \leq 0,$$

and with the reset map at bounces

$$\mathbf{x} := \begin{bmatrix} 1 & 0 \\ 0 & -\kappa \end{bmatrix} \mathbf{x},$$

where $\kappa \in [0, 1]$ is the restitution coefficient.

Solving the system (9.1) for the output \mathbf{y} yields

$$\mathbf{y} = x_1(t_0) + x_2(t - t_0) - \frac{g}{2}(t - t_0)^2,$$

and for $\kappa \in [0, 1)$, the time τ_n at which the n -th bounce happens is as follows

$$\tau_n = t_0 + \tau_1 + \frac{2x_2(\tau_1)}{g} \sum_{i=1}^n \kappa^{i-1}, \quad (9.2)$$

where t_0 is the initial time and τ_1 is the first bounce time

$$\tau_1 = t_0 + \frac{x_2(t_0) + \sqrt{x_2^2(t_0) + 2gx_1(t_0)}}{g}.$$

From (9.2), $\tau_\infty := \lim_{n \rightarrow \infty} \tau_n < \infty$. Hence, beyond τ_∞ , the hybrid system is undefined and simulation crashes.

The vertical position of the ball is shown in Figure 9.2. As the ball bounces off the ground, time intervals for the ball to bounce off again get smaller and smaller although it never stops bouncing. Hence, the ball bounces infinitely many times in finite time, which is called the Zeno time. Denote by τ_∞ the Zeno time. For this bouncing ball example,

$$\tau_\infty = \frac{\sqrt{\frac{8x_1}{g}}}{1 - \kappa} - \sqrt{\frac{2x_1}{g}},$$

for $x_2 = 0$.

9.1.1 Numerical results of bouncing ball

For the numerical scheme, denote by y^n and v^n the position and velocity variables, respectively. For the spatial discretization, explicit Euler scheme is employed

$$y^{n+1} = y^n + \Delta t y^n,$$

where $v^n = \dot{y}^n$ from equations of motions $\Delta t > 0$ is the time step, which is assumed to be $\Delta t = 0.01$.

If the ball has not touched the ground yet; i.e., $y^{n+1} > 0$, implicit Euler step is applied for the velocity

$$v^{n+1} = v^n + \Delta t(-g), \quad (9.3)$$

where g is the gravitational acceleration an assumed to be $g = 9.8$.

The initial time is $t = 0$, number of iteration is $N = 1000$, final time $t_{\max} = N\Delta t$, the restitution coefficient is assumed to be $\kappa = 0.9$, and initial conditions are given as $y^0 = 1$, $v^0 = 0$.

Once the ball touches the ground; i.e., $y^{n+1} \leq 0$,

$$\Delta v = -(1 + \kappa)v^n,$$

and if $\Delta v > -g$; i.e., the ground cannot pull, then the velocity v^{n+1} at t^{n+1} is updated as

$$v^{n+1} = v^n + \Delta v,$$

if $\Delta v > -g$ does not hold, then the implicit Euler step (9.3) applies to the velocity variable.

Figure 9.2 shows the result of a ball that is dropped from a height $x_1 = 1$ comes to rest in finite amount of time, which is the Zeno-time $\tau_\infty = 8.5833$, with infinitely many bounces.

9.2 Algorithm for the power grid example

Below, the algorithm for the example – power grid with switching transformer – is provided.

Algorithm 1 Coupled power grid

Input: $t_0, t_{\max}, x_{\min}, x_{\max}, N, \mathcal{C}, u, y, t_{s1}, t_{s2}, C_{D1}, C_{D2}, v_G$, parameters **Output:**

- u, y
- 1: discretize x ,
- 2: $\Delta x \leftarrow (x_{\max} - x_{\min})/N$
- 3: $\lambda_{\max} \leftarrow 0$

4: $(I_1 \ V_1 \ I_2 \ V_2 \ I_3 \ V_3 \ I_4 \ V_4) \leftarrow u$
 5: $(z_1 \ i_{12} \ i_{13} \ v_{12} \ v_{13} \ z_{24} \ z_{34}) \leftarrow y$

6: **function** GHOSTCELLS&EIGENVALUES(I_k, V_k, λ_{\max}) **Output:** $u, w, y, R_k, \lambda_P^k, \lambda_N^k, \lambda_{\max}$
 7: **for** $k \leftarrow 1$ to 4 **do**
 8: create ghost cells for each \mathcal{E}_k , copy values from neighboring cells
 9: $[D_k \ R_k] \leftarrow$ eigenvalues & eigenvectors of A_k -matrix
 10: $\lambda_N^k \leftarrow$ negative & $\lambda_P^k \leftarrow$ positive eigenvalue
 11: $\lambda_{\max} \leftarrow \max(\lambda_{\max}, |\lambda_k|)$
 12: $w_k \leftarrow \begin{bmatrix} w_{k1} \\ w_{k2} \end{bmatrix} \leftarrow$ inverse coordinate change & $u_k \leftarrow \begin{bmatrix} I_k \\ V_k \end{bmatrix}$
 13: **end for**
 14: update u, w
 15: **end function**

16: **procedure** COUPLEDSCHEME(swDAE,PDE)
 17: **while** $t < t_{\max}$ **do**
 18: $\Delta t \leftarrow \mathcal{C}(\Delta x / \lambda_{\max})$
 19: $t \leftarrow t + \Delta t$

20: **function** BOUNDARYCONDITIONS(z_1, w) **Output:** I_2, I_3, I_4
 21: $w_{21}(N+2) \leftarrow 2w_{41}(1) - w_{22}(N+2)$
 22: $w_{42}(1) \leftarrow 2w_{22}(N+2) - w_{41}(1)$
 23: $w_{41}(N+2) \leftarrow -2/3w_{32}(N+2) + 1/3w_{42}(N+2)$
 24: $w_{31}(N+2) \leftarrow 1/3w_{32}(N+2) - 2/3w_{42}(N+2)$
 25: $w_{12}(1) \leftarrow z_1 + w_{11}(1)$
 26: $I_4(1) \leftarrow w_{41}(1) + w_{42}(1)$
 27: $I_2(N+2) \leftarrow w_{21}(N+2) + w_{22}(N+2)$
 28: $I_3(N+2) \leftarrow w_{31}(N+2) + w_{32}(N+2)$
 29: $I_4(N+2) \leftarrow w_{41}(N+2) + w_{42}(N+2)$
 30: update I_k, w_k for $k = 1, \dots, 4$
 31: **end function**

32: **function** IMPLICITEULER($y, t, t_{s_1}, t_{s_2}, \Delta t, v_G, w_{12}, I_2, I_3, I_4, C_{D_1}, C_{D_2}$, parameters)
Output: y, w , Voltage
 33: $z_1 \leftarrow v_G$
 34: $z_{24} \leftarrow R_{24}(I_4(1) - I_2(N+2))$
 35: $z_{34} \leftarrow R_{34}(I_3(N+2) + I_4(N+2))$
 36: **if** $t < t_{s_1}$ or $t > t_{s_2}$ **then**
 37: $v_{12} \leftarrow \frac{v_{12} + 2w_{12}(N+1) - 2w_{12}(N+2)}{1 + \Delta t}$
 38: $w_{11}(N+2) \leftarrow w_{12}(N+1) - v_{12}$
 39: $i_{12} \leftarrow w_{12}(N+1) + w_{11}(N+2)$
 40: $i_p \leftarrow i_{13}$
 41: $i_{13} \leftarrow 0$
 42: $v_{13} \leftarrow L_{13} \frac{i_{13} - i_p}{\Delta t}$
 43: update y
 44: Voltage $\leftarrow C_{D_1} y$
 45: **else**
 46: $i_p \leftarrow i_{12}$
 47: $i_{12} \leftarrow 0$
 48: $v_{12} \leftarrow L_{12} \frac{i_{12} - i_p}{\Delta t}$

```

49:          $v_p \leftarrow v_{13}$ 
50:          $v_{13} \leftarrow \frac{v_p + 2w_3 - 2w_4}{1 + \Delta t}$ 
51:          $w_{11}(N+2) \leftarrow w_{12}(N+1) - v_{13}$ 
52:          $i_{13} \leftarrow w_{12}(N+1) + w_{11}(N+2)$ 
53:         update  $y$ 
54:         Voltage  $\leftarrow C_{D_2} y$ 
55:     end if
56:     update  $w$  with  $w_{11}(N+2)$ 
57: end function

```

```

58: procedure BOUNDARYCONDITIONS(Voltage,  $w$ )   Output:  $w$ 
59:      $w_{22}(1) \leftarrow \text{Voltage}(1) + w_{21}(1)$ 
60:      $w_{32}(1) \leftarrow \text{Voltage}(3) + w_{31}(1)$ 
61:     update  $w$  with  $w_{22}(1)$ ,  $w_{32}(1)$ 
62: end procedure

```

```

63: function UPWIND( $w$ ,  $x$ ,  $\Delta t$ ,  $\Delta x$ ,  $\lambda_N^k$ ,  $\lambda_P^k$ )   Output:  $u_k$ ,  $w_k$ 
64:     for  $k \leftarrow 1$  to 4 do
65:          $j \leftarrow 1$  to length( $x$ )
66:          $w_{k1}(j+1) \leftarrow w_{k1}(j) - \lambda_N^k \frac{\Delta t}{\Delta x} (w_{k1}(j+1) - w_{k1}(j))$ 
67:          $j \leftarrow 2$  to length( $x$ ) + 1
68:          $w_{k2}(j+1) \leftarrow w_{k2}(j) - \lambda_P^k \frac{\Delta t}{\Delta x} (w_{k2}(j) - w_{k2}(j-1))$ 
69:          $w_k \leftarrow \begin{bmatrix} w_{k1} \\ w_{k2} \end{bmatrix}$    &    $u_k \leftarrow \begin{bmatrix} I_k \\ V_k \end{bmatrix} \leftarrow R_k \begin{bmatrix} w_{k1}(j-1) \\ w_{k2}(j) \end{bmatrix}$ 
70:     end for
71: end function

```

```

72: end while
73: end procedure

```

9.3 Algorithm for the circulatory system example

Below, the algorithm for the example – simplified circulatory system in the left heart is given.

Algorithm 2 Coupled circulatory system

Input: t_0 , t_{\max} , x_{\min} , x_{\max} , N , \mathcal{C} , u , y , parameters **Output:** u , y

- 1: $(u_{pv} \ u_{aa}) \leftarrow u$
- 2: discretize x
- 3: $\Delta x \leftarrow (x_{\max} - x_{\min})/N$
- 4: $\lambda_{\max} \leftarrow 0$
- 5: create ghost cells for I^{pv} , I^{aa} , copy values from neighboring cells
- 6: **while** $t < t_{\max}$ **do**

Pulmonary venous

- 7: **function** BOUNDARYCONDITIONS&OUTPUT(u_{pv} , p_{la} , parameters) **Output:** u_{pv} , Q_{pv}^I
- 8: solve for A_{pv}^I , then update $A_{pv}(N+2)$ and $P_{pv}(N+2)$
- 9: $Q_{pv}(N+2) \leftarrow Q_{pv}(N+1)$, update $V_{pv}(N+2)$, and V_{pv}^I
- 10: construct A_{pv}^I -matrix, $[D \ R] \leftarrow$ eigenvalues & eigenvectors of A
- 11: find $\vec{\alpha}_{pv}$, D_{pv}^- and Q_{pv}^I at $x_{N+3/2}$
- 12: update u_{pv} with boundary values
- 13: **end function**

Ascending aorta

```

14: function BOUNDARYCONDITIONS&OUTPUT( $u_{aa}$ ,  $q_{av}$ , parameters) Output:  $u_{aa}$ ,
 $P_{aa}^I$ 
15:     update values in  $I_0^{aa}$  by fsolve via  $\vec{\alpha}_{aa}$ ,  $D_{aa}^-$ 
16:     find  $A_{aa}^I$  and  $P_{aa}^I$ 
17:      $u_{aa}(N+2) \leftarrow u_{aa}(N+1)$ 
18:     update  $u_{aa}$  with boundary values
19: end function

```

```

20: function FLUCTUATIONS( $u_{pv}$ ,  $u_{aa}$ , parameters) Output:  $\lambda_{max}$ ,  $D_{pv}^-$ ,  $D_{pv}^+$ ,  $D_{aa}^-$ ,
 $D_{aa}^+$ 
21:     construct  $\mathbf{A}_{pv}$ - and  $\mathbf{A}_{aa}$ -matrices via  $A_{pv}^I$ ,  $V_{pv}^I$ ,  $A_{aa}^I$ ,  $V_{aa}^I$  at each interface
22:     for  $i \leftarrow 1$  to  $N+2$  do
23:          $[D_{pv} \ R_{pv}]$ ,  $[D_{aa} \ R_{aa}] \leftarrow$  eigenvalues & eigenvectors of  $\mathbf{A}_{pv}^I$ ,  $\mathbf{A}_{aa}^I$ 
24:          $\lambda_{pv} \leftarrow \max(0, \lambda_{pv})$  &  $\lambda_{aa} \leftarrow \max(0, \lambda_{aa})$ 
25:         find  $\vec{\alpha}_{pv}$ ,  $\vec{\alpha}_{aa}$ ,  $D_{pv}^-$ ,  $D_{pv}^+$ ,  $D_{aa}^-$ ,  $D_{aa}^+$ 
26:     end for
27:      $\lambda_{max} \leftarrow \max(\lambda_{pv}, \lambda_{aa})$ 
28: end function

```

```

29:  $\Delta t \leftarrow \mathcal{C} \Delta x / \lambda_{max}$ 
30:  $t \leftarrow t + \Delta t$ 
31: update  $u_{pv}$  and  $u_{aa}$  by Roe scheme &  $u \leftarrow (u_{pv} \ u_{aa})$ 

```

Left heart

```

32: function ( $t$ ,  $y$ ,  $u$ ,  $P_{aa}^I$ , parameters) Output:  $y$ 
33:      $t^* \leftarrow t \bmod T_0$ 
34:      $E_{la} \leftarrow \mathcal{F}(t^*, e_{la})$ ,  $E_{lv} \leftarrow \mathcal{F}(t^*, e_{lv})$ 
35:     update  $v_{la}$ ,  $v_{lv}$ 
36:      $p_{la} \leftarrow E_{la} v_{la}$ ,  $p_{lv} \leftarrow E_{lv} v_{lv}$ 
37:     if  $p_{la} > p_{lv}$  then
38:         update  $q_{mv}$ 
39:     else
40:          $q_{mv} \leftarrow 0$ 
41:     end if
42:     if  $p_{lv} > P_{aa}^I$  then
43:         update  $q_{av}$ 
44:     else
45:          $q_{av} \leftarrow 0$ 
46:     end if
47:     update  $y$ 
48: end function

```

```

49: end while

```

Bibliography

- [1] ALASTRUHEY, J., PARKER, K., PEIRO, J., AND SHERWIN, S. Lumped parameter outflow models for 1-D blood flow simulations: Effect on pulse waves and parameter estimation. *Communications in Computational Physics* 4 (08 2008), 317–336.
- [2] AMADORI, D. Initial-boundary value problems for nonlinear systems of conservation laws. *NoDEA Nonlinear Differential Equations Appl.* 4, 1 (1997), 1–42.
- [3] AMBROSIO, L., BRESSAN, A., HELBING, D., KLAR, A., AND ZUAZUA, E. *Modelling and optimisation of flows on networks*, vol. 2062 of *Lecture Notes in Mathematics*. Springer, Heidelberg; Fondazione C.I.M.E., Florence, 2013. Lectures from the Centro Internazionale Matematico Estivo (C.I.M.E.) Summer School held in Cetraro, June 15–19, 2009, Edited by Benedetto Piccoli and Michel Rascle, Fondazione CIME/CIME Foundation Subseries.
- [4] AMES, A. D., ABATE, A., AND SASTRY, S. Sufficient conditions for the existence of Zeno behavior in a class of nonlinear hybrid systems via constant approximations. In *2007 46th IEEE Conference on Decision and Control* (Dec 2008), pp. 4033–4038.
- [5] AMIN, S., HANTE, F. M., AND BAYEN, A. M. Exponential stability of switched linear hyperbolic initial-boundary value problems. *IEEE Trans. Automat. Control* 57, 2 (2012), 291–301.
- [6] ANAVEKAR, N., AND OH, J. Doppler echocardiography: A contemporary review. *Journal of cardiology* 54 (12 2009), 347–58.
- [7] ARMBRUSTER, D., DEGOND, P., AND RINGHOFER, C. A Model for the Dynamics of large Queuing Networks and Supply Chains. *SIAM Journal of Applied Mathematics* 66 (01 2006), 896–920.
- [8] ASCHER, U. M., AND PETZOLD, L. R. *Computer methods for ordinary differential equations and differential-algebraic equations*. Society for Industrial and Applied Mathematics, Philadelphia, 1998.
- [9] ASHLEY, E. A., AND NIEBAUER, J. *Cardiology Explained*. Remedica, London, 2004.
- [10] BANDA, M., HERTY, M., AND KLAR, A. Gas flow in pipeline networks. *Networks and Heterogeneous Media* 1 (03 2006), 41–56.
- [11] BASTIN, G., AND CORON, J.-M. *Stability and boundary stabilization of 1-D hyperbolic systems*, vol. 88 of *Progress in Nonlinear Differential Equations and their Applications*. Birkhäuser/Springer, [Cham], 2016. Subseries in Control.
- [12] BAYEN, A., RAFFARD, R., AND TOMLIN, C. Adjoint-based control of a new Eulerian network model of air traffic flow. *Control Systems Technology, IEEE Transactions on* 14 (10 2006), 804 – 818.

- [13] BENNO, F. Eine assoziative Algebra über einem Unterraum der Distributionen. *Mathematische Annalen* 178 (12 1968), 302–314.
- [14] BERGER, T., ILCHMANN, A., AND TRENN, S. The quasi-Weierstraß form for regular matrix pencils. *Linear Algebra Appl.* 436, 10 (2012), 4052–4069. published online February 2010.
- [15] BESSONOV, N., SEQUEIRA, A., SIMAKOV, S., AND VASSILEVSKII, Y. Methods of Blood Flow Modelling. *Mathematical Modelling of Natural Phenomena* 11 (01 2016), 1–25.
- [16] BLANCHARD, P., AND BRÜNING, E. *Mathematical Methods in Physics*. Progress in Mathematical Physics. Birkhäuser, Boston, MA, 2003.
- [17] BORSCHKE, R. *Modeling and Simulation of Sewer Networks and coupled Surface Flow*. PhD thesis, Technische Universität Kaiserslautern, Verlag Dr. Hut, 2011.
- [18] BORSCHKE, R., COLOMBO, R. M., AND GARAVELLO, M. On the coupling of systems of hyperbolic conservation laws with ordinary differential equations. *Nonlinearity* 23, 11 (2010), 2749–2770.
- [19] BORSCHKE, R., COLOMBO, R. M., AND GARAVELLO, M. Mixed systems: ODEs - balance laws. *J. Differential Equations* 252, 3 (2012), 2311–2338.
- [20] BORSCHKE, R., COLOMBO, R. M., GARAVELLO, M., AND MEURER, A. Differential equations modeling crowd interactions. *J. Nonlinear Sci.* 25, 4 (2015), 827–859.
- [21] BORSCHKE, R., EIMER, M., AND SIEDOW, N. A local time stepping method for thermal energy transport in district heating networks. *Appl. Math. Comput.* 353 (2019), 215–229.
- [22] BORSCHKE, R., KLAR, A., KÜHN, S., AND MEURER, A. Coupling traffic flow networks to pedestrian motion. *Mathematical Models and Methods in Applied Sciences* 24 (12 2013).
- [23] BRANICKY, M. *Introduction to Hybrid Systems*. Birkhäuser Boston, 01 2005, pp. 91–116.
- [24] BRESSAN, A. *Hyperbolic systems of conservation laws*, vol. 20 of *Oxford Lecture Series in Mathematics and its Applications*. Oxford University Press, Oxford, 2000. The one-dimensional Cauchy problem.
- [25] BRESSAN, A., AND PICCOLI, B. *Introduction to the Mathematical Theory of Control*, vol. 2 of *AIMS Series on Applied Mathematics*. American Institute of Mathematical Sciences (AIMS), Springfield, MO, 2007.
- [26] CAMLIBEL, M. K., AND SCHUMACHER, J. M. On the Zeno behavior of linear complementarity systems. In *Proceedings of the 40th IEEE Conference on Decision and Control (Cat. No.01CH37228)* (Dec 2001), vol. 1, pp. 346–351 vol.1.
- [27] CENGLER, Y. A., AND CIMBALA, J. M. *Essentials of Fluid Mechanics : Fundamentals and Applications*, 3rd. ed. Boston : McGraw-Hill Higher Education, 2014.
- [28] CHAHAL, N., DRAKOPOULOU, M., GONZALEZ-GONZALEZ, A., MANIVARMANE, R., KHATTAR, R., AND SENIOR, R. Resting Aortic Valve Area at Normal Transaortic Flow Rate Reflects True Valve Area in Suspected Low Gradient Severe Aortic Stenosis. *JACC. Cardiovascular imaging* 8 (09 2015).

- [29] CHALONS, C., DELLE MONACHE, M. L., AND GOATIN, P. A conservative scheme for non-classical solutions to a strongly coupled PDE-ODE problem. *Interfaces Free Bound.* 19, 4 (2017), 553–570.
- [30] CHOQUET-BRUHAT, Y. *Distributions Théorie et problèmes*. MASSON ET CIE, 1973.
- [31] CHOW, V. T. *Open-channel hydraulics*. McGraw-Hill, New York, 1959.
- [32] COCLITE, G., GARAVELLO, M., AND PICCOLI, B. Traffic Flow on a Road Network. *SIAM J. Math. Anal.* 36 (03 2002), 1862–1886 (electronic).
- [33] COLOMBO, R. Hyperbolic Phase Transitions in Traffic Flow. *SIAM J. Appl. Math.* 63 (01 2003), 708–721.
- [34] COLOMBO, R. M., AND MARCELLINI, F. A mixed ODE-PDE model for vehicular traffic. *Math. Methods Appl. Sci.* 38, 7 (2015), 1292–1302.
- [35] COLOMBO, R. M., AND ROSSI, E. On the micro-macro limit in traffic flow. *Rend. Semin. Mat. Univ. Padova* 131 (2014), 217–235.
- [36] DANILOV, V. G., AND SHELKOVICH, V. M. Dynamics of propagation and interaction of δ -shock waves in conservation law systems. *J. Differential Equations* 211, 2 (2005), 333–381.
- [37] DE MARCHI, S. F., BODENMÜLLER, M., LAI, D. L., AND SEILER, C. Pulmonary venous flow velocity patterns in 404 individuals without cardiovascular disease. *Heart (British Cardiac Society)* 85(1) (2001), 23–29.
- [38] DELLE MONACHE, M., AND GOATIN, P. Scalar conservation laws with moving constraints arising in traffic flow modeling: An existence result. *Journal of Differential Equations* 257, 11 (2014), 4015–4029.
- [39] DIAZ, A., GALLI, C., TRINGLER, M., RAMIREZ, A., AND FISCHER, E. Reference Values of Pulse Wave Velocity in Healthy People from an Urban and Rural Argentinian Population. *International Journal of Hypertension* 2014 (08 2014), 1–7.
- [40] DONOGHUE, W. F. *Distributions and Fourier transforms*, vol. 32. Academic Press, 1969.
- [41] EGGER, H., AND KUGLER, T. Damped wave systems on networks: exponential stability and uniform approximations. *Numer. Math.* 138, 4 (2018), 839–867.
- [42] EGGER, H., KUGLER, T., AND STROGIES, N. Parameter identification in a semilinear hyperbolic system. *Inverse Problems* 33, 5 (2017), 055022, 25.
- [43] EPSTEIN, S., WILLEMET, M., CHOWIENCZYK, P., AND ALASTRUEY, J. Reducing the number of parameters in 1D arterial blood flow modeling: Less is more for patient-specific simulations. *AJP Heart and Circulatory Physiology* 309 (04 2015), H222–H234.
- [44] EVANS, L. C. *Partial differential equations*. American Mathematical Society, Providence, R.I., 2010.
- [45] FEHER, J. *Quantitative Human Physiology*. Academic Press, Boston, 2012.
- [46] FIGUROVÁ, M., AND KULINOVÁ, V. Ultrasonographic Examination of Some Vessels in Dogs and the Characteristics of Blood Flow in These Vessels. *Folia Veterinaria* 61 (12 2017).

- [47] FILBET, F., LAURENCOT, P., AND PERTHAME, B. Derivation of hyperbolic models for chemosensitive movement. *J Theor Biol* 50 (01 2003), 189–207.
- [48] FORMAGGIA, L., LAMPONI, D., TUVERI, M., AND VENEZIANI, A. Numerical modeling of 1D arterial networks coupled with a lumped parameters description of the heart. *Computer methods in biomechanics and biomedical engineering* 9 (11 2006), 273–88.
- [49] FORMAGGIA, L., NOBILE, F., QUARTERONI, A., AND VENEZIANI, A. Multiscale modelling of the circulatory system: A preliminary analysis. *Comput. Vis. Sci.* 2 (12 1999).
- [50] FORMAGGIA, L., AND VENEZIANI, A. Reduced and multiscale models for the human cardiovascular system. Tech. rep., Politecnico di Milano, Department of Mathematics, 10 2015.
- [51] FORMAGGIA L., PERKTOLD K., Q. A. Basic mathematical models and motivations. In *Cardiovascular Mathematics : Modeling and Simulation of the Circulatory System*. MS&A, L. Formaggia, A. Quarteroni, and A. Veneziani, Eds. Springer, 2009.
- [52] FUCHSSTEINER, B. Algebraic foundation of some distribution algebras. *Studia Mathematica* 77, 5 (1984), 439–453.
- [53] FÜGENSCHUH, A., GÖTTLICH, S., HERTY, M., KIRCHNER, C., AND MARTIN, A. Efficient reformulation and solution of a nonlinear PDE-controlled flow network model. *Computing* 85, 3 (2009), 245–265.
- [54] GALDERISI, M., LANCELLOTTI, P., DONAL, E., CARDIM, N., EDVARDSEN, T., HABIB, G., MAGNE, J., MAURER, G., AND POPESCU, B. A. European multicentre validation study of the accuracy of E/e' ratio in estimating invasive left ventricular filling pressure: EURO-FILLING study. *European heart journal cardiovascular imaging* 15 (03 2014).
- [55] GANTMACHER, F. R. *The Theory of Matrices. Vol I and Vol II*. Chelsea Publishing Company, Newyork, 1959.
- [56] GARAVELLO, M., GOATIN, P., LIARD, T., AND PICCOLI, B. A multiscale model for traffic regulation via autonomous vehicles. *Journal of Differential Equations* (2020).
- [57] GARAVELLO, M., HAN, K., AND PICCOLI, B. *Models for vehicular traffic on networks*, vol. 9 of *AIMS Series on Applied Mathematics*. American Institute of Mathematical Sciences (AIMS), Springfield, MO, 2016.
- [58] GARAVELLO, M., AND PICCOLI, B. Boundary coupling of microscopic and first order macroscopic traffic models. *NoDEA Nonlinear Differential Equations Appl.* 24, 4 (2017), Paper No. 43, 18.
- [59] GHIGO, A. *Reduced-order models for blood flow in networks of large arteries*. PhD thesis, Université Pierre et Marie Curie, 09 2017.
- [60] GODLEWSKI, E., AND RAVIART, P.-A. *Numerical Approximation of Hyperbolic Systems of Conservation Laws*. Springer Publishing Company, Incorporated, 2014.
- [61] GODUNOV, S. Finite difference method for numerical computation of discontinuous-solutions of the equations of fluid dynamics. *Matematicheskij sbornik, Steklov Mathematical Institute of Russian Academy of Sciences* 47 (89) (3) (1959), 271–306. translated by I. Bohachevsky.

- [62] GÖTTLICH, S., HERTY, M., AND KLAR, A. Network models for supply chains. *Communications in mathematical sciences* 3 (12 2005).
- [63] GÖTTLICH, S., HERTY, M., AND SCHILLEN, P. Electric transmission lines: control and numerical discretization. *Optimal Control Appl. Methods* 37, 5 (2016), 980–995.
- [64] GROESDONK, H., W, D., U, D., GALM, C., MUTH, C.-M., AND DINSE, A. Un-recognized peripartum cardiomyopathy: Case series and comprehensive review of the literature. *Applied Cardiopulmonary Pathophysiology* 13 (01 2009).
- [65] GROSSWINDHAGER, S., VOIGT, A., AND KOZEK, M. Efficient Physical Modelling of District Heating Networks. In *22nd IASTED International Conference "Modelling and Simulation"* (Calgary, 07 2011), pp. 346–351 vol.1.
- [66] GRUNDEL, S., JANSEN, L., HORNING, N., CLEES, T., TISCHENDORF, C., AND BENNER, P. Model Order Reduction of Differential Algebraic Equations Arising from the Simulation of Gas Transport Networks. In *Progress in Differential-Algebraic Equations. Differential-Algebraic Equations Forum* (10 2014), Springer, Berlin, Heidelberg, pp. 183–205.
- [67] GUALA, A., CAMPOREALE, C., TOSELLO, F., CANUTO, C., AND RIDOLFI, L. Modelling and Subject-Specific Validation of the Heart-Arterial Tree System. *Annals of Biomedical Engineering* (10 2014).
- [68] HADDAD, W., CHELLABOINA, V., AND NERSESOV, S. Impulsive and Hybrid Dynamical Systems: Stability, Dissipativity and Control. *Impulsive and Hybrid Dynamical Systems: Stability, Dissipativity, and Control* (01 2006).
- [69] HAN, E., WARNECKE, G., TORO, E. F., AND SIVIGLIA, A. On Riemann solutions to weakly hyperbolic systems: part 1. Modelling subcritical flows in arteries. Tech. Rep. NI15003NPA, Isaac Newton Institute for Mathematical Sciences, University of Cambridge, Cambridge, UK, 2015a.
- [70] HAN, K., FRIESZ, T., AND YAO, T. A Variational Approach for Continuous Supply Chain Networks. *SIAM Journal on Control and Optimization* 52 (02 2014), 663–686.
- [71] HANTE, F. *Hybrid Dynamics Comprising Modes Governed by Partial Differential Equations: Modeling, Analysis and Control for Semilinear Hyperbolic Systems in One Space Dimension*. PhD thesis, 08 2010.
- [72] HANTE, F. M., LEUGERING, G., AND SEIDMAN, T. I. Modeling and analysis of modal switching in networked transport systems. *Appl. Math. Optim.* 59, 2 (2009), 275–292.
- [73] HANTE, F. M., LEUGERING, G., AND SEIDMAN, T. I. An augmented BV setting for feedback switching control. *J. Syst. Sci. Complex.* 23, 3 (2010), 456–466.
- [74] HEYMANN, M., LIN, F., MEYER, G., AND RESMERITA, S. Analysis of Zeno behaviors in a class of hybrid systems. *Automatic Control, IEEE Transactions on* 50 (04 2005), 376 – 383.
- [75] HOLDEN H., R. N. *A Mathematical Model of Traffic Flow on a Network of Roads*, vol. 43. Vieweg+Teubner Verlag, 1993, pp. 329–335.
- [76] IZQUIERDO, J., AND IGLESIAS, P. L. Mathematical modelling of hydraulic transients in simple systems. *Math. Comput. Modelling* 35, 7-8 (2002), 801–812.

- [77] JANSEN, L., AND PADE, J. Global Unique Solvability for a Quasi-Stationary Water Network Model. Preprint, 21 pages, 2013.
- [78] JANTSCHER, L. *Distributionen*. Walter de Gruyter, 1971.
- [79] JOVANOVIĆ, B. S., AND SÜLI, E. *Analysis of Finite Difference Schemes*, 1 ed., vol. 46. Springer-Verlag, London, 2014.
- [80] KOLB, O. *Simulation and Optimization of Gas and Water Supply Networks*. PhD thesis, TU Darmstadt, 2011.
- [81] KUNKEL, P., AND MEHRMANN, V. *Differential-Algebraic Equations. Analysis and Numerical Solution*. European Mathematical Society Publishing House, Zurich, Switzerland, 2006.
- [82] LANGEWOUTERS, G., WESSELING, K., AND GOEDHARD, W. The static elastic properties of 45 human thoracic and 20 abdominal aortas in vitro and the parameters of a new model. *Journal of biomechanics* 17 (02 1984), 425–35.
- [83] LEVEQUE, R. J. *Numerical methods for conservation laws (2. ed.)*. Lectures in mathematics. Birkhäuser, 1992.
- [84] LEVEQUE, R. J. *Finite Volume Methods for Hyperbolic Problems*. Cambridge Texts in Applied Mathematics. Cambridge University Press, 2002.
- [85] LI, J., AND YANG, H. Delta-shocks as limits of vanishing viscosity for multidimensional zero-pressure gas dynamics. *Quarterly of Applied Mathematics* LIX (06 2001), 315–342.
- [86] LIANG, F., HIMENO, R., AND LIU, H. Biomechanical characterization of ventricular-arterial coupling during aging: A multi-scale model study. *Journal of biomechanics* 42 (05 2009), 692–704.
- [87] LYGEROS, J., JOHANSSON, K., SIMIC, S., AND SASTRY, S. Dynamical Properties of Hybrid Automata. *IEEE Transactions on Automatic Control* 48 (06 2003).
- [88] MAREELS, I., WEYER, E., OOI, S., CANTONI, M., LI, Y., AND NAIR, G. Systems engineering for irrigation systems: Successes and challenges. *Annual Reviews in Control* 29 (07 2005), 191–204.
- [89] MATHIS, W. Recent developments in numerical integration of differential equations. *International Journal of Numerical Modelling: Electronic Networks, Devices and Fields* 7 (03 1994), 99 – 125.
- [90] MENALDI, J. L. *Distributions and Function Spaces*. 23. Mathematics Faculty Research Publications, 2016.
- [91] METGER, G., AND VABRE, J. *Transmission Lines With Pulse Excitation*. Academic Press, 1969.
- [92] MICHAL, V. On the low-power design, stability improvement and frequency estimation of the CMOS ring oscillator. In *Proceedings of 22nd International Conference Radioelektronika 2012* (2012), pp. 1–4.
- [93] MILISIC, V., AND QUARTERONI, A. Analysis of lumped parameter models for blood flow simulations and their relation with 1D models. *Mathematical Modelling and Numerical Analysis* 38 (07 2004).

- [94] MÜLLER, L. O., AND TORO, E. F. A global multiscale mathematical model for the human circulation with emphasis on the venous system. *Int. J. Numer. Methods Biomed. Eng.* 30, 7 (2014), 681–725.
- [95] MYNARD, J. P., DAVIDSON, M. R., PENNY, D. J., AND SMOLICH, J. J. A simple, versatile valve model for use in lumped parameter and one-dimensional cardiovascular models. *International Journal for Numerical Methods in Biomedical Engineering* 28, 6-7 (2012), 626–641.
- [96] OLUFSEN, M. *A One-Dimensional Fluid Dynamic Model of the Systemic Arteries*, vol. 124. Springer, 07 2011, pp. 167–187.
- [97] OSHER, S., AND SOLOMON, F. Upwind Difference Schemes for Hyperbolic Systems of Conservation Laws. *Mathematics of Computation - Math. Comput.* 38 (05 1982).
- [98] OTTESEN, J. Valveless pumping in a fluid-filled closed elastic tube-system: One-dimensional theory with experimental validation. *Journal of mathematical biology* 46 (05 2003), 309–32.
- [99] OTTESEN, J. T., OLUFSEN, M. S., AND LARSEN, J. K. *Applied Mathematical Models in Human Physiology*, 1st. ed. Society for Industrial and Applied Mathematics, 2004.
- [100] PERTHAME, B. *Transport Equations in Biology*. Birkhäuser Basel, 2007.
- [101] QUARTERONI, A., FORMAGGIA, L., AND NOBILE, F. *A One Dimensional Model for Blood Flow: Application to Vascular Prosthesis*. Springer, Berlin, Heidelberg, 01 2002, pp. 137–154.
- [102] QUARTERONI, A., FORMAGGIA, L., AND VENEZIANI, A. *Complex systems in biomedicine*. 2006.
- [103] QUARTERONI, A., RAGNI, S., AND VENEZIANI, A. Coupling between lumped and distributed models for blood flow problems. *Computing and Visualization in Science* 4, 2 (2001), 111–124.
- [104] QUARTERONI, A., AND VENEZIANI, A. Analysis of a geometrical multiscale model based on the coupling of odes and pdes for blood flow simulations. *Multiscale Modeling and Simulation* 1, 2 (2003), 173–195.
- [105] QUARTERONI, A., VENEZIANI, A., AND ZUNINO, P. Mathematical and Numerical Modeling of Solute Dynamics in Blood Flow and Arterial Walls. *SIAM Journal on Numerical Analysis* 39 (01 2002).
- [106] RADEMACHER, H. Über partielle und totale differenzierbarkeit von Funktionen mehrerer Variablen und über die Transformation der Doppelintegrale. *Mathematische Annalen* 79 (1919), 340–359.
- [107] ROE, P. Approximate Riemann solvers, parameter vectors, and difference schemes. *Journal of Computational Physics* 43, 2 (1981), 357 – 372.
- [108] SANDERS, S. P., YEAGER, S., AND WILLIAMS, R. G. Measurement of systemic and pulmonary blood flow and QP/QS ratio using doppler and two-dimensional echocardiography. *The American Journal of Cardiology* 51, 6 (1983), 952 – 956.
- [109] SCHWARTZ, L. *Théorie des Distributions*. Hermann, Paris, 1957.

- [110] SHERWIN, S., FORMAGGIA, L., PEIRO, J., AND FRANKE, V. Computational Modeling of 1D Blood Flow with Variable Mechanical Properties and Application to the Simulation of Wave Propagation in the Human Arterial System. *Int. J. Numer. Meth. Fluids* 43 (10 2003), 673–700.
- [111] SHERWIN, S., FRANKE, V., PEIRO, J., AND KH, P. One-dimensional modelling of a vascular network in space-time variables. *Journal of Engineering Mathematics* 47 (01 2003), 217–250.
- [112] SHI, Y., LAWFORD, P., AND HOSE, R. Review of 0-D and 1-D Models of Blood Flow in the Cardiovascular System. *Biomedical engineering online* 10 (04 2011), 33.
- [113] SIMIĆ, S., JOHANSSON, K., SASTRY, S., AND LYGEROS, J. Towards a Geometric Theory of Hybrid Systems. In *Dynamics of Continuous, Discrete and Impulsive Systems. Series B: Applications and Algorithms* (10 2007), vol. 12, pp. 421–436.
- [114] STEINBACH, M. C. Topological Index Criteria in DAE for Water Networks. Tech. Rep. 05-49, ZIB, Takustr. 7, 14195 Berlin, 2005.
- [115] STOLZMANN, P., SCHEFFEL, H., TRINDADE, P., AR, P., HUSMANN, L., LESCHKA, S., GENONI, M., MARINCEK, B., KAUFMANN, P., AND ALKADHI, H. Left ventricular and left atrial dimensions and volumes: Comparison between dual-source CT and echocardiography. *Investigative Radiology* 43 (05 2008).
- [116] SUGA, H., SAGAWA, K., AND SHOUKAS, A. A. Load independence of the instantaneous pressure-volume ratio of the canine left ventricle and effects of epinephrine and heart rate on the ratio. *Circulation Research* 32, 3 (1973), 314–322.
- [117] SUN, Y., BESHARA, M., LUCARIELLO, R., AND CHIARAMIDA, S. A comprehensive model for right-left heart interaction under the influence of pericardium and baroreflex. *The American journal of physiology* 272 (04 1997), H1499–515.
- [118] SUN, Y., JANEROT-SJÖBERG, B., ASK, P., LOYD, D., AND WRANNE, B. Mathematical model that characterizes transmitral and pulmonary venous flow velocity patterns. *The American journal of physiology* 268 (02 1995), H476–89.
- [119] TAKAHASHI, E. A. *Doppler Ultrasonography*. Springer, Cham, 2019, pp. 137–154.
- [120] TAN, D., ZHANG, T., CHANG, T., AND ZHENG, Y. Delta-shock waves as limits of vanishing viscosity for hyperbolic systems of conservation laws. *Journal of Differential Equations* 112, 1 (1994), 1 – 32.
- [121] TANWANI, A., AND TRENN, S. On observability of switched differential-algebraic equations. In *Proceedings of the IEEE Conference on Decision and Control* (01 2011), pp. 5656 – 5661.
- [122] TERMAN, F. E. *Radio Engineers' Handbook*. McGraw-Hill Book Company, 1943.
- [123] THEIN, F., AND HANTKE, M. Singular and selfsimilar solutions for Euler equations with phase transitions. *Bull. Braz. Math. Soc. (N.S.)* 47, 2 (2016), 779–786.
- [124] TISCHENDORF, C. *Topological index calculation of DAEs in circuit simulation*. Humboldt-Universität zu Berlin, Mathematisch-Naturwissenschaftliche Fakultät II, Institut für Mathematik, 2005.
- [125] TORO, E. *Riemann Solvers and Numerical Methods for Fluid Dynamics*. Springer, 2009.

- [126] TORO, E., AND SIVIGLIA, A. Flow in Collapsible Tubes with Discontinuous Mechanical Properties: Mathematical Model and Exact Solutions. *Communications in Computational Physics* 13 (11 2012).
- [127] TORO, E. F. *Godunov Methods Theory and Applications*. Springer, 2001.
- [128] TOUMI, I. A Weak Formulation of Roe's Approximate Riemann Solver. *Journal of Computational Physics* 102 (1992), 360–373.
- [129] TOZEREN, A. Elastic Properties of Arteries and Their Influence on the Cardiovascular System. *Journal of Biomechanical Engineering* 106, 2 (05 1984), 182–185.
- [130] TRENN, S. *Distributional differential algebraic equations*. PhD thesis, Institut für Mathematik, Technische Universität Ilmenau, Universitätsverlag Ilmenau, Germany, 2009.
- [131] TRENN, S. Regularity of distributional differential algebraic equations. *Math. Control Signals Syst.* 21, 3 (2009), 229–264.
- [132] TRENN, S. Switched differential algebraic equations. In *Dynamics and Control of Switched Electronic Systems - Advanced Perspectives for Modeling, Simulation and Control of Power Converters*, F. Vasca and L. Iannelli, Eds. Springer, London, 2012, ch. 6, pp. 189–216.
- [133] TRENN, S., AND UNGER, B. Delay regularity of differential-algebraic equations. In *Proc. 58th IEEE Conf. Decision Control (CDC) 2019* (Nice, France, 2019). to appear.
- [134] WANG, X., SONG, Y., AND IRVING, M. *Modern Power Systems Analysis*, 1st. ed. Springer US, 2008.
- [135] WEIERSTRASS, K. Zur Theorie der bilinearen und quadratischen Formen. *Monatsbericht der Berliner Akademie der Wissenschaften* (05 1868), 310–338.
- [136] WESSELING, P. *Principles of Computational Fluid Dynamics*. Springer, 2001.
- [137] WHITHAM, G. B. *Linear and Nonlinear Waves*. John Wiley & Sons, 06 1999.
- [138] WIJNBERGEN, P., AND TRENN, S. Impulse controllability of switched differential-algebraic equations. In *Proc. European Control Conference (ECC 2020)* (Saint Petersburg, Russia, 2020). to appear.
- [139] WILLEMET, M., AND ALASTRUEY, J. Arterial pressure and flow wave analysis using time-domain 1-D hemodynamics. *Annals of Biomedical Engineering* 43 (08 2015), 190–206.
- [140] WONG, K. The Eigenvalue Problem $\lambda Tx + Sx$. *Journal of Differential Equations* 16, 2 (1974), 270 – 280.
- [141] YANG, H. Riemann problems for a class of coupled hyperbolic systems of conservation laws. *J. Differential Equations* 159, 2 (1999), 447–484.
- [142] YEH, J. J. *Metric In Measure Spaces*. World Scientific, 2019.
- [143] ZHANG, J., JOHANSSON, K. H., LYGEROS, J., AND SASTRY, S. Dynamical Systems Revisited: Hybrid Systems with Zeno Executions. In *Hybrid Systems: Computation and Control* (Berlin, Heidelberg, 2000), N. Lynch and B. H. Krogh, Eds., Springer Berlin Heidelberg, pp. 451–464.

- [144] ZOBIRI, F., WITRANT, E., AND BONNE, F. PDE Observer Design for Counter-Current Heat Flows in a Heat-Exchanger. *IFAC-PapersOnLine* 50, 1 (2017), 7127 – 7132. 20th IFAC World Congress.

Publications

- 2020** Switched Hyperbolic Balance Laws and Differential Algebraic Equations
– *Borsche, Raul and Garavello, Mauro*
- 2019** A Distributional Solution Framework for Linear Hyperbolic PDEs
Coupled to Switched DAEs – *Borsche, Raul and Trenn, Stephan*

Akademischer Lebenslauf

- 2017** Annahme als Doktorandin an der AG Technomathematik der Technischen Universität Kaiserslautern (TUK) unter Prof. Dr. Stephan Trenn.
Masterabschluss in Mathematik.
Thema der Masterarbeit: **Shallow Water Equations with Sediment Transport on Networks**
- 2014** Immatrikulation an der Technical University of Kaiserslautern, Deutschland.
Bachelorabschluss in Mathematik.
- 2009** Immatrikulation im Bachelorstudiengang Mathematik an der Technischen Universität des Nahen Ostens (METU), Ankara, Türkei.
- 2004 - 2008** Kalaba anatolisches Gymnasium , Ankara, Türkei.
- 1996 - 2004** Grundschule Beytepe, Ankara, Türkei.

Academic curriculum vitae

- 2017** Accepted as a doctoral candidate at the Technomathematics Group at the Technical University of Kaiserslautern (TUK) with Prof. Dr. Stephan Trenn.
Master of Science (M.Sc.) degree in mathematics.
Topic of the master thesis: **Shallow Water Equations with Sediment Transport on Networks**
- 2014** Matriculation at the Technical University of Kaiserslautern, Germany.
Bachelor of Science (B.Sc.) in mathematics.
- 2009** Matriculation at the Middle East Technical University (METU), Ankara, Turkey.
- 2004 - 2008** Kalaba Anatolian Grammar School , Ankara, Turkey.
- 1996 - 2004** Primary education at Elementary School Beytepe, Ankara, Turkey.

